Developing Parasite-Resistant Systems in Tomatoes to Control Infestations of *Cuscuta campestris*

By

MIN-YAO JHU
DISSERTATION

Submitted in partial satisfaction of the requirements for the degree of

DOCTOR OF PHILOSOPHY

in

Plant Biology

in the

OFFICE OF GRADUATE STUDIES

of the

UNIVERSITY OF CALIFORNIA

DAVIS

Approved:

Neelima Sinha, Chair

Savithramma Dinesh-Kumar

Siobhan Brady

Committee in Charge 2021

Acknowledgments

First of all, I would like to thank Neelima Sinha for her guidance during the past six years. I am especially grateful that Neelima provided many great learning opportunities for me, including writing a comprehensive review article, giving presentations at conferences and seminars, introducing me to other scientists, and reviewing other researchers' research articles. All of these experiences help me develop into an independent scientist. Neelima is always open-minded to trying new analysis methods and technologies to solve the questions we want to ask. Her creativity and courage also inspired me to be a curious scientist to explore different research topics.

Second, I would like to thank my dissertation committee, Savithramma Dinesh-Kumar and Siobhan Brady, for their helpful suggestions on my research projects during our meetings. I thank Dinesh for providing a lot of useful information and sharing his research experiences to help me with the protein-protein interaction experiments. I really appreciate Siobhan for sharing her research career experiences with me in our informational interview and encouraging me to start looking for jobs at least one year before I planned to graduate. As an international student, I often encountered imposter syndrome at the beginning of my Ph.D. career. Thanks to Siobhan's encouragement, I felt confident enough to take on many challenges. I also want to thank my QE committee: Siobhan Brady, Savithramma Dinesh-Kumar, John Yoder, Daniel Runcie, and Li Tian, for all of their suggestions on my research proposal. My Ph.D. qualifying exam was an exciting, impressive, and precious experience for me. I gained a lot of interdisciplinary knowledge during the preparation process and during the exam itself.

Third, thanks to all the Sinha Lab current and previous lab members, and many people from other labs who provided valuable suggestions and assistance to help me with troubleshooting many experiments. Many thanks to Moran Farhi, Yasunori Ichihashi, and Aashish Ranjan for

starting different *Cuscuta* projects and establishing many tools and resources, so I could continue to investigate this fascinating research topic. Thanks so much to Hokuto Nakayama for always being willing to share his research experiences and inspiring me to be a well-organized scientist. Many thanks to Kristina Zumstein for being a fantastic lab manager and helping with a lot of troubleshooting. Thanks to Li Wang, Richard Philbrook, and Caitlin Wong for all their hard work and contributions to our projects. Thanks to all undergrads: Chiharu Ito, Joana Tanurahardja, Junqi Lu, and Kaiwen Zhang, for helping with some parts of the experiments or image analysis. Thanks to Aaron Leichty, Steven Rowland, Siyu Li, Karo Czarnecki for all their feedback and suggestions during lab meetings. Many thanks to people from Harada lab, Shih Lab, Liu lab, Dinesh lab for providing help or sharing resources or experiment techniques.

Fourth, I am grateful for all instructors who provided me opportunities to work as a teaching assistant in their class: Terence Murphy, Steven Theg, Patrick Shih (PLB111), John Harada (PLB112), Geoffrey Benn (BIS2C), and Joel Ledford (BIS15L). During the past three years, I have gained a lot of valuable teaching experience, which helped me find my passion for teaching, learn how to explain a complex concept in an easy-to-understand way, and also be better at interpersonal communication. I enjoyed the opportunity to put what I had learned into practice in teaching students. These experiences also helped me understand how important it is for scientists to reach outside the ivory tower and start communicating science to the public. In addition, I would like to also thank Julin Maloof for holding the R club and John Davis for helping with code troubleshooting. From Statistical Rethinking, Python for Data Analysis, to Deep learning, I have learned a lot from our weekly meetings during the past four years, and I started to enjoy and feel more confident about programming.

Fifth, thanks to my family members, especially my mom. It was not easy for her to raise two kids by herself. I learned diligence and perseverance from her, which are valuable merits that helped me go through these life adventures. I also appreciate all fellowships, scholarships, financial aid, and student loans provided by the government, universities, high schools, and private agencies. As a student living below the poverty line in Taiwan, I never imagined that I would be able to complete my Ph.D. degree in the US one day. Thanks to all my biologist friends and dance friends for keeping me company in different moments of my life.

Last but not least, to my husband, Eli Marable. Thank you for always being supportive and helping me go through the difficult times in life. Thank you for inspiring me to accept myself and letting me see the unique beauty in imperfection. Thank you so much for willing to move with me to wherever my next job landed. Because of your love and support, I can wholeheartedly immerse myself in research without concern. I really appreciate it. Looking forward to our new adventure in the UK.

Developing Parasite-Resistant Systems in Tomatoes to Control Infestations of *Cuscuta campestris*

Abstract

Unlike most autotrophic plants, parasitic plants evolved to have a heterotrophic lifestyle and to steal water and nutrients from their host through specialized parasitic organs, haustoria. Some species of parasitic angiosperms parasitize major crop plants, which causes severe agricultural losses and threatens food security in many regions. Understanding how host plants sense and resist parasitic plants not only reveals the underlying mechanisms of various resistance systems, but also provides the foundation for agricultural improvements. Chapter One of this dissertation reviews the current knowledge on how host plants perceive stem and root parasitic plants and utilize different pre-attachment and post-attachment defense responses to deter these parasites.

Cuscuta species (dodders) are stem holoparasitic angiosperms, which lack functional leaves and roots. *Cuscuta campestris* (*C. campestris*) is one of the most broadly distributed *Cuscuta* species and has a wide host range, which includes many important vegetable and fruit crops. Domesticated tomato (*Solanum lycopersicum*) is one of the crop plants that are vulnerable to *C. campestris* and reduces 70% yield upon *Cuscuta* infestations. Understanding the molecular mechanism of *C. campestris* haustorium formation will assist in parasitic weed management and the development of parasitic plant-resistant crops. Chapter Two of this dissertation investigated the transcriptome of six *C. campestris* tissues and identified *LATERAL ORGAN BOUNDARIES DOMAIN 25* (*CcLBD25*) as a critical regulator in haustorium development.

On the other hand, even though most cultivated tomatoes are usually susceptible to *C. campestris*, some specific Heinz hybrid tomato cultivars were discovered to be resistant to *Cuscuta* species. These tomato cultivars are used as a biocontrol method in the field, but the resistance mechanism remains unknown. Chapter Three of this dissertation dives into the underlying mechanism and genes involved in this lignin-based defense response. These resistant Heinz cultivars trigger post-attachment lignification in the stem cortex upon *C. campestris* infection.

Although some studies have identified factors required for parasitic plant haustorium induction as well as genes involved in host defense responses, the signals involved in haustorium development at specific developmental stages and tissue-resolution communication between host and parasite during the haustorium penetration process are largely unknown. Chapter Four of this dissertation focused on the interface between the host and parasite. *C. campestris* haustorial tissue and tomato host tissue immediately surrounding haustoria were collected by laser-capture microdissection (LCM) to obtain tissue-resolution RNA-Seq profiles. These profiles were used to identify key genes regulating haustorial development and host responses, and describes my attempt to validate the function of these genes.

Finally, Chapter Five summarizes the major discoveries of each research project and the potential of utilizing these findings in agriculture. This dissertation provides an overview of both haustorium development in *C. campestris* and defense response in tomato host plants. Therefore, this work will be of interest to academic researchers in plant biology and researchers interested in developing potential agricultural translational applications.

Table of Contents

Acknowledgments ii

Abstract v

Table of Contents vii

Chapter 1: Introduction - Parasitic Plants: An Overview of Mechanisms by which Plants Perceive and Respond to Parasites 1

Abstract 1

I. Introduction 2

II. Perception of parasites 4

III. Defense mechanisms in resistance responses 8

IV. A new definition of stem and root parasites: Cross-organ parasitism 21

V. Conclusion and future perspectives 24

VI. Figures 25

VII. References 35

Chapter 2: *LATERAL ORGAN BOUNDARIES DOMAIN 25* functions as a key regulator of haustorium development in dodders 48

Abstract 48

Introduction 50

Results 52

Discussion 62

Conclusions 65

Materials and Methods 66

Figures 73

References 88

Supplemental Data 96

Chapter 3: Lignin-based resistance to *Cuscuta campestris* parasitism in Heinz resistant tomato cultivars 111

Abstract 111

Introduction 113

Results 117

Discussion 132

Materials and Methods 136

Figures 149

References 162

Supplemental Data 175

Chapter 4: Investigating host and parasitic plant interaction by tissue-specific gene analyses on tomato and dodder interface at three haustorial developmental stages 207

Abstract 207

Introduction 208

Results 210

Discussion 221

Materials and Methods 229

Figures 236

References 248

Supplemental Data 258

Chapter 5: Conclusions 266

Chapter 1: Introduction - Parasitic Plants: An Overview of Mechanisms by which Plants Perceive and Respond to Parasites

*This chapter is submitted and will be published in Volume 73 of the Annual Review of Plant Biology.

Keywords: parasitic plants, signal perception, resistance responses, cross-organ parasitism, organ-specific defense.

Abstract

In contrast to most autotrophic plants, parasitic plants obtain water and nutrients by parasitizing host plants. Many important crop plants are infested by these heterotrophic plants, leading to severe agricultural loss and reduced food security. Understanding how host plants perceive and resist parasitic plants provides insight into underlying defense mechanisms and the potential for agricultural applications. In this review, we offer a comprehensive overview of the current understanding of host perception of parasitic plants and the pre-attachment and post-attachment defense responses mounted by the host. We also summarize the current understanding and cases of cross-organ parasitism that have been reported but lack systematic review, and most current research overlooks the role of organ specificity in resistance responses. Understanding how different tissue types respond to parasitic plants could provide the potential for developing a universal resistance mechanism in crops that can resist both root and stem parasitic plants.

I. Introduction

Most land plants are autotrophic: they can conduct photosynthesis to convert inorganic carbon into carbohydrates, using captured light as energy. However, some plants have evolved a heterotrophic lifestyle and are known as parasitic plants. Using a specialized organ known as a haustorium, these plants can parasitize other plants to obtain water and nutrients from their hosts. Parasitic weeds have a major negative impact on agricultural crops, forests, and the dynamics of ecological systems (Musselman et al., 2001; Agrios, 2005; Bardgett et al., 2006; Parker, 2009; Fisher et al., 2013). It has been estimated that about 4500 angiosperms belonging to 28 families have adopted heterotrophy, to different extents, and can attach to and invade other plants to extract nutrients and water for their own use. Based on the invaded host tissue, parasitic weeds can be classified as stem or root parasites and based on host-dependence can be described as obligate hemiparasitic, facultative hemiparasitic, or holoparasitic (Agrios, 2005). Many of these parasitic plants are listed as noxious weeds and parasitize major crop plants, severely reducing yield and affecting food security. However, because of the tight physiological connection between host and parasites, most traditional herbicides and control methods, like hand weeding, are ineffective, too expensive, or labor-intensive to regulate parasitic plant infestations. Most parasitic plants produce numerous small seeds that remain viable for many years, sometimes needing host cues for germination. This makes it impossible to control these plants by seed depletion strategies.

Reducing the impact and spread of parasitic weeds requires knowledge of the molecular processes that underlie interactions between the parasite and the host. This will enable us to deploy modern directed strategies of classical or molecular breeding to make crops resistant to these weeds. However, this approach is currently limited by our understanding of the genetic and biochemical mechanisms underlying the interactions between host plants and parasitic weeds, which often

derive from multiple plant clades. Most of the research focuses on root parasites of the order Lamiales, including the hemiparasitic *Striga*, and factors needed for germination, host recognition, and haustorium induction (Shen et al., 2006; Cui et al., 2007; López-Ráez et al., 2009; Yoder and Scholes, 2010). Previous studies have focused on investigating host responses in major crops and defense mechanisms in specific cultivars, mutants, or species that are resistant against parasitic plants, often revealing the underlying resistance mechanisms or pathways that will aid in developing parasitic plant-resistant crops. The availability of next-generation sequencing has also facilitated research on these interactions, and several genes involved in resistance responses have been identified. Several excellent review articles were recently published and have focused on different specific aspects of parasitic plant and host interactions (Saucet and Shirasu, 2016; Albert et al., 2020; Delavault, 2020; Hu et al., 2020; Fishman and Shirasu, 2021; Mutuku et al., 2021).

Here, we provide a comprehensive review of how different hosts perceive stem and root parasitic plants and utilize diverse defense responses to resist parasitism. Depending on whether defense mechanisms functions before or after haustorial attachment, defense responses can be classified into two categories: pre-attachment and post-attachment responses. Interestingly, while reviewing current knowledge of post-attachment defense responses, we noticed that several resistance mechanisms, like lignin accumulation, had been reported against both root and stem parasitic plants but with distinct anatomical distribution in structures in aboveground and belowground organs. These observations indicated that some types of defense mechanisms might be organ-specific or tissue-specific. Although traditionally parasitic plants can be categorized as root or stem parasitic plants based on the position of their haustorial attachment on the host, recently unconventional haustorial connections have been reported but lack clear definition and systematic review. Therefore, we define cross-organ parasitism and summarize recent

observations and our understanding of cross-organ parasitism. This also raises the question of whether our current understanding of resistance applies to cross-organ parasitism. Finally, we discuss critical future research directions on resistance mechanisms to both major organ parasitism and cross-organ parasitism.

II. Perception of parasites

Most plants are vulnerable to parasitic plant attacks because they lack adequate defense mechanisms. However, some plants evolved to have resistance responses to protect themselves from parasitic weed infestation. One fundamental hypothesis states that the ability to perceive parasitic plants is an essential first step for host plants to trigger defensive responses. Recent discoveries in crop plants provide evidence that, similar to the systems recognizing bacterial and fungal pathogens, host plants can identify stem and root parasitic plants by utilizing the receptors and signal perception mechanisms.

i. How host plants perceive stem parasites

The recently discovered perception mechanism in domesticated tomatoes (*Solanum lycopersicum*) that activates in response to *Cuscuta* spp. provides valuable support for the hypothesis that host plants can sense parasitic plants (Hegenauer et al., 2016; Hegenauer et al., 2020). Hegenauer *et al.* found that the *CUSCUTA RECEPTOR 1* (*CuRe1*) encodes a leucine-rich repeat receptor-like protein (LRR-RLP). This cell surface receptor-like protein has been identified as a necessary element for the perception of the molecular pattern associated with parasitic plants (Figure 1). On the other hand, other related Solanaceae species that are susceptible to *C. reflexa*, like cultivated tobacco *(Nicotiana tabacum), N. benthamiana,* potato (*S. tuberosum),* and wild

tomato species *S. pennellii, lack fully functional CuRe1*, therefore, *are not able to* induce defense responses (Hegenauer et al., 2016).

Their subsequent research further described the molecular patterns of parasitic plants, *Cuscuta* factors, which serve as ligands of CuRe1 (Hegenauer et al., 2020). One 11 kDa *Cuscuta* factor was purified from *C. reflexa* extracts and classified as a glycine-rich protein (GRP). Both GRP and its minimal peptide epitope Crip21 are ligands of CuRe1 and can trigger the CuRe1-dependent resistance responses, including hypersensitive responses (HRs), releasing reactive oxygen (ROS) species, and increased ethylene synthesis (Figure 1) (Hegenauer et al., 2020). This result also indicates that host plants perceive parasitic plants in a way analogous to recognizing microbial pathogens. The host plant's ability to perceive the molecular patterns of parasitic plants is the first step of generating resistance responses that is similar to pathogen-associated molecular pattern (PAMP)-triggered immunity (PTI).

In addition to PTI, studies report that host plants might have evolved a second layer of immunity, effector-triggered immunity (ETI), to resist stem parasitic plants. ETI usually starts with intracellular nucleotide-binding and leucine-rich repeat (NLR) receptors that are encoded by resistance (R) genes. These NLR receptors detect effectors and then trigger downstream strong resistance responses to counteract the effector effects. Recent research reports a gene, *Cuscuta R-gene for Lignin-based Resistance 1* (*CuRLR1*), encoding an N-terminal coiled-coil nucleotide-binding site leucine-rich repeat protein (CC-NBS-LRR) in specific resistant Heinz tomato (Figure 1). CuRLR1 may be engaged in sensing signaling pathways or function as a receptor for perceiving *C. campestris* signals or effectors. Activation of CuRLR1 then induced lignin accumulation in the tomato stem cortex region, creating a physical boundary to prevent haustorium penetration (Figure 1).

The *Cuscuta* signals or effectors that trigger this lignin-based defense response appear to be large heat-sensitive proteins ranging from 30 kDa to 100 kDa, and therefore, distinct from the previously identified 11 kDa *Cuscuta* GRP factor or its minimal peptide epitope Crip21 that CuRe1 recognizes (Hegenauer et al., 2016; Hegenauer et al., 2020). More detailed characteristics or functions of these unknown Cuscuta signals or effectors would be worthy of future investigation.

Interestingly, perceiving parasites does not always lead to activation of the same defense mechanisms. For example, sensing *C. reflexa* leads to HRs, ethylene synthesis, ROS production, and cell wall modifications that form suberin-like wound tissue at the penetration site that blocks parasite growth in tomatoes (Albert et al., 2008; Johnsen et al., 2015; Kaiser et al., 2015). However, while sensing *C. campestris* does trigger ethylene production in tomato, suberin accumulation is not observed, and *C. campestris* can still overcome this defense response and parasitize most tomato cultivars and many wild relatives of tomato. These results indicate the perception mechanisms and resistance responses have species-specificity. This also suggests that some parasitic plants might have evolved to dodge the host perception systems or release effectors to suppress the resistance responses triggered by the sensing mechanisms.

ii. How host plants perceive root parasites

Similar perception mechanisms have also been found to play an important role in the perception of root parasitic plants. Duriez et al. discovered that *Helianthus annuus Orobanche* resistance 7 (*HaOr7*) encodes a membrane-bound leucine-rich repeat (LRR) receptor-like kinase (Figure 2, the upper panel). The fully functional HAOR7 protein is only present in sunflower lines resistant to sunflower broomrape *O. cumana* (Duriez et al., 2019). In susceptible sunflower lines, a truncated HAOR7 protein, lacking transmembrane and kinase domains, is found.

Thus, a fully functional HAOR7 protein appears necessary for host plants to display resistance against *O. cumana* during the early stages of interaction.

The fully functional HAOR7 protein has been reported to recognize an avirulence protein (AVROR7) from *O. cumana* using the LRR domain (Duriez et al., 2019). Perceiving AVROR7 likely enables signal transduction through the kinase domain of the HAOR7 protein and prevents haustorial connection of *O. cumana* to the sunflower root vascular system (Figure 2, the upper panel). This incompatible attachment leads to resistance in these specific sunflower lines. The main elements of the signaling pathways triggered by HAOR7 protein, and how resistance responses lead to incompatible attachments are questions waiting to be elucidated. The discovery of HAOR7 further confirms that the ability to perceive parasite molecular patterns is the crucial first step to trigger a signal transduction cascade and generate the following resistance response during parasitic plant invasion.

In addition to PTI, ETI has also been reported in mechanisms leading to resistance to root parasitic plants. Li and Timko identified an R gene, *RSG3-301,* leading to resistance to *Striga gesnerioides* (*S. gesnerioides*) race 3 and race 4 in the resistant *cowpea* (*Vigna unguiculata*) cultivar B301 (Li and Timko, 2009). *RSG3-301* encodes a CC-NBS-LRR protein, which triggers hypersensitive response and necrosis upon *S. gesnerioides infestation* (Figure 2, the lower panel). Knocking-down *RSG3-301 with virus-induced gene silencing (VIGS) makes* resistant *cowpea* B301 susceptible to *S. gesnerioides (Li and Timko, 2009).*

Intriguingly, the *S. gesnerioides race 4z* which localized to Zakpota, south-western Benin, *can parasitize* the resistant cultivar B301. *Race 4z overcomes RSG3-301-mediated resistance by secreting a* small effector, Suppressor of Host Resistance 4z (SHR4z) (Figure 2, lower panel) (Su

et al., 2020). Based on phylogenetic analyses, the LRR domain of SHR4z is similar to that seen in proteins in the SOMATIC EMBRYOGENESIS RECEPTOR-LIKE KINASE (SERK) gene family. When SHR4z enters the host cell, it can interact with a BTB-BACK domain-containing ubiquitin E3 ligase (VuPOB1) and cause ubiquitination and degradation of VuPOB1 (Figure 2, the lower panel). Since VuPOB1 is a positive regulator of hypersensitive response in *cowpea*, the SHR4z-triggered VuPOB1 degradation leads to reduced hypersensitive response and makes the resistant cultivar B301 susceptible to *S. gesnerioides race 4z (Su et al., 2020). This discovery indicates the ongoing arms race between parasitic plants and their hosts in the co-evolution process.*

III. Defense mechanisms in resistance responses

Host plants attacked by parasitic plants display induction of defense response pathways that can lead to resistance (prevention or limitation of attachment and growth) or tolerance (the ability to maintain biomass and yield despite the infestation) (Medel, 2001; Pagán and García-Arenal, 2018). A recently published review nicely summarizes the theory and experimental evidence for tolerance responses to parasitic plants and pathogens (Pagán and García-Arenal, 2018). In this review, we focus on the mechanisms underpinning resistance responses. Based on whether the resistant mechanism functions before or after parasitic plants attach to their hosts, resistance responses can be classified as pre-attachment and post-attachment resistance.

i. Pre-attachment resistance

Some host plants trigger defense responses only after sensing parasitic plants, but other resistant host plants take a more preventive strategy by making themselves invisible to parasitic plants. For example, being able to perceive hosts prior to seed germination and grow towards the host immediately after germination is a critical step in the root parasitic plant life cycle. The group

of important compounds in host root exudates that stimulate root parasitic plant germination have been identified and named as strigolactones (SLs) (Cook et al., 1966; Xie et al., 2010). Previous studies showed that disrupting the strigolactone biosynthesis pathway, via a carotenoid cleavage dioxygenase 8 (*ccd8*) mutation, leads to strigolactone deficiency. Orobanche seeds exposed to *ccd8* pea plant root exudates have a lower germination rate compared with seeds exposed to wild-type pea plant exudates. This indicates that *ccd8* mutant plants are not able to produce sufficient strigolactones in their root exudates to serve as host signals that can be recognized by Orobanche.

Furthermore, based on previous studies, a mutation in the *LGS1* (*LOW GERMINATION STIMULANT 1*) gene leads to the reduction in Striga germination stimulant activity (Figure 3). This low-stimulant phenotype is commonly found in sorghum plants that are resistant to the root parasitic plant, Striga spp (Gomez-Roldan et al., 2008; Umehara et al., 2008). Gobena et al. discovered that the LGS1 gene codes for a sulfotransferase. Loss-of-function of the gene changes the relative abundance of different types of SLs in sorghum root exudates. Originally, the dominant SL in root exudates is 5-deoxystrigol, which is a highly active Striga germination stimulant (Figure 3, left-hand side). On the other hand, an SL with the opposite stereochemistry to 5-deoxystrigol is orobanchol, which does not stimulate germination of Striga (Figure 3, right-hand side). The mutation at *LGS1* changes the dominant SL in sorghum root exudates from 5-deoxystrigol to orobanchol and leads to low Striga germination rates, which makes these hosts less likely to be parasitized by these root parasitic plants (Gobena et al., 2017).

Other than simply avoiding induction of parasite seed germination, some hosts have evolved to secrete toxic compounds to prevent seed germination or seedling development (Serghini et al., 2001; Echevarría-Zomeño et al., 2006). For example, the germination rate of *O. cernua* seeds in the presence of resistant sunflower plants was 50% lower than that in the presence

of susceptible sunflowers (Figure 4). Moreover, the germinated *O. cernua* seeds next to resistant sunflower had browning symptoms and stunted growth, or died (Serghini et al., 2001). Serghini and coworkers discovered that the resistant sunflower varieties produced 7-hydroxylated simple coumarins, which are defensive secondary metabolites and created a toxic environment for *O. cernua* (Figure 4) *(Serghini et al., 2001).*

Besides reducing germination, reducing haustorium initiation is another approach seen in pre-attachment resistance. Many studies indicate that haustorium initiation requires the induction of host-derived haustorium inducing factors (HIFs) in root parasitic plants (Chang and Lynn, 1986; Riopel and Timko, 1995; Albrecht et al., 1999). An excellent review on HIFs that induce prehaustorium formation in the Orobanchaceae family was recently published (Goyet et al., 2019). Therefore, here we focus on reviewing the reports on pre-attachment resistance mechanisms that interfere with the function of HIFs.

Reducing haustorium induction has been observed as one striga-resistance mechanism. Some specific wild accessions of sorghums (*Sorghum bicolor*) have a low capacity to induce *Striga asiatica* haustorium initiation (Rich et al., 2004). The detailed mechanism is currently unknown, but research proposes the possibility that host roots can exude inhibitors of haustorial induction, like auxins, to suppress haustorium initiation (Keyes et al., 2000). Furthermore, several studies indicated that using various inhibitors to interfere with ROS formation, ethylene signaling (Cui et al., 2020), auxin efflux and activity (Ishida et al., 2016), and Ca^{2+} signaling reduced the number of haustoria. These results indicate that the HIF triggered signaling pathways are vital during the haustorium initiation process, and repressing these signaling pathways can reduce haustoria formation. Whether the host plant can also deploy this

strategy and secret similar inhibitors as an approach for pre-attachment resistance remains to be elucidated.

ii. Post-attachment resistance

In comparison to pre-attachment resistance, more studies have been conducted on post-attachment resistance to parasitic plants. Many of them indicate similarity to plant-pathogen defense mechanisms, which are triggered after sensing the invaders. These resistance mechanisms include hormone signaling, hypersensitive responses, cell wall reinforcement, and defensive secondary metabolites accumulation. Below we summarize the latest research on different aspects of post-attachment resistance.

a. Hypersensitive response

Hypersensitive response (HR), leading to localized cell death and necrosis at the infection site, is a common mechanism that is used to defend against pathogens and prevent infection from spreading (Balint-Kurti, 2019). Similar phenomena and mechanisms have also been observed in host resistance responses that interfere with the haustorium penetration process of both stem and root parasites (Swarbrick et al., 2008; Runyon et al., 2010).

For stem parasitic plants, several studies have shown that hosts deploy HR to *Cuscuta* species. For example, as mentioned in the parasite perception section of this article, cultivated tomato (*S. lycopersicum*) is resistant to *Cuscuta reflexa* via CuRe1-mediated hypersensitive response (Figure 1) (Hegenauer et al., 2016; Hegenauer et al., 2020). Several previous reports also indicate that hypersensitive response in tomato is elicited upon *C. pentagona (Runyon et al., 2010) and C. campestris (Jhu et al., 2020)* infestation. These *Cuscuta*-induced

hypersensitive responses are located explicitly at the haustorial attachment site and interfere with establishing successful host-parasite vascular connections.

Similarly, hypersensitive responses specifically located at the haustorial attachment site are also triggered by various root-parasitic plant infestations in different host systems. For example, cowpea with RSG3-301 is resistant to *S. gesnerioides* races 3 and 4 (Li and Timko, 2009). Upon perceiving an unknown parasite signal or Avr, RSG-301 then triggers downstream signaling cascades and activated VuPOB1, which is a positive regulator of hypersensitive response (Figure 2, the lower panel) (Su et al., 2020). A similar case is reported in sunflower-*O. cumana* interactions. Sunflower recognizes AVROR7 from *O. cumana* via HAOR7, which then activates signaling cascades and induces a following hypersensitive response (Figure 2, the upper panel) (Duriez et al., 2019). Additionally, a rice cultivar, Nipponbare, showed strong post-attachment resistance to *Striga hermonthica* (*S. hermonthica*). HR-related genes were upregulated in Nipponbare upon *S. hermonthica* attack indicating that HR also plays a role in this defense mechanism (Swarbrick et al., 2008). In summary, in the host-parasitic plant coevolution process, some hosts have evolved to acquire the ability to detect parasitic plant-specific signals or effectors using a range of receptors. Perceiving the attack from parasites initiates signal transduction cascades and often leads to a hypersensitive response.

b. Hormone signaling

Phytohormone signaling pathways, especially jasmonic acid (JA) and salicylic acid (SA) signaling, also play an important role in resistance responses. Genes that are involved in the JA biosynthesis pathway are reported to be induced in the early stage of parasitic plant infestations. For example, infestation by *O. cumana* induced the expression of a gene that encodes a lipoxygenase (*LOX*), an enzyme that oxidizes linolenic acid and produces a potential precursor of

JA, in sunflower roots (Letousey et al., 2007; Hiraoka et al., 2008). Similarly, the infestation by *Orobanche crenata* induced the JA pathway in *Medicago truncatula* roots (DITA et al., 2009) and the infestation by *Striga hermonthica* also induced the expression of JA biosynthesis genes, *ALLENE OXIDE CYCLASE* (*OsAOC*) and *ALLENE OXIDE SYNTHASE2* (*OsAOS2*), in rice (Mutuku et al., 2015). Similar phenomena have also been observed in the interaction between host and stem parasitic plants. For instance, the total amount of JA increased dramatically in tomatoes between 24 and 36 hours after *C. pentagona* haustorium attachment (RUNYON et al., 2010). JA-insensitive tomato plants (*jai1*) seem to be more vulnerable to *C. pentagona*, and parasitic plants grown on *jai1* had more biomass than those grown on wild-type tomato (RUNYON et al., 2010). Furthermore, JA has been shown to be involved in cell wall damage-induced lignin biosynthesis (Denness et al., 2011) and HR responses (Runyon et al., 2010). Mutant rice plants with JA biosynthesis deficiency have severe *S. hermonthica* susceptibility and the application of JA can recover their resistance ability (Mutuku et al., 2015). All of these results indicate that JA plays a vital role in host resistance responses against parasitic plants.

SA is another key phytohormone that is required for plant innate immunity against many pathogens and biotic stresses (Ding and Ding, 2020). Based on several previous studies, induction of the SA pathway has also been detected after JA pathway activation (Letousey et al., 2007; RUNYON et al., 2010; Mutuku et al., 2015), and this induction might also be an essential component of defense responses toward parasitic plants. For example, Runyon et al. observed that the maximum induction of JA in tomatoes is 36 hours after *C. pentagona* haustorium attachment, followed by the maximum total amount of SA at 48 hours post-attachment (RUNYON et al., 2010). However, SA-deficient transgenic tomato plants (*NahG*) cannot accumulate SA in response to *C. pentagona* infestation. This is because *NahG* plants produce salicylate hydroxylase, converting SA

immediately to inactive catechol. As a result, *NahG* tomato plants cannot trigger hypersensitive responses and are more susceptible to *C. pentagona* parasitism (RUNYON et al., 2010). On the other hand, SA-deficient *NahG* rice plants were more resistant to *S. hermonthica* (Mutuku et al., 2015). The antagonistic interactions between the SA and JA signaling pathways might be why repression of SA accumulation results in enhanced resistance (Phuong et al., 2020). These results not only show that the balance between JA and SA signaling pathways plays a vital role in the resistance mechanism but also indicate that different host plants might deploy divergent strategies to defend against parasitic plants.

Besides JA and SA, abscisic acid (ABA) is also known as a major phytohormone regulating stress responses. Many studies on model organisms reported that the ABA signaling pathway has crosstalk with the JA and SA signaling pathways to control the balance between biotic and abiotic stress responses (Ku et al., 2018; Berens et al., 2019). Interestingly, several reports indicate that the ABA pathway is involved in the host-parasitic plant interaction, suggesting that ABA might play a role in host resistance against parasitic plants. For example, the infestation of root parasitic plant *Phelipanche ramosa*, branched broomrape, induced increase in ABA levels in both leaves and roots of their tomato host plants (Cheng et al., 2017). The infestation of the root parasitic plant witchweed (*Striga hermonthica*) causes a dramatic increase in ABA concentrations in maize leaves (Taylor et al., 1996). ABA-responsive and biosynthesis genes also have increased expression levels during the early stage of *P. ramosa* infestation (Torres-Vera et al., 2016). With proteomic approaches, the increased production of ABA-responsive proteins was detected only in the resistant, and not susceptible, pea (*Pisum sativum*) cultivar in response to crenate broomrape (*Orobanche crenata*) attacks, which indicates the potential key role of ABA signaling on post-attachment resistance (Ángeles Castillejo et al., 2004). Similar responses were also observed in

the interaction between tomato and the stem parasitic plant *C. pentagona*. The induction of ABA started at 36 hours after *C. pentagona* infestation and continued to accumulate through 120 hours (RUNYON et al., 2010).

In all these cases, the most likely hypothesis to explain this phenomenon is that activation of the ABA signaling pathway is in response to the loss of water experienced by the host due to parasitic plant attachment (Taylor et al., 1996; Cheng et al., 2017). Host plants might use the ABA pathway as a defense strategy to prevent further water losses (Ángeles Castillejo et al., 2004; Cheng et al., 2017). However, some parasitic plants have evolved to overcome this host response and can still continue to obtain water from their hosts. Several studies indicate that parasitic plants accumulate an extremely high level of ABA, even higher than the elevated level in their hosts (Ihl et al., 1987; Taylor et al., 1996; Jiang et al., 2010). For example, the root hemiparasitic plant *Rhinanthus minor* increased ABA biosynthesis dramatically upon attaching to their hosts (Jiang et al., 2010). Several species in the Orobanchaceae family, including *Orobanche hederae* (ivy broomrape), *Lathraea squamaria* (common toothwort), *Melampyrum pratense* (common cow-wheat), also accumulated a high amount of ABA in their sink tissues (Ihl et al., 1987). The exact function of high ABA levels in parasites remains unknown. These phenomena might be a side effect of extremely negative osmotic potentials in parasitic plants. Many parasitic plants are found to produce and accumulate large amounts of mannitol (Jiang et al., 2005) in order to generate very low water potential in the cell sap and force water to flow continuously from the hosts to the parasites.

Ethylene is also known to play a vital role in activating plant defenses against various biotic stress and regulating local and systemic immune responses (Adie et al., 2007; Liu et al., 2013; Tintor et al., 2013; Böhm et al., 2014). Many previous studies also indicate that ethylene has

complex crosstalk with other hormone pathways, including JA, SA, and ABA (Lorenzo et al., 2003; Veselov et al., 2003; Zhao et al., 2004). In the interaction between host and parasitic plants, the production of ethylene has been observed, which suggests ethylene may also play a role in the host defense responses. For example, infestation by *O. ramosa* seedlings induced the expression of the *acc2* gene, which encodes for the aminocyclopropane-1-carboxylic acid (ACC) synthase in *A. thaliana* roots (Dos Santos et al., 2003), suggesting that ethylene biosynthesis was activated. Furthermore, an ethylene-responsive element binding factor, the *AtERF6* gene, was also upregulated in *A. thaliana* upon *O. ramose* infestation (Vieira Dos Santos et al., 2003). Similarly, infestation by *Cuscuta reflexa* induced the emission of ethylene in *N. benthamiana* and *S. lycopersicum (Hegenauer et al., 2016; Hegenauer et al., 2020).* This ethylene induction is CuRe1-dependent and an indicator that the defense response was successfully triggered (Hegenauer et al., 2016; Hegenauer et al., 2020).

Intriguingly, parasitic plants seem to have evolved to also use ethylene as a signal for haustorium penetration and host recognition. Cui et al. found that ethylene signaling is required for the haustorium penetration process in the root parasitic plant *Phtheirospermum japonicum*, and the disruption of host ethylene production can interfere with *P. japonicum* invasion (Cui et al., 2020). Goldwasser et al. also reported that perturbed ethylene pathways in *Arabidopsis* interfere with haustorium formation in the root parasitic plant *Triphysaria versicolor* (Goldwasser et al., 2002; Kokla and Melnyk, 2018). All these examples indicate that parasitic plants utilize this common stress-triggered defense hormone to help with the parasitism process.

c. Cell wall modification

Modifying cell wall composition to reinforce the physical boundary is a resistance mechanism against parasitic plants reported in many host species. Among different types of cell wall modification, lignin deposition is one of the most common methods deployed by many resistant host species (PÉRez-De-Luque et al., 2005; Pérez-de-Luque et al., 2007; Pérez-de-Luque et al., 2008; Huang et al., 2012; Yang et al., 2017; Mutuku et al., 2019). Previous reports used anatomical observation to show lignified endodermal cells in resistant vetch (*Vicia* spp.) and faba bean (*Vicia faba*) in response to attack by the root parasite, bean broomrape (*Orobanche crenata*) (PÉRez-De-Luque et al., 2005; Pérez-de-Luque et al., 2007). Notably, based on observations with phloroglucinol–HCl staining, lignin accumulation was distributed locally and only in the endodermal cells that were in contact with a haustorium. This physical boundary blocks *O. crenata* penetration and leads to aborted haustorial connections (PÉRez-De-Luque et al., 2005; Pérez-de-Luque et al., 2007). This result indicates that the lignin-based resistance is precisely regulated and locally expressed.

Similarly, increased lignin content was measured in sunflower (*Helianthus annuus*) resistant cultivars after sunflower broomrape (*Orobanche cumana*) inoculation. Yang et al. also showed that the enzymes involved in lignin biosynthesis, including cinnamyl alcohol dehydrogenase (CAD), ferulate-5-hydroxylase (F5H), and peroxidases, were highly accumulated in these resistant sunflower cultivars (Yang et al., 2017). Likewise, with genetic analysis, induced expression levels of lignin biosynthesis enzyme genes were also observed in *Striga*-resistant rice (*Oryza sativa*) cultivars upon *S. hermonthica* infection and *Striga*-resistant cowpea (*Vigna unguiculata*) cultivars upon *Striga gesnerioides* infection (Huang et al., 2012). With pyrolysis gas chromatography/mass spectrometry (pyrolysis-GCMS), Mutuku et al. further quantified the composition of *p*-hydroxyphenyl- (H), guaiacyl- (G), and syringyl- (S) types of monolignols in

accumulated lignins. Changing the balance and percentage of these lignin monomers by regulating key enzyme-encoding genes makes resistant cultivars susceptible to *S. hermonthica* infection (Mutuku et al., 2019). Their results indicate that specific lignin composition plays a role in cell wall structural integrity and influences host plant defense responses.

Similar resistance responses also have been observed in the interaction between the stem parasite *C. campestris* and tomato. Although cultivated tomatoes are generally susceptible to *C. campestris,* some specific Heinz tomato cultivars are resistant to *C. campestris* (Hembree et al., 1999; Yaakov et al., 2001; Jhu et al., 2020). These resistant tomatoes accumulate a large amount of lignin at the stem cortex, forming a physical barrier that prevents haustorium penetration (Jhu et al., 2020). The genes that are involved in lignin biosynthesis were upregulated in these resistant tomato cultivars upon *C. campestris* infestation, including 4-coumarate CoA ligase (4CL), caffeoyl-CoA *O*-methyltransferase (CCoAOMT), cinnamoyl-CoA reductase (CCR), and laccases (LACs) (Jhu et al., 2020). In summary, these tomato cultivars block the penetration of *C. campestris* haustoria by strengthening their cell wall.

Some of the upstream regulators of this lignin-based resistance response in tomatoes have also been identified. *CuRLR1* is a crucial factor that might function in perceiving the signal from *C. campestris* and conferring host resistance by regulating lignification (Figure 1) (Jhu et al., 2020). *LIF1* (*Lignin Induction Factor 1*, an *AP2*-like transcription factor) and *SlMYB55* are found to be critical positive regulators of lignin biosynthesis (Figure 1). On the other hand, *SlWRKY16* acts as a negative regulator of the lignin-based resistance response and counteracts *LIF1* (Figure 1) (Jhu et al., 2020). In addition, *SlWRKY16* also has a similar gene expression pattern as *CuRe1*, which encode the receptor trigger HR upon sensing *Cuscuta* factors (Figure 1) (Hegenauer et al., 2020; Jhu et al., 2020). This suggests a potential regulatory connection

between different defense mechanisms. Multilayered defense mechanisms against parasitic plants would be of interest for future studies.

Besides lignification, cell wall structural protein cross-linking, callose deposition, and suberization are also reported as defense mechanisms (Echevarría-Zomeño et al., 2006; Pérez-de-Luque et al., 2006; Pérez-de-Luque et al., 2007). Pérez-de-Luque et al. discovered that resistant pea (*Pisum sativum*) plants increased H_2O_2 and peroxidase activity to catalyze oxidative cross-linking of structural proteins. The cross-linking of cell wall structural proteins in the host cortex halted the penetration of *O. crenata* intrusive cells (Pérez-de-Luque et al., 2006). In both resistant faba bean and pea plants, callose accumulation to reinforce cell walls and hamper *O. crenata* penetration was also observed (Pérez-de-Luque et al., 2006; Pérez-de-Luque et al., 2007). Cross-linked cell wall proteins were also detected in resistant sunflower plants in response to sunflower broomrape (*Orobanche cumana*) (Echevarría-Zomeño et al., 2006). Furthermore, in these resistant sunflower cultivars, the cell wall in contact with *O. cumana* was additionally thickened by depositing suberin, preventing haustorium penetration and stopping the parasite from reaching the endodermis (Echevarría-Zomeño et al., 2006). These findings inform us that resistant host plants often deploy various combinations of cell wall reinforcement strategies to establish multilayer defense mechanisms and ensure adequate protection.

d. Secondary metabolites

The accumulation of defensive secondary metabolites is an effective plant defense and competition strategy for deterring herbivores (Olson and Roseland, 1991) and fungal pathogens (Prats et al., 2003; Castillejo et al., 2010) and for allelopathy (Hierro and Callaway, 2003). Previous studies also show that resistant host plants deploy toxic metabolites to defend against the infestation of parasitic weeds (Serghini et al., 2001; PÉREZ-DE-LUQUE et al., 2005; Echevarría-

Zomeño et al., 2006). For example, a higher amount of bound phenolics and free phenolics is detected in resistant vetches (*Vicia atropurpurea*) upon *Orobanche aegyptiaca* attack (Goldwasser et al., 1999). The infestation of broomrape (*O. cernua*) also induced the content of total soluble phenolic compounds in some pea (*Pisum* spp.) genotypes (PÉREZ-DE-LUQUE et al., 2005). These soluble phenolics could serve as precursors of lignin biosynthesis and be phytoalexins, which are toxic for penetrating haustoria (PÉREZ-DE-LUQUE et al., 2005).

Similarly, excreting and locally accumulating toxic compounds, 7-hydroxylated simple coumarins, including scopoletin and ayapin, were observed in sunflower (*H. annuus*) resistant cultivars in response to *O. cernua* parasitism (Figure 4). These sunflower coumarins not only function as allelochemicals by averting *O. cernua* seed germination or killing germinated seedlings (pre-attachment resistance), but also act as phytoalexins by preventing haustorial penetration and the formation of vascular connection (post-attachment resistance) (Figure 4) (Serghini et al., 2001). Furthermore, Echevarría-Zomeño et al. found that the penetration of *O. cumana* haustoria is followed by the local excretion of sunflower phytoalexins into the apoplast. This response is triggered explicitly at the attachment sites, especially in the host cells that are immediately surrounding parasitic plant intrusive cells, to halt the penetration process (Figure 4).

iii. Non-host resistance

Other than developing different pre-attachment and post-attachment mechanisms to defend against parasitic plants, some host plants seem to be simply incompatible with the parasites. This incompatibility is also known as non-host resistance, which might result from parasitic plants not having adapted to these specific host plants. While *C. campestris* is native to the US and has likely co-evolved with the various crop and non-crop hosts, *C. reflexa* is native to Asia, and not usually

seen in fields in the US. Therefore, domesticated tomatoes may have non-host resistance to *C. reflexa*.

Similar examples have also been observed in the interaction between hosts and root parasitic plants. *S. gesnerioides* can parasitize many eudicots, but *S. hermonthica* and *S. asiatica* are unable to parasitize dicots (Ohlson and Timko, 2020). Arabidopsis is resistant to *S. hermonthica* , which is also likely to be an example of non-host resistance. Interesting instances of attachment and penetration but failure to successfully parasitize is seen in the interaction between *S. hermonthica* and Arabidopsis , and *Orobanche minor* and *Lotus japonicus* (Kubo et al., 2008).

While holding a lot of promise for the development of durable resistance, non-host resistance mechanisms are yet to be fully elucidated (Lee et al., 2017). Non-host resistance interactions between the hemiparasitic *Rhinanthus minor* and two forb species *Leucanthemum vulgare* and *Plantago lanceolata* showed encapsulation and lignification at the interface between the parasite and host (CAMERON et al., 2006). A similar encapsulation reaction is reported in the interaction between the holoparasitic *Orobanche ramosa* and its non-host maize (Zehhar et al., 2003). It is likely that this encapsulation barrier prevents the parasite from accessing the host vascular system. Research on detailed mechanisms of non-host interactions is of interest for future research. Understanding the molecular basis for these non-host interactions could lead to better parasitic plant control strategies.

IV. A new definition of stem and root parasites: Cross-organ parasitism

Interestingly, in the process of reviewing the current knowledge of post-attachment defense responses, we noticed that several similar mechanisms have been observed in both roots and stems

and utilized to resist against root and stem parasitic plants, respectively. However, the exact details of the mechanisms utilized are not the same between the above-ground and below-ground organs in host plants. These observations indicate that some types of defense mechanisms might be organ- or tissue-specific and might arise due to morphological and anatomical differences between the various host plant organs.

Descriptions of parasitic plants traditionally have been based on where the haustorial connections are formed on the host, and divided parasitic plants into stem or root parasites. However, more non-conventional haustorial connections have been reported but not systematically reviewed. For example, several previous studies and our recent observations indicate that stem parasites, like *Cuscuta* spp., can attach to not only stems but also other organs of their host plants and form successful vascular connections (Dean, 1938; Vurro et al., 2011; Kaga et al., 2020). Here, we named these non-conventional haustorial connections as cross-organ parasitism. Cross-organ parasitism has not been well investigated, but these discoveries might bring a new aspect to parasitic plant classification and control strategies.

i. Discovery of cross-organ parasitism

Cuscuta spp. are generally categorized as stem parasitic plants (Figure 5A). However, several previous reports showed that *Cuscuta campestris* could form attachment on carrot leaf petioles and *Arabidopsis thaliana* rosette leaves (Kaga et al., 2020). Notably, vascular connections between the host and the parasite were clearly shown on haustorium transverse sections in both reported cases. We also have observed that *C. campestris* haustoria can attach on and penetrate the petiole of a wild tomato *Solanum galapagense* (Figure 5B). Surprisingly, we also discovered that *C. campestris* can form haustorial connections with tomato seedling roots in our *in vitro*

haustorium system (Jhu et al., 2021) and the vascular connections were readily visible (Figure 5C, D). This discovery shows that *Cuscuta* spp. have the ability to parasitize different organs of their hosts, likely due to the ability to adjust their strategies depending on what host tissue types they encounter during the haustorium penetration process. Incidentally, several previous studies have reported various *in vitro* haustorium systems. *C. campestris* and *C. japonica* can form haustorium like structures on their stems in the absence of a host and in response to far red light or blue light and physical contact (Tada et al., 1996; Kaga et al., 2020; Jhu et al., 2021). Therefore, *Cuscuta* may represent a more permissive system for haustorium formation and thus readily allows cross-organ parasitism.

ii. Organ-specific defense responses

The discovery of cross-organ parasitism also raises the question of whether our current understanding of parasitic plant resistance can also be applied to these non-conventional examples of cross-organ parasitism. Intriguingly, based on our *in vitro* system, Heinz 9553 tomato cultivars that are resistant to *C. campestris* attacks on their stems are susceptible to *C. campestris* in their root system (Figure 6). The infestation of *C. campestris* triggers the cell wall modification type of post-attachment resistance response in the stem of H9553 tomato. A thick layer of lignin was accumulated at the stem cortex region to serve as a physical boundary preventing *C. campestris* haustorium penetration (Figure 6, upper panel). However, this post-attachment resistance response was not triggered in the root of H9553 tomato. Therefore, *C. campestris* haustoria were able to penetrate successfully and establish vascular connections with host roots (Figure 6, lower panel). Most studies on parasitic plant resistance have not investigated whether the described resistance mechanisms also occur in other host plant organs. Understanding if similar defense responses have been utilized in both above-ground and under-ground plant

organs could provide a novel perspective on host defense responses and generate new strategies to develop crops resistant to both stem and root parasites.

V. Conclusion and future perspectives

With the world population growing to 8 billion, food security has become a top concern worldwide, intensifying the urgency to radically innovate methods to reduce agricultural loss due to biotic stresses, especially diseases or parasites that are hard to eliminate using traditional methods. Currently, growing crops is hampered by parasitic plant infestations in many countries that already face food shortages. Investigating the mechanisms by which host and parasite perceive each other and existing mechanisms mounted by hosts to resist parasitic plants will aid in developing parasitic plant-resistant crops and should be one of the top priorities in setting parasitic plant future research directions. In addition, understanding whether similar defense responses have been utilized by some host plants to resist both major organ parasitism and cross-organ parasitism could provide new insights into host-parasite interactions. This knowledge might create new potential strategies to develop crops that are resistant to both stem and root parasites and provides a new path forward to introduce resistance into important crops leading to more sustainable crop production and global food security.

VI. Figures

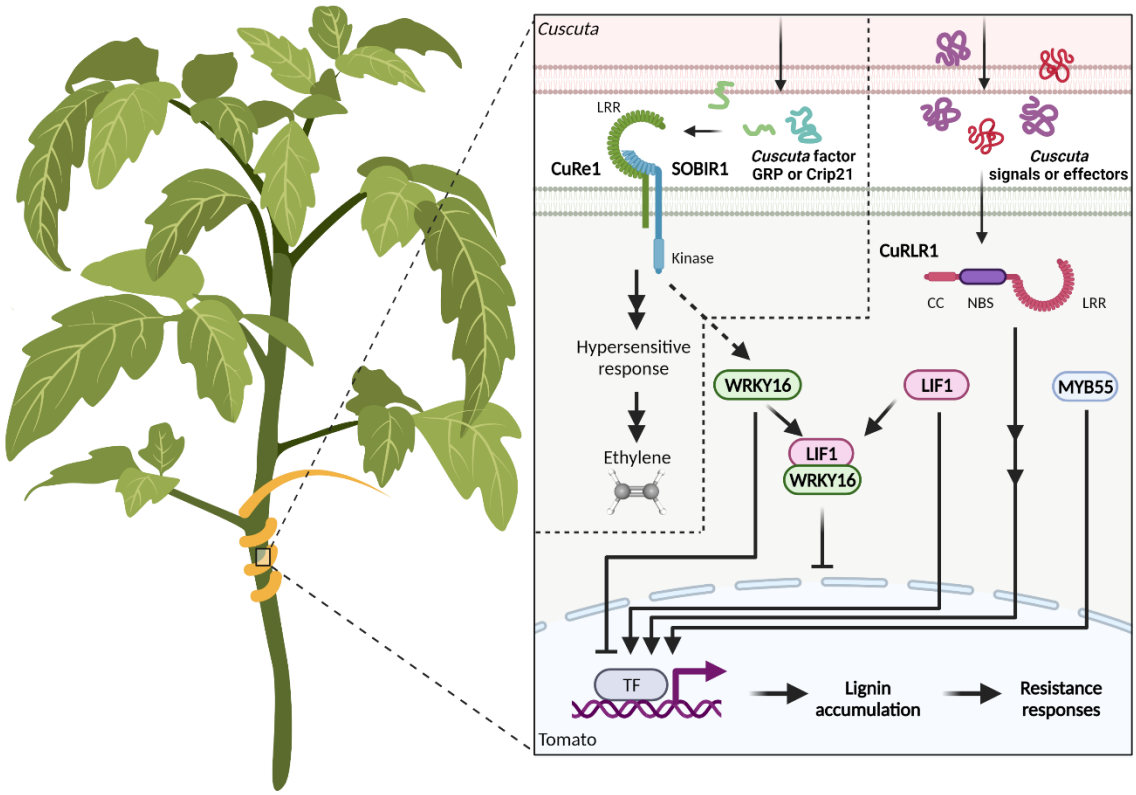

Figure 1. Summary of perception and resistance mechanisms against stem parasitic *Cuscuta* species in tomato host. The left-hand side of the dash line depicts the perception and resistance mechanisms described for *Cuscuta reflexa* in cultivated tomato *Solanum lycopersicum.* CuRe1 is a leucine-rich repeat receptor-like protein (LRR-RLP). This cell surface receptor-like protein perceives an 11 kDa *Cuscuta* factor, a glycine-rich protein (GRP), or its minimal peptide epitope Crip21 secreted by *C. reflexa*. With helps from the co-receptor SlSOBIR1, this recognition process then triggers the CuRe1-dependent resistance responses, including hypersensitive responses (HRs), releasing reactive oxygen (ROS) species, and increased ethylene synthesis. The right-hand side of the dash line shows the perception and resistance mechanisms described for *Cuscuta campestris* in cultivated tomato *S. lycopersicum.* Cuscuta R-gene for Lignin-based Resistance 1 (CuRLR1) is an N-terminal coiled-coil nucleotide-binding site leucine-rich repeat protein (CC-NBS-LRR) in

specific resistant Heinz tomato cultivars. CuRLR1 may be engaged in sensing signaling pathways or function as a receptor for perceiving unknown *C. campestris* signals or effectors. Activation of CuRLR1 starts downstream signaling cascades and induces genes involved in the lignin biosynthesis pathway. This response then triggers lignin accumulation in the tomato stem cortex region, which function as a physical boundary to prevent haustorium penetration. LIF1 (Lignin Induction Factor 1, an AP2-like transcription factor) and SlMYB55 are crucial positive regulators conferring host lignin-based resistance. SlWRKY16 is upregulated upon *C. campestris* infestation and acts as a negative regulator of lignin production and LIF1 function. SlWRKY16 is hypothesized to connect CuRe1 (dashed arrow) to the lignification response. 3D structure image of ethylene is from PubChem (National Center for Biotechnology Information, 2021).

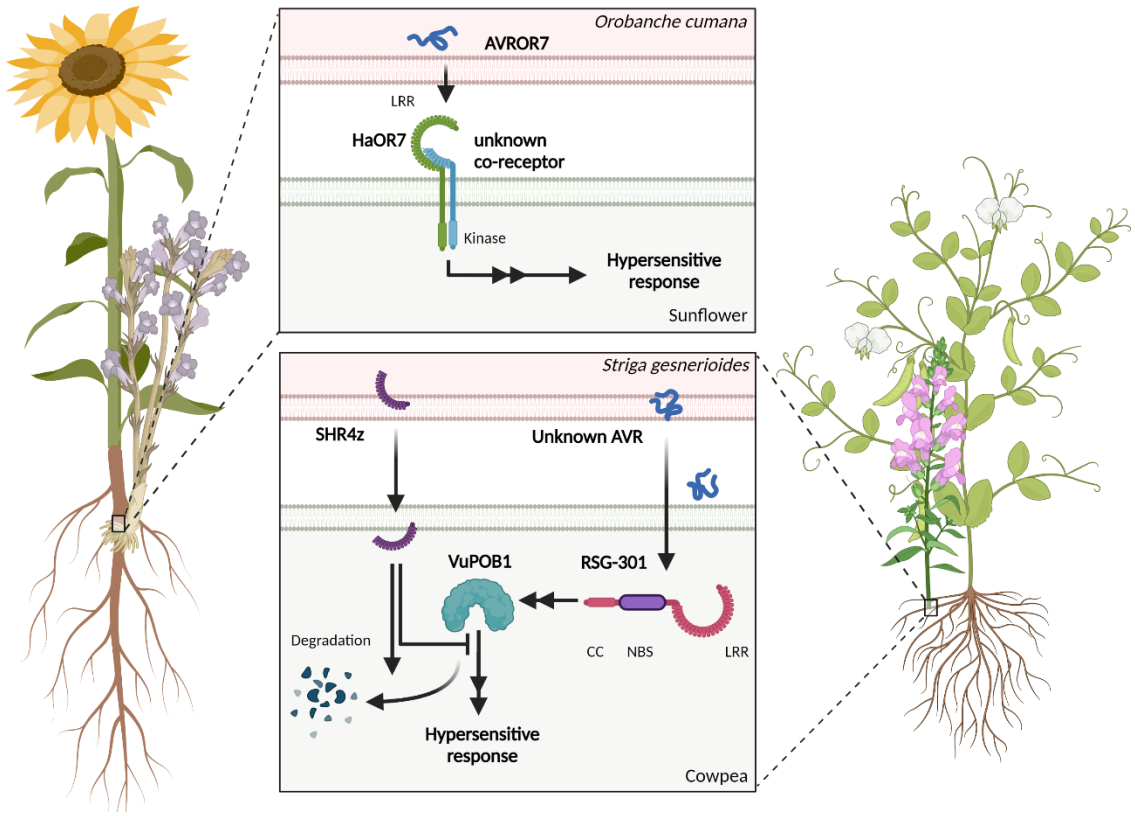

Figure 2. Summary of perception and resistance mechanisms against root parasitic plants *Orobanche cumana* and *Striga gesnerioides* in sunflower and cowpea respectively. The upper panel depicts the perception and resistance mechanisms to *Orobanche cumana* in sunflower *Helianthus annus*. HaOR7 is a membrane-bound leucine-rich repeat (LRR) receptor-like kinase, which recognizes an avirulence protein (AVROR7) from *O. cumana* using the LRR domain. Perceiving AVROR7 with the help of an unknown co-receptor enables signal transduction through the kinase domain of HAOR7. This recognition process then triggers downstream hypersensitive responses and prevents the haustorial connection of *O. cumana* to the sunflower root vascular system. The lower panel shows the perception and resistance mechanisms to *S. gesnerioides* in cowpea *Vigna unguiculata*. RSG3-301 is a CC-NBS-LRR protein. Upon perceiving an unknown parasite signal or AVR protein from *S. gesnerioides*, RSG-301 starts downstream signaling cascades and activates a BTB-BACK domain-containing ubiquitin E3 ligase

VuPOB1, which is a positive regulator of the hypersensitive response. This triggers hypersensitive response and necrosis upon *S. gesnerioides* infestation and confers post-attachment resistance in cowpea. However, the *S. gesnerioides race 4z* can overcome *RSG3-301*-mediated resistance by secreting *a* small effector, Suppressor of Host Resistance 4z (SHR4z). When SHR4z enters the host cell, it can interact with VuPOB1 and inhibit its function by promoting the turnover rate of VuPOB1. Thus, SHR4z-triggered VuPOB1 degradation leads to reduced hypersensitive response and makes the resistant cultivar B301 susceptible to *S. gesnerioides race 4z.*

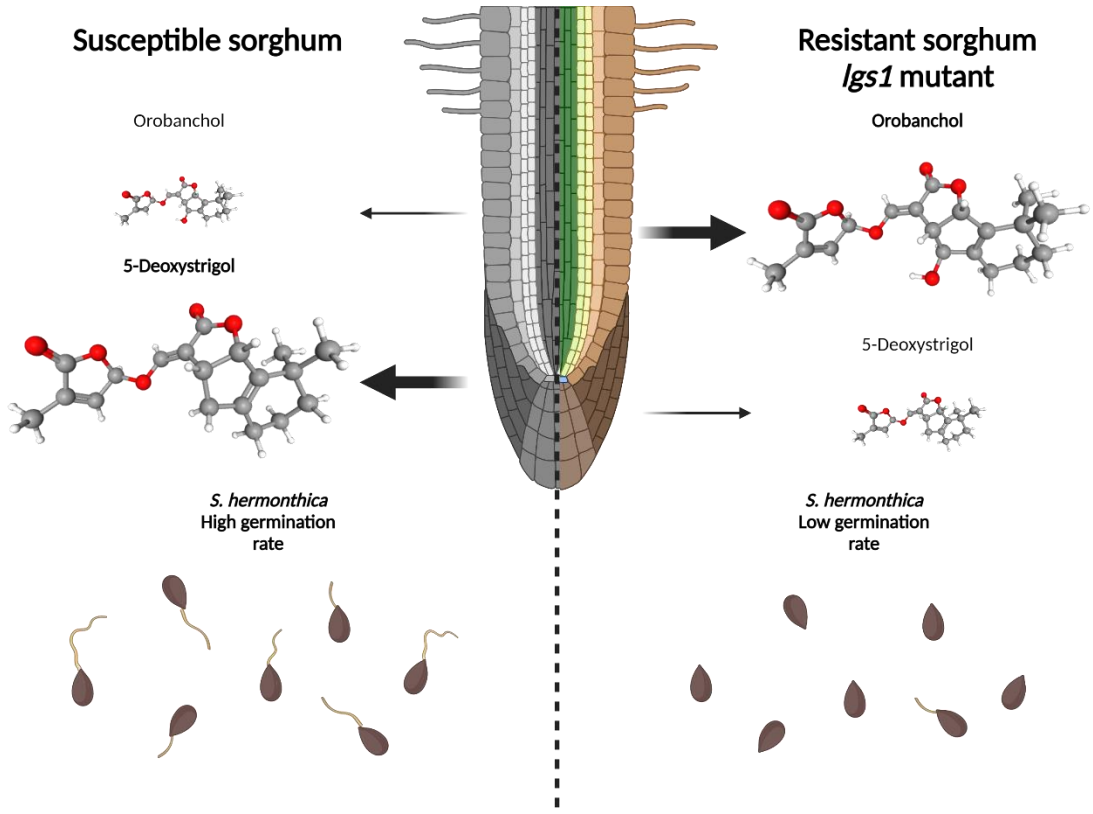

Figure 3. Summary of pre-attachment resistance in sorghum by reducing *Striga hermonthica* germination. The *LGS1* (*LOW GERMINATION STIMULANT 1*) gene codes a sulfotransferase. In susceptible sorghum plants, the dominant SL in root exudates is 5-deoxystrigol, a highly active Striga germination stimulant. However, an SL with the opposite stereochemistry of 5-deoxystrigol is orobanchol, which does not stimulate germination of Striga. A mutation at *LGS1* changes the dominant SL in sorghum root exudates from 5-deoxystrigol to orobanchol, leading to low Striga germination rates. This composition change makes these sorghum hosts less likely to be parasitized by *S. hermonthica* and leads to pre-attachment resistance. 3D structure images of Orobanchol (National Center for Biotechnology Information, 2021) and 5-Deoxystrigol (National Center for Biotechnology Information, 2021) are from PubChem.

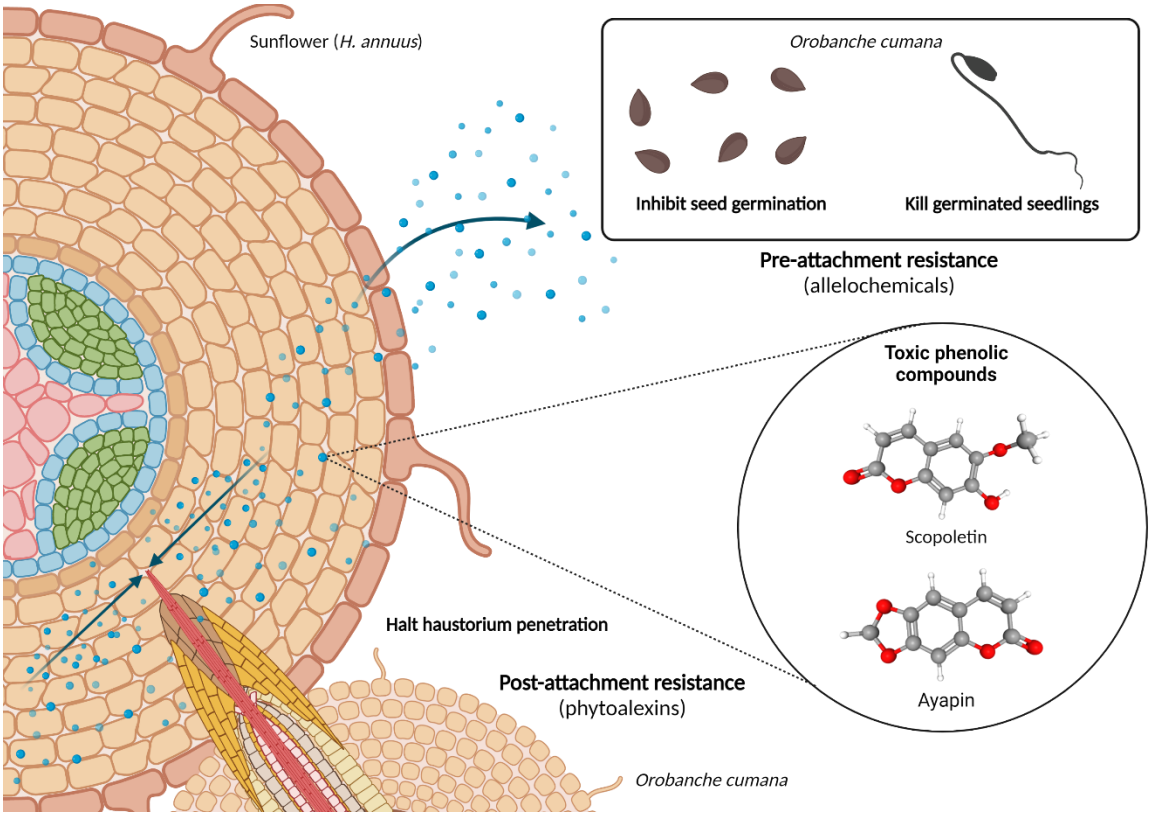

Figure 4. The functions of defensive soluble phenolic compounds in pre-attachment resistance and post-attachment resistance. Sunflower (*H. annuus*) resistant cultivars excrete and accumulate toxic **phenolic** compounds, 7-hydroxylated simple coumarins, including scopoletin and ayapin, upon *O. cernua* parasitism. These sunflower coumarins function as allelochemicals by averting *O. cernua* seed germination or killing germinated seedlings (pre-attachment resistance, upper panel of the figure), and act as phytoalexins by preventing haustorial penetration and the formation of vascular connection (post-attachment resistance, lower panel of the figure). 3D structure images of ayapin (National Center for Biotechnology Information, 2021) and scopoletin (National Center for Biotechnology Information, 2021) are from PubChem.

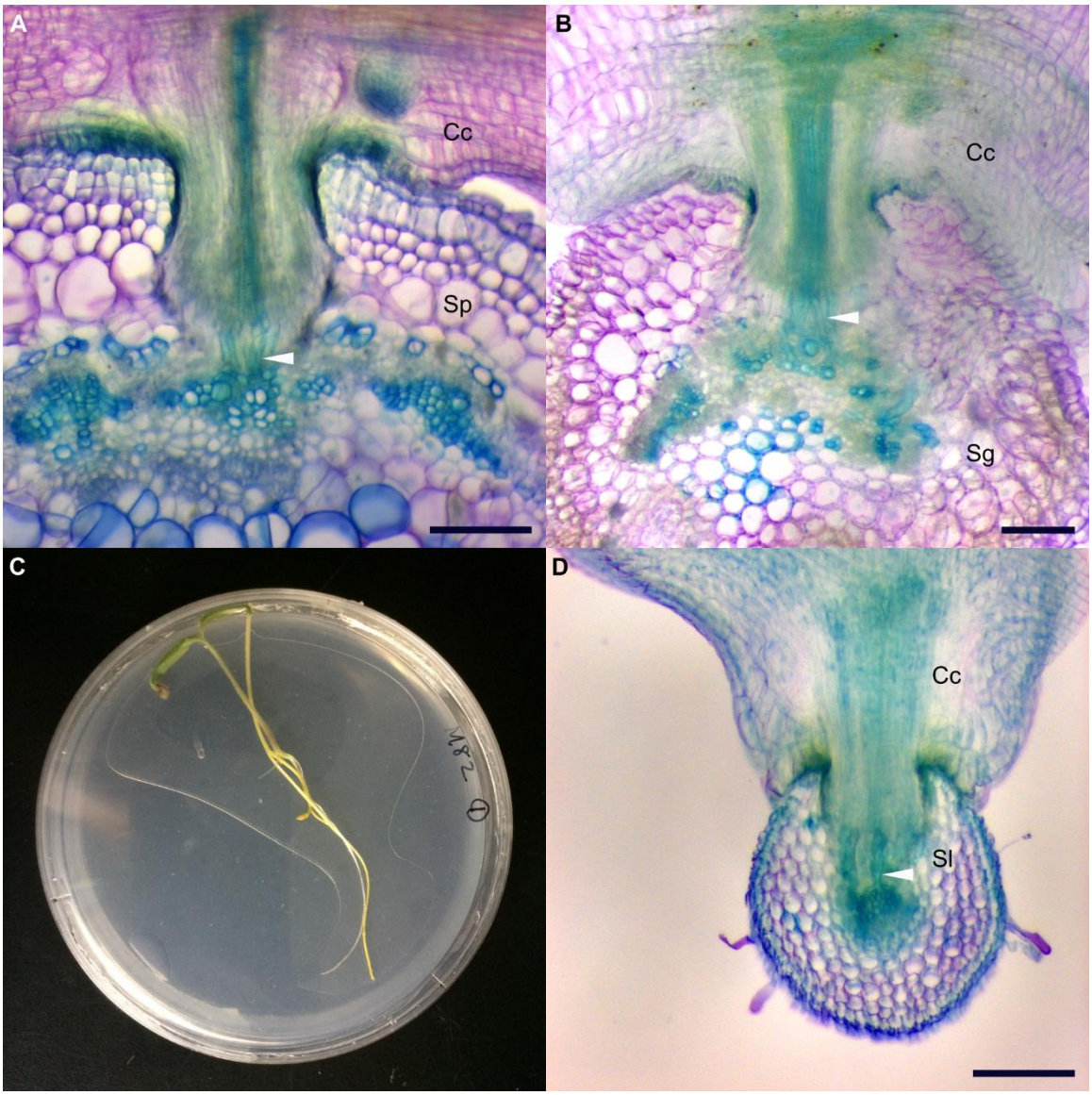

Figure 5. *Cuscuta campestris* haustorial connections with various host organs. (A) A 100 µm thick fresh vibratome section of *C. campestris (Cc)* haustorium parasitizing the stem of a wild tomato *Solanum pennellii (Sp)*. (B) A 100 µm thick fresh vibratome section of *C. campestris (Cc)* haustorium parasitizing the petiole of a wild tomato *Solanum galapagense (Sg)*. (C) An *in vitro* haustorium induction plate with a *C. campestris* strand and a domesticated tomato (*Solanum lycopersicum*) seedling. The *C. campestris (Cc)* strand and the tomato seedling were sandwiched between two agar layers to provide sufficient physical pressure and promote haustorium formation.

(D) A 100 µm thick fresh vibratome section of *C. campestris (Cc)* haustorium parasitizing the root of a tomato (Sl) seedling. (A, B, D) Scale bars = 200 µm. Sections were stained with Toluidine Blue O. White arrowheads indicate the haustorial vascular connection.

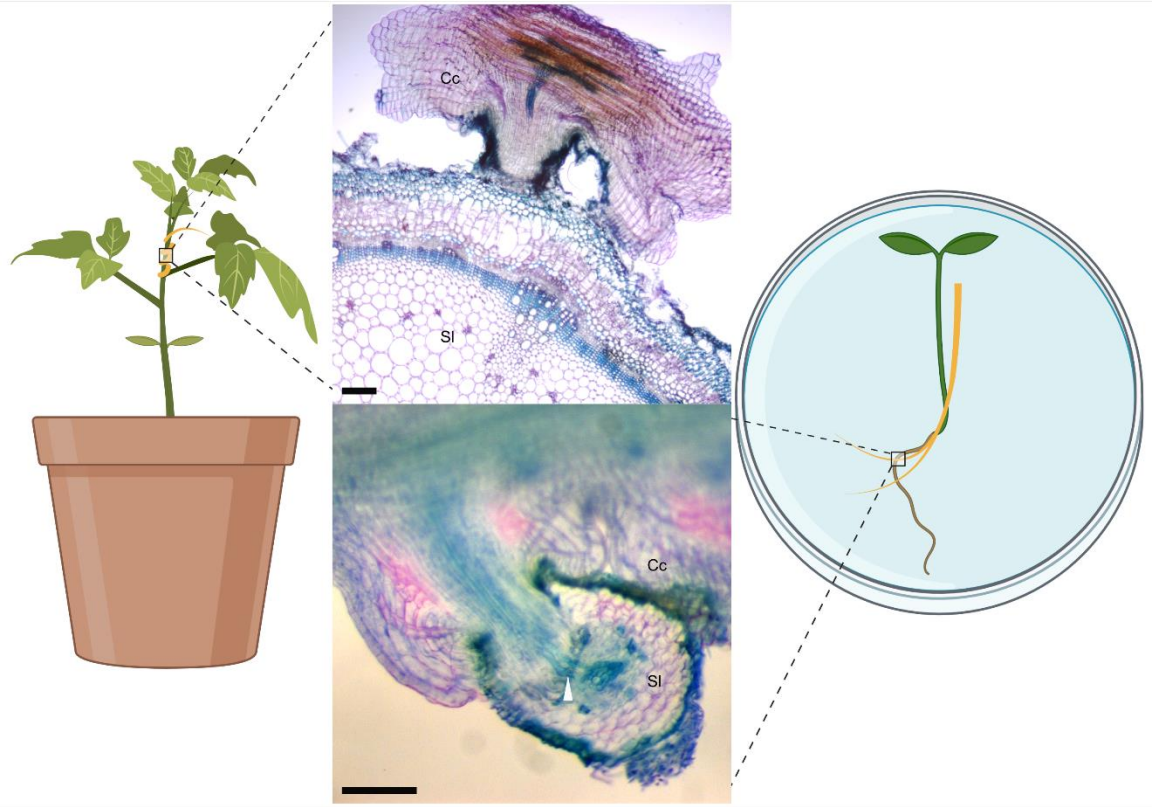

Figure 6. Organ-specific defense responses in the resistant tomato cultivar Heinz 9553. H9553 tomato plants are resistant to *C. campestris* attacks on their stems, but they are susceptible to *C. campestris* on their roots. The upper panel of the figure is a 100 µm thick fresh vibratome section of *C. campestris* (Cc) haustorium parasitizing the stem of an H9553 tomato (Sl). The lower panel of the figure is a 100 µm thick fresh vibratome section of *C. campestris* (Cc) haustorium parasitizing the root of an H9553 tomato (Sl). Scale bars = 200 µm. Sections were stained with Toluidine Blue O. White arrowhead indicates the haustorial vascular connection.

Acknowledgments

The authors acknowledge support from the US Department of Agriculture National Institute of Food and Agriculture award 2014-67013-21700 (N. R. S.), Hatch award CA-D-PLB-7412-H (N. R. S.), NSF IOS-185674 (N. R. S.), and by the UC Davis Graduate Research Award (M-Y. J.), and Loomis Robert S. and Lois Ann Graduate Award in Agronomy (M-Y. J.). Figure 1, 2, 3, 4, 6 were created using BioRender.com.

VII. References

1. Adie B, Chico JM, Rubio-Somoza I, Solano R. 2007. Modulation of Plant Defenses by Ethylene. *Journal of Plant Growth Regulation* 26:160-77
2. Agrios GN. 2005. chapter thirteen - PLANT DISEASES CAUSED BY PARASITIC HIGHER PLANTS, INVASIVE CLIMBING PLANTS, AND PARASITIC GREEN ALGAE. In *Plant Pathology (Fifth Edition)*:705-22. San Diego: Academic Press. Number of 705-22 pp.
3. Albert M, Axtell MJ, Timko MP. 2020. Mechanisms of resistance and virulence in parasitic plant–host interactions. *Plant Physiology* 185:1282-91
4. Albert M, Belastegui-Macadam XM, Bleischwitz M, Kaldenhoff R. 2008. Cuscuta spp: "Parasitic Plants in the Spotlight of Plant Physiology, Economy and Ecology". In *Progress in Botany*, ed. U Lüttge, W Beyschlag, J Murata:267-77. Berlin, Heidelberg: Springer Berlin Heidelberg. Number of 267-77 pp.
5. Albrecht H, Yoder JI, Phillips DA. 1999. Flavonoids Promote Haustoria Formation in the Root ParasiteTriphysaria versicolor1. *Plant Physiology* 119:585-92
6. Ángeles Castillejo M, Amiour N, Dumas-Gaudot E, Rubiales D, Jorrín JV. 2004. A proteomic approach to studying plant response to crenate broomrape (Orobanche crenata) in pea (Pisum sativum). *Phytochemistry* 65:1817-28
7. Böhm H, Albert I, Fan L, Reinhard A, Nürnberger T. 2014. Immune receptor complexes at the plant cell surface. *Current Opinion in Plant Biology* 20:47-54
8. Balint-Kurti P. 2019. The plant hypersensitive response: concepts, control and consequences. *Molecular plant pathology* 20:1163-78

9. Bardgett RD, Smith RS, Shiel RS, Peacock S, Simkin JM, et al. 2006. Parasitic plants indirectly regulate below-ground properties in grassland ecosystems. *Nature* 439:969-72

10. Berens ML, Wolinska KW, Spaepen S, Ziegler J, Nobori T, et al. 2019. Balancing trade-offs between biotic and abiotic stress responses through leaf age-dependent variation in stress hormone cross-talk. *Proceedings of the National Academy of Sciences* 116:2364-73

11. CAMERON DD, COATS AM, SEEL WE. 2006. Differential Resistance among Host and Non-host Species Underlies the Variable Success of the Hemi-parasitic Plant Rhinanthus minor. *Annals of Botany* 98:1289-99

12. Castillejo MÁ, Curto M, Fondevilla S, Rubiales D, Jorrín JV. 2010. Two-Dimensional Electrophoresis Based Proteomic Analysis of the Pea (Pisum sativum) in Response to Mycosphaerella pinodes. *Journal of Agricultural and Food Chemistry* 58:12822-32

13. Chang M, Lynn DG. 1986. The haustorium and the chemistry of host recognition in parasitic angiosperms. *Journal of Chemical Ecology* 12:561-79

14. Cheng X, Floková K, Bouwmeester H, Ruyter-Spira C. 2017. The Role of Endogenous Strigolactones and Their Interaction with ABA during the Infection Process of the Parasitic Weed Phelipanche ramosa in Tomato Plants. *Frontiers in Plant Science* 8

15. Cook CE, Whichard LP, Turner B, Wall ME, Egley GH. 1966. Germination of Witchweed (Striga lutea Lour.): Isolation and Properties of a Potent Stimulant. *Science* 154:1189-90

16. Cui H, Levesque MP, Vernoux T, Jung JW, Paquette AJ, et al. 2007. An Evolutionarily Conserved Mechanism Delimiting SHR Movement Defines a Single Layer of Endodermis in Plants. *Science* 316:421-5

17. Cui S, Kubota T, Nishiyama T, Ishida JK, Shigenobu S, et al. 2020. Ethylene signaling mediates host invasion by parasitic plants. *Science Advances* 6:eabc2385

18. Dean HL. Fruit Hypertrophy Caused by Cuscuta. *Proc. Proceedings of the Iowa Academy of Science, 1938,* 45:95-7:

19. Delavault P. 2020. Are root parasitic plants like any other plant pathogens? *New Phytologist* 226:641-3

20. Denness L, McKenna JF, Segonzac C, Wormit A, Madhou P, et al. 2011. Cell Wall Damage-Induced Lignin Biosynthesis Is Regulated by a Reactive Oxygen Species- and Jasmonic Acid-Dependent Process in Arabidopsis. *Plant Physiology* 156:1364-74

21. Ding P, Ding Y. 2020. Stories of Salicylic Acid: A Plant Defense Hormone. *Trends in Plant Science* 25:549-65

22. DITA MA, DIE JV, ROMÁN B, KRAJINSKI F, KÜSTER H, et al. 2009. Gene expression profiling of Medicago truncatula roots in response to the parasitic plant Orobanche crenata. *Weed Research* 49:66-80

23. Dos Santos CV, Letousey P, Delavault P, Thalouarn P. 2003. Defense Gene Expression Analysis of Arabidopsis thaliana Parasitized by Orobanche ramosa. *Phytopathology*® 93:451-7

24. Duriez P, Vautrin S, Auriac M-C, Bazerque J, Boniface M-C, et al. 2019. A receptor-like kinase enhances sunflower resistance to Orobanche cumana. *Nature Plants* 5:1211-5

25. Echevarría-Zomeño S, Pérez-de-Luque A, Jorrín J, Maldonado AM. 2006. Pre-haustorial resistance to broomrape (Orobanche cumana) in sunflower (Helianthus annuus): cytochemical studies. *Journal of Experimental Botany* 57:4189-200

26. Fisher JP, Phoenix GK, Childs DZ, Press MC, Smith SW, et al. 2013. Parasitic plant litter input: a novel indirect mechanism influencing plant community structure. *New Phytologist* 198:222-31

27. Fishman MR, Shirasu K. 2021. How to resist parasitic plants: pre- and post-attachment strategies. *Current Opinion in Plant Biology* 62:102004

28. Gobena D, Shimels M, Rich PJ, Ruyter-Spira C, Bouwmeester H, et al. 2017. Mutation in sorghum LOW GERMINATION STIMULANT 1 alters strigolactones and causes Striga resistance. *Proceedings of the National Academy of Sciences* 114:4471-6

29. Goldwasser Y, Hershenhorn J, Plakhine D, Kleifeld Y, Rubin B. 1999. Biochemical factors involved in vetch resistance toOrobanche aegyptiaca. *Physiological and Molecular Plant Pathology* 54:87-96

30. Goldwasser Y, Westwood JH, Yoder JI. 2002. The Use of Arabidopsis to Study Interactions between Parasitic Angiosperms and Their Plant Hosts. *Arabidopsis Book* 1:e0035-e

31. Gomez-Roldan V, Fermas S, Brewer PB, Puech-Pagès V, Dun EA, et al. 2008. Strigolactone inhibition of shoot branching. *Nature* 455:189-94

32. Goyet V, Wada S, Cui S, Wakatake T, Shirasu K, et al. 2019. Haustorium Inducing Factors for Parasitic Orobanchaceae. *Frontiers in Plant Science* 10

33. Hegenauer V, Fürst U, Kaiser B, Smoker M, Zipfel C, et al. 2016. Detection of the plant parasite *Cuscuta reflexa* by a tomato cell surface receptor. *Science* 353:478-81

34. Hegenauer V, Slaby P, Körner M, Bruckmüller J-A, Burggraf R, et al. 2020. The tomato receptor CuRe1 senses a cell wall protein to identify Cuscuta as a pathogen. *Nature Communications* 11:5299

35. Hembree KJ, Lanini W, Va N. Tomato varieties show promise of dodder control. *Proc. Proc. Calif. Weed Sci. Soc, 1999,* 51:205-6:

36. Hierro JL, Callaway RM. 2003. Allelopathy and exotic plant invasion. *Plant and Soil* 256:29-39

37. Hiraoka Y, Ueda H, Sugimoto Y. 2008. Molecular responses of Lotus japonicus to parasitism by the compatible species Orobanche aegyptiaca and the incompatible species Striga hermonthica. *Journal of Experimental Botany* 60:641-50

38. Hu L, Wang J, Yang C, Islam F, Bouwmeester HJ, et al. 2020. The Effect of Virulence and Resistance Mechanisms on the Interactions between Parasitic Plants and Their Hosts. *International Journal of Molecular Sciences* 21:9013

39. Huang K, Mellor KE, Paul SN, Lawson MJ, Mackey AJ, Timko MP. 2012. Global changes in gene expression during compatible and incompatible interactions of cowpea (Vigna unguiculata L.) with the root parasitic angiosperm Striga gesnerioides. *BMC Genomics* 13:402

40. Ihl B, Jacob F, Meyer A, Sembdner G. 1987. Investigations on the endogenous levels of abscisic acid in a range of parasitic phanerogams. *Journal of Plant Growth Regulation* 5:191-205

41. Ishida JK, Wakatake T, Yoshida S, Takebayashi Y, Kasahara H, et al. 2016. Local Auxin Biosynthesis Mediated by a YUCCA Flavin Monooxygenase Regulates Haustorium Development in the Parasitic Plant Phtheirospermum japonicum *The Plant Cell* 28:1795-814

42. Jhu M-Y, Farhi M, Wang L, Philbrook RN, Belcher MS, et al. 2020. Lignin-based resistance to Cuscuta campestris parasitism in Heinz resistant tomato cultivars. *bioRxiv*:706861

43. Jhu M-Y, Farhi M, Wang L, Philbrook RN, Belcher MS, et al. 2020. Lignin-based resistance to *Cuscuta campestris* parasitism in Heinz resistant tomato cultivars. *bioRxiv*:706861

44. Jhu M-Y, Ichihashi Y, Farhi M, Wong C, Sinha NR. 2021. LATERAL ORGAN BOUNDARIES DOMAIN 25 functions as a key regulator of haustorium development in dodders. *Plant Physiology*

45. Jiang F, Dieter Jeschke W, Hartung W. 2005. Contents and flows of assimilates (mannitol and sucrose) in the hemiparasiticRhinanthus minor/Hordeum vulgare association. *Folia Geobotanica* 40:195-203

46. Jiang F, Jeschke WD, Hartung W, Cameron DD. 2010. Interactions Between Rhinanthus minor and Its Hosts: A Review of Water, Mineral Nutrient and Hormone Flows and Exchanges in the Hemiparasitic Association. *Folia Geobotanica* 45:369-85

47. Johnsen HR, Striberny B, Olsen S, Vidal-Melgosa S, Fangel JU, et al. 2015. Cell wall composition profiling of parasitic giant dodder (Cuscuta reflexa) and its hosts: a priori differences and induced changes. *New Phytologist* 207:805-16

48. Kaga Y, Yokoyama R, Sano R, Ohtani M, Demura T, et al. 2020. Interspecific Signaling Between the Parasitic Plant and the Host Plants Regulate Xylem Vessel Cell Differentiation in Haustoria of Cuscuta campestris. *Frontiers in Plant Science* 11

49. Kaga Y, Yokoyama R, Sano R, Ohtani M, Demura T, et al. 2020. Interspecific Signaling Between the Parasitic Plant and the Host Plants Regulate Xylem Vessel Cell Differentiation in Haustoria of Cuscuta campestris. *Frontiers in Plant Science* 11

50. Kaiser B, Vogg G, Fürst UB, Albert M. 2015. Parasitic plants of the genus Cuscuta and their interaction with susceptible and resistant host plants. *Frontiers in Plant Science* 6:45

51. Keyes WJ, O'Malley RC, Kim D, Lynn DG. 2000. Signaling Organogenesis in Parasitic Angiosperms: Xenognosin Generation, Perception, and Response. *Journal of Plant Growth Regulation* 19:217-31

52. Kokla A, Melnyk CW. 2018. Developing a thief: Haustoria formation in parasitic plants. *Developmental Biology* 442:53-9

53. Ku Y-S, Sintaha M, Cheung M-Y, Lam H-M. 2018. Plant Hormone Signaling Crosstalks between Biotic and Abiotic Stress Responses. *International journal of molecular sciences* 19:3206

54. Kubo M, Ueda H, Park P, Kawaguchi M, Sugimoto Y. 2008. Reactions of Lotus japonicus ecotypes and mutants to root parasitic plants. *Journal of plant physiology* 166:353-62

55. López-Ráez JA, Matusova R, Cardoso C, Jamil M, Charnikhova T, et al. 2009. Strigolactones: ecological significance and use as a target for parasitic plant control. *Pest Management Science* 65:471-7

56. Lee H-A, Lee H-Y, Seo E, Lee J, Kim S-B, et al. 2017. Current Understandings of Plant Nonhost Resistance. *Molecular Plant-Microbe Interactions*® 30:5-15

57. Letousey P, De Zélicourt A, Vieira Dos Santos C, Thoiron S, Monteau F, et al. 2007. Molecular analysis of resistance mechanisms to Orobanche cumana in sunflower. *Plant Pathology* 56:536-46

58. Li J, Timko MP. 2009. Gene-for-Gene Resistance in *Striga*-Cowpea Associations. *Science* 325:1094-

59. Liu Z, Wu Y, Yang F, Zhang Y, Chen S, et al. 2013. BIK1 interacts with PEPRs to mediate ethylene-induced immunity. *Proceedings of the National Academy of Sciences* 110:6205-10

60. Lorenzo O, Piqueras R, Sánchez-Serrano JJ, Solano R. 2003. ETHYLENE RESPONSE FACTOR1 Integrates Signals from Ethylene and Jasmonate Pathways in Plant Defense[W]. *The Plant Cell* 15:165-78

61. Medel R. 2001. Assessment of correlational selection on tolerance and resistance traits in a host plant–parasitic plant interaction. *Evolutionary Ecology* 15:37-52

62. Musselman LJ, Yoder JI, Westwood JH. 2001. Parasitic Plants Major Problem to Food Crops. *Science* 293:1434-

63. Mutuku JM, Cui S, Hori C, Takeda Y, Tobimatsu Y, et al. 2019. The Structural Integrity of Lignin Is Crucial for Resistance against *Striga hermonthica* Parasitism in Rice. *Plant Physiology* 179:1796-809

64. Mutuku JM, Cui S, Yoshida S, Shirasu K. 2021. Orobanchaceae parasite–host interactions. *New Phytologist* 230:46-59

65. Mutuku JM, Yoshida S, Shimizu T, Ichihashi Y, Wakatake T, et al. 2015. The WRKY45-Dependent Signaling Pathway Is Required For Resistance against Striga hermonthica Parasitism *Plant Physiology* 168:1152-63

66. Mutuku JM, Yoshida S, Shimizu T, Ichihashi Y, Wakatake T, et al. 2015. The WRKY45-Dependent Signaling Pathway Is Required For Resistance against Striga hermonthica Parasitism. *Plant Physiology* 168:1152-63

67. National Center for Biotechnology Information. 2021. *PubChem Compound Summary for CID 137676, Ethylene-d1*. https://pubchem.ncbi.nlm.nih.gov/compound/Ethylene-d1

68. National Center for Biotechnology Information. 2021. *PubChem Compound Summary for CID 3083597, Ayapin.* https://pubchem.ncbi.nlm.nih.gov/compound/Ayapin

69. National Center for Biotechnology Information. 2021. *PubChem Compound Summary for CID 5280460, Scopoletin.* https://pubchem.ncbi.nlm.nih.gov/compound/Scopoletin

70. National Center for Biotechnology Information. 2021. *PubChem Compound Summary for CID 10665247, Orobanchol.* https://pubchem.ncbi.nlm.nih.gov/compound/Orobanchol

71. National Center for Biotechnology Information. 2021. *PubChem Compound Summary for CID 15102684, 5-Deoxystrigol.* https://pubchem.ncbi.nlm.nih.gov/compound/5-Deoxystrigol

72. Ohlson EW, Timko MP. 2020. Race Structure of Cowpea Witchweed (*Striga gesnerioides*) in West Africa and Its Implications for *Striga* Resistance Breeding of Cowpea. *Weed Science* 68:125-33, 9

73. Olson MM, Roseland CR. 1991. Induction of the Coumarins Scopoletin and Ayapin in Sunflower by Insect–Feeding Stress and Effects of Coumarins on the Feeding of Sunflower Beetle (Coleoptera: Chrysomelidae). *Environmental Entomology* 20:1166-72

74. Pérez-de-Luque A, González-Verdejo CI, Lozano MD, Dita MA, Cubero JI, et al. 2006. Protein cross-linking, peroxidase and β-1,3-endoglucanase involved in resistance of pea against Orobanche crenata. *Journal of Experimental Botany* 57:1461-9

75. Pérez-de-Luque A, Lozano MD, Moreno MT, Testillano PS, Rubiales D. 2007. Resistance to broomrape (Orobanche crenata) in faba bean (Vicia faba): cell wall changes associated with prehaustorial defensive mechanisms. *Annals of Applied Biology* 151:89-98

76. Pérez-de-Luque A, Moreno MT, Rubiales D. 2008. Host plant resistance against broomrapes (Orobanche spp.): defence reactions and mechanisms of resistance. *Annals of Applied Biology* 152:131-41

77. Pagán I, García-Arenal F. 2018. Tolerance to Plant Pathogens: Theory and Experimental Evidence. *International journal of molecular sciences* 19:810

78. Parker C. 2009. Observations on the current status of Orobanche and Striga problems worldwide. *Pest Management Science* 65:453-9

79. PÉREZ-DE-LUQUE A, JORRÍN J, CUBERO JI, RUBIALES D. 2005. Orobanche crenata resistance and avoidance in pea (Pisum spp.) operate at different developmental stages of the parasite. *Weed Research* 45:379-87

80. PÉRez-De-Luque A, Rubiales D, Cubero JI, Press MC, Scholes J, et al. 2005. Interaction between Orobanche crenata and its Host Legumes: Unsuccessful Haustorial Penetration and Necrosis of the Developing Parasite. *Annals of Botany* 95:935-42

81. Phuong LT, Fitrianti AN, Luan MT, Matsui H, Noutoshi Y, et al. 2020. Antagonism between SA- and JA-signaling conditioned by saccharin in Arabidopsis thaliana renders resistance to a specific pathogen. *Journal of General Plant Pathology* 86:86-99

82. Prats E, Bazzalo ME, León A, Jorrín JV. 2003. Accumulation of soluble phenolic compounds in sunflower capitula correlates with resistance to Sclerotinia sclerotiorum. *Euphytica* 132:321-9

83. Rich PJ, Grenier C, Ejeta G. 2004. Striga Resistance in the Wild Relatives of Sorghum. *Crop Science* 44:2221-9

84. Riopel J, Timko M. 1995. Haustorial initiation and differentiation. *Parasitic plants* 39:79

85. Runyon JB, Mescher MC, De Moraes CM. 2010. Plant defenses against parasitic plants show similarities to those induced by herbivores and pathogens. *Plant signaling & behavior* 5:929-31

86. RUNYON JB, MESCHER MC, FELTON GW, DE MORAES CM. 2010. Parasitism by Cuscuta pentagona sequentially induces JA and SA defence pathways in tomato. *Plant, Cell & Environment* 33:290-303

87. Runyon JB, Mescher MC, Felton GW, De Moraes CM. 2010. Parasitism byCuscuta pentagonasequentially induces JA and SA defence pathways in tomato. *Plant, Cell & Environment* 33:290-303

88. Saucet SB, Shirasu K. 2016. Molecular Parasitic Plant–Host Interactions. *PLOS Pathogens* 12:e1005978

89. Serghini K, de Luque AP, Castejón-Muñoz M, García-Torres L, Jorrín JV. 2001. Sunflower (Helianthus annuus L.) response to broomrape (Orobanche cernua Loefl.) parasitism: induced synthesis and excretion of 7-hydroxylated simple coumarins. *Journal of Experimental Botany* 52:2227-34

90. Shen H, Ye W, Hong L, Huang H, Wang Z, et al. 2006. Progress in Parasitic Plant Biology: Host Selection and Nutrient Transfer. *Plant Biology* 8:175-85

91. Su C, Liu H, Wafula EK, Honaas L, de Pamphilis CW, Timko MP. 2020. SHR4z, a novel decoy effector from the haustorium of the parasitic weed Striga gesnerioides, suppresses host plant immunity. *New Phytologist* 226:891-908

92. Swarbrick PJ, Huang K, Liu G, Slate J, Press MC, Scholes JD. 2008. Global patterns of gene expression in rice cultivars undergoing a susceptible or resistant interaction with the parasitic plant *Striga hermonthica*. *New Phytologist* 179:515-29

93. Tada Y, Sugai M, Furuhashi K. 1996. Haustoria of Cuscuta japonica, a Holoparasitic Flowering Plant, Are Induced by the Cooperative Effects of Far-Red Light and Tactile Stimuli. *Plant and Cell Physiology* 37:1049-53

94. Taylor A, Martin J, Seel WE. 1996. Physiology of the parasitic association between maize and witchweed (Striga hermonthica): is ABA involved? *Journal of Experimental Botany* 47:1057-65

95. Tintor N, Ross A, Kanehara K, Yamada K, Fan L, et al. 2013. Layered pattern receptor signaling via ethylene and endogenous elicitor peptides during *Arabidopsis* immunity to bacterial infection. *Proceedings of the National Academy of Sciences* 110:6211-6

96. Torres-Vera R, García JM, Pozo MJ, López-Ráez JA. 2016. Expression of molecular markers associated to defense signaling pathways and strigolactone biosynthesis during the early interaction tomato-Phelipanche ramosa. *Physiological and Molecular Plant Pathology* 94:100-7

97. Umehara M, Hanada A, Yoshida S, Akiyama K, Arite T, et al. 2008. Inhibition of shoot branching by new terpenoid plant hormones. *Nature* 455:195-200

98. Veselov D, Langhans M, Hartung W, Aloni R, Feussner I, et al. 2003. Development of Agrobacterium tumefaciens C58-induced plant tumors and impact on host shoots are controlled by a cascade of jasmonic acid, auxin, cytokinin, ethylene and abscisic acid. *Planta* 216:512-22

99. Vieira Dos Santos C, Delavault P, Letousey P, Thalouarn P. 2003. Identification by suppression subtractive hybridization and expression analysis of Arabidopsis thaliana putative defence genes during Orobanche ramosa infection. *Physiological and Molecular Plant Pathology* 62:297-303

100. Vurro E, Ruotolo R, Ottonello S, Elviri L, Maffini M, et al. 2011. Phytochelatins govern zinc/copper homeostasis and cadmium detoxification in Cuscuta campestris parasitizing Daucus carota. *Environmental and Experimental Botany* 72:26-33

101. Xie X, Yoneyama K, Yoneyama K. 2010. The Strigolactone Story. *Annual Review of Phytopathology* 48:93-117

102. Yaakov G, Lanini WT, Wrobel RL. 2001. Tolerance of Tomato Varieties to Lespedeza Dodder. *Weed Science* 49:520-3

103. Yang C, Xu L, Zhang N, Islam F, Song W, et al. 2017. iTRAQ-based proteomics of sunflower cultivars differing in resistance to parasitic weed Orobanche cumana. *PROTEOMICS* 17:1700009

104. Yoder JI, Scholes JD. 2010. Host plant resistance to parasitic weeds; recent progress and bottlenecks. *Current Opinion in Plant Biology* 13:478-84

105. Zehhar N, Labrousse P, Arnaud M-C, Boulet C, Bouya D, Fer A. 2003. Study of Resistance to Orobanche ramosa in Host (Oilseed Rape and Carrot) and Non-host (Maize) Plants. *European Journal of Plant Pathology* 109:75-82

106. Zhao J, Zheng SH, Fujita K, Sakai K. 2004. Jasmonate and ethylene signalling and their interaction are integral parts of the elicitor signalling pathway leading to β-thujaplicin biosynthesis in Cupressus lusitanica cell cultures. *Journal of Experimental Botany* 55:1003-12

Chapter 2: *LATERAL ORGAN BOUNDARIES DOMAIN 25* functions as a key regulator of haustorium development in dodders

*This chapter is published: Min-Yao Jhu, Yasunori Ichihashi, Moran Farhi, Caitlin Wong, Neelima R Sinha, *LATERAL ORGAN BOUNDARIES DOMAIN 25* functions as a key regulator of haustorium development in dodders, *Plant Physiology*, 2021, kiab231, https://doi.org/10.1093/plphys/kiab231

One-sentence summary:

CcLBD25 plays a pivotal role in haustorium initiation, regulating pectin digestion, and searching hyphae development during the haustorium penetration process.

Short title:

LBD25 regulates dodder haustorium development.

Abstract

Parasitic plants reduce crop yield worldwide. Dodder (*Cuscuta campestris)* is a stem parasite that attaches to its host, using haustoria to extract nutrients and water. We analyzed the transcriptome of six *C. campestris* tissues and identified a key gene, *LATERAL ORGAN BOUNDARIES DOMAIN 25* (*CcLBD25*), as highly expressed in prehaustoria and haustoria. Gene co-expression networks (GCN) from different tissue types and laser-capture microdissection (LCM) RNA-Seq data indicated that *CcLBD25* could be essential for regulating cell wall loosening and organogenesis. We employed host-induced gene silencing (HIGS) by generating transgenic tomato

(*Solanum lycopersicum*) hosts that express hairpin RNAs to target and down-regulate *CcLBD25* in the parasite. Our results showed that *C. campestris* growing on *CcLBD25* RNAi transgenic tomatoes transited to the flowering stage earlier and had reduced biomass compared with *C. campestris* growing on wild-type hosts, suggesting that parasites growing on transgenic plants were stressed due to insufficient nutrient acquisition. We developed an *in vitro* haustorium (IVH) system to assay the number of prehaustoria produced on strands from *C. campestris*. *C. campestris* grown on *CcLBD25* RNAi tomatoes produced fewer prehaustoria than those grown on wild type tomatoes, indicating that down-regulating *CcLBD25* may affect haustorium initiation. *C. campestris* haustoria growing on *CcLBD25* RNAi tomatoes exhibited reduced pectin digestion and lacked searching hyphae, which interfered with haustorium penetration and formation of vascular connections. The results of this study elucidate the role of *CcLBD25* in haustorium development and might contribute to developing parasite-resistant crops.

Introduction

Parasitic plants are heterotrophic, reducing the yields of crops worldwide (Agrios, 2005; Yoder and Scholes, 2010). They parasitize host plants using specialized organs known as haustoria, which extract nutrients and water from the hosts. *Cuscuta* species (dodders) are stem holoparasites without functional roots and leaves. Stems of *Cuscuta* spp. coil counterclockwise around their host and then form a series of haustoria along their own stems to attach to the hosts (Furuhashi et al., 2011; Alakonya et al., 2012). *Cuscuta campestris* is one of the most widely distributed and destructive parasitic weeds (Parker, 2021). A better understanding of the underlying molecular mechanisms of *C. campestris* haustorium development will aid in applying parasitic weed control and producing parasitic plant-resistant crops.

Many previous studies have identified the key factors needed for seed germination, host recognition, and haustorium induction and growth in root parasites (Shen et al., 2006; López-Ráez et al., 2009; Yoder and Scholes, 2010). Focusing on haustorium development, a previous study indicated that root parasitic plants co-opted the mechanism of lateral root formation in haustorium organogenesis (Ichihashi et al., 2017). The LATERAL ORGAN BOUNDARIES DOMAIN (LBD) family of transcription factors (TFs) are reported to be crucial in both lateral root formation in non-parasitic plants and haustorium developmental programming in root parasites (Ichihashi et al., 2020). In non-parasitic model plants, like Arabidopsis, LBD genes are shown to be involved in auxin signaling, interact with AUXIN RESPONSE FACTORs (ARFs) and promote lateral root formation (Mangeon et al., 2010; Porco et al., 2016). During the haustorium development stage, LBD orthologs are reported to be upregulated at attachment sites of root parasitic plants like *Thesium chinense* (Ichihashi et al., 2017) and *Striga hermonthica* (Yoshida et al., 2019). On the other hand, the molecular pathways regulating haustorium development in stem parasitic plants

are still largely unexplored. Although a few gene orthologs that regulate auxin accumulation during lateral root development in non-parasitic plants are found to be expressed in *Cuscuta* seedlings and stems, whether these genes are also involved haustorium formation remains unknown (Ranjan et al., 2014). Our previous studies showed that *SHOOT MERISTEMLESS*-like (*STM*) plays a role in *Cuscuta* spp. haustorium development (Alakonya et al., 2012). These results suggest that *Cuscuta* spp. might have repurposed the shoot developmental programs into haustorium organogenesis, but a recent study indicates that some genes that are involved in root development were also expressed in *Cuscuta australis* prehaustoria and haustoria (Sun et al., 2018), suggesting that the lateral root programming system was co-opted into haustorium development.

In this study, we provide an insight into the gene regulatory mechanisms of haustorium organogenesis and identify one of the LBD transcription factors, *CcLBD25*, as a vital regulator of *C. campestris* haustorium development. This discovery supports the hypothesis that stem parasitic plants adapted both shoot and root molecular machinery into haustorium formation. Using detailed transcriptome analysis and gene coexpression networks coupled with cellular and developmental phenotype assays, we also show that *CcLBD25* is not only involved in haustorium initiation through auxin signaling, but also participates in other aspects of haustorial developmental reprogramming, including cell wall loosening, searching hyphae development, and other phytohormone mediated signaling pathways. The results of this study will not only shed light on the field of haustorium development in stem parasitic plants but will also help develop a potentially universal parasitic weed-resistant system in crops to reduce economic losses caused by both root and stem parasites.

Results

Establishing genomic resources for *C. campestris* and constructing gene coexpression networks that regulate haustorium formation

In this study, we analyzed the transcriptome of different *C. campestris* tissues, including seeds, seedlings, stems, prehaustoria, haustoria, and flowers, grown on the tomato (*Solanum lycopersicum*) Heinz 1706 (H1706) cultivar and *Nicotiana benthamiana* (*N. benthamiana*) (Ranjan et al., 2014) by mapping reads to the recently available genome of *C. campestris* (Vogel et al., 2018). In general, seed tissues have distinctively different gene expression profiles compared to all other tissues (Supplemental Fig. S1). In addition, the expression patterns in invasive tissues (prehaustoria and haustoria) and non-invasive tissues are also disparate (Supplemental Fig. S1). We conducted principal component analysis (PCA) analysis and noticed that the genes that are highly expressed in invasive tissues can be separated from the genes that are highly expressed in non-invasive tissues on PC1 (Fig. 1A, B). To identify the genes that might be involved in haustorium development, we performed clustering analysis using self-organizing maps (SOM) in R, and identified a cluster enriched with genes that are highly expressed in both prehaustoria and haustoria tissues (SOM9 - Fig. 1, Supplemental Fig. S2, Supplemental Table S1).

We focused on the genes contained in this SOM9 cluster and constructed a gene coexpression network (GCN). Using the fast greedy modularity optimization algorithm to analyze the GCN community structure (Clauset et al., 2004) and visualizing the network using Cytoscape (Cline et al., 2007), we noticed this SOM9 GCN is composed of three major modules (Fig. 2A, Supplemental Table S2). Since the current gene annotation of *C. campestris* genome is not as complete as that of most model organisms, we used BLAST to combine our previously annotated transcriptome with current *C. campestris* genome gene IDs (Supplemental Table S3). With this

more comprehensive annotation profile, we conducted GO enrichment analysis using the TAIR ID for each *C. campestris* gene in the network to identify the major GO term for each module (Supplemental Table S4). Based on our GO enrichment results, the major biological process of module 1 can be classified as "plant-type cell wall loosening", and the cellular component of module 1 is "extracellular region and intracellular membrane-bounded organelle" (Fig. 2, Supplemental Table S4). This result indicates the genes contained in module 1 are mostly involved in cell wall loosening, which is needed for the haustorium to penetrate through the host tissue. On the other hand, the major biological processes of module 3 include "transport, response to hormones, secondary metabolite biosynthetic process, and regulation of lignin biosynthetic process". The molecular function of module 3 is "transmembrane transporter activity", and the cellular component of module 3 is "plasma membrane" (Fig. 2A, Supplemental Table S4). This analysis suggests that these genes might be involved in later stages of development and nutrient transport from the host to the parasite once a connection is established between the host and the parasite.

To identify the key regulators in the haustorium penetration process, we focused on genes in module 1 and calculated the degree centrality and betweenness centrality scores of each gene within this group. Many central hub genes in module 1 are proteins or enzymes involved in cell wall modifications, like pectin lyases, pectinesterase inhibitors, and expansins (Fig. 2B, Supplemental Table S2). To find the upstream regulators of these pathways, we focused on transcription factors that are classified in module 1. Intriguingly, only three transcription factors are included in module 1: *CcLBD25* (Lateral Organ Boundaries Domain gene 25; Cc019141), *CcLBD4* (Cc017015), and *CcWRKY71* (Cc004070) (Fig. 2B, Supplemental Table S2). According to the gene coexpression network of SOM9, we noticed that *CcLBD25*, *CcLBD4*, and *CcWRKY71*

share several common first layer neighbors (Fig. 2). Based on previous reports, *AtLBD25* regulates lateral root development in *Arabidopsis* by promoting auxin signaling (Dean et al., 2004; Mangeon et al., 2010). Furthermore, an *LBD25* orthologue (*TcLBD25*) in *Thesium chinense*, a root parasitic plant in the Santalaceae family, was also detected to be upregulated during the haustorium development process (Ichihashi et al., 2017). Using *CcLBD25* nucleotide sequence alignments and a *LBD25* phylogenetic tree constructed using MEGA X (Kumar et al., 2018) (Supplemental Fig. S3, Supplemental Dataset S1), we confirmed orthology between the *TcLBD25, AtLBD25* and *CcLBD25* genes. Based on these serendipitous pieces of evidence, we suspected that *CcLBD25* may also regulate haustorium formation and the parasitism process in *C. campestris*.

To understand the role of *CcLBD25* and the potential connection with other genes, we included genes in SOM2 (genes that are only highly expressed in haustoria) and SOM3 (genes that are only highly expressed in prehaustoria) to build a more comprehensive GCN (Fig. 1, Supplemental Fig. S2). Based on the community structure analysis, this comprehensive network is composed of three major modules (Fig. 3A, Supplemental Table S5). Based on our GO enrichment results, the major biological process of module 3 is plant-type cell wall loosening and the major biological processes of module 1 include morphogenesis of a branching structure, plant organ formation, and several hormone responses and biosynthetic processes (Supplemental Table S6). *CcLBD25* itself is placed in module 1 (Supplemental Table S5), but *CcLBD25* has many first layer connections with genes that are classified in module 1 or module 3 (Fig. 3A, C). This result indicates that *CcLBD25* might play a role in connecting genes involved in different pathways or aspects of haustorium development. Furthermore, by coloring the network with their corresponding SOM groups, we noticed that even though *CcLBD25* itself is in SOM9, many of the *CcLBD25* first and second layer neighbors are in SOM2 and SOM3 (Fig. 3B, D). Thus,

CcLBD25 might be a key regulator of the haustorium development process in both early and late stages of haustorium development and may also play a critical role in coordinating the function of genes that are expressed only during discrete developmental stages.

Zooming into tissue specific expression using laser-capture microdissection (LCM) coupled with RNA-seq

Our first transcriptome data came from hand collected tissue samples. To further dissect *Cuscuta* haustorium developmental stages, we used laser-capture microdissection (LCM) with RNA-seq to analyze only pure haustorial tissues from three different haustorium developmental stages (Fig. 4A-E). Based on a previous study, changes in the levels of jasmonic acid (JA) and salicylic acid (SA) are observed about 36-48 hours after first haustorial swelling, which is about 4 days post attachment (DPA) (RUNYON et al., 2010). We also noticed that haustorium growth is a continuous process for *C. campestris*, so all developmental stages of haustoria can be found on the same strand at the 4 DPA time point. Therefore, we focused on 4 DPA and defined three developmental stages based on their haustorium structure: early (the haustorium has just contacted the host), intermediate (the haustorium has developed searching hyphae but has not formed vascular connections), and mature (a mature haustorium with continuous vasculature between host and parasite) (Fig. 4A-C). *C. campestris* haustorium tissues, especially the protruding region of haustoria, were collected from *C. campestris* using LCM at these three developmental stages attached to H1706 and subjected to RNA-Seq (Fig. 4D-E).

Next, we mapped our LCM RNA-Seq data to the *C. campestris* genome. Visualizing the gene expression changes using multidimensional scaling showed that the expression profile of the mature stage is distinct from the early and intermediate stages (Supplemental Fig. S4). We then conducted clustering analyses using SOM to group genes based on their expression patterns at

these three different developmental stages (Fig. 4F-G). According to our PCA analysis, PC1 obviously separated genes that are specifically expressed in the mature stage from those expressed in the other two stages, and PC2 distinguished the genes expressed in the early stage from those expressed in the intermediate stage (Supplemental Fig. S5). Interestingly, and similar to what was seen in our tissue type transcriptome data, *CcLBD25* is grouped in SOM6, which is the cluster of genes that are relatively highly expressed in both early-stage and mature-stage (Fig. 4F-G, and Supplemental Fig. S6, Supplemental Table S7). Notably, *CcLBD25* expression in intermediate-stage is relatively reduced compared with early-stage or mature-stage but is still much higher compared with other non-invasive tissues like seed, seedlings, stems and flowers. Genes with low expression levels were often not detectable in LCM RNA-Seq data, which might be caused by the preparation process of LCM tissues, including fixation, sectioning, and dissection processes, which are likely to lead to loss of some RNAs due to unpreventable degradation. To investigate gene regulatory dynamics within the haustorium developmental process, we used the same gene list from tissue type RNA-Seq SOM9 and constructed another GCN of these genes that was based on the LCM RNA-Seq expression profiles (Fig. 4H). By using the same gene list, but the expression dataset from samples of precisely collected haustorial cells, we obtained detailed regulatory connections between genes by comparing the tissue type GCN and LCM GCN (Fig. 2A, 4H). Based on the fast greedy community structure analysis, this LCM GCN is composed of three major modules with *CcLBD25* in module 1 (Fig. 4H, Supplemental Table S8). According to our GO enrichment results, the major biological process for module 1 is plant-type cell wall loosening, and for module 3, is brassinosteroid mediated signaling pathway (Fig. 4H, Supplemental Table S9). In addition to cell wall loosening related enzyme encoding genes forming central hubs, we noticed *CcLBD25* is the TF with the highest number of connections in module 1. *CcLBD25* has 13 first

layer neighbors and 70 second layer neighbors, including many cell wall loosening-related genes (Fig. 4H-I, Supplemental Table S8). Zooming in to focus on *CcLBD25*, we noticed that the *CcLBD25* first and second layer neighbors are genes classified in module 1 or module 3, indicating that *CcLBD25* might play a role in connecting these two pathways. Many of the *CcLBD25* first and second layer neighbors are pectin degradation related genes like *PL* and *PMEI*. On the other hand, *CcLBD4* is not in the LCM GCN, and *CcWRKY71* is at a marginal location with only one connection. This result provided further support for our hypothesis that *CcLBD25* is the major TF regulating cell wall modification in the haustorium penetration process. *CcLBD4* and *CcWRKY71* might also be key regulators but are likely involved in a different aspect of haustorium development. Thus, we focused our attention on understanding the function of *CcLBD25* in haustorium development.

Cross-species RNAi (Host-Induced Gene Silencing) *CcLBD25* effects whole-plant phenotypes and reduces parasite fitness

In our previous studies, we found cross-species transport of mRNAs and siRNAs between *C. campestris* and their hosts (when the initial haustoria are successfully connected with host vascular tissue), and demonstrated host-induced gene silencing (HIGS) (Runo et al., 2011; Alakonya et al., 2012). Many previous studies have also shown that large-scale mRNA and small RNAs are transported through the haustorium connections in *Cuscuta* species (Kim et al., 2014; Johnson et al., 2019). Therefore, we generated transgenic host tomatoes with hairpin RNAs that target and down-regulate *CcLBD25* after the parasite forms the first attachment and takes up RNAs from the host (Supplemental Fig. S7). When *C. campestris* grows on wild-type tomato hosts, *CcLBD25* is highly expressed in invasive tissues (Fig. 5A, B). However, *CcLBD25* expression levels are significantly knocked-down in the tissues on and near the initial functional attachment sites of *C.*

campestris plants that are growing on *CcLBD25* RNAi transgenic plants (Fig. 5B). Based on our results, expressing *CcLBD25* RNAi constructs has no effect on tomato plant growth and, with one exception, transgenic *CcLBD25* RNAi tomato plants have the same phenotype as wild-type plants (Supplemental Fig. S8). Notably, *CcLBD25* and *SlLBD25* nucleotide sequences shared low similarity based on results of Blastn with the most recently published tomato genome (ITAG 4.0) (Supplemental Data S1). This also explains why using *CcLBD25* RNAi constructs do not influence tomato growth (Supplemental Fig. S8). We suspect that the p35S:RNAi line 2-2 might be different from wild-type due to tissue culture or insertion effects. Nevertheless, pSUC:RNAi would be a better choice for agricultural application due to specific expression of the RNAi construct in phloem tissues, which would allow efficient transfer of siRNAs to *C. campestris* after establishment of vascular connection. However, for the purpose of verifying the function of *CcLBD25* in *C. campestris*, both p35S:RNAi lines and pSUC:RNAi lines worked well and successfully downregulated the expression of *CcLBD25* in *C. campestris* (Fig. 5B). If *CcLBD25* is important in haustorium development and parasitism, then down-regulating *CcLBD25* should influence haustorium structure or formation, and might also affect nutrient transport. To verify our hypothesis, we measured flowering time in *C. campestris* growing on various tomato hosts. The result showed that parasites growing on *CcLBD25* RNAi transgenic tomatoes transitioned to the flowering stage and subsequently senesced earlier than those growing on wild types (Fig. 5C). Based on previous studies, many plant species respond to environmental stress factors by inducing flowering (Wada and Takeno, 2010; Riboni et al., 2014). This early transition to the reproductive stage and senescence in *C. campestris* grown on *CcLBD25* RNAi plants suggests that *C. campestris* was growing under stress, likely because of nutrient deficiency.

To verify if down-regulating *CcLBD25* affects the ability of the parasite to acquire resources from the host, we also measured the biomass of *C. campestris* grown on wild-type H1706 and *CcLBD25* RNAi transgenic plants. At 14 days post attachment (DPA), we noticed that *C. campestris* plants grown on *CcLBD25* RNAi transgenic tomatoes had less biomass compared with the *C. campestris* plants grown on wild-type H1706 (Fig. 5D). Both whole-plant level phenotypes suggest that *CcLBD25* might be involved in haustorium development and knocking down the expression level of *CcLBD25* influences the ability of *C. campestris* to establish connections with hosts and interferes with parasite nutrient acquisition.

Using an *in vitro* haustoria (IVH) system to investigate the impact of *CcLBD25* on early-stage haustorium development

Previous studies indicate that several auxin-inducible *LBD* genes function in lateral root initiation (Goh et al., 2012). We noticed that auxin efflux carriers and auxin-responsive genes are also in the SOM9 gene co-expression network (Fig. 2). Therefore, we proposed that *CcLBD25* might regulate early-stage haustorium development in *C. campestris*. In order to assay the role of *CcLBD25* in *C. campestris* haustorium initiation, we developed an *in vitro* haustorium (IVH) system coupled with HIGS (Fig. 6A). This method is inspired by the previous discovery that *Cuscuta* haustoria can be induced by physical contact and far-red light signals (Tada et al., 1996) and many studies confirmed that small RNAs and mRNAs can move cross-species through the haustorial phloem connection (David-Schwartz et al., 2008; Alakonya et al., 2012; Kim et al., 2014; Johnson et al., 2019). Therefore, we took the *C. campestris* strands growing near the haustorium attachment sites on wild-type and *CcLBD25 RNAi* transgenic tomato (Fig. 6B) and sandwiched these strands between two layers of agar to provide sufficient physical contact (Fig. 6A, C). We then illuminated these plates under far-red light for 5 days, at which point prehaustoria are readily

visible (Fig. 6D-E). Since the IVH induction is rapid and these prehaustoria can easily be separated from the agar, this method allowed us to count prehaustoria numbers under the microscope and validate the effect of *CcLBD25* RNAi on haustorium initiation. The strands from the *C. campestris* grown on *CcLBD25 RNAi* transgenic tomatoes produced many fewer prehaustoria than the strands from those grown on wild type (Fig. 6F). This result indicates that reduced *CcLBD25* expression impeded haustorium initiation and confirms that *CcLBD25* is a key regulator of early-stage haustorium development, as suggested by our LCM RNA-Seq analysis results.

Down-regulation of *CcLBD25* leads to structural changes in haustoria

To verify the crucial role *CcLBD25* plays in haustorium development and to investigate how down-regulating *CcLBD25* affects haustorium structure and the parasitism process, we prepared 100 µm-thick fresh haustorium sections using a vibratome, and stained them with Toluidine Blue O (O'Brien et al., 1964). In sections of haustoria growing on wild-type plants, we could observe searching hyphae that had penetrated the host cortex region and transformed into xylic or phloic hyphae as they had connected to host xylem and phloem (Fig. 7A, C, E). However, we observed that many haustoria growing on *CcLBD25* RNAi transgenic tomatoes had formed a dome shape structure and lacked searching hyphae (Fig. 7B, D, F, Supplemental Fig. S9, Supplemental Table S10 and S11). This result indicates that *CcLBD25* might be involved in development of searching hyphae. Therefore, knocking down of *CcLBD25* affects the ability of *C. campestris* to establish connections with the host vascular system and leads to nutrient deficiency, as observed in the whole-plant level phenotypes.

We also noticed the down-regulation of *CcLBD25* influenced the parasite penetration process. Fresh tissue sections of the haustoria growing on wild type showed a clear zone in tomato cortex tissues near haustorium tissues (Fig. 7A, C, E). Since the metachromatic staining of

Toluidine Blue O is based on cell wall composition and pH values and a pink to purple color indicates pectin presence, this result indicates that the pectins in tomato cortex tissues may have been digested or the pH condition in the cell wall had been changed in the haustorium penetration process (Fig. 7A, C, E). On the other hand, the *C. campestris* growing on *CcLBD25* RNAi transgenic tomatoes still showed pink to purple color in the cortex near the haustorium attachment sites (Fig. 7B, D). Hence, less pectin digestion or cell wall modification happened in tomato cortex tissues near these *CcLBD25* downregulated haustorium tissues compared to the haustoria growing on wild-type. These haustorium structural phenotypes correspond well with our SOM9 GCN from the *C. campestris* tissue transcriptome. *CcLBD25* is one of the transcription factor central hub genes in module 1, with many first and second layers of connection to genes involved in cell wall modification, including pectin lyases and pectin methyl-esterase inhibitors (PMEIs). Based on many previous studies, the interplay between pectin methylesterase (PME) and PMEI is an important determinant of cell wall loosening, strengthening, and organ formation (Wormit and Usadel, 2018). Therefore, we hypothesized that PMEIs might be one of the key regulators that cause the haustorium phenotype in *CcLBD25*-downregulated haustorium tissues. To test if the down-regulation of *CcLBD25* would affect *PMEI* expression levels, we conducted qPCR to detect *CcPMEI* expression levels in the tissues of *C. campestris* plants that are growing on *CcLBD25* RNAi transgenic plants. Our results show that *CcPMEI* expression levels are also significantly reduced when *CcLBD25* is knocked-down (Fig. 7G, H). Thus, *CcLBD25* might directly or indirectly regulate *CcPMEI* at the transcriptional level. These results verify the hypothesis that *CcLBD25* plays an important role in haustorium development and might regulate cell wall modification.

Discussion

In this study, we demonstrate that *CcLBD25* is a crucial regulator of several aspects of *C. campestris* haustorium development, including haustorium initiation, cell-wall loosening, and searching hyphae growth. We use transcriptome of six *C. campestris* tissue types and RNA-Seq data of LCM captured haustoria at three developmental stages to reveal the potential molecular mechanisms and the complexity of gene networks that are regulated during the haustorium formation process. Our results provide a comprehensive analysis of the *CcLBD25* centered regulatory system and illustrate that *CcLBD25* might directly or indirectly coordinate different groups of genes that are expressed only at the early or mature stage during haustorium development.

Lateral root development and haustorium development

In non-parasitic plants, like Arabidopsis, *AtLBD25* was also named *DOWN IN DARK AND AUXIN1* (*DDA1*) because *lbd25* mutant plants exhibited reduced sensitivity to auxin and reduced number of lateral roots (Mangeon et al., 2010). These phenotypes indicate that *AtLBD25* functions in lateral root formation by promoting auxin signaling (Mangeon et al., 2010). In the root parasitic plant, *Thesium chinense*, *TcLBD25* was highly expressed during haustorium formation (Ichihashi et al., 2017). This supports the hypothesis that root parasitic plants co-opted the lateral root formation machinery into haustorium organogenesis. However, whether rootless stem parasitic plants *Cuscuta* spp. also followed the same path to generating haustoria was unknown. In this study, we identified *CcLBD25* as playing a key role in *Cuscuta* haustorium development. Our SOM9 gene co-expression network shows that auxin efflux carriers and auxin-responsive genes are also remotely connected with *CcLBD25*, but not in the first or second layers of neighbors (Fig. 2). Our hypothesis is that the increased expression of *CcLBD25* might induce the genes that are involved in auxin signaling, which was observed in the Arabidopsis lateral root development

system (Dean et al., 2004; Mangeon et al., 2010). These pieces of evidence suggest that *Cuscuta* spp. adapted not only the shoot developmental programs (Alakonya et al., 2012), but also the lateral root programming system, into haustorium organogenesis. According to our *LBD25* gene phylogenetic tree, *CcLBD25* and *TcLBD25* likely evolved convergently to function in haustorium development (Supplemental Fig. S3, Supplemental Data S1).

Development of searching hyphae

Down-regulating *CcLBD25* reduced searching hyphae formation (Fig. 7B, D, F, Supplemental Fig. S9), indicating that *CcLBD25* is involved in searching hyphae development. Surprisingly, *AtLBD25* is not only expressed in roots but is also expressed in pollen (Mangeon et al., 2010). Previous reports indicate that *AtLBD25* is especially highly expressed during the pollen late developmental stage (Kim et al., 2016). Intriguingly, many genes that are involved in haustoria development also play important roles in flower and pollen development (Yang et al., 2015; Yoshida et al., 2019). Recent research on haustoria 3D structures also indicates that the growth pattern of intrusive cells is similar to the rapid polar growth of pollen tubes (Masumoto et al., 2020). Taken together with our results in this study and previous findings in other organisms, we suggest that the genes that regulate pollen development or pollen tube growth, like *LBD25*, might be adapted by parasitic plants for development of haustorium intrusive cells and searching hyphae. This discovery also confirmed the hypothesis that parasitic plants co-opted the developmental reprogramming process from multiple sources instead of just a single organ.

Cell adhesion and cell wall loosening in parasitism

The mechanical properties and chemical conditions of cell walls have been reported to be critical for regulating plant organ morphogenesis (Chebli and Geitmann, 2017; Zhao et al., 2018). By

remodeling cell wall composition or extracellular environments, plants generate local cell wall loosening and strengthening, which allows anisotropic growth processes to occur (Chebli and Geitmann, 2017). Recent studies also indicate that the interaction between pectin and other cell wall components is an important determinant for plant organogenesis (Chebli and Geitmann, 2017; Saffer, 2018), and the interplay between PME and PMEI plays a vital role in regulating physical properties of the cell wall (Wormit and Usadel, 2018). In the root parasitic plant, *Orobanche cumana*, a PME is shown to be present at the host and parasite interface and to have pectolytic activity (Losner-Goshen et al., 1998). These results suggest that parasitic plants produce PME to degrade pectin in the host cell wall and help with haustorium penetration. Our SOM9 GCNs shows that *CcLBD25* is co-expressed with many pectin lyases and PMEIs (Fig. 2B, 3C-D, 4H-I), implying that *CcLBD25* might be the key transcription factor regulating expression of the enzymes involved in pectin remodeling. The haustoria grown on *CcLBD25* RNAi transgenic plants failed to penetrate host tissues and were unable to create a clear zone at the host and parasite interface (Fig. 7A-F), supporting the existence of a tight connection between *CcLBD25* and pectin-modifying enzymes. *CcLBD25* and PMEIs were co-expressed in the mature stage of haustorium (Fig. 4H-I), when cell wall loosening occurs for haustorium penetration.

On the other hand, since the patterns of de-methylesterification on homogalacturonans (HG) determines cell wall loosening or strengthening, pectin properties also play a role in cell adhesion, which is regulated by PME and PMEI (Wormit and Usadel, 2018). Previous studies also indicate that *Cuscuta* spp. secrete pectin-rich adhesive materials to help with adhesion and allow attachment to their hosts (Vaughn, 2002; Shimizu and Aoki, 2019). This is consistent with our discovery that both *CcLBD25* and *PMEI*s are highly expressed in the early stage of haustorium development, which would be responsible for the adhesion process in *C. campestris* (Fig. 4H-I).

Conclusions

Our detailed bioinformatic analysis on previously published *C. campestris* tissue type transcriptome coupled with LCM of RNA-Seq data from three haustorium developmental stages helped us discern the molecular mechanism of parasitic plant haustorium development. The discovery that *CcLBD25* plays a pivotal role in many aspects of haustorium formation shows that the regulatory machinery of haustorium development is potentially shared by both root and stem parasites. Although previous studies have indicated that parasitic plants evolved independently in about 13 different families, this conserved molecular mechanism supports the hypothesis that stem parasitic plants also adapted the lateral root formation programming of non-parasitic plants into haustorium development. The results of this study not only provide an insight into molecular mechanisms by which LBD25 may regulate parasitic plant haustorium development, but also raise potential for developing a universal parasitic weed-resistant crop that can defend against both stem and root parasitic plants at the same time.

Materials and Methods

Cuscuta campestris materials

We thank W. Thomas Lanini for providing dodder seeds collected from tomato field in California. These dodder materials were previously identified as *Cuscuta pentagona* (Yaakov et al., 2001), a species closely related to *Cuscuta campestris (Costea et al., 2015)*. We used molecular phylogenetics of plastid *trnL-F* intron/spacer region, plastid ribulose-1,5-bisphosphate carboxylase/oxygenase large subunit (*rbcL*), nuclear internal transcribed spacer (*nrITS*), and nuclear large-subunit ribosomal DNA (*nrLSU*) sequences (Stefanović et al., 2007; García et al., 2014; Costea et al., 2015) to verify our dodder isolate is the same as *Cuscuta campestris* 201, Rose 46281 (WTU) from USA, CA (Jhu et al., 2020) by comparing with published sequences (Costea et al., 2015).

RNA-Seq data mapping and processing

For *C. campestris* tissue type RNA-Seq analysis, we used the raw data previously published (Ranjan et al., 2014). This RNA-Seq data contain six different *C. campestris* tissues, including seeds, seedlings, stems, prehaustoria, haustoria, and flowers, grown on the tomato (*Solanum lycoperscum*) Heinz 1706 (H1706) cultivar and *Nicotiana benthamiana* (*N. benthamiana*). We mapped both *C. campestris* tissue type and LCM RNA-Seq data to the genome of *C. campestris* (Vogel et al., 2018) with Bowtie 2 (Langmead and Salzberg, 2012) and used EdgeR (Robinson et al., 2009) to get normalized trimmed mean of M values (TMM) for further analysis.

MDS and PCA with SOM clustering

After normalization steps, we used cmdscale in R stats package to create multidimensional scaling (MDS) data matrix and then generate MDS plots. For *C. campestris* tissue types RNA-Seq data, we selected genes with coefficient of variation > 0.85 for PCA analysis. We calculated principal

component values using prcomp function in R stats package. Selected genes are clustered for multilevel six-by-two hexagonal SOM using som function in the kohonen package (Wehrens and Buydens, 2007). We visualized the SOM clustering results in PCA plots. The complete gene lists for all SOM units in *C. campestris* tissue type RNA-Seq data with SOM distances and PCA principal component values are included in Supplemental Table S1. For *C. campestris* LCM RNA-Seq data, genes in the upper 50% quartile of coefficient of variation were selected for further analysis. Selected genes were then clustered for multilevel three-by-two hexagonal SOM. The complete gene lists for all SOM units in LCM RNA-Seq data with SOM distances and PCA principal component values are included in Supplemental Table S7.

Construct gene coexpression networks

We used the genes that are classified in selected SOM groups to build GCNs. The R script is modified from our previously published method (Ichihashi et al., 2014) and the updated script is uploaded to GitHub and included in code availability. The SOM9 GCNs for *C. campestris* tissue type data was constructed with normal quantile cutoff = 0.93. The SOM2+3+9 GCNs for *C. campestris* tissue type data was constructed with normal quantile cutoff =0.94. For the GCN of *C. campestris* LCM data, we used the SOM9 gene list from tissue type RNA-Seq and constructed the GCN of these genes based on the expression profiles in LCM RNA-Seq data with normal quantile cutoff =0.94. These networks were then visulaized using Cytoscape version 3.8.0.

Functional annotation and GO enrichment analysis of RNA-Seq data

Since many genes are not functionally annotated in the recently published *C. campestris* genome (Vogel et al., 2018), we used BLASTN with 1e-5 as an e-value threshold to compare our previously annotated transcriptome final contigs with current *C. campestris* genome genes and only kept the top 1 scored hit for each gene (Supplemental Table S3). After we obtained this master list, we

combined the functional annotation of our published transcriptome based on the NCBI nonredundant database and TAIR10 (Ranjan et al., 2014) with the *C. campestris* genome gene IDs to create a more complete functional annotation (Supplementary Table S9). TAIR ID hits were used for GO Enrichment Analysis on http://geneontology.org/ for gene clusters and modules.

LCM RNA-seq library preparation and sequencing

We infested approximately four-leaves-stage Heinz 1706 tomato plants with *C. campestris* strands. Tomato stems with haustoria were collected at 4 days post attachment (DPA) and fixed in formaldehyde – acetic acid – alcohol (FAA). These samples were dehydrated by the ethanol series and embedded in paraffin (Paraplast X-TRA, Thermo Fisher Scientific). We prepared 10 μm thick sections on a Leica RM2125RT rotary microtome. Approximately 30 regions of 10 um thickness each were cut from each slide, and three to four slides used per library preparation. Tissue was processed within one month of fixation to ensure RNA quality. Haustorial tissues of the 3 defined developmental stages were dissected on a Leica LMD6000 Laser Microdissection System. Tissue was collected in lysis buffer from RNAqueous-Micro Total RNA Isolation Kit (Ambion) and stored at -80 °C. RNA was extracted using RNAqueous-Micro Total RNA Isolation Kit (Ambion) and amplified using WT-Ovation Pico RNA Amplification System (ver. 1.0, NuGEN Technologies Inc.) following manufacturer instructions. RNA-seq libraries for Illumina sequencing were constructed following a previously published method (Kumar et al., 2012) with slight modifications. Libraries were quantified, pooled to equal amounts, and their quality was checked on a Bioanalyzer 2100 (Agilent). Libraries were sequenced on a HiSeq2000 Illumina Sequencer at the Vincent J Coates Genomics Sequencing Laboratory at UC Berkeley.

***CcLBD25* RNAi transgenic plants and HIGS efficiency verification**

We used the pTKO2 vector (Snowden et al., 2005; Brendolise et al., 2017), which enables streamlined cloning by using two GATEWAY cassettes positioned at opposite directions, separated by an Arabidopsis ACT2 intron, and under the control of the 35S constitutive promoter. We have previously shown that producing the RNAi construct in phloem cells specifically using the SUC2 promoter was effective for dodder HIGS (Alakonya et al., 2012). Therefore, we replaced the 35S promoter with the SUC2 promoter and generated pTKOS (Supplemental Fig. S7). We used BLAST to identify a 292 bp fragment that was specific to *CcLBD25* and different from tomato genes (Supplemental Dataset S2). This RNAi fragment was amplified from *C. campestris* gDNA, TOPO cloned into pCR8/GW-TOPO (Life Technologies) and LR recombined into pTKO2 and pTKOS (Supplemental Dataset S3). These constructs were then sent to the UC Davis Plant Transformation Facility to generate *CcLBD25* RNAi transgenic tomato plants.

All T0 transgenic plants were selected by kanamycin resistance and their gDNAs were extracted and PCR performed to verify they contained *CcLBD25* RNAi constructs. To validate HIGS efficiency and quantify the expression level of *CcLBD25* and *CcPMEI* in *C. campestris*, dodder tissues were harvested from both *C. campestris* grown on wild-type plants and T2 *CcLBD25* RNAi transgenic plants. For validating the downregulation of *CcLBD25*, we collected the stem segment with haustoria and prehaustoria at the initial attachment site from *C. campestris* grown on wild-type and RNAi transgenic plants. About 100 mg tissues were used for each RNA extraction for each genotype sample. We froze tissues in liquid nitrogen and ground them in extraction buffer using a bead beater (Mini Beadbeater 96; BioSpec Products). Following our previously published poly-A based RNA extraction method (Townsley et al., 2015), we obtained total mRNA from *C. campestris* and then used Superscript III reverse transcriptase (Invitrogen) for reverse transcription to synthesize cDNA as described by the manufacturer instructions. Real-time qPCR was performed

using a Bio-Rad iCycler iQ real-time thermal cycler with Bio-Rad IQ SYBR Green super mix. The sequences of qPCR primer pairs are included in Supplemental Table S12.

Whole-plant phenotype assays

Based on previous studies, many plant species are reported to have early flowering phenotypes in response to environmental stresses (Wada and Takeno, 2010; Riboni et al., 2014). Therefore, we grew *C. campestris* on wild-type Heinz 1706 tomatoes and *CcLBD25* RNAi T1 transgenic tomato plants and then quantified how fast these *C. campestris* plants transitioned to their reproductive stage. The number of *C. campestris* plants that transitioned to the flowering stage were counted at 9, 10, and 14 days post attachment (DPA) to test whether a stress-induced flowering phenotype could be observed.

To quantify the effect of *CcLBD25* downregulation on *C. campestris* growth, we infested 3-weeks-old tomato plants with about 10 cm stem segments *C. campestris*, which were originally grown on wild-type H1706. We harvested all *C. campestris* tissues grown on wild-type H1706 and *CcLBD25* RNAi T2 transgenic plants at 14 DPA. These *C. campestris* tissues were then carefully separated from their host plant stems by hand, and their fresh weights were measured using chemical weighing scales.

***In vitro* haustoria (IVH) system**

Inspired by the previous discovery that *Cuscuta* haustoria can be induced by physical contact and far-red light signals (Tada et al., 1996), we developed an *in vitro* haustoria (IVH) system for haustorium induction without hosts. In this method, we detached *Cuscuta* stem segments, which were right next to a stable haustorium attachment, from the *C. campestris* grown on wild-type plants and T2 *CcLBD25* RNAi transgenic plants. *Cuscuta* strands with shoot apices detached from a host plant were sandwiched between 3% Phytagel agar containing 0.5X Murashige and Skoog

medium to provide tactile stimuli (Fig. 6A-C). These combined plates were then irradiated with far-red light for two hours. After 5 days of growth in darkness in a 22 °C growth chamber, prehaustoria were readily visible (Fig. 6D-E). We then counted the number of prehaustoria under a Zeiss SteREO Discovery, V12 microscope for quantification. Since the RNAi silencing signal is systemic (Alakonya et al., 2012; David-Schwartz et al., 2008) and IVH induction is rapid, we could validate the effect of *CcLBD25* RNAi on haustoria development. We are aware of a similar system that was reported recently (Kaga et al., 2020). However, we used two layers of agar gel instead of one layer of gel with one glass slide. This prevented prehaustoria from attaching to the glass slide, making it easier to detach prehaustoria for further analysis without damaging their structure. Second, we used far-red light instead of blue light irradiation. Both methods seem to be effective.

Fresh tissue sectioning and histology

For fresh vibratome sections of haustoria attached to wild-type and *CcLBD25 RNAi* host stems, we collected samples and embedded them in 7% Plant Tissue Culture Agar. We then fixed these agar blocks in FAA (final concentration: 4% formaldehyde, 5% glacial acetic acid, and 50% ethanol) overnight, 50% ethanol for one hour, and then transferred the samples to 70% ethanol for storage. These agar blocks were then sectioned using Lancer Vibratome Series 1000 to prepare 100 μm sections. We kept these sections in 4°C water and then conducted Toluidine Blue O Staining. We followed the published protocol (O'Brien et al., 1964) with some modifications. The sections were immersed in the stain for 30 seconds, and then washed with water three times for 30 seconds each wash. After removing the agar from around the sections using forceps, we mounted the sections with water on a slide and imaged using a Zeiss SteREO Discovery, V12 microscope, and a Nikon Eclipse E600 microscope.

Competing interests: The authors declare that they have no competing interests.

Code availability

Updated R scripts for MDS, PCA and SOM analysis and gene coexpression network analysis are all deposited on GitHub (Link: https://github.com/MinYaoJhu/CcLBD25_project.git).

Data availability

All data is available in the main text or the supplementary materials. LCM RNA-Seq raw data are deposited on NCBI SRA PRJNA687611.

Acknowledgements

We are grateful to the UC Davis Plant Transformation Facility for generating *CcLBD25* RNAi transgenic tomato plants. We thank Kristina Zumstein for help in maintaining transgenic tomato seed stocks, and Richard Philbrook, Kaiwen Zhang, and Junqi Lu for helping with some parts of experiments and vibratome sectioning. We also thank Aaron Leichty, Steven Rowland and Karo Czarnecki for their input on bioinformatics analyses. **Funding:** This work was funded by USDA-NIFA (2013-02345). M.-Y. J. was supported by Yen Chuang Taiwan Fellowship, Taiwan Government Scholarship (GSSA), Elsie Taylor Stocking Memorial Fellowship, Katherine Esau Summer Graduate Fellowship, Loomis Robert S. and Lois Ann Graduate Fellowship in Agronomy, and the UCD Graduate Research Award. Y. I. was supported by Grant-in-Aid for Young Scientists from the Ministry of Education, Culture, Sports, Science and Technology, Japan [B; grant no. 15K18589 to YI].

Figures

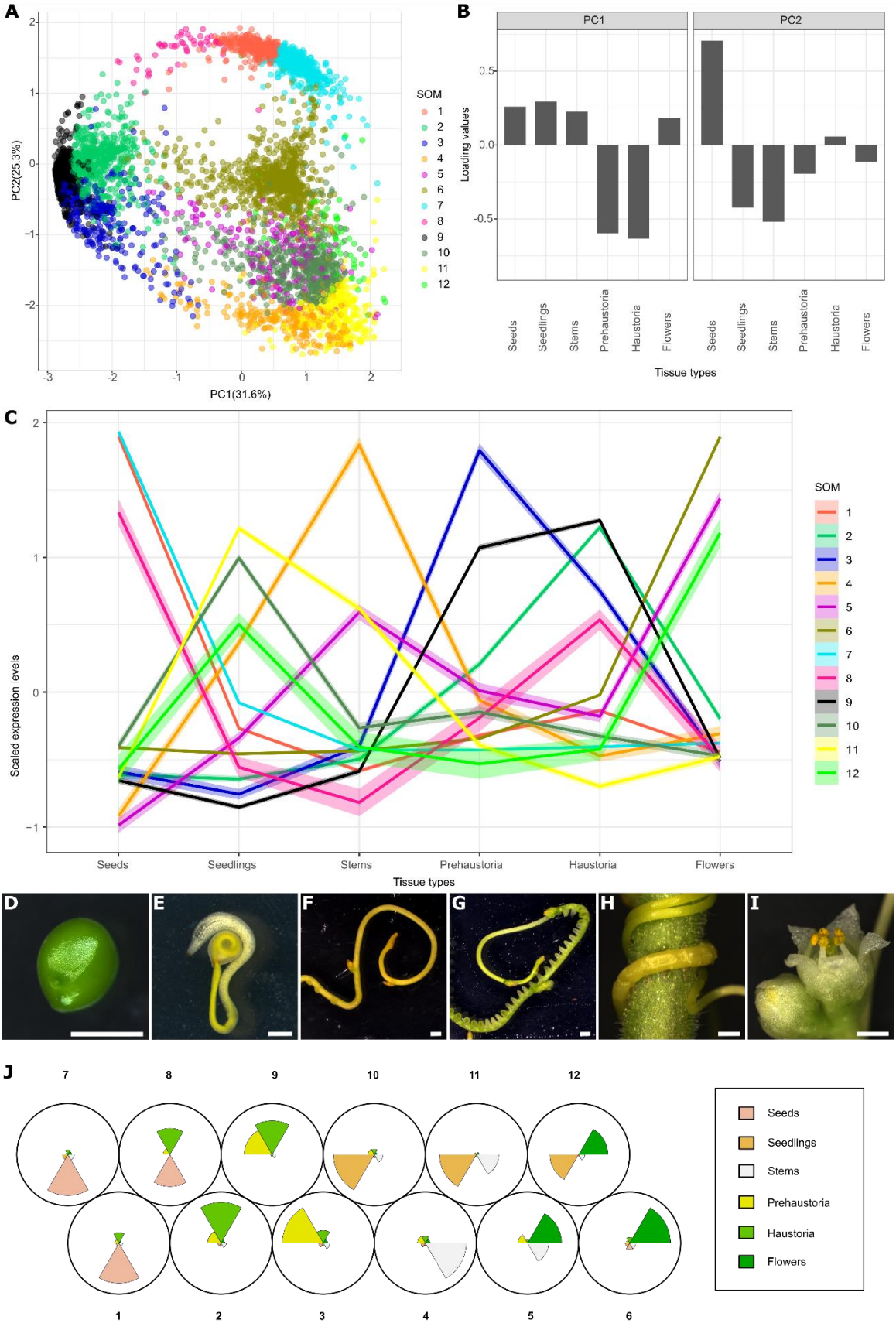
A
PC2(25.3%)
PC1(31.6%)
SOM
1
2
3
4
5
6
7
8
9
10
11
12
B
PC1
PC2
Loading values
Seeds
Seedlings
Stems
Prehaustoria
Haustoria
Flowers
Tissue types
C
Scaled expression levels
Tissue types
D
E
F
G
H
I
J
7
8
9
10
11
12
1
2
3
4
5
6
Seeds
Seedlings
Stems
Prehaustoria
Haustoria
Flowers

Figure 1. Principal component analysis (PCA) and self-organizing maps (SOM) clustering of gene expression in *C. campestris* tissue type RNA-Seq data mapped to *C. campestris* genome. (A) PCA analysis based on gene expression across different *C. campestris* tissues. Each dot represents a gene and is in the color indicating its corresponding SOM group. The percentage next to each axis indicates the proportion of variance that can be explained by the principal component. (B) Loading values of PC1 and PC2. PC1 separates the genes that are specifically expressed in intrusive tissues (prehaustoria and haustoria) from those that are expressed in non-intrusive tissues. PC2 divides the seed-specific genes from other genes. (C) Scaled expression levels of each SOM group across different *C. campestris* tissue types. Each line is colored based on the corresponding SOM groups. The highlighting around the lines indicates a 95% confidence interval. (D-I) The six different tissue types that were used in this transcriptomic study. Scale bars = 1 mm. (D) Seed. (E) Seedling. (F) Stem. (G) Prehaustoria. (H) Haustoria. White arrowheads indicate haustoria. (I) Flowers. (J) A code plot of SOM clustering based on gene expression in *C. campestris* tissue type RNA-Seq data mapped to the *C. campestris* genome. Each sector represents a tissue type and is in the color indicating its corresponding tissue type. The size of each sector illustrates the amount of expression from each tissue type in SOM groups.

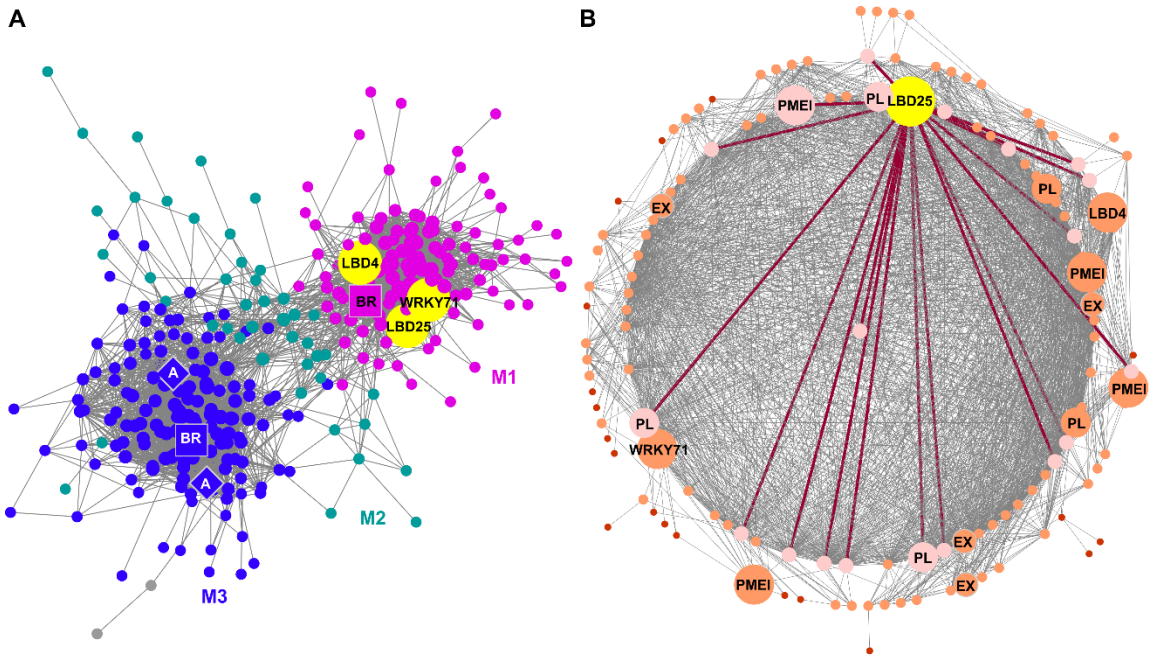

Figure 2. SOM9 gene-coexpression networks (GCNs) from *C. campestris* tissue type RNA-Seq data. (A) GCN of genes that are classified in SOM9, which includes genes that are highly expressed in both prehaustoria and haustoria. This SOM9 GCN is composed of three major modules. Magenta indicates genes in Module 1, which has enriched biological process GO term "plant-type cell wall loosening." Cyan indicates genes in Module 2. Blue indicates genes in Module 3, which has enriched biological process GO terms "transport, response to hormones, secondary metabolite biosynthetic process, and regulation of lignin biosynthetic process". The only three transcription factors (TFs) in module 1 are enlarged and labeled in yellow. The genes involved in auxin transport are labeled in diamonds. The genes involved in brassinosteroid signaling are labeled in squares. (B) GCN of genes that are classified in SOM9 Module 1. Dark red lines indicate the connection between *CcLBD25* (yellow) and its first layer neighbors. The genes that are first layer neighbors of *CcLBD25* are labeled in pink. The genes that are second layer neighbors of *CcLBD25* are labeled in orange with medium size dots. The genes that are outside the second layer neighbors of *CcLBD25* are labeled in red with small size dots. The only three TFs as well as cell wall loosening

related genes are enlarged, highlighted and labeled in the network. (A, B) PL, pectin lyase. PMEI, pectin methyl-esterase inhibitor. EX, expansin. A, auxin efflux carrier-like protein. BR, brassinosteroid insensitive 1-associated receptor kinase 1-like.

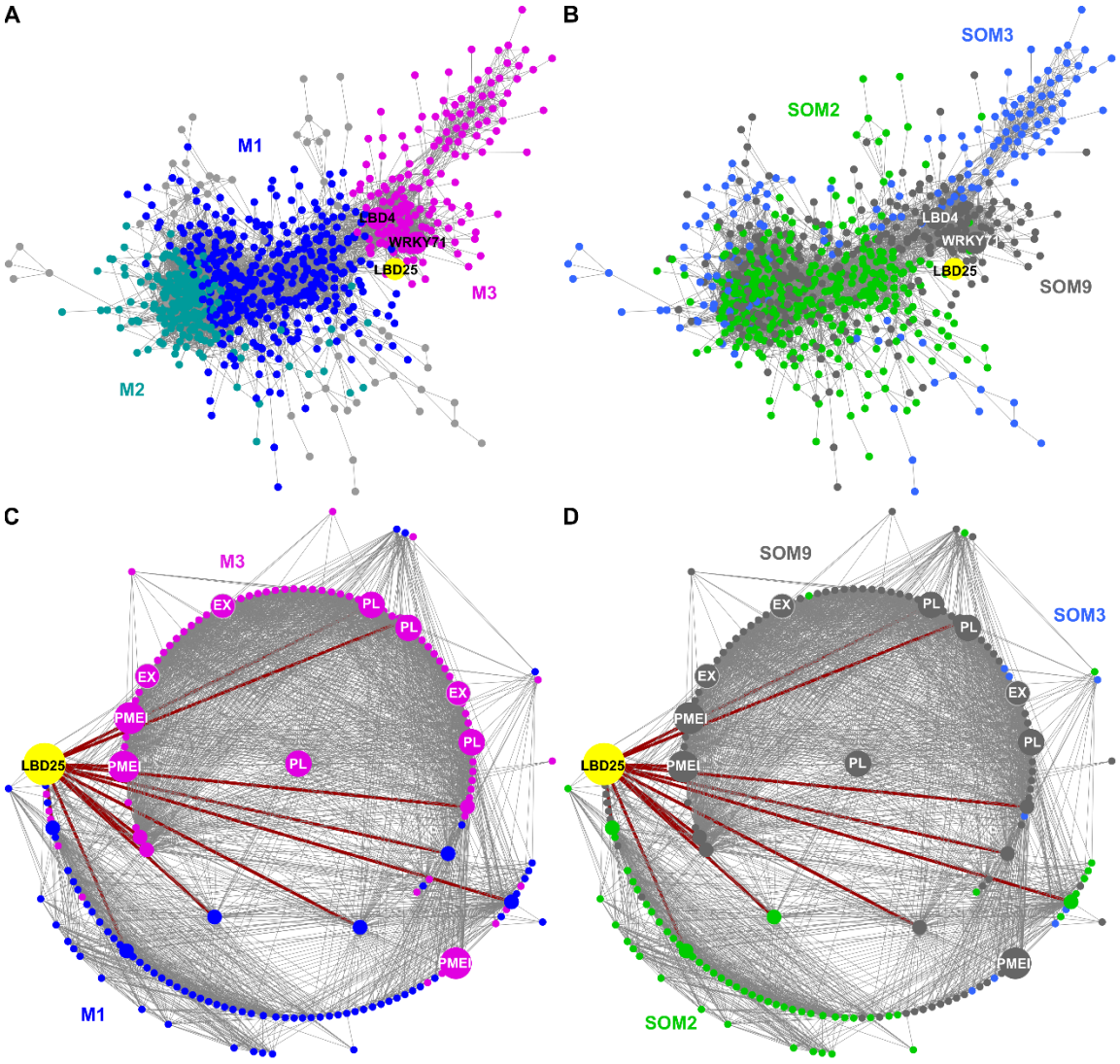

Figure 3. GCNs of SOM2, 3, 9 genes based on *C. campestris* tissue type RNA-Seq data. (A) GCN of genes that are in SOM2, SOM3, and SOM9 with colors based on network modules. This SOM2+SOM3+SOM9 GCN is composed of three major modules. Blue indicates genes in Module 1, which has the biological process GO enrichment "morphogenesis of a branching structure, plant organ formation, strigolactone responses and biosynthetic processes." Cyan indicates genes in Module 2, which has the biological process GO enrichment "response to karrikin, hormone-mediated signaling pathway and defense response." Magenta indicates genes in Module 3, which has the biological process GO enrichment "plant-type cell wall loosening." Light grey indicates

genes that are not included in Module 1, 2, or, 3. (B) GCN of genes that are in SOM2, SOM3, and SOM9, with colors based on SOM clustering groups. Green indicates genes in SOM2. Blue indicates genes in SOM3. Grey indicates genes in SOM9, which includes the genes that are highly expressed in both prehaustoria and haustoria. SOM2 includes genes that are only highly expressed in haustoria and SOM3 includes genes that are only highly expressed in prehaustoria. (C) GCN of *CcLBD25* and its first and second layer neighbors with colors based on network modules as in A. (D) GCN of *CcLBD25* and its first and second layer neighbors with colors based on SOM clustering groups as in B. (C, D) Dark red lines indicate the connection between *CcLBD25* and its first layer neighbors. The genes that are second layer neighbors of *CcLBD25* are labeled with medium size dots. The genes that are outside the second layer neighbors of *CcLBD25* are labeled with small size dots. *CcLBD25* and cell wall loosening related genes are enlarged, highlighted and labeled in the network. PL, pectin lyase. PMEI, pectin methyl-esterase inhibitor. EX, expansin.

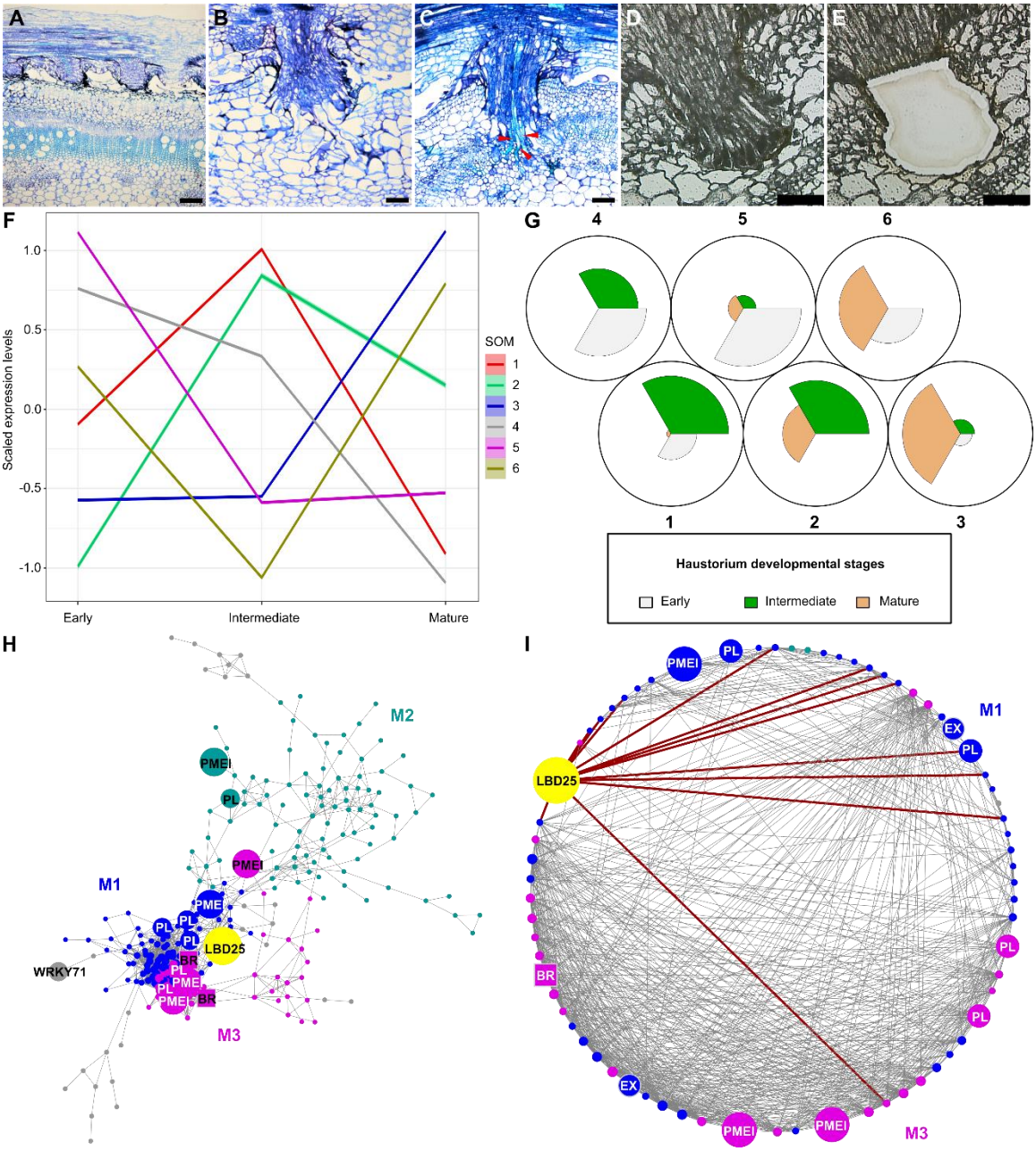

Figure 4. SOM clustering and GCNs of gene expression in *C. campestris* haustoria across three developmental stages (from the LCM RNA-Seq data). (A-E) Sections of developmental stages for laser-capture microdissection (LCM) RNA-Seq. (A-C) Three developmental stages for LCM RNA-Seq. Paraffin sections stained with Toluidine Blue. (A) Early stage. (B) Intermediate stage. (C) Mature stage. The red arrowheads indicate vascular connections between host and *C.*

campestris. (D-E) The *C. campestris* haustorium tissues were collected using LCM. (A, C) Scale bars = 250 µm (B, D E) Scale bars = 100 µm. (F) Scaled expression levels of each SOM group across three haustorium developmental stages. Each line is colored based on the corresponding SOM group. The highlighting around the lines indicates a 95% confidence interval. (G) A code plot of SOM clustering illustrating which developmental stages are highly represented in each SOM group by the size of sectors. Each sector represents a developmental stage and is in the color indicating its corresponding developmental stage. (H) GCN based on LCM RNA-Seq expression profiles with genes in tissue type RNA-Seq SOM9. Blue indicates genes in Module 1, which has enriched biological process GO term "plant-type cell wall loosening." Cyan indicates genes in Module 2, which has enriched biological process GO term "respiratory burst." Magenta indicates genes in Module 3, which has enriched biological process GO term "brassinosteroid mediated signaling pathway." Light grey indicates genes that are not included in Module 1, 2, or, 3. *CcLBD25*, *CcWRKY71* and pectin degradation related genes are enlarged, highlighted and labeled in the network. The genes involved in brassinosteroid signaling are labeled in squares. (I) GCN of *CcLBD25* and its first and second layer neighbors with colors based on network modules as in H. Dark red lines indicate the connection between *CcLBD25* and its first layer neighbors. *CcLBD25* and cell wall loosening related genes are enlarged, highlighted and labeled in the network. (H-I) PL, pectin lyase. PMEI, pectin methyl-esterase inhibitor. EX, expansin. BR, brassinosteroid insensitive 1-associated receptor kinase 1-like.

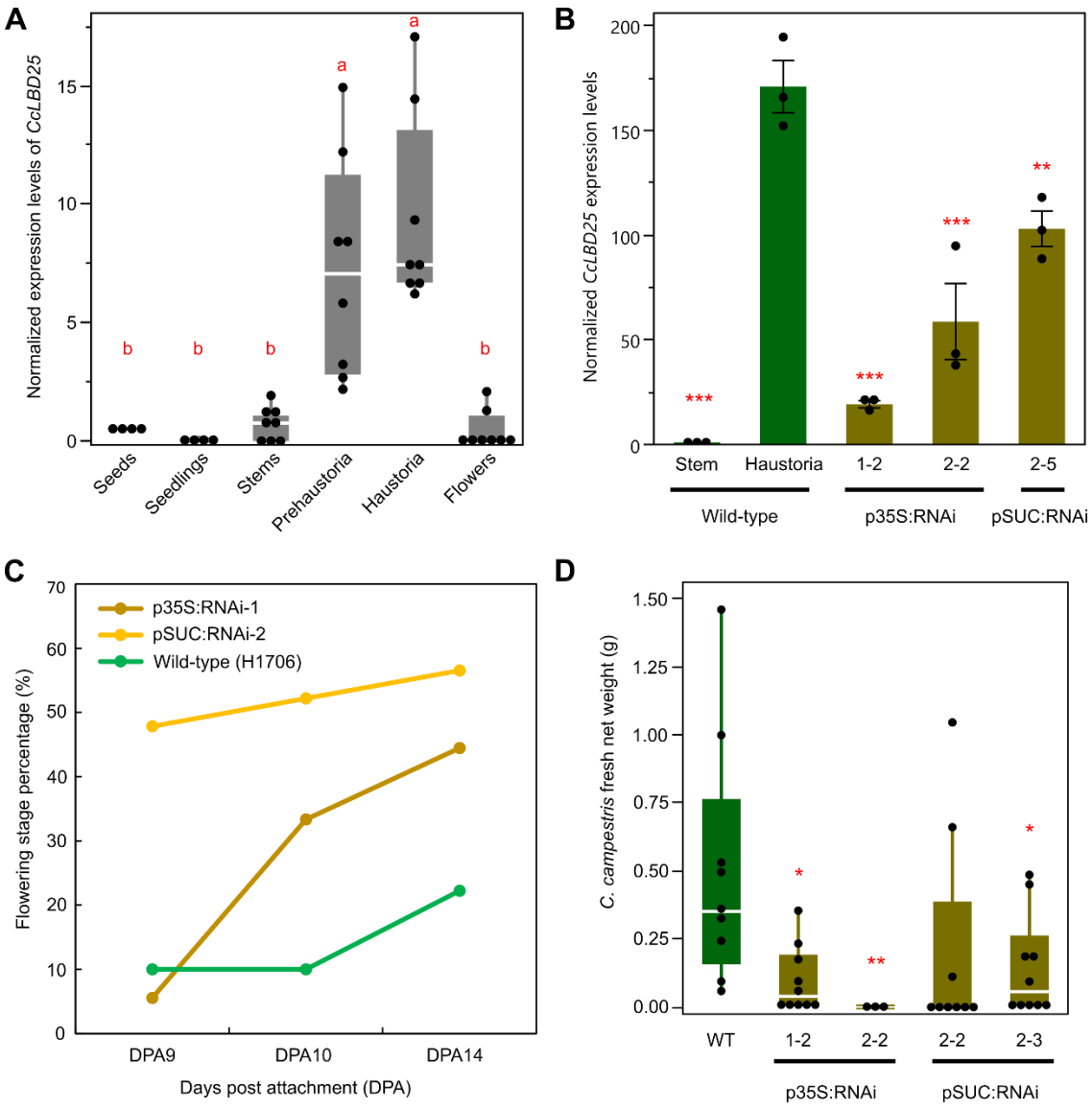

Figure 5. Gene expression levels and whole-plant phenotypes of *C. campestris* growing on Host-Induced Gene Silencing (HIGS) *CcLBD25* RNAi transgenic plants. (A) The normalized expression level of *CcLBD25* in six different tissue types of *C. campestris* (from RNA-Seq data). Data presented are assessed using pair-wise comparisons with the Tukey test. P-values of the contrasts between "a" and "b" are less than 0.001. (B) Expression levels of *CcLBD25* in *C. campestris* haustoria grown on wild-type tomatoes and T2 *CcLBD25* RNAi transgenic plants (by RT-qPCR). Data presented are assessed using one-tailed Welch's t-test with wild-type haustoria as

control. “*” p-value < 0.05. “**” p-value < 0.01. “***” p-value < 0.005. The error bars indicate standard errors of the data. All data points are plotted as black dots. (C) The flowering time of *C. campestris* growing on wild-type tomatoes and T1 *CcLBD25* RNAi transgenic plants. The early transition to the flowering stage indicates that *C. campestris* may be growing under stress conditions because they might not obtain sufficient nutrients from their host. DPA, days post attachment. Quantification was assessed with the whole plant as a unit. Sample size: wild-type, 9 biological replicates; p35S:RNAi-1, 18 biological replicates; pSUC:RNAi-2, 23 biological replicates. (D) Biomass of *C. campestris* growing on wild-type tomatoes and T2 *CcLBD25* RNAi transgenic plants. Fresh net weights of *C. campestris* were measured in grams (g). Data presented are assessed using one-tailed Welch's t-test with wild-type (WT) as control. “*” p-value < 0.05. “**” p-value < 0.01. (B, C, D) p35S:RNAi indicates the transgenic plants with the 35S promoter driving the *CcLBD25* RNAi construct. pSUC:RNAi indicates the transgenic plants with the SUC2 promoter driving the *CcLBD25* RNAi construct. (A, D) The centerline in the box indicates the median. The bottom and top of the box indicate the 25th and 75th quantiles. The whiskers represent the expected variation of the data. The whiskers extend 1.5 times the interquartile range from the top and bottom of the box. All measured data points are plotted as black dots.

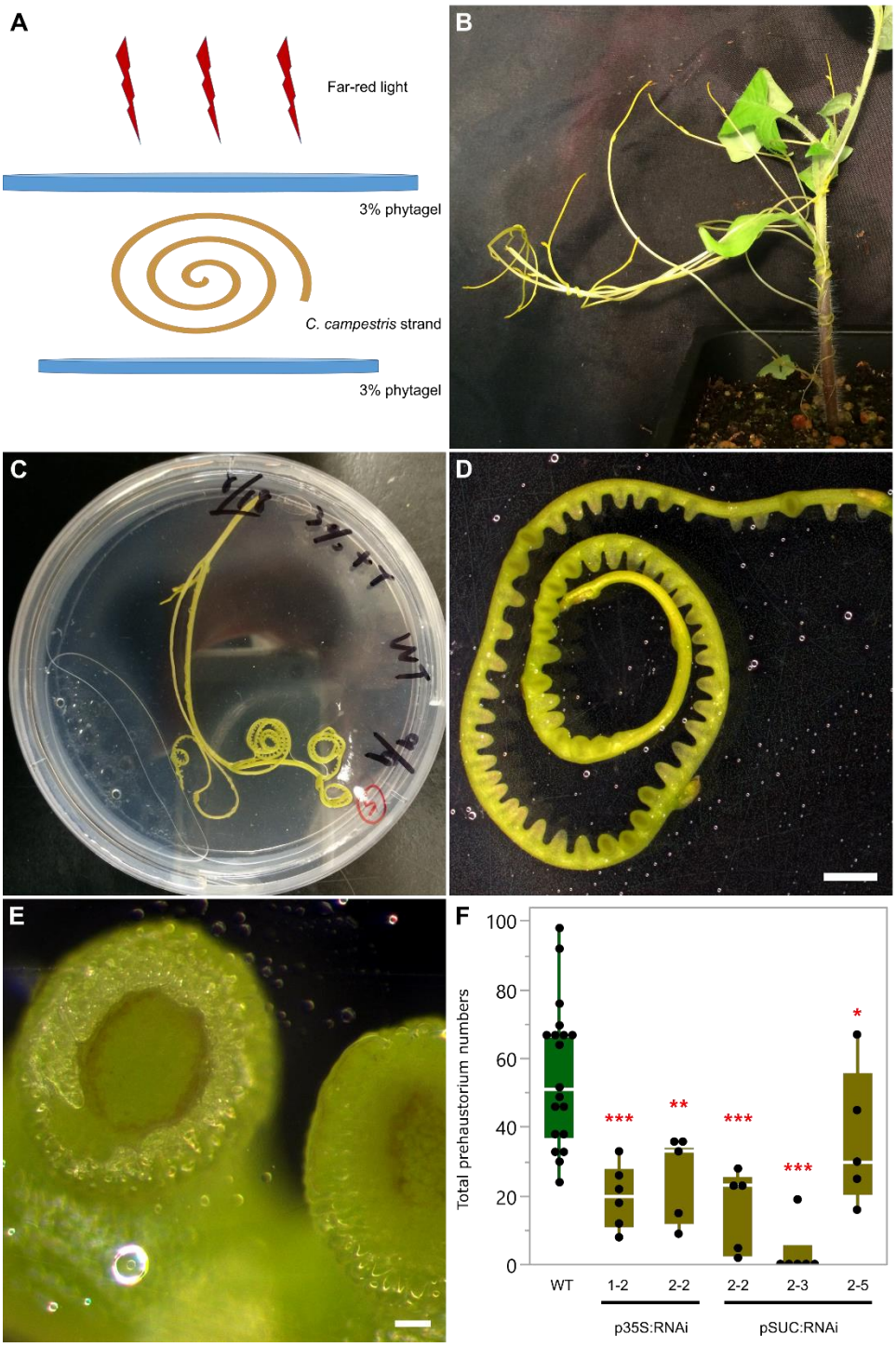

Figure 6. Far-red light-induced *in vitro* haustorium (IVH) phenotypes of *C. campestris* growing on T2 HIGS *CcLBD25* RNAi transgenic plants. (A) An illustration of the setup for the IVH system. Each *C. campestris* strand that was used in the IVH system is about 10 centimeters long. (B) *C.*

campestris strands near the haustorium attachment sites. (C) An IVH plate with a *C. campestris* strand sandwiched in between two layers of agar to provide sufficient physical contact signals. (D, E) After illuminating these plates under far-light for 5 days, prehaustoria are readily visible. (D) Scale bar = 2 mm. (E) Scale bar = 100 μm. (F) *C. campestris* strands were detached and subjected to IVH, and the numbers of prehaustoria were counted. Data presented are assessed using one-tailed Welch's t-test with wild-type (WT) as control. "*" p-value < 0.06. "**" p-value < 0.001. "***" p-value < 0.0005. p35S:RNAi indicates the transgenic plants with the 35S promoter driving the *CcLBD25* RNAi construct. pSUC:RNAi indicates the transgenic plants with the SUC2 promoter driving the *CcLBD25* RNAi construct. The centerline in the box indicates the median. The bottom and top of the box indicate the 25th and 75th quantiles. The whiskers represent the expected variation of the data. The whiskers extend 1.5 times the interquartile range from the top and bottom of the box. All measured data points are plotted as black dots.

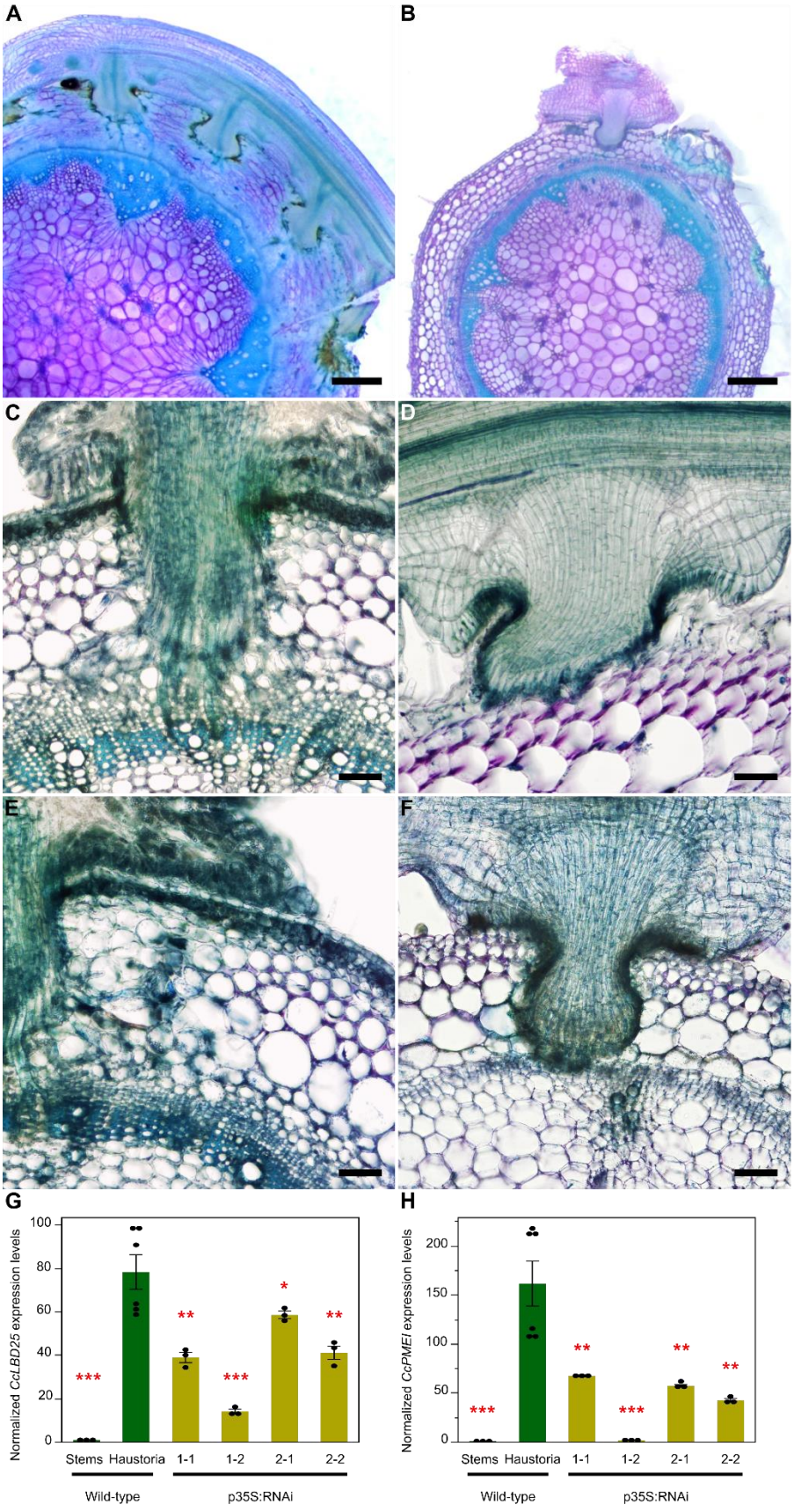
A
B
C
D
E
F
G
H
Normalized CcLBD25 expression levels
100
80
60
40
20
0
***
**
***
*
**
Stems
Haustoria
1-1
1-2
2-1
2-2
Wild-type
p35S:RNAi
Normalized CcPMEI expression levels
200
150
100
50
0
***
**
***
**
**
Stems
Haustoria
1-1
1-2
2-1
2-2
Wild-type
p35S:RNAi

Figure 7. Haustorium phenotypes and gene expression levels of *C. campestris* growing on HIGS *CcLBD25* RNAi transgenic plants. (A, C, E) *C. campestris* haustoria growing on a wild-type H1706 host. (B, D, F) *C. campestris* haustoria growing on T2 *CcLBD25* RNAi transgenic tomato plants. (B) p35S:RNAi line 1-1. (D) pSUC:RNAi line 1-2. (F) p35S:RNAi line 1-2. (A, B) Scale bars = 500 µm. (C, D, E, F) Scale bars = 100 µm. (A-F) 100 µm thick vibratome sections of fresh haustorium stained with Toluidine Blue O. (G, H) Expression levels of *CcLBD25* and *CcPMEI* in *C. campestris* haustoria grown on wild-type tomatoes and *CcLBD25* RNAi transgenic plants. Data presented are assessed using one-tailed Welch's t-test with wild-type haustoria as control. "*" p-value < 0.05. "**" p-value < 0.005. "***" p-value < 0.001. p35S:RNAi indicates the transgenic plants with the 35S promoter driving *CcLBD25* RNAi construct. The error bars indicate standard errors of the data.

References

Agrios GN (2005) chapter thirteen - PLANT DISEASES CAUSED BY PARASITIC HIGHER PLANTS, INVASIVE CLIMBING PLANTS, AND PARASITIC GREEN ALGAE. *In* Plant Pathology (Fifth Edition). Academic Press, San Diego, pp 705-722

Alakonya A, Kumar R, Koenig D, Kimura S, Townsley B, Runo S, Garces HM, Kang J, Yanez A, David-Schwartz R, Machuka J, Sinha N (2012) Interspecific RNA Interference of SHOOT MERISTEMLESS-Like Disrupts Cuscuta pentagona Plant Parasitism. The Plant Cell **24:** 3153-3166

Brendolise C, Montefiori M, Dinis R, Peeters N, Storey RD, Rikkerink EH (2017) A novel hairpin library-based approach to identify NBS–LRR genes required for effector-triggered hypersensitive response in Nicotiana benthamiana. Plant Methods **13:** 32

Chebli Y, Geitmann A (2017) Cellular growth in plants requires regulation of cell wall biochemistry. Current Opinion in Cell Biology **44:** 28-35

Clauset A, Newman MEJ, Moore C (2004) Finding community structure in very large networks. Physical Review E **70:** 066111

Cline MS, Smoot M, Cerami E, Kuchinsky A, Landys N, Workman C, Christmas R, Avila-Campilo I, Creech M, Gross B, Hanspers K, Isserlin R, Kelley R, Killcoyne S, Lotia S, Maere S, Morris J, Ono K, Pavlovic V, Pico AR, Vailaya A, Wang P-L, Adler A, Conklin BR, Hood L, Kuiper M, Sander C, Schmulevich I, Schwikowski B, Warner GJ, Ideker T, Bader GD (2007) Integration of biological networks and gene expression data using Cytoscape. Nat. Protocols **2:** 2366-2382

Costea M, García MA, Baute K, Stefanović S (2015) Entangled evolutionary history of Cuscuta pentagona clade: A story involving hybridization and Darwin in the Galapagos. TAXON **64:** 1225-1242

David-Schwartz R, Runo S, Townsley B, Machuka J, Sinha N (2008) Long-distance transport of mRNA via parenchyma cells and phloem across the host–parasite junction in Cuscuta. New Phytologist **179:** 1133-1141

Dean G, Casson S, Lindsey K (2004) KNAT6 gene of Arabidopsis is expressed in roots and is required for correct lateral root formation. Plant Molecular Biology **54:** 71-84

Furuhashi T, Furuhashi K, Weckwerth W (2011) The parasitic mechanism of the holostemparasitic plant Cuscuta. Journal of Plant Interactions **6:** 207-219

García MA, Costea M, Kuzmina M, Stefanović S (2014) Phylogeny, character evolution, and biogeography of Cuscuta (dodders; Convolvulaceae) inferred from coding plastid and nuclear sequences. American Journal of Botany **101:** 670-690

Goh T, Joi S, Mimura T, Fukaki H (2012) The establishment of asymmetry in *Arabidopsis* lateral root founder cells is regulated by LBD16/ASL18 and related LBD/ASL proteins. Development **139:** 883-893

Ichihashi Y, Aguilar-Martínez JA, Farhi M, Chitwood DH, Kumar R, Millon LV, Peng J, Maloof JN, Sinha NR (2014) Evolutionary developmental transcriptomics reveals a gene network module regulating interspecific diversity in plant leaf shape. Proceedings of the National Academy of Sciences **111:** E2616-E2621

Ichihashi Y, Hakoyama T, Iwase A, Shirasu K, Sugimoto K, Hayashi M (2020) Common Mechanisms of Developmental Reprogramming in Plants—Lessons From Regeneration, Symbiosis, and Parasitism. Frontiers in Plant Science **11**

Ichihashi Y, Kusano M, Kobayashi M, Suetsugu K, Yoshida S, Wakatake T, Kumaishi K, Shibata A, Saito K, Shirasu K (2017) Transcriptomic and Metabolomic Reprogramming from Roots to Haustoria in the Parasitic Plant, Thesium chinense. Plant and Cell Physiology **59:** 729-738

Jhu M-Y, Farhi M, Wang L, Philbrook RN, Belcher MS, Nakayama H, Zumstein KS, Rowland SD, Ron M, Shih PM, Sinha NR (2020) Lignin-based resistance to *Cuscuta campestris* parasitism in Heinz resistant tomato cultivars. bioRxiv**:** 706861

Johnson NR, dePamphilis CW, Axtell MJ (2019) Compensatory sequence variation between trans-species small RNAs and their target sites. eLife **8:** e49750

Kaga Y, Yokoyama R, Sano R, Ohtani M, Demura T, Kuroha T, Shinohara N, Nishitani K (2020) Interspecific Signaling Between the Parasitic Plant and the Host Plants Regulate Xylem Vessel Cell Differentiation in Haustoria of Cuscuta campestris. Frontiers in Plant Science **11**

Kim G, LeBlanc ML, Wafula EK, dePamphilis CW, Westwood JH (2014) Genomic-scale exchange of mRNA between a parasitic plant and its hosts. Science **345:** 808-811

Kim M, Kim M-J, Pandey S, Kim J (2016) Expression and Protein Interaction Analyses Reveal Combinatorial Interactions of LBD Transcription Factors During Arabidopsis Pollen Development. Plant and Cell Physiology **57:** 2291-2299

Kumar R, Ichihashi Y, Kimura S, Chitwood D, Headland L, Peng J, Maloof J, Sinha N (2012) A High-Throughput Method for Illumina RNA-Seq Library Preparation. Frontiers in Plant Science **3**

Kumar S, Stecher G, Li M, Knyaz C, Tamura K (2018) MEGA X: Molecular Evolutionary Genetics Analysis across Computing Platforms. Molecular Biology and Evolution **35:** 1547-1549

López-Ráez JA, Matusova R, Cardoso C, Jamil M, Charnikhova T, Kohlen W, Ruyter-Spira C, Verstappen F, Bouwmeester H (2009) Strigolactones: ecological significance and use as a target for parasitic plant control. Pest Management Science **65:** 471-477

Langmead B, Salzberg SL (2012) Fast gapped-read alignment with Bowtie 2. Nature Methods **9:** 357-359

Losner-Goshen D, Portnoy VH, Mayer AM, Joel DM (1998) Pectolytic Activity by the Haustorium of the Parasitic PlantOrobancheL. (Orobanchaceae) in Host Roots. Annals of Botany **81:** 319-326

Mangeon A, Bell EM, Lin W-c, Jablonska B, Springer PS (2010) Misregulation of the LOB domain gene DDA1 suggests possible functions in auxin signalling and photomorphogenesis. Journal of Experimental Botany **62:** 221-233

Masumoto N, Suzuki Y, Cui S, Wakazaki M, Sato M, Kumaishi K, Shibata A, Furuta KM, Ichihashi Y, Shirasu K, Toyooka K, Sato Y, Yoshida S (2020) Three-dimensional reconstructions of the internal structures of haustoria in parasitic Orobanchaceae. bioRxiv**:** 2020.2005.2007.083055

O'Brien TP, Feder N, McCully ME (1964) Polychromatic staining of plant cell walls by toluidine blue O. Protoplasma **59:** 368-373

Parker C (2021) *Cuscuta campestris* (field dodder) in Invasive Species Compendium. *In*. CAB International, Wallingford, UK

Porco S, Larrieu A, Du Y, Gaudinier A, Goh T, Swarup K, Swarup R, Kuempers B, Bishopp A, Lavenus J, Casimiro I, Hill K, Benkova E, Fukaki H, Brady SM, Scheres B, Péret B, Bennett MJ (2016) Lateral root emergence in *Arabidopsis* is dependent on transcription factor LBD29 regulation of auxin influx carrier *LAX3*. Development **143:** 3340-3349

Ranjan A, Ichihashi Y, Farhi M, Zumstein K, Townsley B, David-Schwartz R, Sinha NR (2014) De Novo Assembly and Characterization of the Transcriptome of the Parasitic Weed Dodder Identifies Genes Associated with Plant Parasitism. Plant Physiology **166:** 1186-1199

Riboni M, Robustelli Test A, Galbiati M, Tonelli C, Conti L (2014) Environmental stress and flowering time: The photoperiodic connection. Plant Signaling & Behavior **9:** e29036

Robinson MD, McCarthy DJ, Smyth GK (2009) edgeR: a Bioconductor package for differential expression analysis of digital gene expression data. Bioinformatics **26:** 139-140

Runo S, Alakonya A, Machuka J, Sinha N (2011) RNA interference as a resistance mechanism against crop parasites in Africa: a 'Trojan horse' approach. Pest Management Science **67:** 129-136

Runyon JB, Mescher MC, Felton GW, De Moraes CM (2010) Parasitism by Cuscuta pentagona sequentially induces JA and SA defence pathways in tomato. Plant, Cell & Environment **33:** 290-303

Saffer AM (2018) Expanding roles for pectins in plant development. Journal of Integrative Plant Biology **60:** 910-923

Shen H, Ye W, Hong L, Huang H, Wang Z, Deng X, Yang Q, Xu Z (2006) Progress in Parasitic Plant Biology: Host Selection and Nutrient Transfer. Plant Biology **8:** 175-185

Shimizu K, Aoki K (2019) Development of Parasitic Organs of a Stem Holoparasitic Plant in Genus Cuscuta. Frontiers in plant science **10:** 1435-1435

Snowden KC, Simkin AJ, Janssen BJ, Templeton KR, Loucas HM, Simons JL, Karunairetnam S, Gleave AP, Clark DG, Klee HJ (2005) The *Decreased apical dominance1/Petunia hybrida CAROTENOID CLEAVAGE DIOXYGENASE8* Gene Affects Branch Production and Plays a Role in Leaf Senescence, Root Growth, and Flower Development. The Plant Cell **17:** 746-759

Stefanović S, Kuzmina M, Costea M (2007) Delimitation of major lineages within Cuscuta subgenus Grammica (Convolvulaceae) using plastid and nuclear DNA sequences. American Journal of Botany **94:** 568-589

Sun G, Xu Y, Liu H, Sun T, Zhang J, Hettenhausen C, Shen G, Qi J, Qin Y, Li J, Wang L, Chang W, Guo Z, Baldwin IT, Wu J (2018) Large-scale gene losses underlie the genome evolution of parasitic plant Cuscuta australis. Nature Communications **9**

Tada Y, Sugai M, Furuhashi K (1996) Haustoria of Cuscuta japonica, a Holoparasitic Flowering Plant, Are Induced by the Cooperative Effects of Far-Red Light and Tactile Stimuli. Plant and Cell Physiology **37:** 1049-1053

Townsley BT, Covington MF, Ichihashi Y, Zumstein K, Sinha NR (2015) BrAD-seq: Breath Adapter Directional sequencing: a streamlined, ultra-simple and fast library preparation protocol for strand specific mRNA library construction. Frontiers in Plant Science **6**

Vaughn KC (2002) Attachment of the parasitic weed dodder to the host. Protoplasma **219:** 227-237

Vogel A, Schwacke R, Denton AK, Usadel B, Hollmann J, Fischer K, Bolger A, Schmidt MHW, Bolger ME, Gundlach H, Mayer KFX, Weiss-Schneeweiss H, Temsch EM,

Krause K (2018) Footprints of parasitism in the genome of the parasitic flowering plant Cuscuta campestris. Nature Communications **9:** 2515

Wada KC, Takeno K (2010) Stress-induced flowering. Plant Signaling & Behavior **5:** 944-947

Wehrens R, Buydens L (2007) Self- and Super-organizing Maps in R: The kohonen Package. Journal of Statistical Software **21:** 1-19

Wormit A, Usadel B (2018) The Multifaceted Role of Pectin Methylesterase Inhibitors (PMEIs). International journal of molecular sciences **19:** 2878

Yaakov G, Lanini WT, Wrobel RL (2001) Tolerance of Tomato Varieties to Lespedeza Dodder. Weed Science **49:** 520-523

Yang Z, Wafula EK, Honaas LA, Zhang H, Das M, Fernandez-Aparicio M, Huang K, Bandaranayake PCG, Wu B, Der JP, Clarke CR, Ralph PE, Landherr L, Altman NS, Timko MP, Yoder JI, Westwood JH, dePamphilis CW (2015) Comparative transcriptome analyses reveal core parasitism genes and suggest gene duplication and repurposing as sources of structural novelty. Molecular biology and evolution **32:** 767-790

Yoder JI, Scholes JD (2010) Host plant resistance to parasitic weeds; recent progress and bottlenecks. Current Opinion in Plant Biology **13:** 478-484

Yoshida S, Kim S, Wafula EK, Tanskanen J, Kim Y-M, Honaas L, Yang Z, Spallek T, Conn CE, Ichihashi Y, Cheong K, Cui S, Der JP, Gundlach H, Jiao Y, Hori C, Ishida JK, Kasahara H, Kiba T, Kim M-S, Koo N, Laohavisit A, Lee Y-H, Lumba S, McCourt P, Mortimer JC, Mutuku JM, Nomura T, Sasaki-Sekimoto Y, Seto Y, Wang Y, Wakatake T, Sakakibara H, Demura T, Yamaguchi S, Yoneyama K, Manabe R-i, Nelson DC, Schulman AH, Timko MP, dePamphilis CW, Choi D, Shirasu K (2019)

Genome Sequence of *Striga asiatica* Provides Insight into the Evolution of Plant Parasitism. Current Biology **29:** 3041-3052.e3044

Zhao F, Chen W, Traas J (2018) Mechanical signaling in plant morphogenesis. Current Opinion in Genetics & Development **51:** 26-30

Supplemental Data

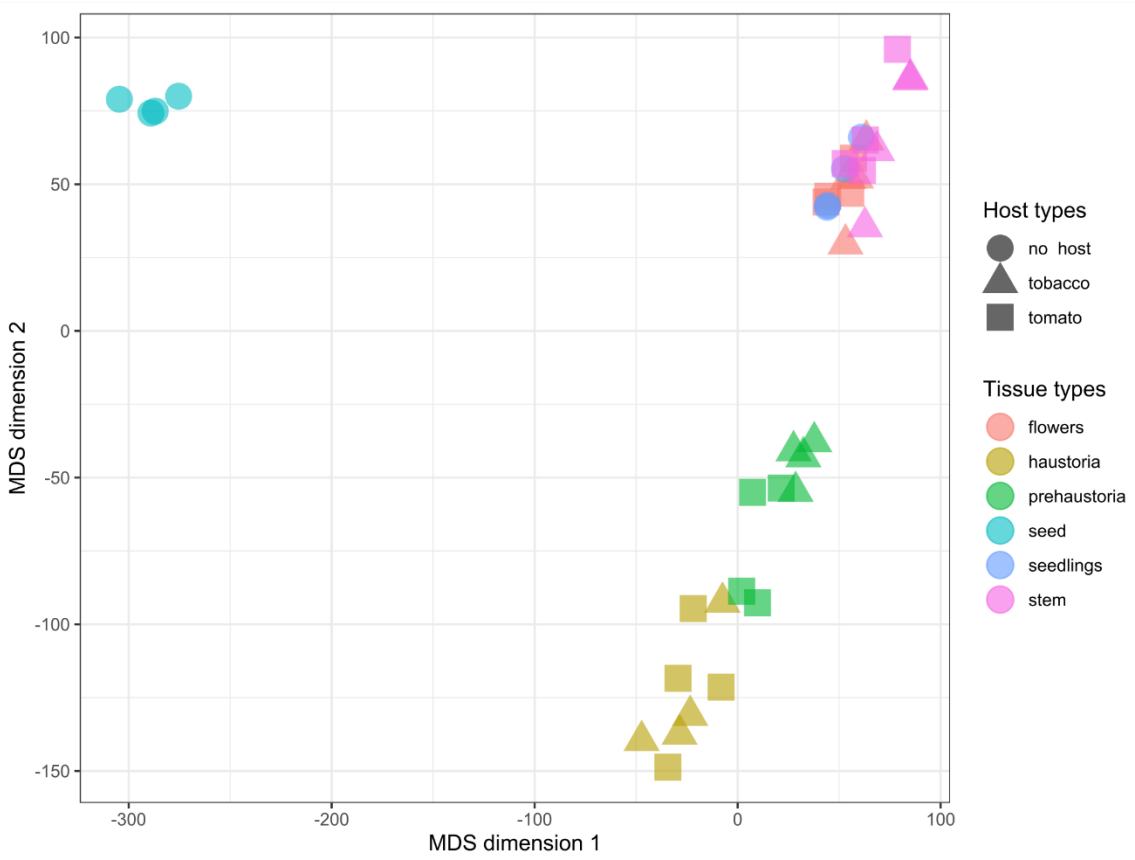

Supplemental Figure S1. Multidimensional scaling (MDS) plot of expression profiles of all libraries from 6 different *C. campestris* tissue types mapped to the *C. campestris* genome. Stem, prehaustorium, haustorium, and flower tissue types have 8 libraries for each. Triangles represent the 4 libraries using tissue collected from *C. campestris* grown on *N. benthamiana*. Squares represent the 4 libraries using tissue collected from *C. campestris* grown on *S. lycoperscum*. Seed and seedling tissue types have 4 libraries for each. Circles represent seed and seedling libraries that are not dependent on hosts.

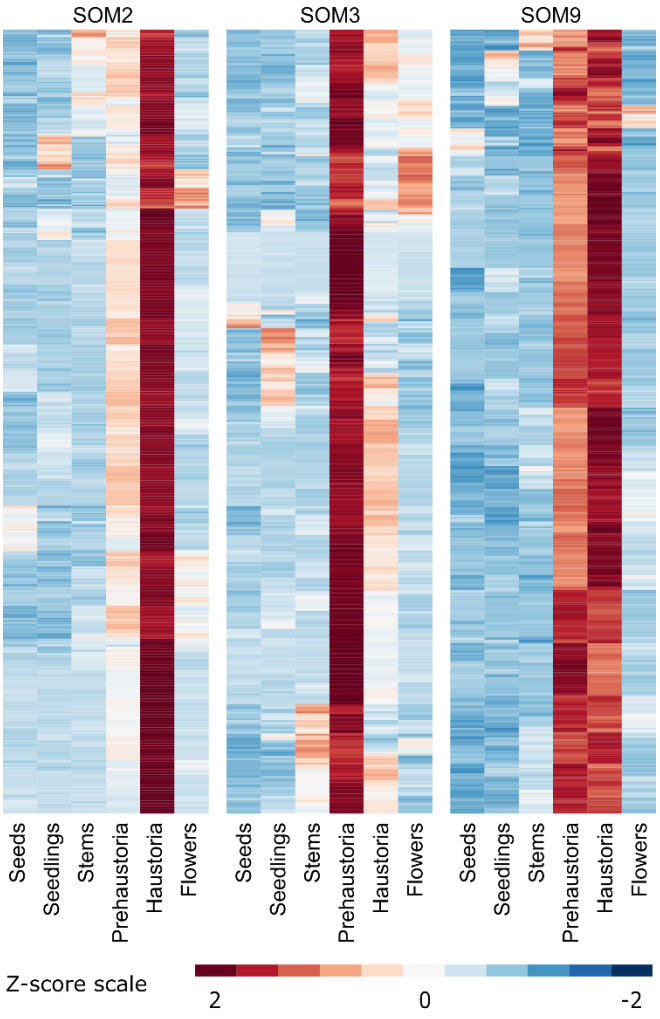

Supplemental Figure S2. Heatmaps of gene expression profiles in z-scores for SOM2, SOM3, and SOM9 from *C. campestris* tissue type RNA-Seq data mapped to *C. campestris* genome. The complete gene lists for all SOM units with SOM distances and PCA principal component values are included in Supplemental Table S1.

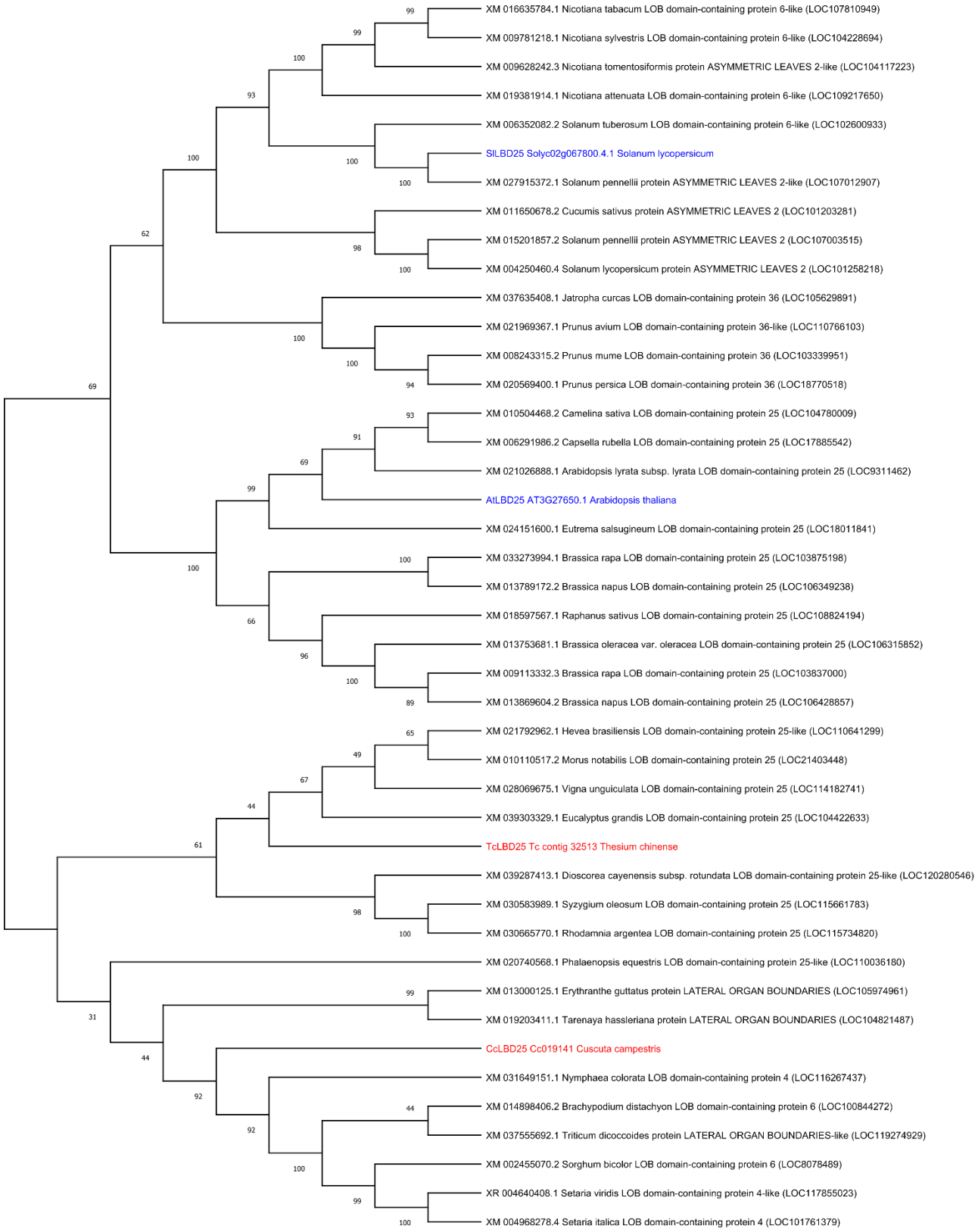
XM 016635784.1 Nicotiana tabacum LOB domain-containing protein 6-like (LOC107810949)
XM 009781218.1 Nicotiana sylvestris LOB domain-containing protein 6-like (LOC104228694)
XM 009628242.3 Nicotiana tomentosiformis protein ASYMMETRIC LEAVES 2-like (LOC104117223)
XM 019381914.1 Nicotiana attenuata LOB domain-containing protein 6-like (LOC109217650)
XM 006352082.2 Solanum tuberosum LOB domain-containing protein 6-like (LOC102600933)
SlLBD25 Solyc02g067800.4.1 Solanum lycopersicum
XM 027915372.1 Solanum pennellii protein ASYMMETRIC LEAVES 2-like (LOC107012907)
XM 011650678.2 Cucumis sativus protein ASYMMETRIC LEAVES 2 (LOC101203281)
XM 015201857.2 Solanum pennellii protein ASYMMETRIC LEAVES 2 (LOC107003515)
XM 004250460.4 Solanum lycopersicum protein ASYMMETRIC LEAVES 2 (LOC101258218)
XM 037635408.1 Jatropha curcas LOB domain-containing protein 36 (LOC105629891)
XM 021969367.1 Prunus avium LOB domain-containing protein 36-like (LOC110766103)
XM 008243315.2 Prunus mume LOB domain-containing protein 36 (LOC103339951)
XM 020569400.1 Prunus persica LOB domain-containing protein 36 (LOC18770518)
XM 010504468.2 Camelina sativa LOB domain-containing protein 25 (LOC104780009)
XM 006291986.2 Capsella rubella LOB domain-containing protein 25 (LOC17885542)
XM 021026888.1 Arabidopsis lyrata subsp. lyrata LOB domain-containing protein 25 (LOC9311462)
AtLBD25 AT3G27650.1 Arabidopsis thaliana
XM 024151600.1 Eutrema salsugineum LOB domain-containing protein 25 (LOC18011841)
XM 033273994.1 Brassica rapa LOB domain-containing protein 25 (LOC103875198)
XM 013789172.2 Brassica napus LOB domain-containing protein 25 (LOC106349238)
XM 018597567.1 Raphanus sativus LOB domain-containing protein 25 (LOC108824194)
XM 013753681.1 Brassica oleracea var. oleracea LOB domain-containing protein 25 (LOC106315852)
XM 009113332.3 Brassica rapa LOB domain-containing protein 25 (LOC103837000)
XM 013869604.2 Brassica napus LOB domain-containing protein 25 (LOC106428857)
XM 021792962.1 Hevea brasiliensis LOB domain-containing protein 25-like (LOC110641299)
XM 010110517.2 Morus notabilis LOB domain-containing protein 25 (LOC21403448)
XM 028069675.1 Vigna unguiculata LOB domain-containing protein 25 (LOC114182741)
XM 039303329.1 Eucalyptus grandis LOB domain-containing protein 25 (LOC104422633)
TcLBD25 Tc contig 32513 Thesium chinense
XM 039287413.1 Dioscorea cayenensis subsp. rotundata LOB domain-containing protein 25-like (LOC120280546)
XM 030583989.1 Syzygium oleosum LOB domain-containing protein 25 (LOC115661783)
XM 030665770.1 Rhodamnia argentea LOB domain-containing protein 25 (LOC115734820)
XM 020740568.1 Phalaenopsis equestris LOB domain-containing protein 25-like (LOC110036180)
XM 013000125.1 Erythranthe guttatus protein LATERAL ORGAN BOUNDARIES (LOC105974961)
XM 019203411.1 Tarenaya hassleriana protein LATERAL ORGAN BOUNDARIES (LOC104821487)
CcLBD25 Cc019141 Cuscuta campestris
XM 031649151.1 Nymphaea colorata LOB domain-containing protein 4 (LOC116267437)
XM 014898406.2 Brachypodium distachyon LOB domain-containing protein 6 (LOC100844272)
XM 037555692.1 Triticum dicoccoides protein LATERAL ORGAN BOUNDARIES-like (LOC119274929)
XM 002455070.2 Sorghum bicolor LOB domain-containing protein 6 (LOC8078489)
XR 004640408.1 Setaria viridis LOB domain-containing protein 4-like (LOC117855023)
XM 004968278.4 Setaria italica LOB domain-containing protein 4 (LOC101761379)

Supplemental Figure S3. *LBD25* phylogenetic tree with top significant sequences aligned with *CcLBD25*, *TcLBD25*, *AtLBD25* and *SlLBD25*. According to BLAST E-value, the top 10 most significant aligned sequences were obtained using Blastn based on *CcLBD25, TcLBD25, AtLBD25* and *SlLBD25* nucleotide sequences. The evolutionary relationships were inferred using the Maximum Likelihood method and Tamura-Nei model. The bootstrap consensus tree was built from 500 replicates. The number next to each node indicates the percentage of replicate trees in which the associated taxa clustered together in the bootstrap test. Evolutionary analysis was conducted in MEGA X. *CcLBD25* and *TcLBD25* are labeled in red. *AtLBD25* and *SlLBD25* are labeled in blue. The sequence alignment that is used for building this gene phylogenetic tree is included in Supplemental Data S1.

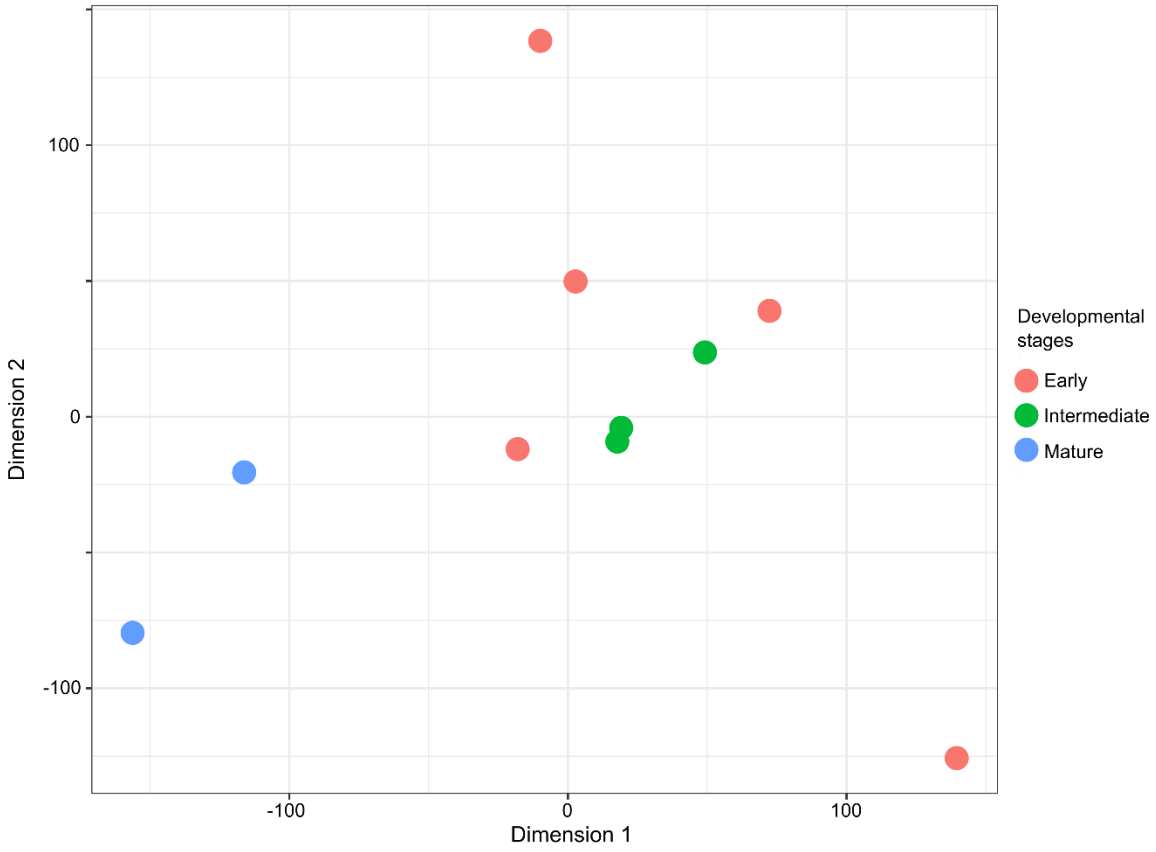

Supplemental Figure S4. MDS plot of RNA expression profile in all libraries from LCM of three different *C. campestris* developmental stages mapped to *C. campestris* genome. Early-stage has 5 libraries. Intermediate-stage has 3 libraries. Mature-stage has 2 libraries.

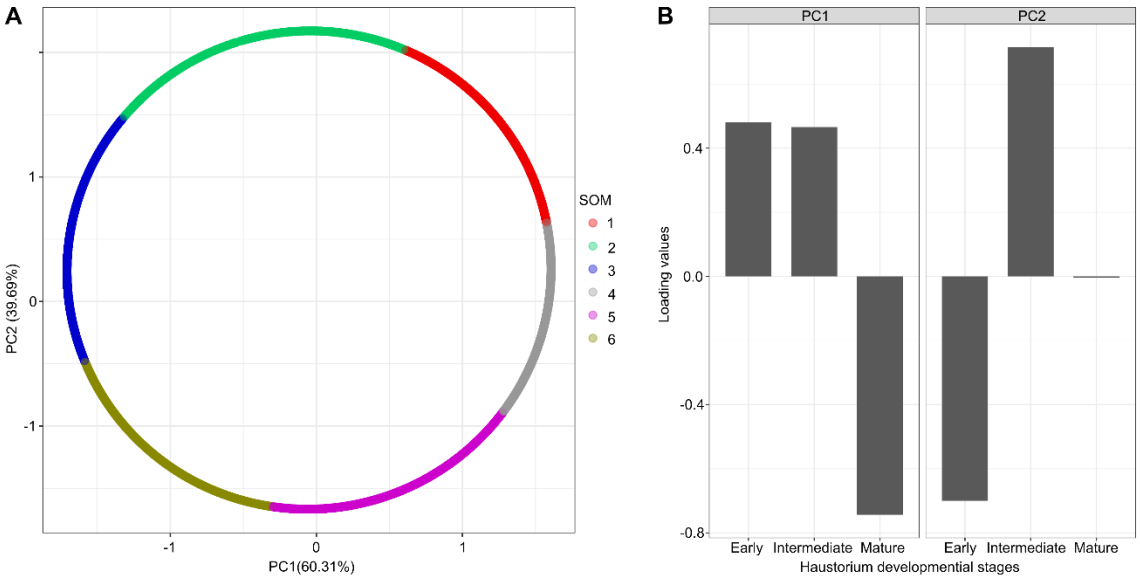

Supplemental Figure S5. PCA analysis with SOM clustering and GCNs of gene expression in *C. campestris* haustoria across three developmental stages in LCM RNA-Seq data. (A) PCA analysis based on gene expression pattern across three developmental stages, early, intermediate, and mature. Each dot represents a gene and is in the color indicating their corresponding SOM groups. (B) Loading values of PC1 and PC2. PC1 separates the genes that are specifically expressed in mature-stage from those that are expressed in the early and intermediate-stages. PC2 divides the early-stage-specific genes from intermediate-stage-specific genes.

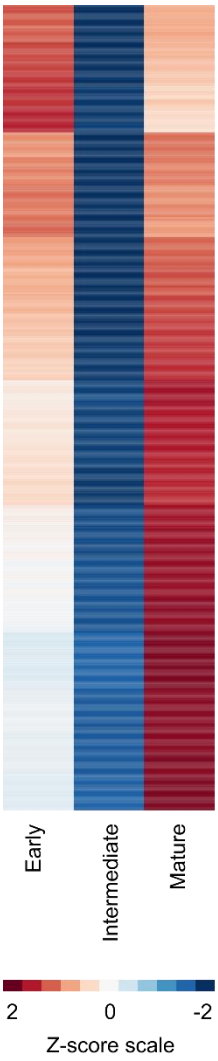

Supplemental Figure S6. Heatmap of gene expression profiles in z-scores for SOM6 from *C. campestris* LCM RNA-Seq data mapped to *C. campestris* genome.

A

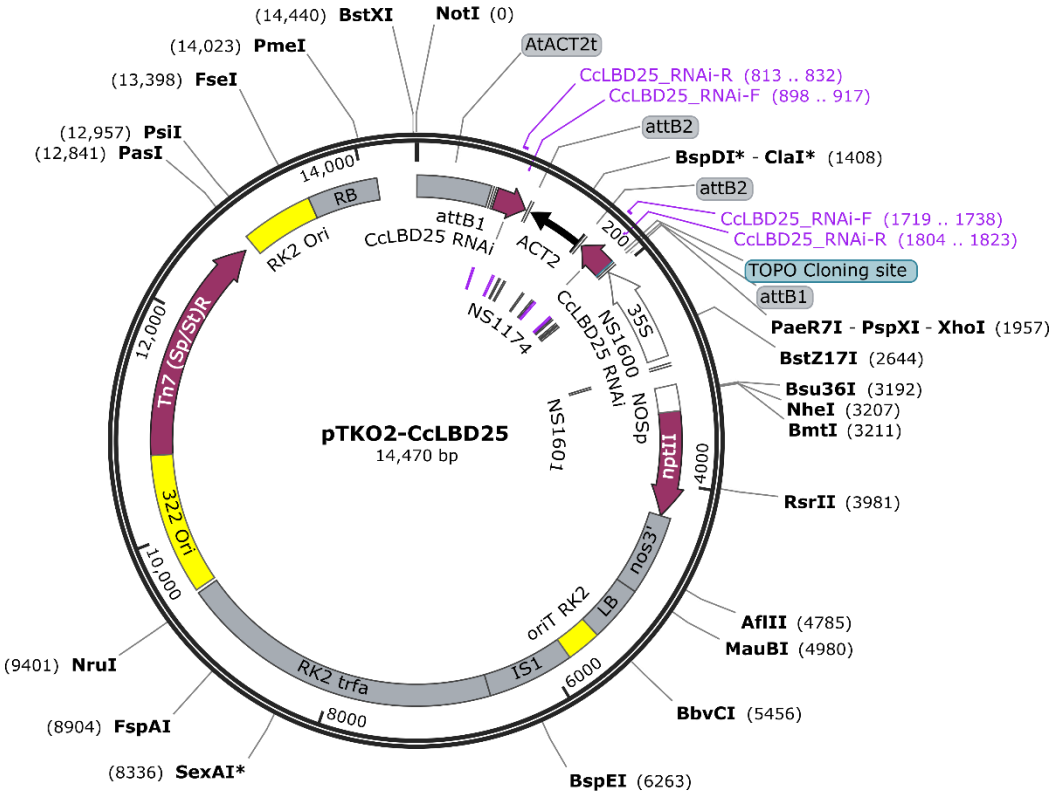
(14,440) BstXI
NotI (0)
(14,023) PmeI
(13,398) FseI
(12,957) PsiI
(12,841) PasI
AtACT2t
CcLBD25_RNAi-R (813 .. 832)
CcLBD25_RNAi-F (898 .. 917)
attB2
BspDI* - ClaI* (1408)
attB2
CcLBD25_RNAi-F (1719 .. 1738)
CcLBD25_RNAi-R (1804 .. 1823)
TOPO Cloning site
attB1
PaeR7I - PspXI - XhoI (1957)
BstZ17I (2644)
Bsu36I (3192)
NheI (3207)
BmtI (3211)
RsrII (3981)
AflII (4785)
MauBI (4980)
BbvCI (5456)
BspEI (6263)
(8336) SexAI*
(8904) FspAI
(9401) NruI
pTKO2-CcLBD25
14,470 bp
RB
RK2 Ori
attB1
CcLBD25 RNAi
ACT2
NS1174
CcLBD25 RNAi
NS1600
35S
NS1601
NOSp
nptII
nos3'
LB
oriT RK2
IS1
RK2 trfa
322 Ori
Tn7 (Sp/St)R
14,000
2000
4000
6000
8000
10,000
12,000

B

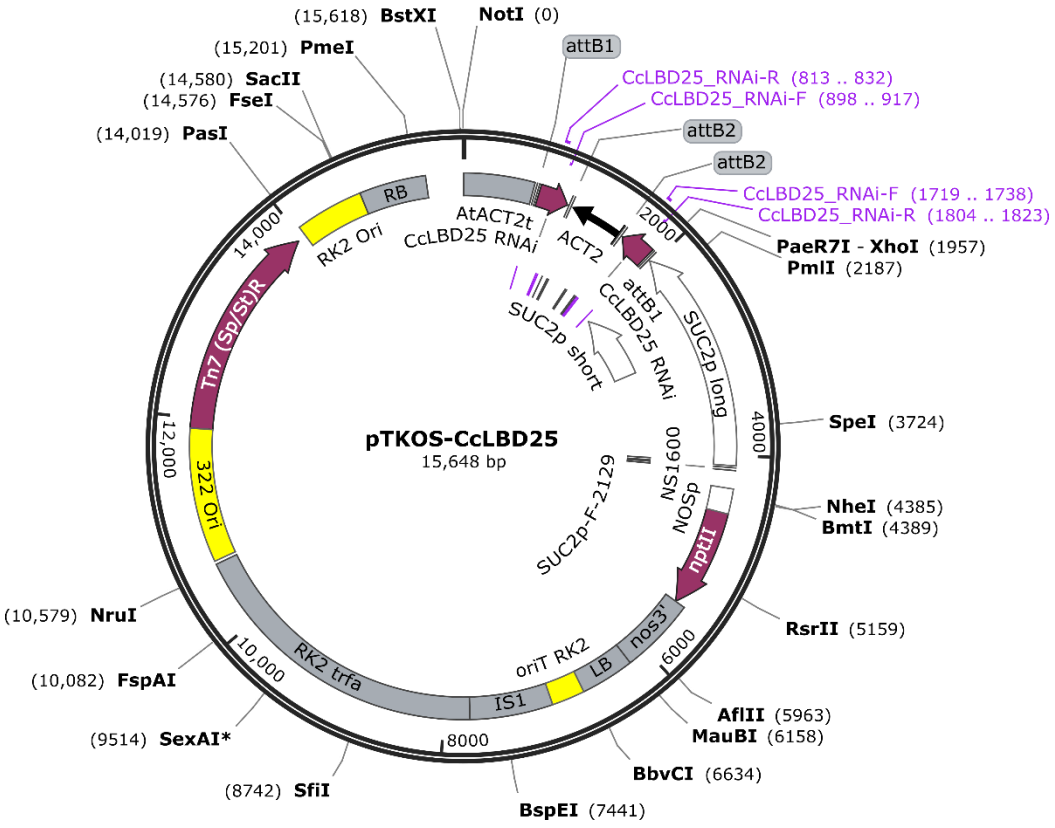
(15,618) BstXI
NotI (0)
(15,201) PmeI
(14,580) SacII
(14,576) FseI
(14,019) PasI
attB1
CcLBD25_RNAi-R (813 .. 832)
CcLBD25_RNAi-F (898 .. 917)
attB2
attB2
CcLBD25_RNAi-F (1719 .. 1738)
CcLBD25_RNAi-R (1804 .. 1823)
PaeR7I - XhoI (1957)
PmlI (2187)
SpeI (3724)
NheI (4385)
BmtI (4389)
RsrII (5159)
AflII (5963)
MauBI (6158)
BbvCI (6634)
BspEI (7441)
SfiI (8742)
(9514) SexAI*
(10,082) FspAI
(10,579) NruI
pTKOS-CcLBD25
15,648 bp
RB
RK2 Ori
AtACT2t
CcLBD25 RNAi
ACT2
SUC2p short
attB1
CcLBD25 RNAi
SUC2p long
SUC2p-F-2129
NS1600
NOSp
nptII
nos3'
LB
oriT RK2
IS1
RK2 trfa
322 Ori
Tn7 (Sp/St)R
14,000
2000
4000
6000
8000
10,000
12,000

Supplemental Figure S7. *CcLBD25* RNAi constructs for host-induced gene silencing (HIGS). (A) pTKO2 has 35S promoter to drive *CcLBD25* RNAi construct. (B) pTKOS has SUC2 promoter to drive *CcLBD25* RNAi construct. The segment of CcLBD25 sequence used for RNAi construct is included in Supplemental Data S2. The complete SUC2 promoter sequence is included in Supplemental Data S3.

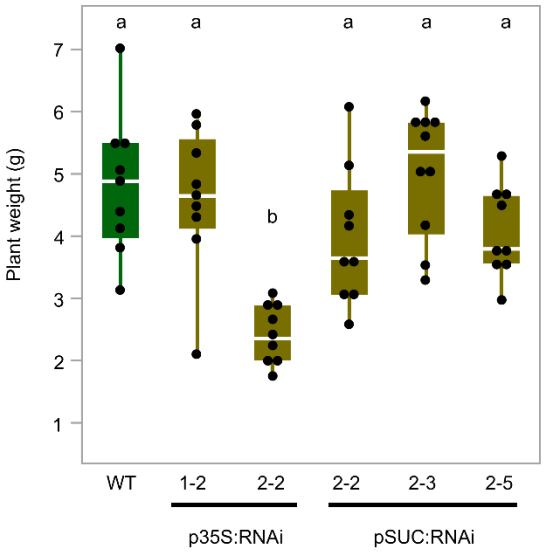
a
a
a
a
a
7
6
5
4
3
2
1
Plant weight (g)
b
WT
1-2
2-2
2-2
2-3
2-5
p35S:RNAi
pSUC:RNAi

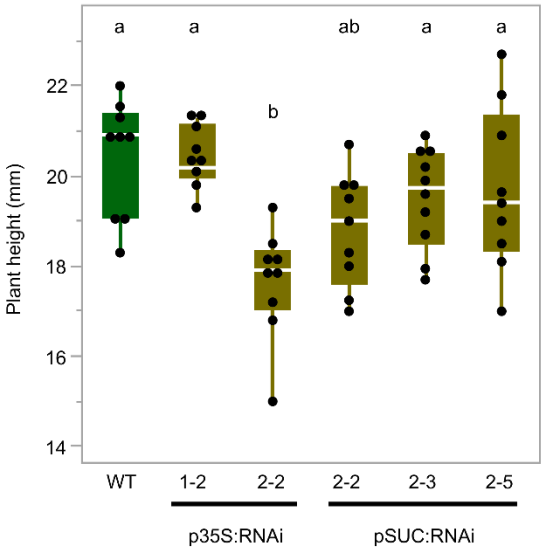
a
a
ab
a
a
22
20
18
16
14
Plant height (mm)
b
WT
1-2
2-2
2-2
2-3
2-5
p35S:RNAi
pSUC:RNAi

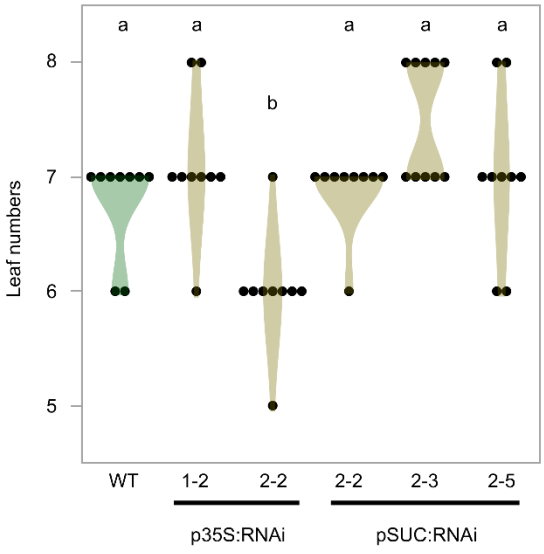
a
a
a
a
a
8
7
6
5
Leaf numbers
b
WT
1-2
2-2
2-2
2-3
2-5
p35S:RNAi
pSUC:RNAi

Supplemental Figure S8. Whole-plant phenotypes of *CcLBD25* RNAi transgenic tomato plants without *C. campestris* infestation treatment. (A) Comparison of 4-week-old tomato plant biomass (above ground fresh weight). Data are presented in grams. (B) Comparison of 4-week-old tomato plant height. Data are presented in centimeters. (C) Comparison of 4-week-old tomato plant leaf number. (A-C) Data presented are assessed using pair-wise comparisons with the Tukey test. P-value of the contrasts between "a" and "b" is less than 0.05.

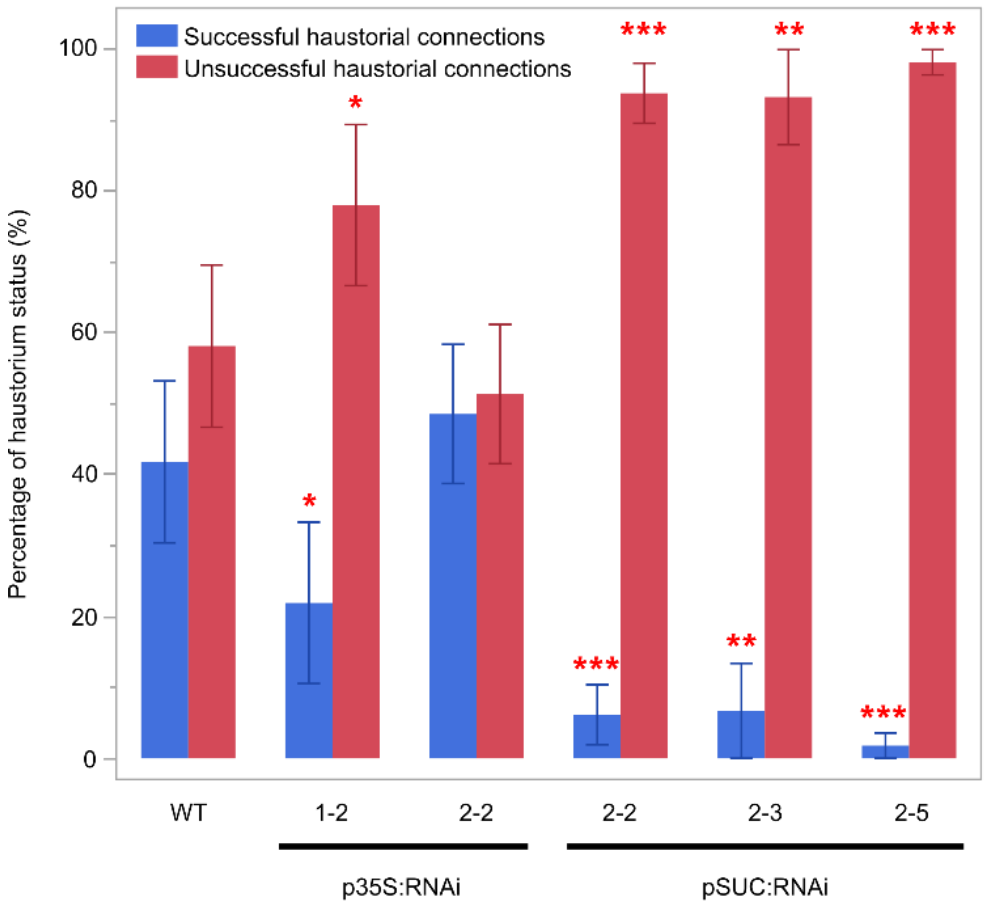

Supplemental Figure S9. Quantification of haustorium status on *CcLBD25* RNAi HIGS and wild-type plants. p35S:RNAi indicates the transgenic plants with the 35S promoter driving *CcLBD25* RNAi construct. pSUC:RNAi indicates the transgenic plants with the SUC2 promoter driving *CcLBD25* RNAi construct. Successful haustorial connections include the haustoria that formed vascular connections with the host or the haustoria with searching hyphae penetrated into the host cortex. Unsuccessful haustorial connections include the haustoria penetrated into the host cortex but without searching hyphae, or the haustoria that are only attached on the host stem surface. Data presented are assessed using one-tailed Welch's t-test with wild-type (WT) as control. "*" p-value < 0.13. "**" p-value < 0.05. "***" p-value < 0.01. Sample size: H1706, 136 sections from 8

biological replicates; p35S:RNAi 1-2, 55 sections from 4 biological replicates; p35S:RNAi 2-2, 105 sections from 4 biological replicates; pSUC:RNAi 2-2, 103 sections from 8 biological replicates; pSUC:RNAi 2-3, 69 sections from 7 biological replicates; pSUC:RNAi 2-5, 12 sections from 7 biological replicates. Complete quantification tables by sections and by samples are included in Supplemental Table S11 and S12.

All Supplemental Tables are available on the Plant Physiology Website. Please follow the hyperlink for each table or directly access them all at: https://doi.org/10.1093/plphys/kiab231.

Supplemental Table S1. The SOM clustering gene list in *C. campestris* tissue type RNA-seq data and results of PCA analysis and multilevel SOM clustering using selected genes with coefficient of variation >0.85.

Supplemental Table S2. The gene list of SOM9 GCN modules from *C. campestris* tissue type RNA-seq data.

Supplemental Table S3. Combined annotation of *C. campestris* genes and transcriptome.

Supplemental Table S4. The GO enrichment results and statistics of SOM9 GCN modules from *C. campestris* tissue type RNA-seq data.

Supplemental Table S5. The gene list of SOM2, 3, 9 combined GCN modules from *C. campestris* tissue type RNA-seq data.

Supplemental Table S6. The GO enrichment results and statistics of SOM2, 3, 9 combined GCN modules from *C. campestris* tissue type RNA-seq data.

Supplemental Table S7. The SOM clustering gene list in LCM RNA-seq data and results of PCA analysis and multilevel SOM clustering using selected genes in the upper 50% quartile of coefficient of variation.

Supplemental Table S8. The gene list in the modules of the GCN based on LCM RNA-seq expression with genes in tissue type RNA-seq SOM9.

Supplemental Table S9. The GO enrichment results and statistics of the modules of the GCN based on LCM RNA-seq expression with genes in tissue type RNA-seq SOM9.

Supplemental Table S10. Quantification and statistics of haustorium status on *CcLBD25* RNAi HIGS and WT plants by section ID.

Supplemental Table S11. Quantification and statistics of haustorium status on *CcLBD25* RNAi HIGS and WT plants by sample ID.

Supplemental Table S12. The primer pairs that are used for making the construct and quantifying expression level of *CcLBD25* by quantitative reverse transcriptase PCR (RT-qPCR).

Supplemental Dataset S1. Nucleotide sequence alignments with *CcLBD25*, *TcLBD25*, *AtLBD25*, *SlLBD25*, and their top 10 significant aligned sequences.

Supplemental Dataset S2. Sequence of the *CcLBD25* fragment that is used for making *CcLBD25* RNAi construct.

Supplemental Dataset S3. Sequence of the SUC2 promoter that is used for driving CcLBD25 RNAi construct in pTKOS.

Chapter 3: Lignin-based resistance to *Cuscuta campestris* parasitism in Heinz resistant tomato cultivars

*This chapter is submitted to the Plant Cell and is available on BioRxiv doi: https://doi.org/10.1101/706861.

Short title: Lignin-based resistance blocks dodder entry

One-sentence summary: Four key regulators confer lignin accumulation in the tomato stem cortex to block *C. campestris* host penetration upon infection.

Abstract

Cuscuta species (dodders) are agriculturally destructive parasitic angiosperms. These parasitic plants use haustoria as physiological bridges to extract nutrients and water from hosts. *Cuscuta campestris* has a broad host range and wide geographical distribution. While some wild tomato relatives are resistant, cultivated tomatoes are generally susceptible to *C. campestris* infestations. However, some specific Heinz tomato hybrid cultivars exhibit resistance to dodders in the field, but their defense mechanism was unknown. Here, we discovered that the stem cortex in these resistant lines responds with local lignification upon *C. campestris* attachment, preventing parasite entry into the host. *LIF1* (*Lignin Induction Factor 1*, an *AP2*-like transcription factor), *SlMYB55*, and *CuRLR1* (*Cuscuta R-gene for Lignin-based Resistance 1*, a *CC-NBS-LRR*) are identified as crucial factors conferring host resistance by regulating lignification. *SlWRKY16* is upregulated upon *C. campestris* infestation and acts as a negative regulator of *LIF1* function. Intriguingly, *CuRLR1* may play a role in signaling or function as a receptor for receiving *Cuscuta* signals or effectors to regulate lignification-based resistance. In summary, these four regulators control the

lignin-based resistance response in specific Heinz tomato cultivars, preventing *C. campestris* from parasitizing these resistant tomatoes. This discovery provides a foundation for investigating multilayer resistance against *Cuscuta* species and has potential for application in other essential crops attacked by parasitic plants.

Main Text

Introduction

Parasitic plants directly attach to hosts using specialized haustorial organs known as haustoria. These connections function as physiological bridges to extract nutrients and water from the hosts, making most traditional herbicides and control methods, including management of soil fertility, hand weeding, and sanitation, either too cost-intensive, labor-intensive, or ineffective in regulating parasitic plant infestations. Therefore, parasitic angiosperms are among the most devastating pests, reducing the yields of agricultural crops each year by billions of dollars worldwide (Agrios, 2005; Yoder and Scholes, 2010). Members of the *Cuscuta* genus (family Convolvulaceae), also known as dodders, occur worldwide and *Cuscuta* infestations in tomato alone lead to 50–72% yield reductions (Yaakov et al., 2001). Despite serious agricultural problems caused by *Cuscuta*, our understanding of the interactions between *Cuscuta* and its hosts is relatively limited compared to our knowledge of pathogenic fungi, bacteria, and viruses. Only recently, the first receptor (*CUSCUTA RECEPTOR 1*, *CuRe1*, Solyc08g016270), an LRR receptor-like serine/threonine-protein kinase (RLP), from *Cuscuta* was identified in tomatoes (Hegenauer et al., 2016; Hegenauer et al., 2020). *CuRe1* initiates PAMP (Pathogen-associated molecular pattern)-triggered immunity (PTI) to *Cuscuta reflexa* (Hegenauer et al., 2016; Hegenauer et al., 2020). However, plants that lack *CuRe1* are still fully resistant to *C. reflexa*. This result indicates that other layers of defense, besides *CuRe1*, must also be involved in the responses to these parasites. Therefore, further investigating the potential multilayered resistance mechanisms will aid in developing parasitic plant-resistant crops.

Potential immune responses and defense responses to parasitic plants have been observed in several crop plants, including rice, tomato, cowpea, and sunflower (Mutuku et al., 2015;

Hegenauer et al., 2016; Duriez et al., 2019; Su et al., 2020). Notably, most previous reports indicated that hypersensitive response is the major mechanism that contributes to plant immunity to parasitic plants (Lane et al., 1993; Hegenauer et al., 2016; Su et al., 2020). A few studies indicated that secondary cell-wall modification and formation in the resistant rice (*Oryza sativa*) cultivar 'Nipponbare' also contribute to defense against root parasitic plants, like *Striga hermonthica* (Yoshida and Shirasu, 2009; Mutuku et al., 2019). Plants often modify their cell walls in response to pathogen infection and herbivore feeding (Moura et al., 2010). Among different modifications, lignification is considered a major mechanism for resistance in plants (Vance et al., 1980; Moura et al., 2010; Bellincampi et al., 2014; Malinovsky et al., 2014). Lignified cell walls have higher mechanical strength, are impermeable to water, and less accessible to cell wall-degrading enzymes (Bhuiyan et al., 2009; Barros et al., 2015). Several previous reports indicated that lignified endodermal cells were found in resistant host roots, like vetch (*Vicia* spp.) and faba bean (*Vicia faba*), in response to root parasitic plant attack (Pérez-de-Luque et al., 2005; Pérez-de-Luque et al., 2007). However, how secondary cell-wall modification and lignin are involved in the defense responses to stem parasitic plants still needs to be elucidated. Thus, we specifically investigated host cell wall composition and the lignin biosynthesis pathways aiming to discover the potential additional layers of resistance to *Cuscuta* spp.

Cuscuta campestris (*C. campestris*) attacks a wide range of crop species worldwide (Lanini and Kogan, 2005). Although cultivated tomatoes are usually susceptible (Ashton, 1976), some specific Heinz tomato cultivars that are resistant to *Cuscuta* spp. were discovered in the field (Hembree et al., 1999; Yaakov et al., 2001). These resistant cultivars have been used in the field to control the infestation of *Cuscuta* spp., but the resistance mechanism remains unknown. Therefore, to identify the underlying mechanism and genes involved in these defense responses,

these dodder-resistant Heinz tomatoes were used for further study. We discovered that the resistance response in these Heinz cultivars is based on post-attachment lignification in the host stem cortex upon *C. campestris* infection. Recent work described the involvement of lignin in the resistance responses to root parasitic plants, including *Orobanche cumana*, *Orobanche minor*, *Phtheirospermum japonicum*, and *Striga hermonthica* (Labrousse et al., 2001; Kusumoto et al., 2007; Cui et al., 2018). However, considering the differences in the anatomy of stems and roots, whether host plants deploy similar mechanisms to stop stem parasitic plants remains under-investigated. Based on our comparative transcriptomics, virus-induced gene silencing, and gain-of-function studies in susceptible cultivars, we identified two transcription factors, *SlMYB55* (Solyc10g044680) and *LIF1* (Solyc02g079020, *Lignin induction Factor 1*, an *AP2*-like protein), that regulate the biosynthesis of lignin in the cortex. Moreover, *CuRLR1* (Solyc04g009110, a *CC-NBS-LRR*) may be engaged in signaling or function as a receptor for perceiving *C. campestris* signals or effectors, leading to lignification-based resistance. Overexpression of *CuRLR1* in susceptible tomato only induced strong lignification upon *C. campestris* attachment or *C. campestris* extract injection. To investigate whether these newly discovered lignin-based resistance responses connect with previously identified *CuRe1* mediated resistance responses, we conducted comprehensive RNA-Seq profiling, clustering and gene-coexpression analysis. Our gene coexpression networks indicate that *CuRe1* is also connected with *CuRLR1, LIF1, and SlMYB55* in resistant cultivars under *C. campestris* infested condition and also helped us identify another transcription factor, *SlWRKY16* (Solyc07g056280), which has a similar expression pattern as *CuRe1*. CRISPR-mediated mutants of *SlWRKY16* showed lignification in the cortex and were more resistant to *C. campestris*. This result indicates that *SlWRKY16* functions as a negative regulator of the lignin-based resistance. Furthermore, we noticed that the lignin-based resistance

responds to a large protein molecule from *C. campestris* extracts, which might represent potential novel *C. campestris* signals or effectors. In summary, we discovered four key regulators control the lignin-based resistance response in the stem cortex upon *C. campestris* infection, and this lignification blocks *C. campestris* strands from parasitizing selected Heinz tomato cultivars.

Results

Response to *C. campestris* in the resistant cultivars

While most tomato cultivars can be parasitized by *C. campestris*, the Heinz hybrids 9492 and 9553 (H9492 and H9553) exhibit resistance to dodders (Yaakov et al., 2001). *C. campestris* strands grew well on the susceptible H1706 (genome sequenced) and H9775 (Heinz hybrid 9775 – closely related to the resistant cultivars) (Figure 1A). On the other hand, *C. campestris* strands could not form good attachments with H9492 and H9553, and haustoria detached from the host stem, preventing parasite growth (Figure 1B). Based on the biomass ratio of *C. campestris* and host (relative growth rate), H9492 and H9553 cannot support long-term (>45 days) growth of *C. campestris*, in contrast to H9775 and H1706 (Figure 1C).

To identify the basis for resistance, we analyzed *C. campestris* attachments on susceptible and resistant lines using anatomy and cell wall-specific staining with Toluidine Blue O and Phloroglucinol-HCl (Liljegren, 2010). Upon challenging these different cultivars with *C. campestris* strands, lignin accumulation in the stem cortex was observed in the resistant H9492 and H9553, but not in the susceptible H9775 and H1706 (Figure 1D – 1O). The resistance mechanism involved local lignification in the stem cortex, creating a barrier to haustorium penetration, and dodder attachment on the resistant cultivars (Figure 1D – 1O). Little to no lignin accumulates in the cortex of both resistant and susceptible cultivars without *Cuscuta* attachment (Figure 1P). In addition, *Cuscuta* attachment sites usually cause some wounding responses and cell death in both resistant and susceptible cultivars (Figure 1Q).

Identifying the key time point for early host defense responses in host-parasite interactions

Changes in the levels of salicylic acid and jasmonic acid have been reported at 36 to 48 hours after attachment (Runyon et al., 2010). To capture early responses to dodder parasitism, we performed a time-course RNA-Seq analysis on 0, 1, 2, 3, and 4 DPA (days post attachment) of *C. campestris* on tomatoes H1706 (susceptible). At these stages, the dodder strands were not embedded in the host and could be removed to collect the attached stem area. Within the constraints of our ability to identify differentially expressed genes which can be prone to both biological and technical variation, maximal transcriptional changes peaked at 4 DPA (Supplemental Figure 1, Supplemental Data Set 1), suggesting that the Differentially Expressed (DE) genes include core genes involved in the early response to *C. campestris* infection. Accordingly, we chose 4 DPA for further gene expression analysis of the resistant and susceptible cultivars.

Gene expression in the resistant and susceptible host response to *C. campestris*

We challenged the resistant H9492 and H9553, and susceptible H9775 and H1706 with *C. campestris* strands. We collected stem tissues at 4 DPA for RNA-seq and differential gene expression analysis in dodder infested versus uninfested plants. In principal component analysis (PCA) on the transcriptomes of resistant and susceptible cultivars (Supplemental Figure 2), PC1 accounted for 44% of the variation and significantly clustered the data into two separate sets: infested and non-infested samples. However, PCA did not separate different cultivars into distinct genotypic groups. Thus, the transcriptional differences in response to *C. campestris* between the resistant and susceptible genotypes likely involve a small number of genes.

Next, we conducted differential gene expression (DGE) analyses by comparing *C. campestris* infested and uninfested host plants using an interaction design model (design model = infested or uninfested condition + genotype + condition: genotype). Based on our communication with the

Kraft Heinz Company, both H9492 and H9553 were developed in the same breeding program. However, H9553 is more resistant to *C. campestris* than H9492 based on the relative growth rate of *C. campestris* and host results at 45 DPA (Figure 1C). Therefore, we suspected that the enhanced resistance to *C. campestris* is due to alterations in key regulatory gene expression or function. We selected 113 genes that were differentially expressed (Supplemental Data Set 2) between infested H9775 (susceptible) and infested H9553 (resistant) with an adjusted p value cutoff < 0.1 and $\log_2$ fold change > 1. Consistent with our observations of lignin accumulation in resistant tomato cultivars upon *C. campestris* infestation (Figure 1), many of these genes are known to be involved in the lignin biosynthetic pathway, including three laccase genes (*LAC4*, *5* and *17*, Solyc05g052340, Solyc09g010990, Solyc10g085090) and Caffeoyl CoA 3-O-methyltransferase (*CCoAOMT*, Solyc01g107910) (Figure 2).

To narrow down the potential upstream candidates regulating this lignin-based resistance, we focused on transcription factors (TF - based on gene annotations) as possible key regulators of lignin biosynthesis pathways, and membrane-localized or cytosolic receptors that may receive signals from *C. campestris*. Using these two criteria, we identified three candidate genes for further study, including a TF related to *AP2*, a *SlMYB55* TF, and a gene encoding an N-terminal coiled-coil nucleotide-binding site leucine-rich repeat protein (*CC-NBS-LRR*) (Figure 2A-C). Among the 113 differentially expressed genes, Solyc04g009110 was the only *CC-NBS-LRR* gene. Based on multiple comparison adjusted p value, *SlMYB55* (Solyc10g044680) ranked as the first TF, and *AP2* (Solyc02g079020) ranked as the fourth TF. These three candidate genes share a common expression pattern of significantly reduced expression levels upon *C. campestris* infestation in the susceptible cultivars. However, expression of these three candidate genes remained almost unchanged from uninfested or was only mildly reduced upon *C. campestris* infestation in resistant

cultivars. This result suggests that these candidates might play a role in defense against *Cuscuta*, such that when these genes are not repressed during *C. campestris* infestation, the host plants are more resistant to *C. campestris*.

Functional characterization of candidate genes using virus-induced gene silencing (VIGS) and virus-based gene expression (VGE)

To validate the function of these candidate genes, an ideal method would be to generate knockout mutant plants for further study. However, these resistant tomato lines are F1 hybrids in the Heinz background, and the Heinz cultivars are recalcitrant to transformation. Therefore, we used virus-induced gene silencing (VIGS) to knock down our candidate genes in the resistant cultivar H9553 to test the functions of our candidate genes. The *C. campestris* plants grown on *AP2*-like, *SlMYB55*, and *CC-NBS-LRR VIGS* knockdown plants have higher survival rates compared with those growing on mock controls (Supplemental Figure 3). Similar phenotypes were also observed in *CCoAOMT* (Solyc01g107910) and *LACs* (*LAC4*, *5*, *17*, three genes in one construct (Solyc05g052340, Solyc09g010990, Solyc10g085090)) gene knockdown plants (Supplemental Figure 3). These results indicate that these candidate genes might play a role in the lignin-based resistance response. Therefore, when these essential genes were knocked down in resistant tomato cultivars, resistant tomato became more susceptible to *C. campestris*, leading to a higher survival rate of the parasite.

To further evaluate if the candidate genes can confer lignification-based resistance in susceptible tomato cultivars, we cloned coding regions of *GUS*, *AP2*-like, *SlMYB55*, and *CC-NBS-LRR* genes into Virus-based Gene Expression (VGE) vectors (vector map in Supplemental Figure 4; sequence in Supplemental Data Set 3) for transient overexpression in the susceptible H1706, which has similar expression patterns of these three candidate genes (Supplemental Figure 5A-C). We saw

significant GUS expression in the stem around the injection site (Supplemental Figure 5D-F), and a lack of lignification due to the process of injection itself (Figure 3A and D). Hence, we used *GUS*-injected plants as our mock controls for VGE experiments. We sectioned and stained injected stems with lignin-specific Phloroglucinol-HCl for lignin detection. VGE with *SlMYB55* and *AP2*-like successfully overexpressed these genes in the first internode near the injection site and induced stem lignification in the susceptible H1706 without *C. campestris* infestation (Figure 3B–C and G). Therefore, we named this *AP2*-like protein *LIF1* (*Lignin Induction Factor 1*, Solyc02g079020) based on its ability to induce lignin biosynthesis in the cortex. These results indicate that *SlMYB55* and *LIF1* might play a role in regulating some of the critical enzymes in the lignin biosynthesis pathway.

In contrast, the H1706 plants with VGE of *CC-NBS-LRR* had no lignin accumulation phenotype and were very similar to those with GUS VGE under no *C. campestris* infestation conditions (Figure 3E). However, previous studies indicated that many genes in the *NBS-LRR* family encode intracellular receptors that detect pathogens and trigger defense signaling (Padmanabhan et al., 2013). Therefore, we suspected that this *CC-NBS-LRR* might play a role in signaling or function as a receptor for signals from *Cuscuta* that are needed to initiate subsequent defense responses. Hence, *C. campestris* infestation treatment might be needed to see the phenotype difference. To validate this hypothesis, we compared the response differences between *Cuscuta* infested and uninfested susceptible H1706 with *CC-NBS-LRR* VGE (Figure 3E – F and H). Intriguingly, our results showed the overexpression of *CC-NBS-LRR* only induced lignification upon *C. campestris* attachment (Figure 3H), and these results suggest that direct or indirect perception of *C. campestris* signals by this *CC-NBS-LRR* leads to lignification-based resistance. Thus, we named this gene *CuRLR1* (*Cuscuta R-gene for Lignin-based Resistance 1*).

On the other hand, we are also aware that lignin is a complex polymer and phloroglucinol-HCl staining is a fast and efficient lignin detection method, but it only detects the cinnamaldehyde end groups of lignin, preferentially staining the G and S-type aldehyde form monolignols (Pomar et al., 2002; Cass et al., 2015). Therefore, we also conducted an acetyl bromide assay to determine total lignin content, including different types of monolignols and lignin precursors. Consistent with the aforementioned anatomical observations, the overexpression of *SlMYB55* and *LIF1* both increased total lignin content compared with GUS mock controls in this assay (Figure 3I). Surprisingly, the overexpression of *CuRLR1* also increased the total lignin content even without *Cuscuta* signals. With *Cuscuta* signals, the total lignin content was much higher in *CuRLR1* overexpressing plants (Figure 3I). This difference indicates that the composition of induced lignin might be different between *CuRLR1* overexpressing plants with and without *Cuscuta* signals.

To further validate this hypothesis, we used high-performance liquid chromatography (HPLC) and pyrolysis gas chromatography/mass spectrometry (Pyrolysis-GC-MS/PYRO-GC-MS) to analyze the composition of induced lignin. Our HPLC results showed that *p*-coumarate and *trans*-ferulate are both increased in *CuRLR1* overexpressed plants, but the samples with *Cuscuta* signals have much higher levels of these two precursors than the samples without *Cuscuta* signals (Supplemental Figure 6). PYRO-GC-MS analysis showed that samples from *CuRLR1* overexpressing plants without *Cuscuta* signals have the larger percentage of H-lignin and the larger concentration of coumarate derivatives compared to VGE of *GUS*, *LIF1*, and *CuRLR1* with *Cuscuta* (Figure 3J). These results show that *CuRLR1* overexpression alone leads to an increase in the upstream steps of the lignin biosynthesis pathway and production of more lignin precursors and H-type monolignols, while adding *Cuscuta* signals may actually up-regulate the final steps in the biosynthesis pathway leading to more G-type and S-type monolignol formation (Figure 3I and

J). Since H-lignin and coumarate are not incorporated into lignin as aldehydes, they are not detected by phloroglucinol staining, which explains the difference that we observed between the phloroglucinol staining data and acetyl bromide assay. This phenotype of induced lignin precursors and H-lignin also indicates the *CuRLR1* overexpression alone has turned on the baseline of defense mechanisms. Based on previous studies, H-lignin has been correlated with both stress response as well as defense from pathogen intrusion because this is a form of "defense" lignin that can be generated and deposited more rapidly than G or S lignin (Zhang et al., 2007; Moura et al., 2010; Liu et al., 2018). This baseline of defense mechanisms can then be upgraded upon detecting *Cuscuta* signals and start accumulating more G-type and S-type monolignols to reinforce a stronger physical boundary.

Eventually, whether or not the overexpression of these candidate genes makes susceptible tomatoes resistant to *C. campestris* is the central question when evaluating potential agricultural applications. Therefore, we transiently overexpressed *SlMYB55*, *LIF1*, and *CuRLR1* first and then attached *C. campestris* strands to test their resistance status. Based on our results, VGE of *SlMYB55*, *LIF1*, and *CuRLR1* with *C. campestris* all induced lignin accumulation in the cortex and blocked haustorium penetration, which made the susceptible tomato cultivar H1706 more resistant to *C. campestris* (Figure 3K –N, Supplemental Figure 7, and Supplemental Data Set 4).

Regulatory mechanisms and networks leading to resistance responses

Since both H9492 and H9553 hybrid cultivars arose in the same breeding program, enhanced resistance to dodders observed in these two cultivars is likely due to the presence of some unique sequence polymorphisms in these cultivars. Resistance-specific nucleotide polymorphisms (SNPs) could contribute to the regulation or function of our candidate genes, so we specifically identified SNPs that are common in H9553 and H9492 but different from H9775 (Supplemental Data Set 5).

Unexpectedly, there were no resistance-specific SNPs in coding regions of our candidate genes except one SNP located in a *LIF1* exon. This resistance-specific SNP changes 251 Lysine (K, in H1706) to 251 Glutamine (Q, in H9553). However, based on our protein domain prediction using InterProScan (Jones et al., 2014; Mitchell et al., 2018) and protein structure analysis using Phyre2 (Kelley et al., 2015), this amino acid replacement is not located in any known protein domains or structures. We also conducted PROVEAN (Protein Variation Effect Analyzer) analysis, and this K251Q variant only has a 0.619 PROVEAN score, indicating that it is a neutral variant. Thus, we conclude that there are no resistance-specific SNP in coding regions of our candidate genes that might contribute to the regulation of resistance.

We, therefore, specifically focused on resistance-specific SNPs in the promoter regions of our candidate genes (Supplemental Data Set 6). Our SNP analysis detected several resistance-specific SNPs in the *LIF1* promoter region, but no resistance-specific SNPs were detected in other candidate gene promoter regions (within 5 kb upstream). One resistance-specific SNP was detected in the *CuRe1* promoter region (outside 5 kb upstream) located at a putative YABBY binding site. However, this SNP is also located 1184bp upstream of *ULP1* (Solyc08g016275) and may regulate expression of this neighboring gene instead of *CuRe1*. Therefore, we focused on the *LIF1* promoter region for further analysis and conducted transcription factor (TF) binding site predictions.

Based on our phylogenetic network analysis (Solís-Lemus et al., 2017) using 500 kb around the *LIF1* resistance-specific SNP enriched region, these SNPs might be introgressed from wild tomato species (likely coming from *S. galapagense* and/or *S. pennellii*, Supplemental Figure 8). One of these resistance-specific SNPs is located right at a WRKY binding W-box cis-element (TTGACY-core motif (Ciolkowski et al., 2008; Chen et al., 2019)) (Supplemental Figure 9 and Supplemental Data Set 7). This SNP is predicted to interrupt WRKY binding, likely leading to *LIF1* expression

differences between resistant and susceptible cultivars upon *C. campestris* attachment. Hence, we were also interested in searching for potential *WRKY* TFs in our selected gene lists.

To understand the relationships between the three candidate genes and their targets, to identify the potential *WRKY* regulator, and to also investigate whether these newly discovered candidate genes connect with previously identified *CuRe1*-mediated resistance responses (Hegenauer et al., 2016), we conducted DGE analysis with ANOVA and selected 10939 differentially expressed genes (DEG) with FDR less than 0.1 (Supplemental Data Set 8). Next, we used Barnes-Hut t-distributed stochastic neighbor embedding (BH-SNE) to generate gene clusters using RSMod (a pipeline developed by us, script included in code availability) (Ranjan et al., 2016). In this analysis 5941 DEGs are clustered into 48 groups based on their gene expression patterns and 4998 DEGs are in the noise group. Among the 48 gene clusters generated (Supplemental Data Set 9), five clusters were selected based on their GO (Gene Ontology) enrichment terms and the candidate genes they included (Figure 4A-B and Supplemental Data Set 9). The GO term of cluster 39 is "DNA binding", which includes potentially key resistance TFs, like *MYB55*. The GO term of cluster 11 is "lignin biosynthetic and catabolic process", which encapsulates the observed resistance phenotypes, and includes Caffeoyl CoA 3-O-methyltransferase (*CCOMT*) and three Laccase (*Lac*) genes identified in our model-based approach (Supplemental Data Set 2). Cluster 23 includes a *Cinnamoyl-CoA reductase* gene (Solyc03g097170, *CCR*) and is enriched in the "xyloglucan:xyloglucosyl transferase activity" GO term, which may indicate potential cell wall modifications. "Response to biotic stimulus" is the GO term enriched in cluster 17, which also includes the previously identified Cuscuta receptor, *CuRe1*.

Additionally, with comprehensive RNA-Seq clustering and gene-coexpression analysis results, we also noticed *SlWRKY16* (Solyc07g056280) is always clustered with *CuRe1*. *SlWRKY16* was highly

upregulated at 4 DPA in all four Heinz cultivars, an expression pattern similar to that for *CuRe1* (Figure 5A-B). Host tissues surrounding haustoria from the tomato M82 cultivar also show upregulated expression of *SlWRKY16* at 4 DPA in our time-course data with FDR < 0.1 and real-time qPCR data (Supplemental Figure 10). Thus, *SlWRKY16* is a commonly upregulated host response gene across different cultivars and may play an important role in the transduction of *C. campestris* signals upon host attachment. Furthermore, one of the resistance-specific SNPs in the *LIF1* promoter region mentioned above, is located at a WRKY transcription factor W-box (TTGACY-core motif) binding site, which is also the predicted *SlWRKY16* binding site based on homologous genes in the phylogenetic tree of the WRKY domain at the Plant Transcription Factor Database (Jin et al., 2016). Taking all these criteria together, we included *SlWRKY16* in our candidate genes for further analysis.

We focused on these 1676 genes in clusters 11, 17, 23, 39, 46 and included *CuRLR1* (Figure 4A-B and Supplemental Data Set 9) to construct gene co-expression networks (GCNs) for different treatments and cultivars to identify central hub genes (Figure 4, Supplemental Figure 11) (script included in code availability). Interestingly, *CuRLR1*, *SlWRKY16* and *CuRe1* had few connections or almost no connection with other genes in the GCN (with normal quantile cutoff = 0.997) in susceptible cultivars with *Cuscuta* attachments (Figure 4C-D). On the other hand, *CuRe1* and *SlWRKY16* became central hub genes in resistant cultivars only upon *C. campestris* attachments and connected with *CuRLR1* (Figure 4E-F). However, based on our DNA-Seq analysis, we cannot detect any resistance-specific SNPs in the promoter regions or coding regions of *CuRe1* and *CuRLR1*, and *SlWRKY16* (Supplemental Data Set 5). This result indicates that the differential expression of *CuRe1* and *CuRLR*1, and *SlWRKY16* may be controlled by trans-regulatory factors or protein interactions. Based on our GCN analysis and DNA-Seq analysis results, we propose that

all four Heinz tomato cultivars have fully functional *CuRe1*, *CuRLR1*, and *SlWRKY16*. Among them, *SlWRKY16* is a key factor in the transduction of *C. campestris* signals upon attachment of the parasite to the host. However, the differential expression patterns upon *C. campestris* attack and the diverse regulatory connections of these three genes determine whether resistance responses are triggered in these Heinz cultivars or not.

Functional characterization of *SlWRKY16* by CRISPR/Cas9 knockouts and VGE

Since *SlWRKY16* exists in all Heinz resistant and susceptible tomatoes and in the M82 tomato cultivar, we bypassed the transformation limitation in Heinz tomatoes and generated mutant tomato plants in the M82 background for further analysis. To validate the function of *SlWRKY16* and its role in lignification-based resistance, we produced stable *SlWRKY16* edited M82 lines using the CRISPR/Cas9 targeted gene knockout system (Pan et al., 2016). Our homozygous null mutants were generally smaller than M82 wild type (Figure 5C and D) even though both *wrky16* and M82 wild type show the same developmental progression (Figure 5I). Intriguingly, *wrky16* plants are more resistant to *C. campestris* than M82 wild type (Figure 5E – H). Using Phloroglucinol staining, we noticed that homozygous *wrky16* lines continuously produce cortical lignin, which forms a physical boundary and provides a strong resistance to *C. campestris* attachment compared to M82 wild type (Figure 5E – H and J). However, the phenotype of continuously accumulating cortical lignin likely also limits cell growth and leads to the stunted growth phenotype in *wrky16* plants. These results indicate that *SlWRKY16* may function as a negative regulator of the lignin-based resistance response.

The hypothesis that *SlWRKY16* may play a role in the lignin-based resistance response also incorporates our previous SNP analysis and transcription factor binding site prediction results in the *LIF1* promoter region (Supplemental Figure 9). We proposed that the resistance-specific SNP

located at a WRKY binding site in the *LIF1* promoter region could interrupt SlWRKY16 protein binding, leading to *LIF1* expression differences between resistant and susceptible cultivars upon *C. campestris* attachment. Therefore, we conducted real-time qPCR to determine the expression levels of *LIF1* in both susceptible M82 wild type and resistant *wrky16* tomatoes (M82 background). We observed a mild increase in *LIF1* expression in *wrky16* tomatoes compared to M82 tomatoes (Supplemental Figure 12A). Considering LIF1 is an AP2/B3-like transcription factor, any elevation in *LIF1* expression could potentially lead to large differences in the downstream gene expression pathways.

To evaluate the interaction between *SlWRKY16* and the other three candidate genes, we transiently overexpressed *LIF1*, *SlMYB55*, *CuRLR1,* and *GUS* controls in the susceptible H1706, M82 wild type, and resistant *wrky16* tomatoes. In the *GUS* transient overexpression control group, we observed that *wrky16* plants accumulate much more lignin than H1706 and M82 wild type as expected (Supplemental Figure 12B). Overexpression of *LIF1* induced more lignification in H1706, M82, and *wrky16* plants. This result shows additive effects of loss of *SlWRKY16* function and overexpression of *LIF1* in lignification responses (Supplemental Figure 12B), suggesting that *SlWRKY16* may not only regulate *LIF1* expression at the transcriptional level, but also may regulate LIF1 protein function by other mechanisms. Also, overexpression of *MYB55* induced more lignification in H1706 and *wrky16* plants (M82 background) but not in M82 (Supplemental Figure 12B), indicating that the loss of *SlWRKY16* function in M82 allows more lignin accumulation upon *MYB55* overexpression. This result also suggests subtle differences in resistant response between cultivars and that *SlWRKY16* might act upstream of *MYB55*, but more details remain to be elucidated in future research.

On the other hand, overexpression of *CuRLR1* with *C. campestris* infection was able to induce more lignification in M82, but not in *wrky16* tomatoes (Supplemental Figure 13). This epistatic phenotype suggests that either *CuRLR1* and *SlWRKY16* are in the same pathway with WRKY16 downstream of CuRLR1, or that *CuRLR1* and *SlWRKY16* are in two independent pathway that may influence each other. This hypothesis matches with the gene coexpression networks we built, which show that *CuRLR1* and *SlWRKY16* are peripherally positioned in resistant cultivars in the *Cuscuta* treated condition, with multiple layers of genes connecting them. In order to elucidate other layers of regulation between these genes, we conducted protein-protein interaction investigations.

Subcellular localization and interactions between the candidate proteins

One described mechanism for triggering innate immunity following TMV infection in tobacco involved interaction and subsequent nuclear localization of the SPL6 TF with the TIR-NBS-LRR receptor (Padmanabhan et al., 2013; Padmanabhan and Dinesh-Kumar, 2014). Therefore, we investigated the potential interactions between our candidates and their protein subcellular localization to uncover potential regulatory mechanisms. Based on our results using translational GFP fusions, LIF1 and SlWRKY16 are located mainly in the nucleus (Figure 6A), while *CuRLR1* is located in both the nucleus and the cytosol. Bimolecular fluorescence complementation (BiFC) experiments with split YFP using transient infiltration in *N. benthamiana* leaves show that the LIF1 and SlWRKY16 proteins interact and get localized to the cytoplasm (Figure 6B). Interactions between other combinations, CuRLR1-LIF1, CuRLR1-SlWRKY16, or CuRLR1-CuRe1, were not detected in our experiments (Figure 6B).

To further validate the interaction between LIF1 and SlWRKY16 proteins, we used the GAL4 yeast two-hybrid (Y2H) assays with the yeast (*Saccharomyces cerevisiae*) strain AH109 for

examination. Growth on SD/–Ade/–His/–Leu/–Trp/X-α-Gal medium plates and blue colony color confirmed that LIF1 indeed interacted with SlWRKY16 (Figure 6C). To verify the interaction between LIF1 and SlWRKY16 proteins and their subcellular localizations when they interact with each other, we also co-expressed the fusion proteins LIF1-GFP and SlWRKY16-RFP. We found that GFP and RFP signals are located mainly in the nucleus when we only overexpress LIF1-GFP or SlWRKY16-RFP in separate *N. benthamiana* leaves (Figure 6D). However, when we co-express LIF1-GFP and SlWRKY16-RFP in the same leaves, GFP and RFP signals mostly overlap in the cytoplasm (Figure 6D). These results not only further confirm that LIF1 and SlWRKY16 proteins may interact with each other and become cytosol localized, but also validate our hypothesis that SlWRKY16 can regulate LIF1 expression at both the transcriptional and protein interaction levels.

Analysis of the *Cuscuta* signal using *Cuscuta* extract injections

To further discern the nature of the major signals that trigger lignification-based resistance, we injected the first internode of the resistant H9553 with *Cuscuta* extracts subjected to different treatments (Supplemental Figure 14). Untreated or filtered *Cuscuta* extract injections induced the accumulation of lignin in the cortex region (Supplemental Figure 14B-C). On the other hand, alteration of *Cuscuta* extract pH from 5.8 to 9 abolished lignin accumulation (Supplemental Figure 14D-E), suggesting either instability or sequestration of the *Cuscuta* signaling molecules in alkaline conditions. In addition, heat-treated extract and protease-treated extract could not trigger the lignification response (Supplemental Figure 14F-J). Moreover, *Cuscuta* extract injections also induced lignin accumulation in H1706 with VGE overexpressing *CuRLR1*, but not in H1706 with GUS VGE (Supplemental Figure 15). This result indicates that *CuRLR1* may be able to either sense some unknown factors in *Cuscuta* extract or some part of the response to these factors

leading to lignin-based resistant responses. Furthermore, filtration of extracts through devices with different molecular weight cutoffs indicates that fractions smaller than 30kD cannot trigger strong lignification response (Supplemental Figure 16). Thus, the active *Cuscuta* signal for induction of lignin-based resistance is larger than 30kD but smaller than 100kD, and distinct from the previously identified *Cuscuta* signal that binds *CuRe1* (Hegenauer et al., 2016; Hegenauer et al., 2020).

Discussion

Cuscuta spp. cause massive losses in infested tomato fields in the United States, so understanding the resistance mechanism of these specific Heinz tomatoes will provide the potential of developing crop protection systems. Notably, previous studies indicate that different *Cuscuta* species can have diverse host-parasite interactions with the same host species (Ranjan et al., 2014; Kaiser et al., 2015; Hegenauer et al., 2016). For example, although cultivated tomatoes (*S. lycopersicum*) are generally resistant to *Cuscuta reflexa* (Sahm et al., 1995; Hegenauer et al., 2016), most domesticated tomato cultivars are susceptible to *C. campestris*. Therefore, using the Heinz tomato cultivars that have been bred for resistance to dodders helped us understand the multilayered resistance mechanism to *Cuscuta* spp. and how this might aid in developing parasitic plant-resistant crops. This study reveals the underlying resistance mechanism is a lignin-based resistance response in these Heinz resistant tomato cultivars.

Lignin is a complex phenolic polymer, which is generated from three major monolignols, paracoumaryl alcohol, coniferyl alcohol, and sinapyl alcohol, using covalent crosslinks formed via free radical polymerization (Ferrer et al., 2008). Accumulation of lignin in plant stems or roots has been shown to reinforce plant resistance to invading herbivores, parasites and pathogens (Reimers and Leach, 1991; Gayoso et al., 2010; Taheri and Tarighi, 2012; War et al., 2012; Dhakshinamoorthy et al., 2014; Kumari et al., 2016; Zhang et al., 2019). Lignification at the host-parasite interface in roots has been reported in plants that are resistant to root parasitic plants (Goldwasser et al., 1999; PÉRez-De-Luque et al., 2005; CAMERON et al., 2006; Lozano-Baena et al., 2007). However, for stem parasitic plants, most research has focused on hypersensitive response or necrosis as the major mechanisms for host plant defense (LANE et al., 1993; Hegenauer et al., 2016; Su et al., 2020). One previous report of incompatible reactions between

tomato plants and *Cuscuta reflexa* characterized by a visible brownish plaque at infection sites, suggested this might be due to suberized or lignified cell walls (Sahm et al., 1995). Here, we first identified a strong lignin-based resistance response toward *C. campestris* attack in these specific Heinz tomato cultivars, adding another layer on the previous reported hypersensitive-type response mechanism.

This lignin-based resistance response is regulated by three key genes, *LIF1*, *SlMYB55*, and *CuRLR1*. Of these, *CuRLR1* responded to unknown *Cuscuta* signals and further reinforced lignin deposition in the resistant cultivars. The *Cuscuta* signals that trigger the lignin-based defense responses appear to be large heat-sensitive proteins (30 kDa - 100 kDa, Supplemental Figure 16), and distinct from the previously identified small *Cuscuta* signal 11 kDa glycine-rich protein (GRP) or its minimal peptide epitope Crip21 (Hegenauer et al., 2020) that is recognized by *CuRe1* (Hegenauer et al., 2016). It would be of interest to investigate interactions between these potential *Cuscuta* signals or effectors that interact with the two different *Cuscuta* receptors.

In conclusion, we propose a new multilayered model for *Cuscuta* resistance response in tomato (Figure 7). *CuRLR1* is a cytosolic factor, which either receives large signaling molecules from *C. campestris* as a receptor or may be a novel factor which plays a role in downstream signal transduction upon sensing *Cuscuta* signals, and triggers a lignin-based resistance response (Figure 7, red-labeled arrow). Based on previous studies, NBS-LRRs are usually located in the cytoplasm and nucleus and likely to recognize pathogen effectors to induce effector-triggered immunity (ETI) (Dodds and Rathjen, 2010). This matches where we observed CuRLR1 subcellular localization (Figure 6) and might also explain why the *Cuscuta* signals that trigger the lignin-based defense responses are in a different size range compared with the previously identified *Cuscuta* signal. Our

research results shed light on a potential ETI pathway in parasitic plant resistance and provides the foundation for future studies into how these various layers of resistance connect.

In our model, *SlMYB55* and *LIF1* were placed as positive regulators in the lignin biosynthesis pathway (Figure 7, pink and yellow-labeled arrows) because transient overexpression of *SlMYB55* and *LIF1* induced lignin accumulation in the cortex (Figure 3). Other yet undiscovered *Cuscuta* receptors or factors may induce *SlMYB55* and *LIF1* expression upon *Cuscuta* attachment. On the other hand, *wrky16* plants showed lignin accumulation and stronger resistance to *Cuscuta*, suggesting that *SlWRKY16* is a negative regulator of this lignin-based resistance pathway (Figure 7, green-labeled arrow). Based on our DNA-Seq, BiFC, and subcellular localization data (Figure 6, Supplemental Figure 9), we propose that *SlWRKY16* regulates the function of *LIF1* by a combination of inhibition of *LIF1* transcription and physical capture of LIF1 proteins to block their entry into the nucleus (Figure 7, yellow and green-labeled arrows). *CuRe1* is reported to mediate PAMP/MAMP-triggered immunity (PTI/MTI) (Hegenauer et al., 2016) (Figure 7, blue-labeled arrow). GCN analysis indicates a coexpression connection between *CuRe1* and *SlWRKY16* (Figure 4A-D). *CuRe1* and *SlWRKY16* both became central hub genes in resistant cultivars upon *Cuscuta* attachments (Figure 4D), suggesting the hypothesis that *SlWRKY16* may act downstream of *CuRe1* (Figure 7, blue-labeled arrow). Thus, we envision crosstalk between different resistance pathways that may be triggered together to enhance host defense responses.

We conclude from our work that the resistance in these specific Heinz tomato cultivars relies on a lignin-based response. The systematic investigation of this resistance response in tomato plants toward the stem parasitic plant *C. campestris* provides potential implications for enhancing crop resistance to parasitic plants. Interestingly, none of the early-step lignin biosynthetic genes, like PAL, C4H, 4CL, were in the model-based differentially expressed gene list. Changing the

early steps in lignin biosynthetic genes can also change the phenylpropanoid pathway for the biosynthesis of anthocyanins. This further confirms that lignin biosynthesis is specifically triggered in the Heinz resistant cultivars. Notably, overexpression of the CuRLR1 protein induced upregulation of lignin precursors, but extensive lignin accumulation was only triggered by *Cuscuta* extracts. Introducing CuRLR1 protein could provide resistance to *C. campestris* without triggering the crop to continuously spend a lot of resources producing a large amount of cortical lignin with associated stunted growth. The identification of *CuRLR1* might provide a path forward to introduce resistance into other important crops that are also attacked by *C. campestris*. In summary, *CuRLR1*, *SlWRKY16*, *LIF1*, and *SlMYB55* regulate a lignin-based response in the tomato stem cortex, which prevents *C. campestris* strands from parasitizing these resistant Heinz cultivars.

Materials and Methods

Plant materials used in the study

We obtained four different cultivars from Dr. Rich Ozminkowski at HeinzSeed, including the Heinz hybrid cultivars 9492 and 9553 (H9492 and H9553), and the related susceptible Heinz hybrid cultivar 9775 (H9775) and the sequenced susceptible Heinz cultivar 1706 (H1706). Our *Cuscuta* was originally collected from tomato field in California, and we obtained seeds from W. Thomas Lanini. This *Cuscuta* was previously identified as *Cuscuta pentagona* (Yaakov et al., 2001), which is a closely related species to *Cuscuta campestris* (Costea et al., 2015b). To clear up the confusion, we extract DNA to verify species by molecular phylogenetics. Based on phylogenetic analysis of plastid trnL-F, rbcL sequences, and nrITS, nrLSU sequences (Stefanović et al., 2007; García et al., 2014; Costea et al., 2015b), we confirmed that our experimental species is *Cuscuta campestris* (Supplemental Figure 17-21). According to our results, our *Cuscuta campestris* isolate is most similar to *Cuscuta campestris* 201 voucher Rose 46281 WTU from USA, CA (Supplemental Figure 21) that is published by Costea *et al.* in 2015 (Costea et al., 2015a).

Histology and Cell Wall-Specific Staining

For preparing the sections at the *C. campestris* attachment area and Agroinjection sites on tomato stems, we hand-sectioned plants at 200 to 500 μm thickness using razor blades and kept these sections in 4°C water before staining. For preparing the sections of haustoria attached to host, we fixed samples in 7% Plant Tissue Culture Agar and used Lancer Vibratome Series 1000 to prepare 100 μm sections and kept these sections in 4°C water.

For Phloroglucinol-HCl Staining, we followed the published protocols (Liljegren, 2010; Pradhan Mitra and Loqué, 2014) with some modifications. To prevent plasmolysis during staining, we

added an ethanol dehydration process before staining, which is described as follows: we removed the water and then immersed sections in cold 30% ethanol and then 60% ethanol for 5 minutes each. We prepared phloroglucinol-HCl stain (Ph-HCl) or Wiesner stain by preparing a 2:1 mixture of 100% EtOH and concentrated HCl and dissolving powdered phloroglucinol into this solution at a final concentration of 3% w/v. After removing the 60% ethanol, we added phloroglucinol-HCl solution dropwise to the Petri dishes, and let the sections sit in the stain for 5 minutes. The lignified areas of the sections stain bright red within 30 seconds of immersion in the stain. After removing the phloroglucinol-HCl and adding 60% ethanol back, we imaged the sections in the petri dish on a white background using a Zeiss SteREO Discovery, V12 microscope and Nikon Eclipse E600 microscope.

For Toluidine Blue O Staining, we used a published protocol with some modifications (O'Brien et al., 1964). We immersed the sections in the stain for 30 seconds, and then washed with water three times for 30 seconds each. After removing the agar from around the sections using forceps, we mounted the sections with water on a slide and imaged using a Nikon Eclipse E600 microscope.

Image analysis of stem and haustorium sections

To quantify the lignin content of each section, we analyzed images using the image processing software ImageJ (Schneider et al., 2012). We added a Gaussian blur with a sigma radius of 2.00 to reduce image noise. We set the color space of the image to L*a*b* to generate histograms that measure lightness, green-red contrast, and blue-yellow contrast of the image. We adjusted the lightness filter to allow histogram coordinates ranging from zero to the peak of the image histogram, and the green-red filter to allow from the histogram peak to 255, and the blue-yellow filter to allow all histogram coordinates. These coordinates filter for red areas on the image, corresponding to lignified areas in the stem sections. We measured the total area of lignification,

then selected areas corresponding to the lignified xylem of the stem and measured this area. We subtracted the xylem area from the total lignin area to calculate the cortex lignin area.

DNA-seq library construction for resistant and susceptible Heinz cultivars

DNA was extracted from the leaves of three weeks old seedlings using GeneJET Plant Genomic DNA Purification Mini Kit (Thermo Scientific, Waltham, MA, USA) DNA-Seq libraries were prepared using an in-house protocol modified from Breath Adapter Directional sequencing (BrAD-seq) (Townsley et al., 2015). First, 5 µg of genomic DNA was fragmented using a Covaris E220 (Covaris, Inc. Woburn, MA, USA) with the following settings: Peak Incident Power (W) 140; Duty Factor 10%; Cycles per Burst 200 and Treatment Time (s) 90 to obtain an average fragment size of 400 base pairs. Next, the fragmented DNA was end-repaired and A-tailed in a single reaction using DNA End Repair Mix and Taq DNA polymerase (New England Biolabs). Y-type adapters were ligated and an enrichment PCR was performed with as in BrAD-seq (Townsley et al., 2015) using 7 cycles. Individual libraries were quantified by PCR and pooled to equaled amounts. After a final library cleanup with AMPure beads (Beckman Coulter, Brea, CA, USA), DNA-seq libraries were sequenced at the California Institute for Quantitative Biosciences (QB3) at the University of California, Berkeley using the HiSeq 4000 platform at 150 Paired Read (PR). (Illumina Inc. San Diego, CA, USA).

Resistant and susceptible Heinz cultivar DNA-seq SNP analysis, promoter binding site analysis, and protein domain and structure prediction

For single nucleotide polymorphism (SNP) analysis, we mapped DNA-seq read data to sequenced H1706 tomato genome itag 3.0 to identify SNPs using CLC Genomics Workbench 11 (QIAGEN, https://www.qiagenbioinformatics.com/). Next, we compared the SNPs across the resistant and

susceptible tomato cultivars and focus on finding the SNPs that are common in H9553 and H9492 but different from H9775. In other words, we focus on the SNPs that exist in resistant cultivars and named these SNPs as "resistant specific SNPs" (Supplemental Data Set 5). Among our 4 candidate genes, *LIF1* was the only gene that has resistant specific SNPs in the promoter region (Supplemental Data Set 6). In order to identify potential introgression regions, we conducted phylogenetic network analysis using the PhyloNetworks package (Solís-Lemus et al., 2017) in the Julia environment on XSEDE (Dahan et al., 2014) with 500 kb of sequence around the LIF1 resistance-specific SNP enriched region (Supplemental Figure 8). To identify potential transcription factor binding sites in the *LIF1* promoter region, we used PlantPAN 3.0 (http://PlantPAN.itps.ncku.edu.tw) (Chow et al., 2015; Chow et al., 2018) "TF/TFBS Search" and "Promoter Analysis". We also predicted the *SlWRKY16* binding site based on the homologous genes in the phylogenetic tree of WRKY domains on the Plant Transcription Factor Database (PlantTFDB v5.0, http://planttfdb.gao-lab.org; Phylogenetic Tree for Solanum lycopersicum WRKY Family: http://planttfdb.gao-lab.org/phylo_tree.php?sp=Sly&fam=WRKY) (Jin et al., 2016). To determine the consequences of the K251Q amino acid replacement in the LIF1 protein, we predicted potential protein domains of LIF1 using InterProScan (https://www.ebi.ac.uk/interpro/search/sequence/) (Jones et al., 2014; Mitchell et al., 2018). We conducted protein 3D structure prediction and analysis using Phyre2 (Protein Homology/analogY Recognition Engine v 2.0, http://www.sbg.bio.ic.ac.uk/phyre2/html/page.cgi?id=index) (Kelley et al., 2015). We also predicted whether K251Q amino acid substitution is deleterious or neutral using PROVEAN (Choi, 2012; Choi et al., 2012) (Protein Variation Effect Analyzer, http://provean.jcvi.org/seq_submit.php).

Timecourse RNA-Seq library construction and analysis

We challenged H1706 tomato cultivars with strands of *C. campestris* and collected stem tissues at 1, 2, 3, 4 days post attachment (DPA) and 0 DPA as negative controls. Following this, we constructed strand-specific poly-A based libraries for RNA-seq (Townsley et al., 2015). We conducted sequencing of these libraries on two lanes on Illumina HiSeq 2000 at 50bp Single Read (SR).

We used using CLC Genomics Workbench 11 (QIAGEN) for following RNA-seq analysis. First, we mapped resistant and susceptible cultivar RNA-seq read data to sequenced H1706 tomato genome itag 3.0. To see the general pattern across libraries, we conducted principal component analysis (PCA) of gene expression across different DPA. Next, we used ANOVA comparison with DPA factors and cutoff FDR < 0.1 to select differentially expressed genes (DEG) list. Then, we drew Venn diagrams of DEGs at different DPA libraries. 0 DPA libraries are without *Cuscuta* treatments and serve as the negative control for comparisons. The cutoff of these DEGs are FDR < 0.1 and fold change > 1.5. Following, we constructed a heat map of DEGs across different DPA libraries. Euclidean distance and complete linkage are used for this clustering analysis (Supplemental Figure 1).

Resistant and susceptible cultivar RNA-Seq library construction and interaction model-based analysis

We challenged the resistant and susceptible tomato cultivars with strands of *C. campestris* and collected stem tissues at 4 days post attachment (DPA). Following this, we constructed strand-specific poly-A based libraries for RNA-seq from the four tomato cultivars, including the resistant cultivars H9492 and H9553, and the susceptible cultivars H9775 and H1706. We conducted sequencing of these libraries on two lanes on Illumina HiSeq 4000 at 100bp Single Read (SR). We first mapped reads to sequenced H1706 tomato genome itag 2.4. To investigate gene expression

changes across the resistant and susceptible cultivars in dodder infested versus uninfested plants, we conducted a PCA with K-means clustering using the normalized read counts of sequences mapped to the tomato transcriptome (Supplemental Figure 2). Next, we defined differentially expressed genes with the Bioconductor package DESeq2 employing an interaction design (design = ~ Condition + Genotype + Condition: Genotype). Following this, we focused on these 113 genes that display expression changes upon dodder infestation that are different in H9492 and H9553 compared to H1706 and H9775. Within these 113 genes, we picked our three candidate genes based on gene annotation and functions.

Barnes-Hut clustering analysis and gene coexpression network analysis for resistant and susceptible cultivar RNA-Seq

In order to get a more comprehensive differentially expressed gene (DEG) list, we mapped resistant and susceptible cultivar RNA-seq read data to sequenced H1706 tomato genome itag 3.0 by using CLC Genomics Workbench 11 (QIAGEN). Next, we used ANOVA comparison with both factors, all cultivars and with/without *Cuscuta* treatments, and cutoff FDR < 0.1 to select DEG list. In these 10939 genes, we applied Barnes-Hut t-distributed stochastic neighbor embedding (BH-SNE) using RSMod package (script included in code availability) generated 85 gene clusters based on their gene expression patterns. Based on their GO (Gene Ontology) enrichment terms and their included candidate genes, five clusters were selected for further analysis (Supplemental Data Set 9, yellow-labeled genes). We use these selected genes to build gene coexpression networks by using the R script (script included in code availability) that was modified from our previously published method (Ichihashi et al., 2014). We constructed gene coexpression networks for different *C. campestris* treatments in susceptible and resistant cultivars with normal quantile cutoff = 0.997.

Virus-based Gene Expression (VGE) and virus-induced gene silencing (VIGS) in tomatoes

For preparing the binary vector for plant transient expression that carries the ToMoV DNA, we used a modified pSP72-TAV (Gilbertson et al., 1993; Hou and Gilbertson, 1996) that is lacking the capsid protein ORF (CP) and has a restriction enzyme multisite in which a Gateway® cassette (Thermo Fischer Scientific) was cloned by In-Fusion (Takara) in the *NcoI* site. The whole replicon fragment of TAV-GW was amplified from this vector and cloned into a binary vector to generate a vector for Agrobacterium-mediated transient expression in plants (pMR315). Since the ToMoV DNA-B (Carrying the viral movement protein (MP) and the CP are missing, this clone is not an infectious clone and is only serves as a viral replicon by replicating via rolling circle mechanism (Stenger et al., 1991). The gene cloned into this vector is driven by the CP promoter, which is in the non-translated region between the end of the common region and the start codon of the CP gene that was removed (Supplemental Figure 4).

For transiently overexpressing our candidate genes in the susceptible tomato cultivar H1706, we used this Virus-based Gene Expression (VGE) vector pTAV (Supplemental Figure 4). We cloned *GUS, LIF1, SlMYB55* and *CuRLR1* genes into pTAV and transformed these into thermo-competent *Agrobacterium tumefaciens* by heat-shock-transformation. For culturing Agrobacterium and preparing agroinjection, we followed the previously published protocol (Vel et al., 2009) with some modifications. For each experiment, we started from growing transformed Agrobacterium on Lysogeny broth (LB) agar plates with appropriate antibiotic selections at 30° C for 2 days. Following this, we inoculated 10 mL liquid LB with transformed Agrobacteria (AGL1) and incubated at 30° C for 16 hours with 200 r.p.m. shaking. We diluted the primary cultures 1:5 into Induction Media (Vel et al., 2009) supplemented with appropriate antibiotic selections and 200 µM acetosyringone, and then incubated them at 30° C for 24 hours with 200 r.p.m. shaking. When

the O.D. 600 of the culture was around 1, we harvested the transformed Agrobacteria by centrifuging at 3000 x g for 10 minutes and then resuspended Agrobacteria in Inoculation Buffer (10 mM 2-[N-Morpholino] ethane sulfonic acid (MES), 10 mM $MgCl_2$, 200 µM acetosyringone and 0.5 mM dithiothreitol) to an O.D. 600 of 1 culture. Next, we injected this transformed Agrobacterium culture into the first internode of tomato stems using a syringe equipped with a 0.8 mm x 38.1 mm MonoJect needle.

For virus-induced gene silencing (VIGS), we followed the published VIGS in tomato protocol and tobacco rattle virus (TRV)-based vector system (Liu et al., 2002) with slight modifications. This TRV-based VIGS contains TRV-RNA1 (pTRV1) and TRV-RNA2 (pTRV2), which includes multiple cloning sites for building constructs for the genes of interest. Transformed pTRV1 and pTRV2 *Agrobacterium* cultures were mixed in a 1: 1 ratio before infiltration. After about 3.5 hours of incubation on the shaker at room temperature, mixed *Agrobacterium* cultures were infiltrated onto the cotyledons of 9-day-old tomato plants using a 1 ml needleless syringe.

Preparation of *C. campestris* extracts and injection protocols

For one mL *C. campestris* extracts, we collected 100 mg of the stem tissue in microcentrifuge tubes from *C. campestris* growing on H1706 tomato plants. We used the BioSpec Mini-Beadbeater to grind the liquid nitrogen-frozen tissue with five 2.3 mm diameter BioSpec zirconia beads and 1.0 mm diameter BioSpec zirconia beads in the tubes for 1 minute, and then mixed with one mL deionized water. To remove the plant tissue debris, we centrifuged extracts for 30 seconds at 5000 r.c.f., and used only the supernatant for untreated extract injections. For heat-treated extracts, we heated at 95 °C for 5 minutes. For pH treated extracts, we adjusted the pH to 9 by adding 0.1M NaOH. For filtered extracts, we filtered untreated extracts through a VWR 0.2 µm sterile syringe filter. We injected different treated extracts into the first internode of tomato stems using a syringe

equipped with a 0.8 mm x 38.1 mm MonoJect needle. Furthermore, we used 3K, 10K, 30K, and 100K Amicon® Ultra Centrifugal Filter Devices to filter *Cuscuta* extracts. Then, we use flow through extracts to do injection on H9553 stems to test the size of *Cuscuta* signals.

Protein interaction, subcellular localization and co-localization of fusion candidate proteins

For protein interaction assays, we performed *in vivo* using bimolecular fluorescence complementation (BiFC) system (Kerppola, 2008). The plasmids were constructed by using the Gateway-compatible BiFC vectors SPDK1794 (*p35S::cCitrine*) and SPDK1823 (*p35S::nCitrine*). The leaves of four-week-old *Nicotiana (N.) benthamiana* were injected with different combinations of *Agrobacterium (A.) tumefaciens* GV3101 containing the transient expression vectors (Fang and Spector, 2010).

For subcellular localization and co-localization of fusion candidate proteins, we performed with transient expression fluorescent fusion proteins *in vivo*. The plasmids were constructed by using the Gateway-compatible vectors pGWB5 (*p35S::GFP*) and pGWB660 (*p35S::TagRFP*). The leaves of four-week-old *N. benthamiana* were injected with the *A. tumefaciens* GV3101 strain containing one of the plasmids (Sparkes et al., 2006). To verify the interaction between LIF1 and SlWRKY16 proteins and determine their subcellular localizations when they interact with each other, we also co-expressed the fusion proteins LIF1-GFP (*p35S::LIF1-GFP*) and SlWRKY16-RFP (*p35S::SlWRKY16-TagRFP*). To reduce gene-silencing and enhance transient expression of our candidate proteins, we co-expressed the fusion proteins with p19 obtained from Professor Bo Liu's Lab at University of California, Davis. Three individual plants and three adult leaves of each plant were used for each treatment. Fluorescence was observed 2 – 5 days after transfection by a Confocal Laser Scanning Platform Zeiss LSM710 (Zeiss, Germany).

Validation of protein-protein interaction by yeast two-hybrid analysis

To validate the predicted protein-protein interaction between two of our candidate TFs, AP2 and WRKY16, we used the GAL4 yeast two-hybrid system (Clontech). AP2 and WRKY16 were cloned into pGADT7-GW (Addgene Plasmid #61702) and pGBKT7-GW (Addgene Plasmid #61703) plasmids, which were obtained from Yuhai Cui (Lu et al., 2010). Empty pGADT7 (with the GAL4 activation domain, AD) and pGBKT7 (with the GAL4 DNA-binding domain, BD) plasmids were used as negative controls. We use the yeast (*Saccharomyces cerevisiae*) strain AH109 in the MATCHMAKER GAL4 Two-Hybrid System (Clontech), in which *HIS3*, *ADE2*, *MEL1* and *LacZ* are under the control of GAL4 TF. The AD and BD plasmids were co-transformed to yeast AH109 competent cells following Clontech's user manual instructions of the polyethylene glycol (PGE)/lithium acetate method and cultured in YPD Plus Medium for 90 minutes to promote transformation efficiency. Transformed yeast cells were assayed by culturing in SD/-Leu/-Trp medium to select for successful co-transformants and then assayed by culturing in SD/–Ade/–His/–Leu/–Trp medium with 40 μg/ml X-α-Gal, which provides high-stringency selection. The positive protein-protein interactions between two TFs are indicated by growth on SD/–Ade/–His/–Leu/–Trp/X-α-Gal medium plates and blue colony color.

Lignin content and composition analysis

Tomato stem material from specified treatments was flash-frozen in liquid nitrogen and lyophilized at -50°C and ≤ 0.1 mbar for 48 hours in a 6L FreeZone 6 Benchtop Freeze Dry System (Labconco Corp., Kansas City, MO, USA). Lyophilized material was pulverized in a 2ml screw top microcentrifuge tube with a glass bead for 10 minutes at a frequency of 20/s in a TissueLyser (Retsch ballmill, Qiagen, Venlo, Netherlands). The material was AIR prepped and destarched using protocols from Barnes and Anderson (Barnes and Anderson, 2017). Acetyl bromide analysis

was carried out using the same protocol with one exception: samples were incubated at 50°C with gentle swirling every 10 minutes for 2 hours to limit the degradation of xylan, which can lead to the over quantification of lignin present in the sample. Lignin quantification reactions were performed in a 10 mm light path quartz cuvette (VWR, Radnor, PA, USA, catalog number 414004-062) and absorbance measurements were taken on a SPECTRAmax plus 384 (Molecular Devices, San Jose, CA, USA). Acetyl Bromide Soluble Lignin (%ABSL), which indicates percent absorbance of soluble lignin, was calculated using the extinction coefficient of 17.2 (Chen and Dixon, 2007). Presently, no extinction coefficient is available for tomato stem lignin so the extinction coefficient for tobacco stem lignin was used.

Cell wall-bound aromatics and HPLC analysis of liberated aromatics was performed as described by Eudes et al. (Eudes et al., 2015). The remaining cell wall material post-aromatic extraction, now enriched for lignin, was then washed with water 3 times and dried at 30°C overnight. The chemical composition of the lignin enriched cell wall material was analyzed by pyrolysis-gas chromatography (GC) /mass spectrometry (MS) using a previously described method with some modifications (Eudes et al., 2015). Pyrolysis of biomass was performed with a Pyroprobe 6200 (CDS Analytical Inc., Oxford, PA, USA) connected with GC/MS (GCMS-QP2010 Ultra Gas Chromatograph Mass Spectrometer, Shimadzu corp., Kyoto, Japan) equipped with an AgilentHP-5MS column (30 m 9 0.25 mm i.d., 0.25 lm film thickness). The pyrolysis was carried out at 550 °C. The chromatograph was programmed from 50 °C (1 min) to 300 °C at a rate of 30 °C/min; the final temperature was held for 10 min. Helium was used as the carrier gas at a constant flow rate of 1 mL/min. The mass spectrometer was operated in scan mode and the ion source was maintained at 300 °C. The compounds were identified by comparing their mass spectra with those of the NIST library and those previously reported (Ralph and Hatfield, 1991; Gutiérrez et al., 2006). Peak molar

areas were calculated for the lignin degradation products, and the summed areas were normalized per sample.

Data availability

All data is available in the main text or the supplementary materials. All DNA-Seq and RNA-Seq raw data are deposited on NCBI SRA PRJNA550259.

Code availability

All R scripts and package for analysis are deposited on GitHub. R script for RNA-Seq interaction model-based analysis deposited on GitHub (Link: https://github.com/MinYaoJhu/Moran-s-RNA-Seq-analysis-script). R script and RSMod package for Barnes-Hut clustering analysis deposited on GitHub (Link: https://github.com/sdrowland/RSMod). R script for RNA-Seq gene coexpression network analysis deposited on GitHub (Link: https://github.com/Hokuto-GH/gene-coexpression-network-script).

Acknowledgments

We are grateful to S. Dinesh-Kumar, A. B. Britt, S. Brady, and D. Runcie for their input on this research, and S. Dinesh-Kumar, A. B. Britt, S. Brady, and E. D. Marable for editing suggestions. We thank C. Wong, C. Ito, Z. Jaramillo, J. Tanurahardja and J. Lu for helping with some parts of experiments or image analysis, and Axtell Lab and N. Johnson for providing information to help with verifying *Cuscuta* species, and Liu Lab and Y. Lee for providing p19, pGWB5 and pGWB660 plasmid. We also thank R. Ozminkowski, Manager of Agricultural Research from HeinzSeed for providing seeds of three Heinz cultivars, and the UC Davis Plant Transformation Facility for

generating transgenic plants, and CyVerse for online data storage. This work used the Extreme Science and Engineering Discovery Environment (XSEDE) on the Pittsburgh Supercomputing Center (PSC) at the Regular Memory (Bridges) servers through allocation IBN200015. We thank A. Eudes for his recommendations and guiding conversations in lignin analysis, and J. Ortega for her technical support with the pyro-GC/MS instrument. **Funding:** This work was funded by USDA-NIFA (2013-02345). M.-Y. J. was supported by Yen Chuang Taiwan Fellowship, Taiwan Government Scholarship (GSSA), Elsie Taylor Stocking Memorial Fellowship, and Katherine Esau Summer Graduate Fellowship program; M.F. was supported by United States-Israel Binational Agricultural Research and Development Fund (postdoctoral fellowship no. FI–463–12), M.S.B. and P.M.S. were supported by the DOE Joint BioEnergy Institute (http://www.jbei.org) supported by the U.S. Department of Energy, Office of Science, Office of Biological and Environmental Research through contract DE-AC02-05CH11231 between Lawrence Berkeley National Laboratory and the U.S. Department of Energy.

Competing interests: The authors declare that they have no competing interests.

Figures

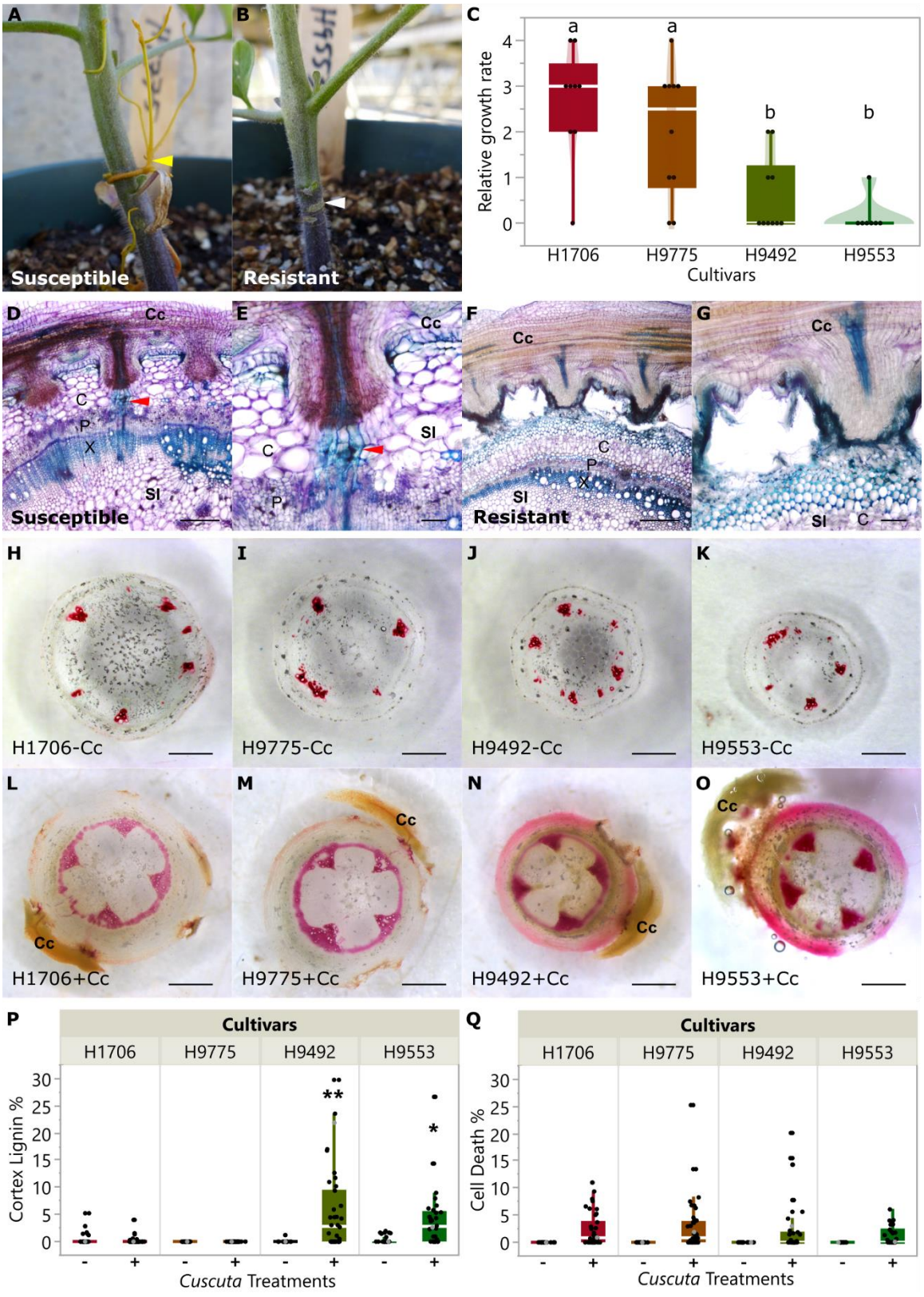
A
Susceptible
B
Resistant
C
Relative growth rate
a
a
b
b
H1706
H9775
H9492
H9553
Cultivars
D
Cc
C
P
X
Sl
Susceptible
E
Cc
Sl
C
P
F
Cc
C
P
X
Sl
Resistant
G
Cc
Sl
C
H
H1706-Cc
I
H9775-Cc
J
H9492-Cc
K
H9553-Cc
L
Cc
H1706+Cc
M
Cc
H9775+Cc
N
Cc
H9492+Cc
O
Cc
H9553+Cc
P
Cultivars
H1706
H9775
H9492
H9553
Cortex Lignin %
**
*
- + - + - + - +
Cuscuta Treatments
Q
Cultivars
H1706
H9775
H9492
H9553
Cell Death %
- + - + - + - +
Cuscuta Treatments

Figure 1 | The comparison of resistance responses to *C. campestris* in tomato cultivars. (A) *C. campestris* grows on the susceptible H9775, (B) and cannot attach on the resistant H9553. (C) The biomass ratio of host and *C. campestris* (*Cuscuta* weight/ tomato weight) on different cultivars. Data were assessed using pair-wise comparisons with Tukey test. P-values between "a" and "b" are < 0.05; H1706, n = 9; H9775, n = 10, H9492, n = 10, H9553 n = 7. Data were collected at 45 days post attachment (DPA). (D-G) 100 μm vibratome longitudinal sections of *C. campestris* haustoria attaching to H1706 (D-E) and H9553 (F-G), and stained with Toluidine Blue O. Lignin is stained as blue. Red arrowhead indicates haustorial vascular connections. Cc indicates *C. campestris; Sl* indicates *S. lycopersicum*. C, cortex; P, phloem; X, xylem. (D and F) Scale bar, 40 μm. (E and G) Scale bar, 10 μm. (H-O) are ~300 μm sections of the haustoria attachment sites stained with Phloroglucinol-HCl. Scale bar, 1 mm. Lignin is stained as red. Stem cross-sections of H1706 (H and L), H9775 (I and M), H9492 (J and N), and H9553 (K and O) without *C. campestris* treatment (labeled with -Cc) and with *C. campestris* attached (labeled with +Cc). (P) Cortex lignin area percentage in different cultivars. Data presented are assessed using multiple comparisons with Dunnett's test. "*": p-values < 0.05, "**": p-values < 0.01. (Q) Cell death area percentage in different cultivars. (P-Q) H1706-Cc, n = 20; H1706+Cc, n = 38; H9775-Cc, n = 19; H9775+Cc, n = 40; H9492-Cc, n = 16; H9492+Cc, n = 38; H9553-Cc, n = 17; H9553+Cc, n = 30. Data were collected at 14 DPA. The data points labeled with grey color indicate the sample that we show in the section picture H-I.

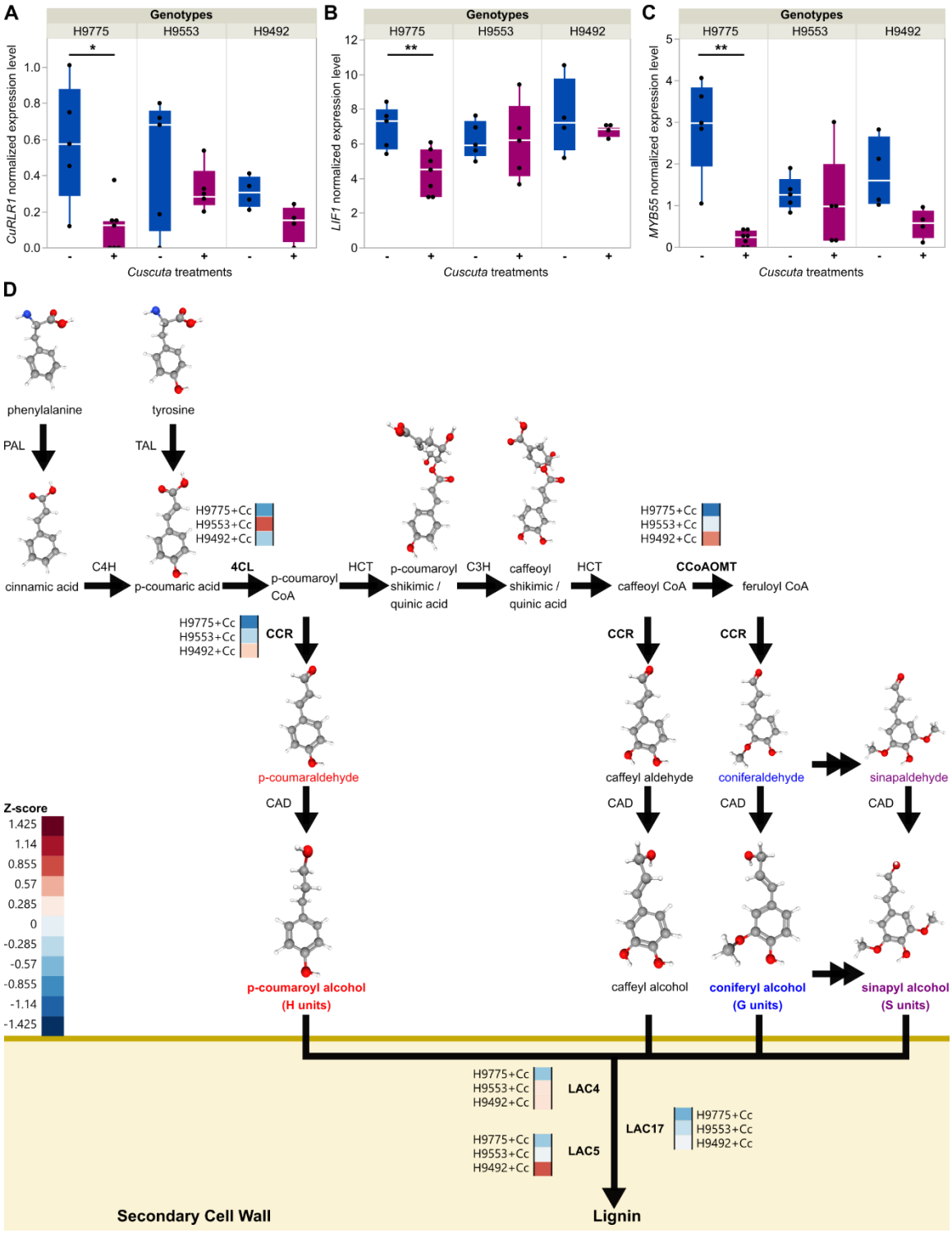

Figure 2 | Key candidate genes and lignin biosynthesis genes that display expression changes upon *C. campestris* infestation. (A-C) The normalized expressions levels (CPM, counts per

million) of genes in susceptible cultivar H9775 and in resistant hybrid cultivar H9553 and H9492 under *C. campestris* infestation. – and + indicates without or with *C. campestris* infection treatments respectively. Biologically independent replicates: RNA-Seq libraries: H9775-Cc, n = 5; H9775+Cc, n = 7; H9492-Cc, n = 4; H9492+Cc, n = 4; H9553-Cc, n = 5; H9553+Cc, n = 5. Data are assessed using two-tailed t test. "*": p-values < 0.04, "**": p-values < 0.01, "***": p-values < 0.005. (D) The lignin biosynthesis pathway with key enzyme expression levels. Genes that are differentially expressed were selected and the normalized expression values across three cultivars were color coded according to z-score. + Cc indicates with *C. campestris* infection treatments. PAL, phenylalanine ammonia-lyase; C4H, cinnamate 4-hydroxylase; TAL, tyrosine ammonia-lyase; 4CL, 4-coumarate CoA ligase; HCT, hydroxycinnamoyl-CoA shikimate / Quinate hydroxycinnamoyltransferase; C3H, *p*-coumarate 3-hydroxylase; CCoAOMT, caffeoyl-CoA *O*-methyltransferase; CCR, cinnamoyl-CoA reductase; CAD, cinnamyl alcohol dehydrogenase; LAC, laccase. 3D structure images of phenylalanine, tyrosine, cinnamic acid, p-coumaric acid, p-coumaroyl shikimic acid, caffeoyl shikimic acid, p-coumaraldehyde, p-coumaryl alcohol, caffeyl aldehyde, caffeyl alcohol, coniferaldehyde, coniferyl alcohol, sinapaldehyde, and sinapyl alcohol are from PubChem (National Center for Biotechnology Information, 2021c, b, d, e, f, g, h, i, j, k, l, m, n, a).

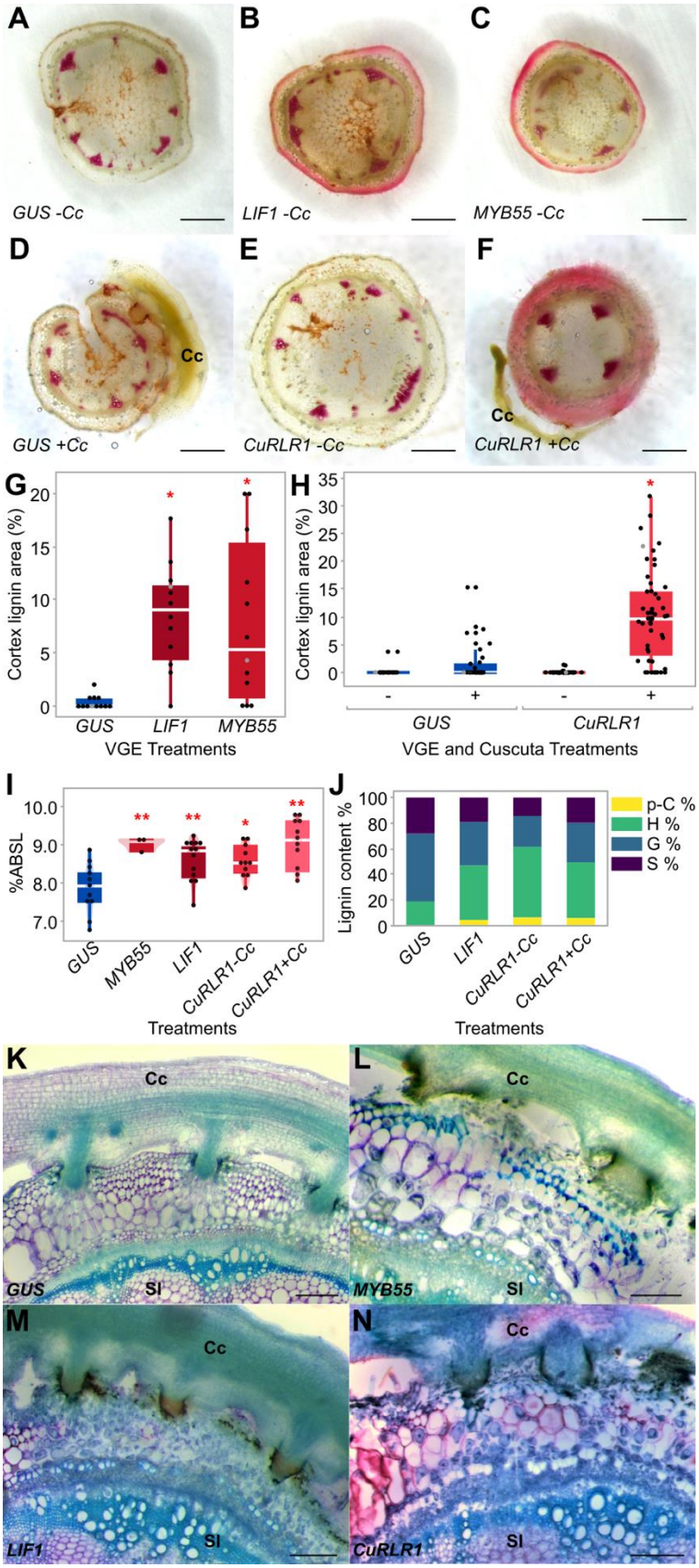
A
GUS -Cc
B
LIF1 -Cc
C
MYB55 -Cc
D
Cc
GUS +Cc
E
CuRLR1 -Cc
F
Cc
CuRLR1 +Cc
G
Cortex lignin area (%)
GUS
LIF1
MYB55
VGE Treatments
H
Cortex lignin area (%)
GUS
CuRLR1
VGE and Cuscuta Treatments
I
%ABSL
GUS
MYB55
LIF1
CuRLR1-Cc
CuRLR1+Cc
Treatments
J
Lignin content %
p-C %
H %
G %
S %
GUS
LIF1
CuRLR1-Cc
CuRLR1+Cc
Treatments
K
Cc
GUS
Sl
L
Cc
MYB55
Sl
M
Cc
LIF1
Sl
N
Cc
CuRLR1
Sl

Figure 3 | Virus-based Gene Expression (VGE) in tomato H1706. (A-F) ~300 μm stem sections near injection sites, Phloroglucinol-HCl stains lignin red. VGE of *GUS* (A), *LIF1* (B), *SlMYB55* (C), and *CuRLR1* (E) in stem without *C. campestris*. VGE of *GUS* (D) and *CuRLR1* (F) with *C. campestris*. (G) Cortex lignin area percentage in VGE of *LIF1* and *SlMYB55* (n = 12 each) and (H) *CuRLR1* with and without *C. campestris* (*GUS*-Cc, n = 18; *GUS*+Cc, n =28; *CuRLR1*-Cc, n = 47; *CuRLR1*+Cc, n = 53). (G-H) Data were collected at 7 days post injection (DPI) and 14 days post attachment (DPA). Data are assessed using Dunnett's test with *GUS*-Cc as negative control. "*": p-values < 0.01. The data points labeled with grey color indicate the sample that we show in the section picture A-F. (I) Acetyl bromide assay for lignin in VGE stems. Acetyl Bromide Soluble Lignin (ABSL) indicates percent absorbance of soluble lignin. Samples were collected at 7 DPI and 6 DPA. Data are assessed using Dunnett's test. "*": p-values < 0.05, "**": p-values < 0.01. Biological replicates for *GUS*, n = 18; *SlMYB55*, n = 10; *LIF1*, n = 18, *CuRLR1*-Cc, n = 18; *CuRLR1*+Cc, n = 18. Technical replicates for acetyl bromide assay; *GUS*, n = 11; *SlMYB55*, n = 3; *LIF1*, n = 13; *CuRLR1*-Cc, n = 11; *CuRLR1*+Cc, n = 11. (J) PYRO-GC assay for monolignols in *CuRLR1* VGE samples with and without *C. campestris*. Samples were collected at 7 DPI and 6 DPA. Biological replicates collected from first internodes; *GUS*, n = 8; *LIF1*, n = 8, *CuRLR1*-Cc, n = 18; *CuRLR1*+Cc, n = 18. PYRO-GC assay technical replicates; *GUS*, n = 3; *LIF1*, n = 3; *CuRLR1*-Cc, n = 5; *CuRLR1*+Cc, n = 5. (K-N) VGE of *CuRLR1*, *LIF1* and *SlMYB55* induces cortical lignin making H1706 resistant to *C. campestris*. Scale bar, 30 μm. Samples were collected at 7 DPI and 6 DPA. Cc indicates *C. campestris; Sl* indicates *S. lycopersicum.*

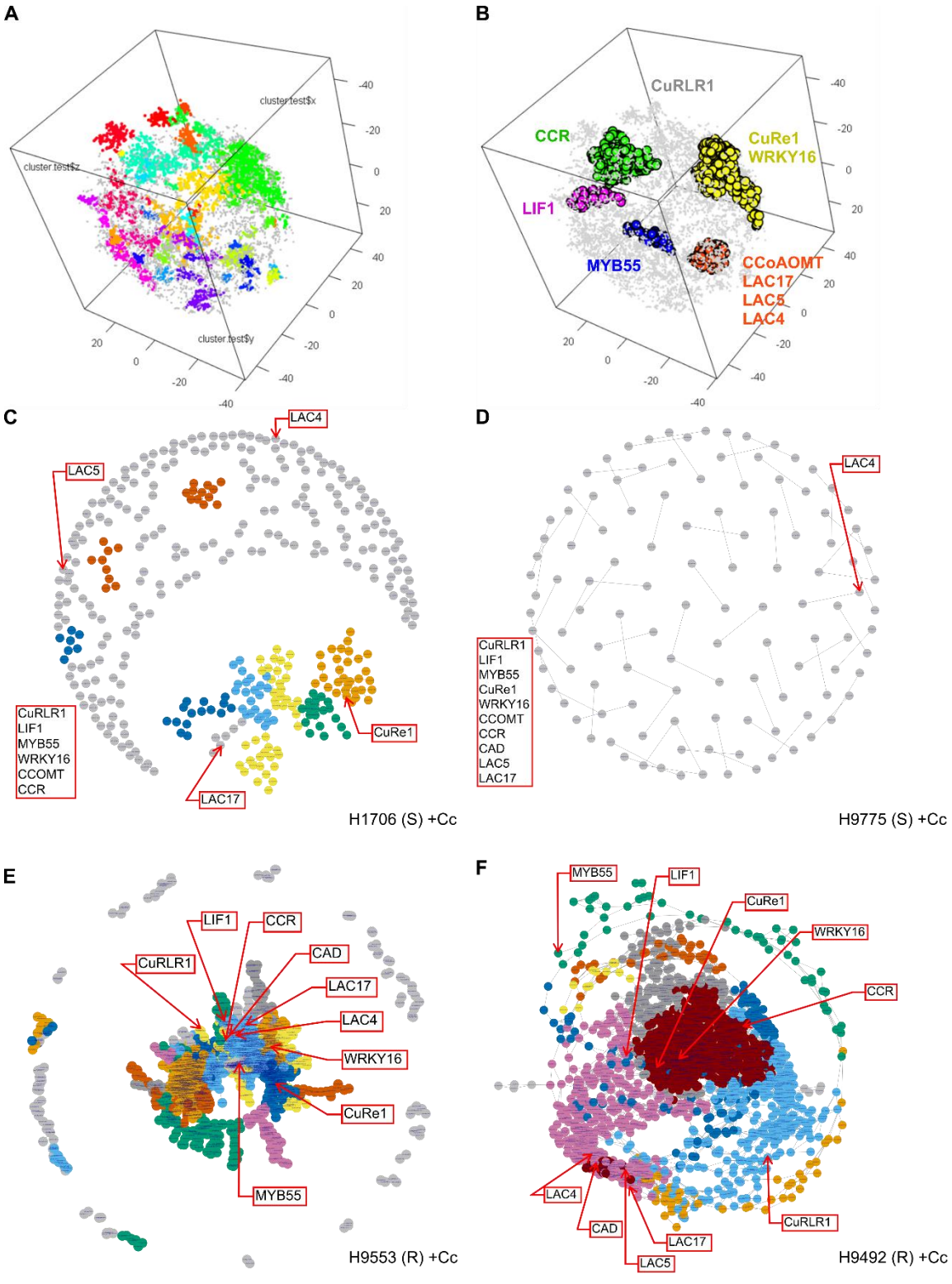

Figure 4 | Barnes-Hut t-distributed stochastic neighbor embedding (BH-SNE) generated gene clusters and gene co-expression network (GCN) analysis. (A) BH-SNE generated gene

clusters based on their gene expression patterns. Total cluster (module) number was 48. (B) The candidate genes that are included in the clusters are labeled with their corresponding colors. The selected gene clusters for GCN are labeled in yellow (CuRe1 and WRKY16 cluster, cluster 17), red (CCOMT and LAC cluster, cluster 11), blue (MYB55 cluster, cluster 39), pink (LIF1 cluster, cluster 46), green (CCR cluster, cluster 23) colors. *CuRLR1* is in the noise cluster, and is labeled in grey color. Parameters used in this analysis: perplexity (perp) = 20, lying = 250, cutoff = 20, seed = 2. (C-F) Gene co-expression networks (GCNs) of four different Heinz susceptible and resistant cultivars upon *C. campestris* treatments. Based on BH-SNE analysis, 1676 genes in cluster 11, 17, 23, 39, 46 and CuRLR1 were selected for building GCNs. +Cc indicates with *C. campestris* infection treatments. The genes that are listed at the left of the GCN and not labeled in the network are the genes that have no coexpression connections with all the other genes in the list.

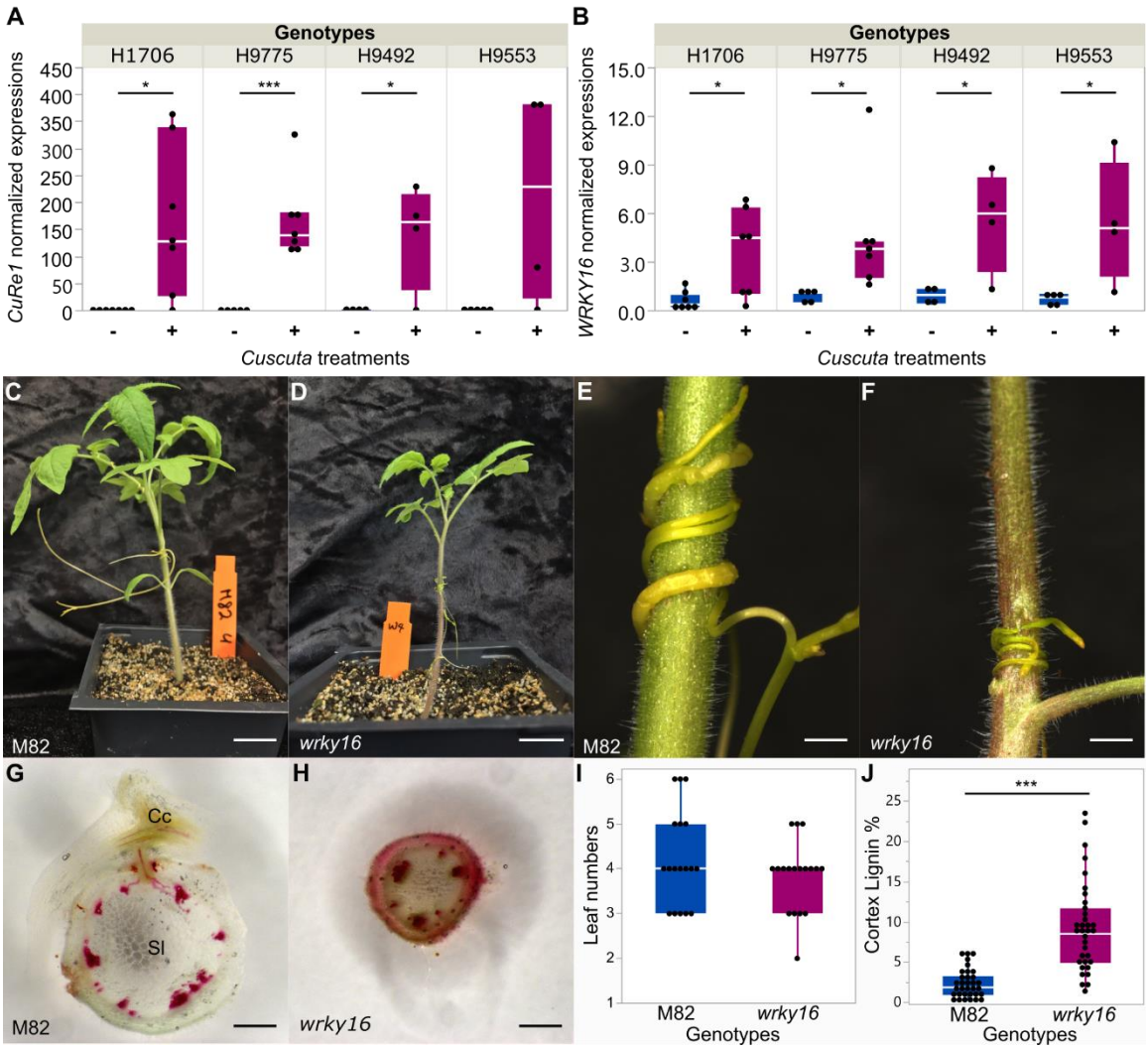

Figure 5 | The role of *SlWRKY16* in *Cuscuta* resistance using CRISPR/Cas9 gene knockouts. (A-B) Normalized *CuRel* and *SlWRKY16* expression level from RNA-Seq data (CPM, counts per million) in different Heinz cultivars with/without *Cuscuta* treatments. Biologically independent replicates: RNA-Seq libraries, H1706-Cc, n = 7; H1706+Cc, n = 7; H9775-Cc, n = 5; H9775+Cc, n = 7; H9492-Cc, n = 5; H9492+Cc, n = 4; H9553-Cc, n = 5; H9553+Cc, n = 5. Data are assessed using one-tailed t test. "*": p-values < 0.05, "**": p-values < 0.01, "***": p-values < 0.005. (C-J) Samples and data were collected at 7 DPA. (C-D) overall phenotype comparison between M82 and homozygous *SlWRKY16* CRISPR lines (*wrky16*). Scale bar, 2 cm. (E-F) *C. campestris* growing on

M82 and *wrky16*. (G-H) ~300 μm hand sections of M82 and *wrky16* stems near *Cuscuta* attachment site stained with Phloroglucinol-HCl. Lignin is stained red. Cc indicates *C. campestris.* (I) Leaf number of *wrky16* and M82. Biological replicates, n = 18 for each. (J) Cortex lignin area percentage in M82 and *wrky16* stems. Data presented are assessed using student's t-test. "***" indicates p-value is less than 0.001. Replicates: M82, n = 33; *wrky16*, n = 34.

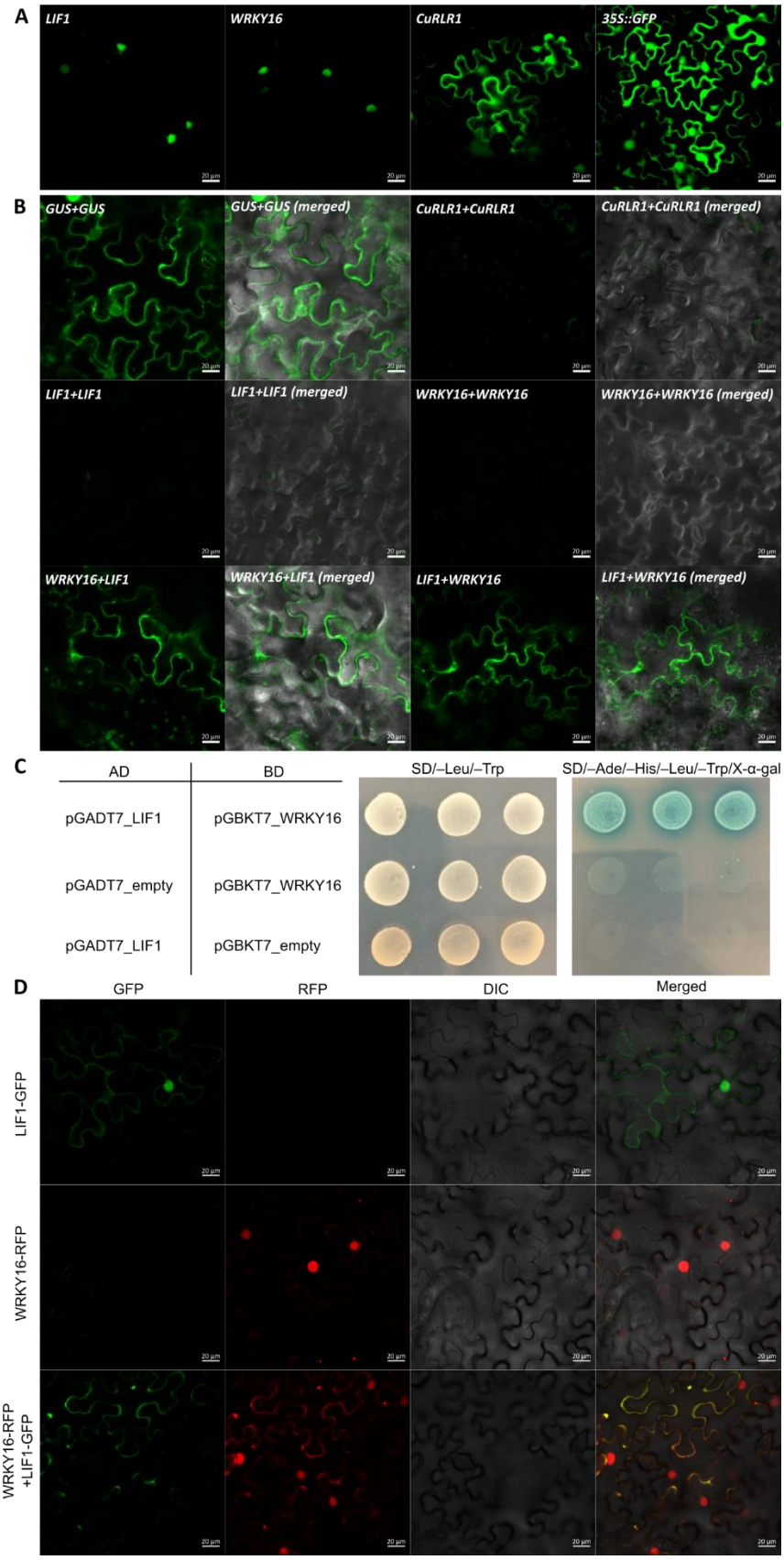
A
LIF1
WRKY16
CuRLR1
35S::GFP
B
GUS+GUS
GUS+GUS (merged)
CuRLR1+CuRLR1
CuRLR1+CuRLR1 (merged)
LIF1+LIF1
LIF1+LIF1 (merged)
WRKY16+WRKY16
WRKY16+WRKY16 (merged)
WRKY16+LIF1
WRKY16+LIF1 (merged)
LIF1+WRKY16
LIF1+WRKY16 (merged)
C
AD
BD
SD/–Leu/–Trp
SD/–Ade/–His/–Leu/–Trp/X-α-gal
pGADT7_LIF1
pGBKT7_WRKY16
pGADT7_empty
pGBKT7_WRKY16
pGADT7_LIF1
pGBKT7_empty
D
GFP
RFP
DIC
Merged
LIF1-GFP
WRKY16-RFP
WRKY16-RFP +LIF1-GFP

Figure 6 | Subcellular localization of candidate genes and protein-protein interactions. (A) Subcellular localizations of LIF1, SlWRKY16, and CuRLR1 proteins. (B) Verification of protein-protein interactions and locations of SlWRKY16 and LIF1 by Bimolecular Fluorescence Complementation (BiFC). The gene with *cCitrine* fusion is listed before the "+" sign and the gene with *nCitrine* fusion is listed after the "+" sign. (C) Yeast two-hybrid (Y2H) results for interaction between LIF1 and SlWRKY16. The plasmids with GAL4 activation domain (AD) and GAL4 DNA binding domain (BD) were co-transformed to yeast AH109 competent cells. Transformed yeast cells were screened on SD/-Leu/-Trp medium plates to select successful co-transformants and then assayed by culturing on high-stringency SD/–Ade/–His/–Leu/–Trp medium plates with 40 μg/ml X-α-Gal. The positive protein-protein interactions between LIF1 and SlWRKY16 are indicated by growth on SD/–Ade/–His/–Leu/–Trp/X-α-Gal medium plates and blue colony color. (D) Co-expression of fusion protein LIF1-GFP and SlWRKY16-RFP to observe subcellular localizations. Yellow color in the merged panel indicates that GFP and RFP signals are overlapped.

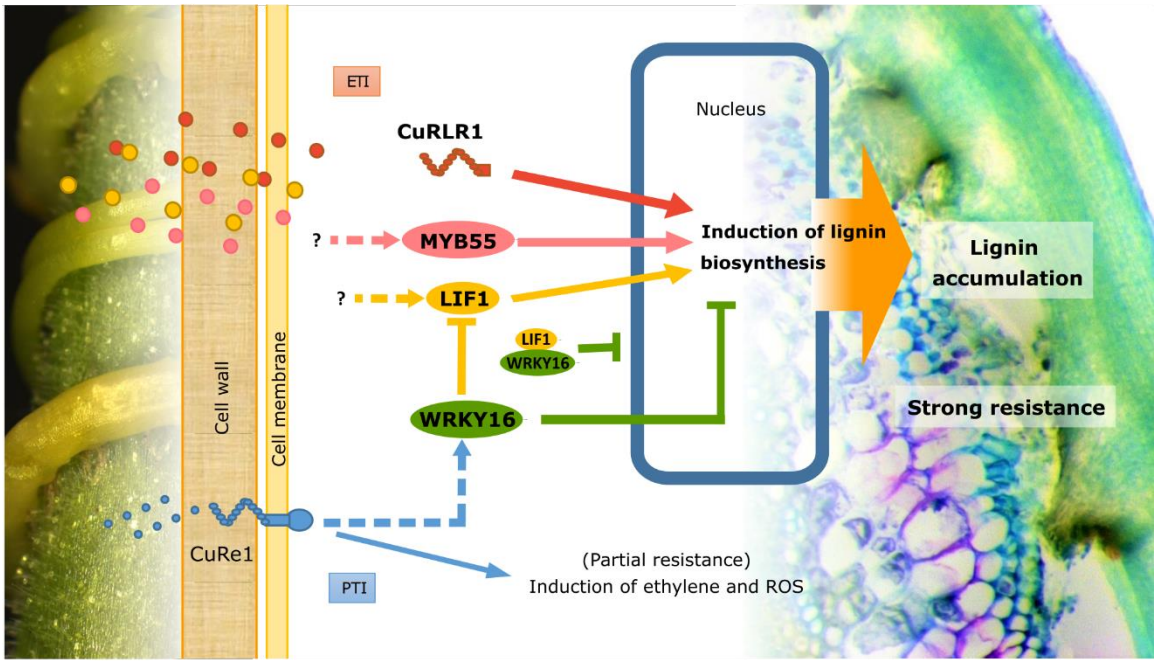

Figure 7 | Model of *C. campestris* resistance response in tomato cultivars. Red-labeled pathway: newly identified cytosolic *CuRLR1*, which may receive large signaling molecules from *C. campestris* or play a role in signal transduction upon *Cuscuta* perception. This triggers downstream signal transduction and induces a lignin-based resistance response. This resistant response may be an effector-triggered immunity (ETI). Pink and yellow-labeled pathway: *SlMYB55* and *LIF1* function as positive regulators in the lignin biosynthesis pathway. Yellow and green-labeled pathway: *SlWRKY16* and *LIF1* mediated lignin-based resistant responses and with a potential connection to *CuRe1*. Blue-labeled pathway: previously identified *CuRe1* mediated PAMP/MAMP-triggered immunity (PTI/MTI) pathway.

References

Agrios, G.N. (2005). chapter thirteen - PLANT DISEASES CAUSED BY PARASITIC HIGHER PLANTS, INVASIVE CLIMBING PLANTS, AND PARASITIC GREEN ALGAE. In Plant Pathology (Fifth Edition) (San Diego: Academic Press), pp. 705-722.

Ashton, F.M. (1976). Cuscuta Spp. (Dodder): A Literature Review of Its Biology and Control. (Division of Agricultural Sciences, University of California).

Barnes, W.J., and Anderson, C.T. (2017). Acetyl Bromide Soluble Lignin (ABSL) Assay for Total Lignin Quantification from Plant Biomass. Bio-protocol **7,** e2149.

Barros, J., Serk, H., Granlund, I., and Pesquet, E. (2015). The cell biology of lignification in higher plants. Annals of botany **115,** 1053-1074.

Bellincampi, D., Cervone, F., and Lionetti, V. (2014). Plant cell wall dynamics and wall-related susceptibility in plant–pathogen interactions. Frontiers in Plant Science **5**.

Bhuiyan, N.H., Selvaraj, G., Wei, Y., and King, J. (2009). Role of lignification in plant defense. Plant signaling & behavior **4,** 158-159.

CAMERON, D.D., COATS, A.M., and SEEL, W.E. (2006). Differential Resistance among Host and Non-host Species Underlies the Variable Success of the Hemi-parasitic Plant Rhinanthus minor. Annals of Botany **98,** 1289-1299.

Cass, C.L., Peraldi, A., Dowd, P.F., Mottiar, Y., Santoro, N., Karlen, S.D., Bukhman, Y.V., Foster, C.E., Thrower, N., Bruno, L.C., Moskvin, O.V., Johnson, E.T., Willhoit, M.E., Phutane, M., Ralph, J., Mansfield, S.D., Nicholson, P., and Sedbrook, J.C. (2015). Effects of PHENYLALANINE AMMONIA LYASE (PAL) knockdown on cell wall composition, biomass digestibility, and biotic and abiotic stress responses in Brachypodium. Journal of Experimental Botany **66,** 4317-4335.

Chen, F., and Dixon, R.A. (2007). Lignin modification improves fermentable sugar yields for biofuel production. Nature Biotechnology **25,** 759.

Chen, X., Li, C., Wang, H., and Guo, Z. (2019). WRKY transcription factors: evolution, binding, and action. Phytopathology Research **1,** 13.

Choi, Y. (2012). A fast computation of pairwise sequence alignment scores between a protein and a set of single-locus variants of another protein. In Proceedings of the ACM Conference on Bioinformatics, Computational Biology and Biomedicine (Orlando, Florida: Association for Computing Machinery), pp. 414–417.

Choi, Y., Sims, G.E., Murphy, S., Miller, J.R., and Chan, A.P. (2012). Predicting the Functional Effect of Amino Acid Substitutions and Indels. PLOS ONE **7,** e46688.

Chow, C.-N., Lee, T.-Y., Hung, Y.-C., Li, G.-Z., Tseng, K.-C., Liu, Y.-H., Kuo, P.-L., Zheng, H.-Q., and Chang, W.-C. (2018). PlantPAN3.0: a new and updated resource for reconstructing transcriptional regulatory networks from ChIP-seq experiments in plants. Nucleic Acids Research **47,** D1155-D1163.

Chow, C.-N., Zheng, H.-Q., Wu, N.-Y., Chien, C.-H., Huang, H.-D., Lee, T.-Y., Chiang-Hsieh, Y.-F., Hou, P.-F., Yang, T.-Y., and Chang, W.-C. (2015). PlantPAN 2.0: an update of plant promoter analysis navigator for reconstructing transcriptional regulatory networks in plants. Nucleic Acids Research **44,** D1154-D1160.

Ciolkowski, I., Wanke, D., Birkenbihl, R.P., and Somssich, I.E. (2008). Studies on DNA-binding selectivity of WRKY transcription factors lend structural clues into WRKY-domain function. Plant Mol Biol **68,** 81-92.

Costea, M., García, M.A., Baute, K., and Stefanović, S. (2015a). Entangled evolutionary history of Cuscuta pentagona clade: A story involving hybridization and Darwin in the Galapagos. TAXON **64,** 1225-1242.

Costea, M., García, M.A., Baute, K., Stefanovi, and Sa. (2015b). Entangled evolutionary history of Cuscuta pentagona clade: A story involving hybridization and Darwin in the Galapagos. Taxon **64,** 1225-1242.

Cui, S., Wada, S., Tobimatsu, Y., Takeda, Y., Saucet, S.B., Takano, T., Umezawa, T., Shirasu, K., and Yoshida, S. (2018). Host lignin composition affects haustorium induction in the parasitic plants Phtheirospermum japonicum and Striga hermonthica. New Phytologist **218,** 710-723.

Dahan, M., Towns, J., Cockerill, T., Dahan, M., Foster, I., Gaither, K., Grimshaw, A., Hazlewood, V., Lathrop, S., Lifka, D., Peterson, G., Roskies, R., Scott, J., and Wilkins-Diehr, N. (2014). XSEDE: Accelerating scientific discovery. Computing in Science and Engineering **16,** 62-74.

Dhakshinamoorthy, S., Mariama, K., Elsen, A., and De Waele, D. (2014). Phenols and lignin are involved in the defence response of banana (Musa) plants to infection. Nematology **16,** 565-576.

Dodds, P.N., and Rathjen, J.P. (2010). Plant immunity: towards an integrated view of plant–pathogen interactions. Nature Reviews Genetics **11,** 539-548.

Duriez, P., Vautrin, S., Auriac, M.-C., Bazerque, J., Boniface, M.-C., Callot, C., Carrère, S., Cauet, S., Chabaud, M., Gentou, F., Lopez-Sendon, M., Paris, C., Pegot-Espagnet, P., Rousseaux, J.-C., Pérez-Vich, B., Velasco, L., Bergès, H., Piquemal, J., and Muños, S.

(2019). A receptor-like kinase enhances sunflower resistance to Orobanche cumana. Nature Plants **5,** 1211-1215.

Eudes, A., Sathitsuksanoh, N., Baidoo, E.E.K., George, A., Liang, Y., Yang, F., Singh, S., Keasling, J.D., Simmons, B.A., and Loqué, D. (2015). Expression of a bacterial 3-dehydroshikimate dehydratase reduces lignin content and improves biomass saccharification efficiency. Plant Biotechnology Journal **13,** 1241-1250.

Fang, Y., and Spector, D.L. (2010). BiFC Imaging Assay for Plant Protein-Protein Interactions. Cold Spring Harbor Protocols **2010,** pdb.prot5380.

Ferrer, J.L., Austin, M.B., Stewart, C., and Noel, J.P. (2008). Structure and function of enzymes involved in the biosynthesis of phenylpropanoids. Plant Physiology and Biochemistry **46,** 356-370.

García, M.A., Costea, M., Kuzmina, M., and Stefanović, S. (2014). Phylogeny, character evolution, and biogeography of Cuscuta (dodders; Convolvulaceae) inferred from coding plastid and nuclear sequences. American Journal of Botany **101,** 670-690.

Gayoso, C., Pomar, F., Novo-Uzal, E., Merino, F., and Martínez de Ilárduya, Ó. (2010). The Ve-mediated resistance response of the tomato to Verticillium dahliae involves H2O2, peroxidase and lignins and drives PALgene expression. BMC Plant Biology **10,** 232.

Gilbertson, R.L., Hidayat, S.H., Paplomatas, E.J., Rojas, M.R., Hou, Y.-M., and Maxwell, D.P. (1993). Pseudorecombination between infectious cloned DNA components of tomato mottle and bean dwarf mosaic geminiviruses. Journal of General Virology **74,** 23-31.

Goldwasser, Y., Hershenhorn, J., Plakhine, D., Kleifeld, Y., and Rubin, B. (1999). Biochemical factors involved in vetch resistance toOrobanche aegyptiaca. Physiological and Molecular Plant Pathology **54,** 87-96.

Gutiérrez, A., Rodríguez, I.M., and del Río, J.C. (2006). Chemical Characterization of Lignin and Lipid Fractions in Industrial Hemp Bast Fibers Used for Manufacturing High-Quality Paper Pulps. Journal of Agricultural and Food Chemistry **54,** 2138-2144.

Hegenauer, V., Fürst, U., Kaiser, B., Smoker, M., Zipfel, C., Felix, G., Stahl, M., and Albert, M. (2016). Detection of the plant parasite *Cuscuta reflexa* by a tomato cell surface receptor. Science **353,** 478-481.

Hegenauer, V., Slaby, P., Körner, M., Bruckmüller, J.-A., Burggraf, R., Albert, I., Kaiser, B., Löffelhardt, B., Droste-Borel, I., Sklenar, J., Menke, F.L.H., Maček, B., Ranjan, A., Sinha, N., Nürnberger, T., Felix, G., Krause, K., Stahl, M., and Albert, M. (2020). The tomato receptor CuRe1 senses a cell wall protein to identify Cuscuta as a pathogen. Nature Communications **11,** 5299.

Hembree, K.J., Lanini, W., and Va, N. (1999). Tomato varieties show promise of dodder control. In Proc. Calif. Weed Sci. Soc, pp. 205-206.

Hou, Y.M., and Gilbertson, R.L. (1996). Increased pathogenicity in a pseudorecombinant bipartite geminivirus correlates with intermolecular recombination. J Virol **70,** 5430-5436.

Ichihashi, Y., Aguilar-Martínez, J.A., Farhi, M., Chitwood, D.H., Kumar, R., Millon, L.V., Peng, J., Maloof, J.N., and Sinha, N.R. (2014). Evolutionary developmental transcriptomics reveals a gene network module regulating interspecific diversity in plant leaf shape. Proceedings of the National Academy of Sciences **111,** E2616-E2621.

Jin, J., Tian, F., Yang, D.-C., Meng, Y.-Q., Kong, L., Luo, J., and Gao, G. (2016). PlantTFDB 4.0: toward a central hub for transcription factors and regulatory interactions in plants. Nucleic Acids Research **45,** D1040-D1045.

Jones, P., Binns, D., Chang, H.-Y., Fraser, M., Li, W., McAnulla, C., McWilliam, H., Maslen, J., Mitchell, A., Nuka, G., Pesseat, S., Quinn, A.F., Sangrador-Vegas, A., Scheremetjew, M., Yong, S.-Y., Lopez, R., and Hunter, S. (2014). InterProScan 5: genome-scale protein function classification. Bioinformatics **30,** 1236-1240.

Kaiser, B., Vogg, G., Fürst, U.B., and Albert, M. (2015). Parasitic plants of the genus Cuscuta and their interaction with susceptible and resistant host plants. Frontiers in Plant Science **6,** 45.

Kelley, L.A., Mezulis, S., Yates, C.M., Wass, M.N., and Sternberg, M.J.E. (2015). The Phyre2 web portal for protein modeling, prediction and analysis. Nature Protocols **10,** 845-858.

Kerppola, T.K. (2008). Bimolecular Fluorescence Complementation (BiFC) Analysis as a Probe of Protein Interactions in Living Cells. Annual Review of Biophysics **37,** 465-487.

Kumari, C., Dutta, T.K., Banakar, P., and Rao, U. (2016). Comparing the defence-related gene expression changes upon root-knot nematode attack in susceptible versus resistant cultivars of rice. Scientific Reports **6,** 22846.

Kusumoto, D., Goldwasser, Y., Xie, X., Yoneyama, K., Takeuchi, Y., and Yoneyama, K. (2007). Resistance of red clover (Trifolium pratense) to the root parasitic plant Orobanche minor is activated by salicylate but not by jasmonate. Ann Bot **100,** 537-544.

Labrousse, P., Arnaud, M.C., Serieys, H., Bervillé, A., and Thalouarn, P. (2001). Several Mechanisms are Involved in Resistance of Helianthus to Orobanche cumana Wallr. Annals of Botany **88,** 859-868.

LANE, J.A., BAILEY, J.A., BUTLER, R.C., and TERRY, P.J. (1993). Resistance of cowpea [Vigna unguiculata (L.) Walp.] to Striga gesnerioides (Willd.) Vatke, a parasitic angiosperm. New Phytologist **125,** 405-412.

Lanini, W.T., and Kogan, M. (2005). Biology and Management of Cuscuta in Crops.

Liljegren, S. (2010). Phloroglucinol Stain for Lignin. Cold Spring Harbor Protocols **2010,** pdb.prot4954.

Liu, Q., Luo, L., and Zheng, L. (2018). Lignins: Biosynthesis and Biological Functions in Plants. International journal of molecular sciences **19,** 335.

Liu, Y., Schiff, M., and Dinesh-Kumar, S.P. (2002). Virus-induced gene silencing in tomato. The Plant Journal **31,** 777-786.

Lozano-Baena, M.D., Prats, E., Moreno, M.T., Rubiales, D., and Pérez-de-Luque, A. (2007). Medicago truncatula as a Model for Nonhost Resistance in Legume-Parasitic Plant Interactions. Plant Physiology **145,** 437.

Lu, Q., Tang, X., Tian, G., Wang, F., Liu, K., Nguyen, V., Kohalmi, S.E., Keller, W.A., Tsang, E.W.T., Harada, J.J., Rothstein, S.J., and Cui, Y. (2010). Arabidopsis homolog of the yeast TREX-2 mRNA export complex: components and anchoring nucleoporin. The Plant Journal **61,** 259-270.

Malinovsky, F.G., Fangel, J.U., and Willats, W.G.T. (2014). The role of the cell wall in plant immunity. Frontiers in Plant Science **5**.

Mitchell, A.L., Attwood, T.K., Babbitt, P.C., Blum, M., Bork, P., Bridge, A., Brown, S.D., Chang, H.-Y., El-Gebali, S., Fraser, M.I., Gough, J., Haft, D.R., Huang, H., Letunic, I., Lopez, R., Luciani, A., Madeira, F., Marchler-Bauer, A., Mi, H., Natale, D.A., Necci, M., Nuka, G., Orengo, C., Pandurangan, A.P., Paysan-Lafosse, T., Pesseat, S., Potter, S.C., Qureshi, M.A., Rawlings, N.D., Redaschi, N., Richardson, L.J., Rivoire, C., Salazar, G.A., Sangrador-Vegas, A., Sigrist, C.J A., Sillitoe, I., Sutton, G.G., Thanki, N., Thomas, P.D., Tosatto, S.C E., Yong, S.-Y., and Finn, R.D. (2018). InterPro in 2019:

improving coverage, classification and access to protein sequence annotations. Nucleic Acids Research **47,** D351-D360.

Moura, J.C.M.S., Bonine, C.A.V., De Oliveira Fernandes Viana, J., Dornelas, M.C., and Mazzafera, P. (2010). Abiotic and Biotic Stresses and Changes in the Lignin Content and Composition in Plants. Journal of Integrative Plant Biology **52,** 360-376.

Mutuku, J.M., Yoshida, S., Shimizu, T., Ichihashi, Y., Wakatake, T., Takahashi, A., Seo, M., and Shirasu, K. (2015). The WRKY45-Dependent Signaling Pathway Is Required For Resistance against Striga hermonthica Parasitism. Plant Physiology **168,** 1152-1163.

Mutuku, J.M., Cui, S., Hori, C., Takeda, Y., Tobimatsu, Y., Nakabayashi, R., Mori, T., Saito, K., Demura, T., Umezawa, T., Yoshida, S., and Shirasu, K. (2019). The Structural Integrity of Lignin Is Crucial for Resistance against *Striga hermonthica* Parasitism in Rice. Plant Physiology **179,** 1796-1809.

National Center for Biotechnology Information. (2021a). PubChem Compound Summary for CID 5280507, Sinapyl alcohol.

National Center for Biotechnology Information. (2021b). PubChem Compound Summary for CID 6057, Tyrosine.

National Center for Biotechnology Information. (2021c). PubChem Compound Summary for CID 6140, Phenylalanine.

National Center for Biotechnology Information. (2021d). PubChem Compound Summary for CID 444539, Cinnamic acid.

National Center for Biotechnology Information. (2021e). PubChem Compound Summary for CID 637542, 4-Hydroxycinnamic acid.

National Center for Biotechnology Information. (2021f). PubChem Compound Summary for CID 101712560, 4-O-(p-coumaroyl)shikimic acid.

National Center for Biotechnology Information. (2021g). PubChem Compound Summary for CID 5281762, 5-O-Caffeoylshikimic acid.

National Center for Biotechnology Information. (2021h). PubChem Compound Summary for CID 641301, 3-(4-Hydroxyphenyl)acrylaldehyde.

National Center for Biotechnology Information. (2021i). PubChem Compound Summary for CID 5280535, p-Coumaryl alcohol.

National Center for Biotechnology Information. (2021j). PubChem Compound Summary for CID 5281871, Caffeic aldehyde.

National Center for Biotechnology Information. (2021k). PubChem Compound Summary for CID 5282096, Caffeyl alcohol.

National Center for Biotechnology Information. (2021l). PubChem Compound Summary for CID 5280536, 4-Hydroxy-3-methoxycinnamaldehyde.

National Center for Biotechnology Information. (2021m). PubChem Compound Summary for CID 1549095, Coniferyl alcohol.

National Center for Biotechnology Information. (2021n). PubChem Compound Summary for CID 5280802, Sinapaldehyde.

O'Brien, T.P., Feder, N., and McCully, M.E. (1964). Polychromatic staining of plant cell walls by toluidine blue O. Protoplasma **59,** 368-373.

Pérez-de-Luque, A., Lozano, M.D., Moreno, M.T., Testillano, P.S., and Rubiales, D. (2007). Resistance to broomrape (Orobanche crenata) in faba bean (Vicia faba): cell wall changes

associated with prehaustorial defensive mechanisms. Annals of Applied Biology **151,** 89-98.

Padmanabhan, M.S., and Dinesh-Kumar, S.P. (2014). The conformational and subcellular compartmental dance of plant NLRs during viral recognition and defense signaling. Current Opinion in Microbiology **20,** 55-61.

Padmanabhan, M.S., Ma, S., Burch-Smith, T.M., Czymmek, K., Huijser, P., and Dinesh-Kumar, S.P. (2013). Novel Positive Regulatory Role for the SPL6 Transcription Factor in the N TIR-NB-LRR Receptor-Mediated Plant Innate Immunity. PLOS Pathogens **9,** e1003235.

Pan, C., Ye, L., Qin, L., Liu, X., He, Y., Wang, J., Chen, L., and Lu, G. (2016). CRISPR/Cas9-mediated efficient and heritable targeted mutagenesis in tomato plants in the first and later generations **6,** 24765.

PÉRez-De-Luque, A., Rubiales, D., Cubero, J.I., Press, M.C., Scholes, J., Yoneyama, K., Takeuchi, Y., Plakhine, D., and Joel, D.M. (2005). Interaction between Orobanche crenata and its Host Legumes: Unsuccessful Haustorial Penetration and Necrosis of the Developing Parasite. Annals of Botany **95,** 935-942.

Pomar, F., Merino, F., and Barceló, A.R. (2002). O-4-Linked coniferyl and sinapyl aldehydes in lignifying cell walls are the main targets of the Wiesner (phloroglucinol-HCl) reaction. Protoplasma **220,** 0017-0028.

Pradhan Mitra, P., and Loqué, D. (2014). Histochemical Staining of Arabidopsis thaliana Secondary Cell Wall Elements. Journal of Visualized Experiments : JoVE**,** 51381.

Ralph, J., and Hatfield, R.D. (1991). Pyrolysis-GC-MS characterization of forage materials. Journal of Agricultural and Food Chemistry **39,** 1426-1437.

Ranjan, A., Ichihashi, Y., Farhi, M., Zumstein, K., Townsley, B., David-Schwartz, R., and Sinha, N.R. (2014). De Novo Assembly and Characterization of the Transcriptome of the Parasitic Weed Dodder Identifies Genes Associated with Plant Parasitism. Plant Physiology **166,** 1186-1199.

Ranjan, A., Budke, J.M., Rowland, S.D., Chitwood, D.H., Kumar, R., Carriedo, L., Ichihashi, Y., Zumstein, K., Maloof, J.N., and Sinha, N.R. (2016). eQTL Regulating Transcript Levels Associated with Diverse Biological Processes in Tomato. Plant Physiology **172,** 328-340.

Reimers, P.J., and Leach, J.E. (1991). Race-specific resistance to Xanthomonas oryzae pv. oryzae conferred by bacterial blight resistance gene Xa-10 in rice (Oryza sativa) involves accumulation of a lignin-like substance in host tissues. Physiological and Molecular Plant Pathology **38,** 39-55.

RUNYON, J.B., MESCHER, M.C., FELTON, G.W., and DE MORAES, C.M. (2010). Parasitism by Cuscuta pentagona sequentially induces JA and SA defence pathways in tomato. Plant, Cell & Environment **33,** 290-303.

Sahm, A., Pfanz, H., Grünsfelder, M., Czygan, F.-C., and Proksch, P. (1995). Anatomy and Phenylpropanoid Metabolism in the Incompatible Interaction of Lycopersicon esculentum and Cuscuta reflexa. Botanica Acta **108,** 358-364.

Schneider, C.A., Rasband, W.S., and Eliceiri, K.W. (2012). NIH Image to ImageJ: 25 years of image analysis. Nature Methods **9,** 671.

Solís-Lemus, C., Bastide, P., and Ané, C. (2017). PhyloNetworks: A Package for Phylogenetic Networks. Molecular Biology and Evolution **34,** 3292-3298.

Sparkes, I.A., Runions, J., Kearns, A., and Hawes, C. (2006). Rapid, transient expression of fluorescent fusion proteins in tobacco plants and generation of stably transformed plants. Nature Protocols **1,** 2019-2025.

Stefanović, S., Kuzmina, M., and Costea, M. (2007). Delimitation of major lineages within Cuscuta subgenus Grammica (Convolvulaceae) using plastid and nuclear DNA sequences. American Journal of Botany **94,** 568-589.

Stenger, D.C., Revington, G.N., Stevenson, M.C., and Bisaro, D.M. (1991). Replicational release of geminivirus genomes from tandemly repeated copies: evidence for rolling-circle replication of a plant viral DNA. Proceedings of the National Academy of Sciences of the United States of America **88,** 8029-8033.

Su, C., Liu, H., Wafula, E.K., Honaas, L., de Pamphilis, C.W., and Timko, M.P. (2020). SHR4z, a novel decoy effector from the haustorium of the parasitic weed Striga gesnerioides, suppresses host plant immunity. New Phytologist **226,** 891-908.

Taheri, P., and Tarighi, S. (2012). The Role of Pathogenesis-Related Proteins in the Tomato-Rhizoctonia solani Interaction. Journal of Botany **2012,** 6.

Townsley, B.T., Covington, M.F., Ichihashi, Y., Zumstein, K., and Sinha, N.R. (2015). BrAD-seq: Breath Adapter Directional sequencing: a streamlined, ultra-simple and fast library preparation protocol for strand specific mRNA library construction. Frontiers in Plant Science **6**.

Vance, C.P., Kirk, T.K., and Sherwood, R.T. (1980). Lignification as a Mechanism of Disease Resistance. Annual Review of Phytopathology **18,** 259-288.

Vel, squez, A., C, Chakravarthy, S., and Martin, G.B. (2009). Virus-induced Gene Silencing (VIGS) in Nicotiana benthamiana and Tomato**,** e1292.

War, A.R., Paulraj, M.G., Ahmad, T., Buhroo, A.A., Hussain, B., Ignacimuthu, S., and Sharma, H.C. (2012). Mechanisms of plant defense against insect herbivores. Plant Signaling & Behavior **7,** 1306-1320.

Yaakov, G., Lanini, W.T., and Wrobel, R.L. (2001). Tolerance of Tomato Varieties to Lespedeza Dodder. Weed Science **49,** 520-523.

Yoder, J.I., and Scholes, J.D. (2010). Host plant resistance to parasitic weeds; recent progress and bottlenecks. Current Opinion in Plant Biology **13,** 478-484.

Yoshida, S., and Shirasu, K. (2009). Multiple layers of incompatibility to the parasitic witchweed, Striga hermonthica. New Phytologist **183,** 180-189.

Zhang, S.-H., Yang, Q., and Ma, R.-C. (2007). Erwinia carotovora ssp. carotovora Infection Induced "Defense Lignin" Accumulation and Lignin Biosynthetic Gene Expression in Chinese Cabbage (Brassica rapa L. ssp. pekinensis). Journal of Integrative Plant Biology **49,** 993-1002.

Zhang, Y., Wu, L., Wang, X., Chen, B., Zhao, J., Cui, J., Li, Z., Yang, J., Wu, L., Wu, J., Zhang, G., and Ma, Z. (2019). The cotton laccase gene GhLAC15 enhances Verticillium wilt resistance via an increase in defence-induced lignification and lignin components in the cell walls of plants. Molecular Plant Pathology **20,** 309-322.

Supplemental Data

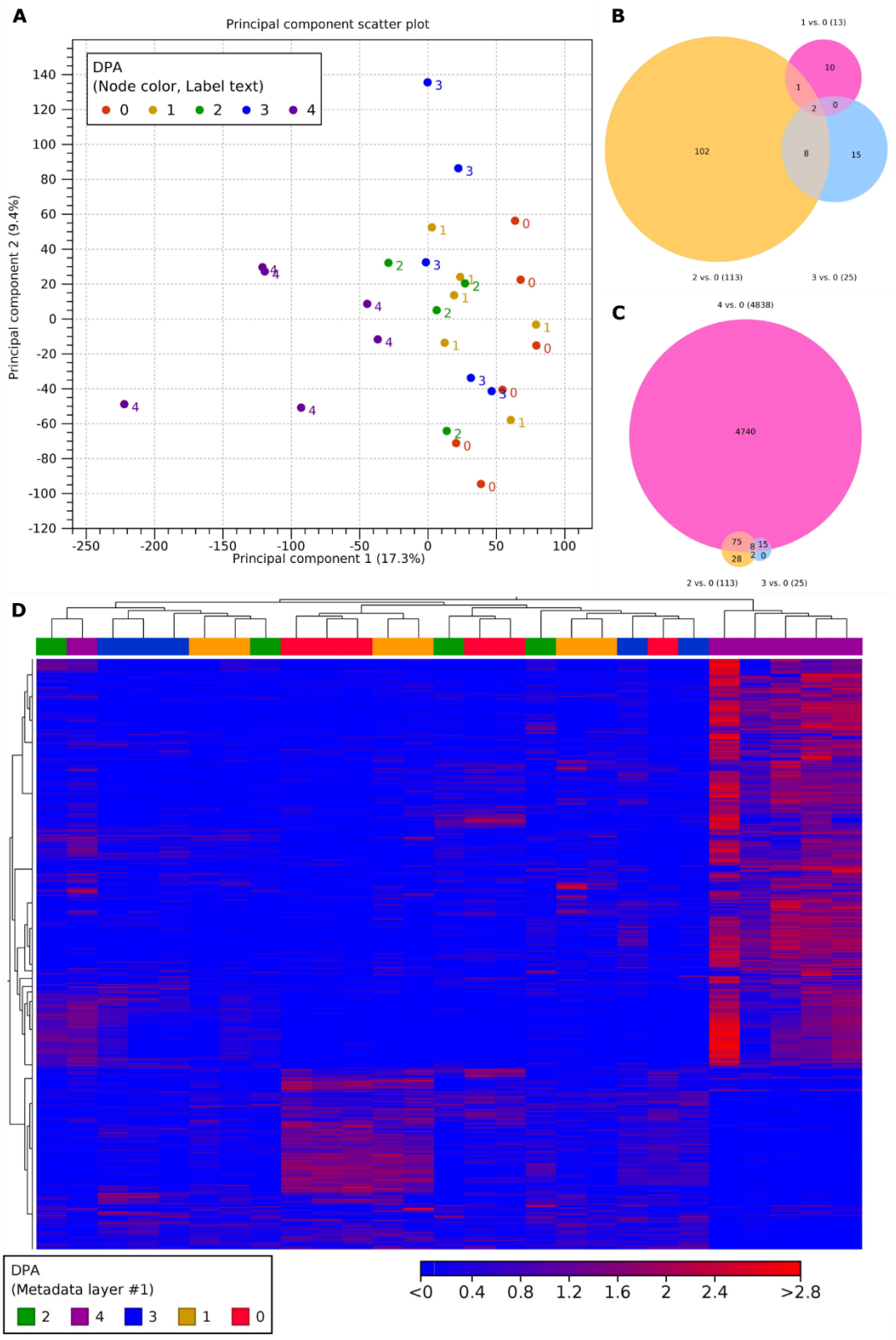

Supplemental Figure 1 | Analysis of time-course RNA-Seq data. (A) Principal component analysis (PCA) of gene expression across different day post attachment (DPA). Library number, 0 PDA, n = 6; 1 DPA, n = 6; 2 DPA, n = 4; 3 DPA, n = 5; 4 DPA, n = 6. (B-C) Venn diagram of differentially expressed genes (DEGs) at different DPA libraries. 0 DPA libraries are without *Cuscuta* treatments and serve as the control for comparisons. The cutoff of these DEGs are FDR < 0.1 and fold change > 1.5. (D) Heat map of DEGs across different DPA libraries. DEGs are selected by ANOVA analysis with cutoff FDR < 0.1. Euclidean distance and complete linkage are used for this clustering analysis.

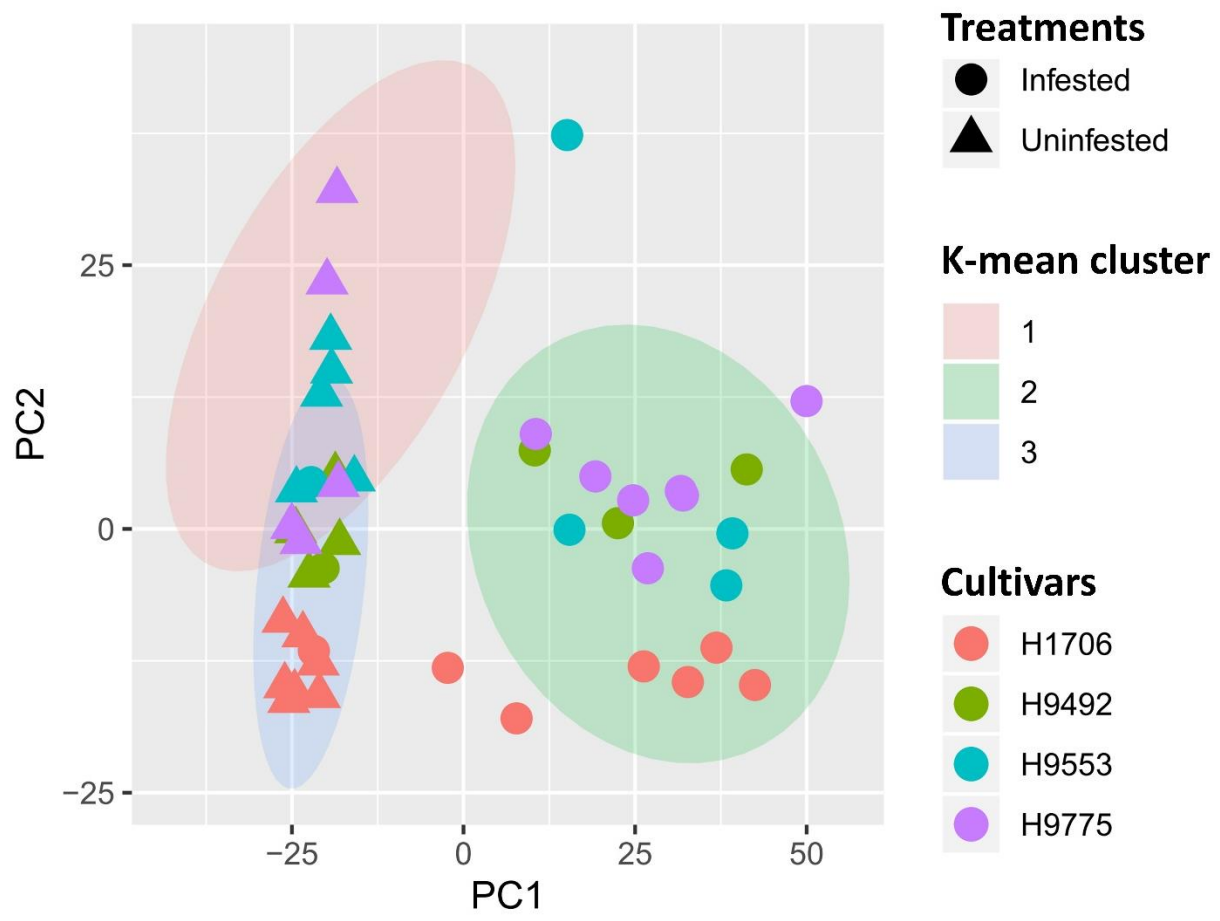

Supplemental Figure 2 | RNA-Seq analysis results of gene expression across resistant and susceptible cultivars at 4 DPA. PCA of gene expression across resistant and susceptible cultivars at 4 DPA. Different treatment conditions are represented by shapes: square dots indicate the uninfested host stem tissue samples; circle dots indicate the infested host stem tissue samples. Different cultivars are represented by different colors.

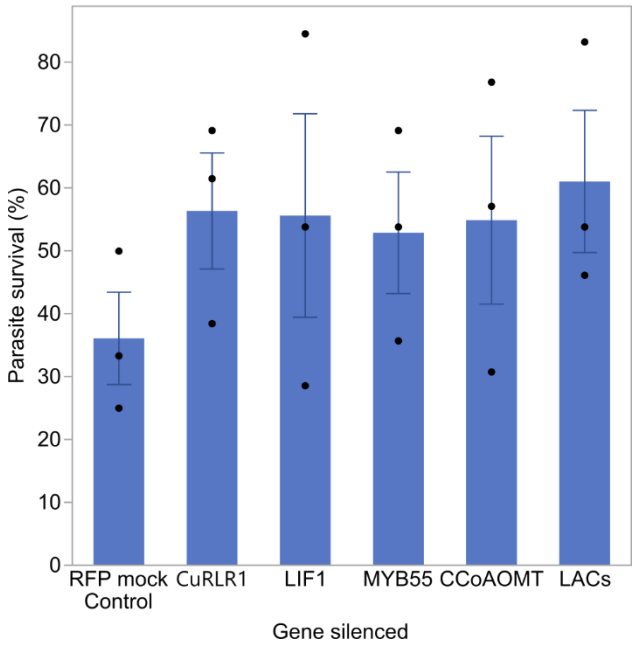

Supplemental Figure 3 | Virus-induced gene silencing (VIGS) in resistant tomato H9553. Plot shows the average *C. campestris* survival rates on different VIGS tomato plants. Survival rates = (the number of *C. campestris* surviving by the end of the experiment/ the total number of *C. campestris* at the beginning of experiment) * 100%. Each dot represents the average survival rate for each experiment, which used 12-14 individual plants (biological replicates) for each VIGSed gene. CCoAOMT, caffeoyl-CoA O-methyltransferase; LAC, laccase.

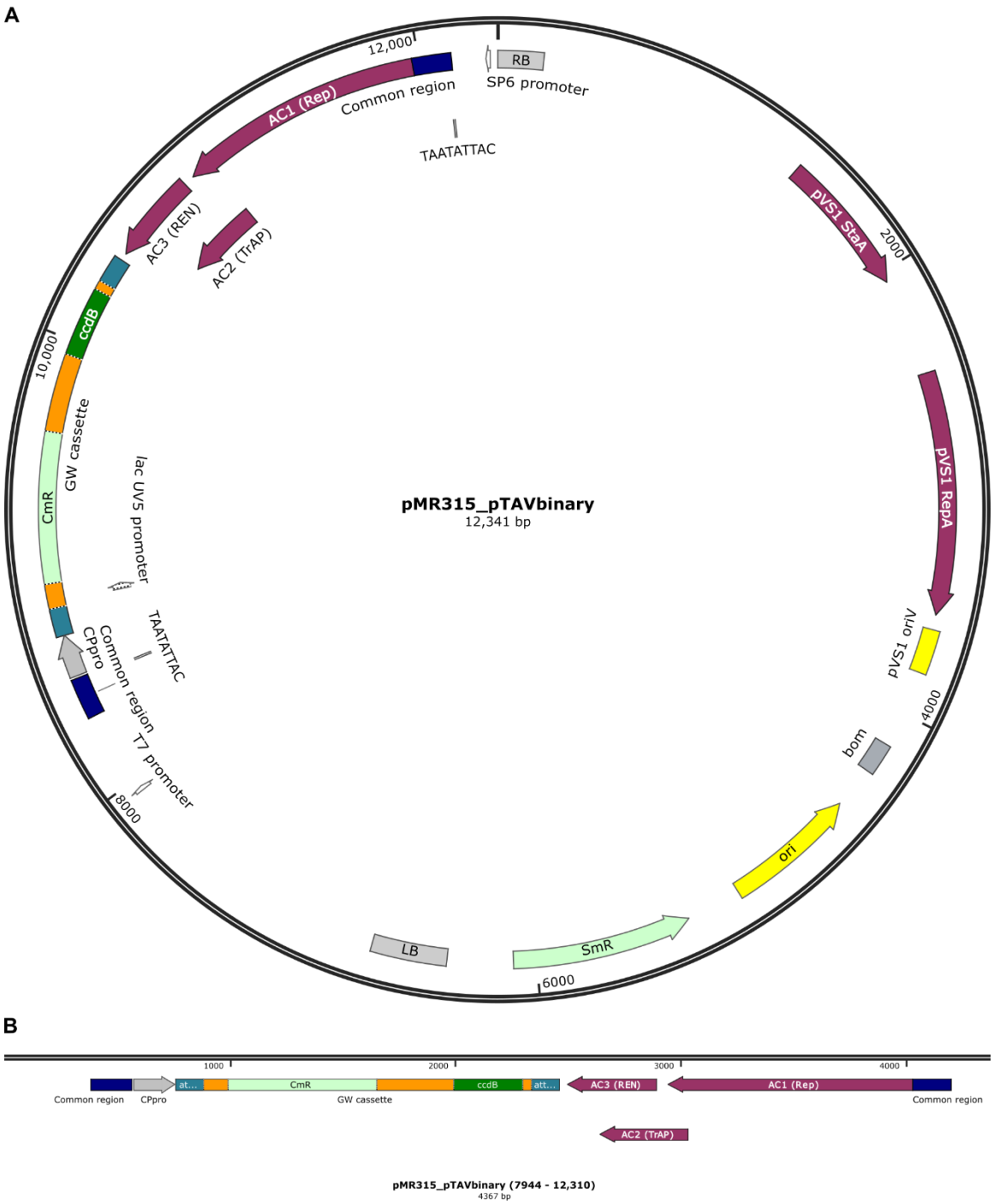

Supplemental Figure 4 | Virus-based Gene Expression vectors (pTAV) map. (A) Full map of pTAV plasmid. (B) Zoom-in view of the Gateway® cassette region. The gene cloned into this vector is driven by the capsid protein promoter (CPpro), which is in the non-translated region between the end of the common region and the start codon of the capsid protein gene that was

removed. CmR indicates chloramphenicol acetyltransferase, which is the Chloramphenicol resistance gene. SmR indicates aminoglycoside adenylyltransferase, which is the Spectinomycin/Streptomycin resistance gene. pVS1 RepA indicates replication protein from the *Pseudomonas* plasmid pVS1. pVS1 StaA indicates stability protein from the *Pseudomonas* plasmid pVS1. Complete sequence of pTAV is attached in Datasets S1.

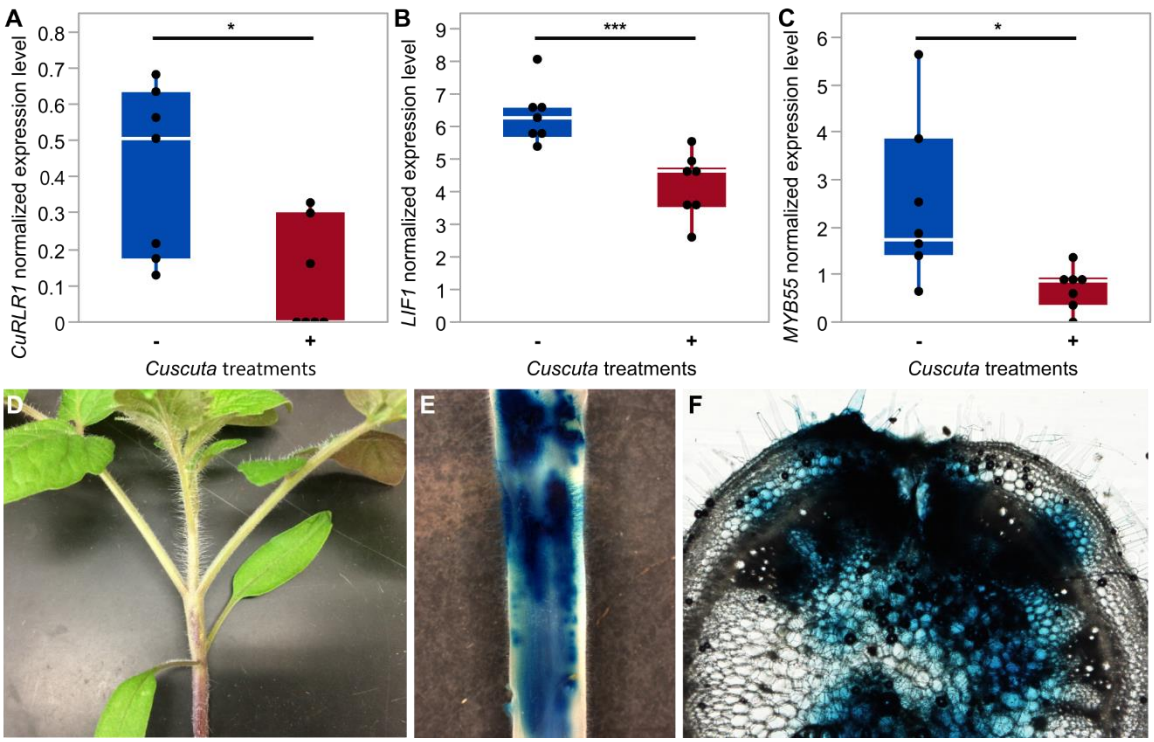

Supplemental Figure 5 | Expression of candidate genes and Virus-based Gene Expression (VGE) of GUS in tomato H1706. (A-C) The normalized expressions levels (CPM, counts per million) of genes in susceptible cultivar H1706 under *C. campestris* infestation. – and + indicates without or with *C. campestris* infection treatments respectively. Biologically independent replicates: RNA-Seq libraries: H1706-Cc, n = 7; H1706+Cc, n = 7. Data are assessed using two-tailed t test. "*": p-values < 0.05, "**": p-values < 0.01, "***": p-values < 0.005. (D) Tomato seedling showing first internode. Arrow points to injection site. (E) The first internode of stem stained for GUS expression from VGE construct in susceptible cultivar H1706. (F) Hand section (about 300 μm) of stem near injection site stained for GUS expression.

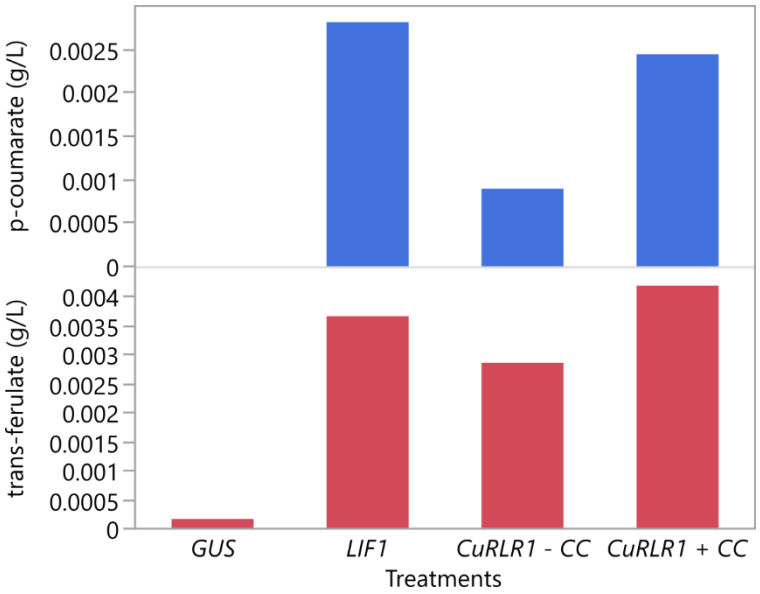

Supplemental Figure 6 | HPLC data for p-coumarate and trans-ferulate levels in different VGE and *C. campestris* infection treatments. HPLC data for p-coumarate and trans-ferulate was generated from ethyl acetate extract of de-starched AIR prepped stem tissue. The unit of this data is g/L. –Cc and +Cc indicate without or with *C. campestris* infection treatments respectively. Biological replicates collected from first internodes; *GUS*, n = 8; *LIF1*, n = 8, *CuRLR1*-Cc, n = 18; *CuRLR1*+Cc, n = 18. HPLC assay technical replicate, n = 1.

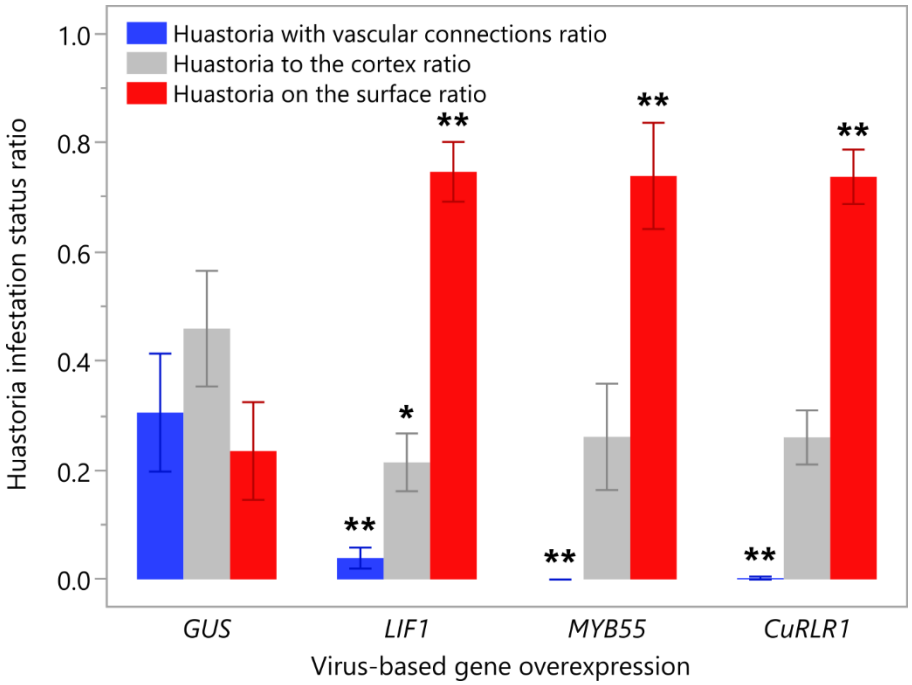

Supplemental Figure 7 | Haustorium infestation status ratio under different VGE treatments. The numbers of haustoria in different infestation status are quantified by examining hand sections and vibratome sections. The ratios are calculated by dividing the number of haustoria in each status by the total number of haustoria on each section. The detailed haustorium number and ratio data are presented in Supplemental Data Set 3. Data are analyzed using Dunnett's test. "*": p-values < 0.05, "**": p-values < 0.01.

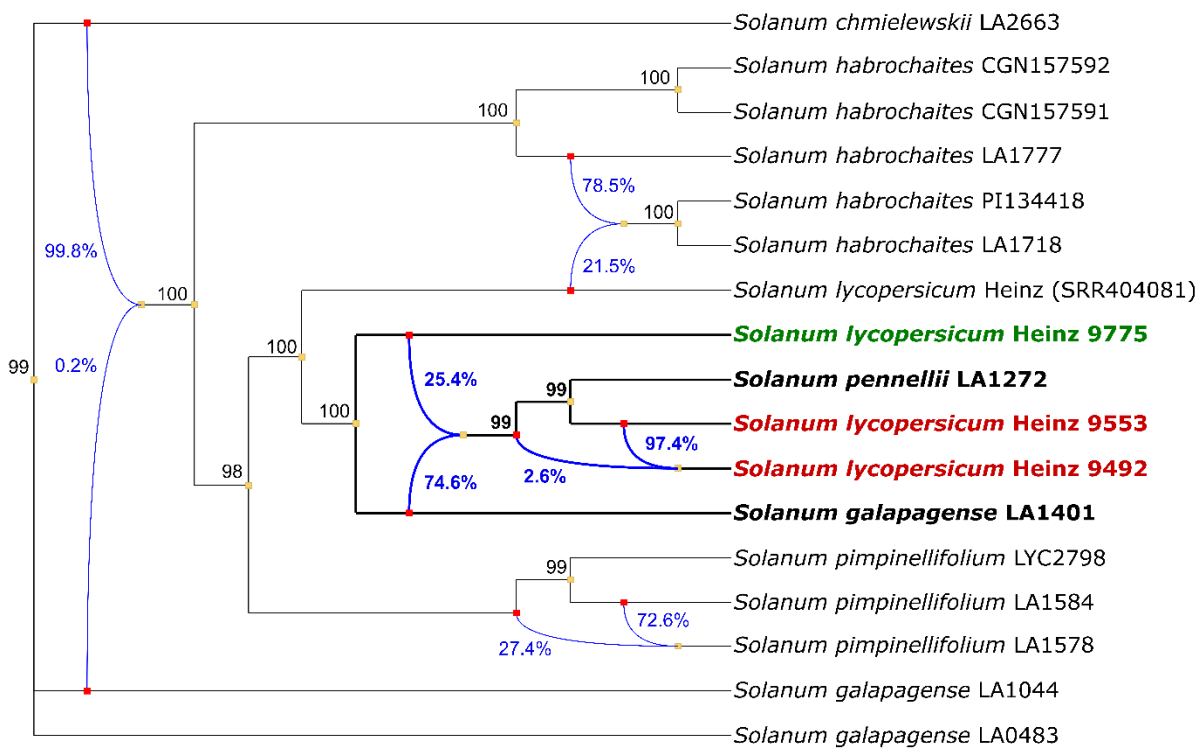

Supplemental Figure 8 | Phylogenetic network analysis using 500 kb sequence around the *LIF1* resistance-specific SNP enriched region. This phylogenetic network analysis was conducted using PhyloNetworks in the Julia environment with 500 kb of sequence around the *LIF1* resistance-specific SNP enriched region (SL3.0 ch02: 43800000 – 44300000). The species and accessions relevant to this work are highlighted in bold front and darker lines. Blue lines indicate potential hybridization events among these tomato cultivars, accessions, and species. Blue percentage numbers represent the gene flow from each potential parent cultivar to the hybridization event. Black numbers next to each node are bootstrap values. Green bold labeled cultivar H9775 is susceptible to *C. campestris* infection. Red bold labeled cultivars H9553 and H9492 are resistant

to *C. campestris* infection. Black bold labeled species are potential tomato wild species introgression sources contributing to the *LIF1* resistance-specific SNP enriched region.

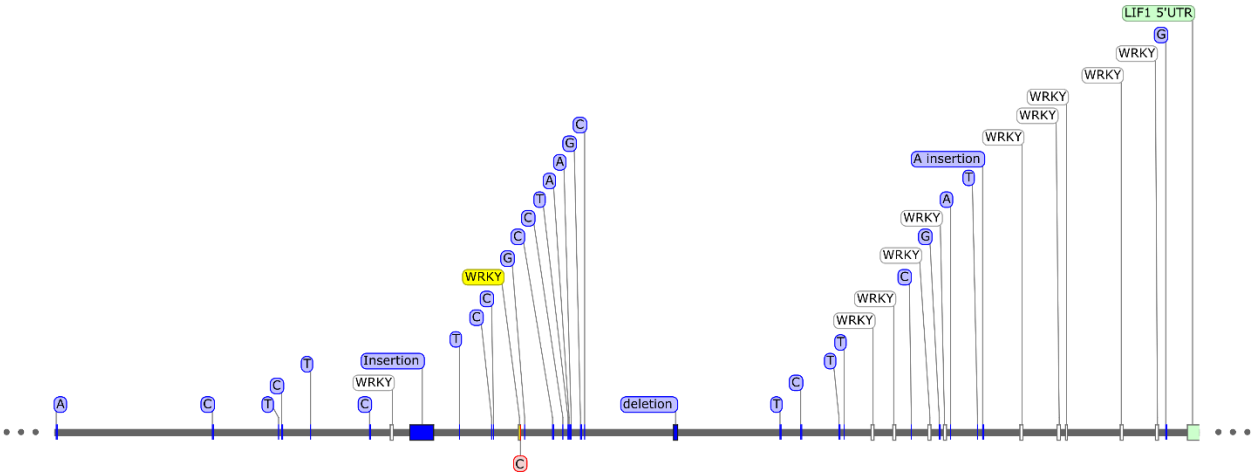

Supplemental Figure 9 | *LIF1* promoter region and transcription factors binding motifs. The *LIF1* promoter DNA sequence is labeled as a gray colored line. Transcription factors binding motifs are labeled as white boxes on the DNA sequence, and the potential key WRKY binding site is labeled as a yellow box. Resistance specific SNPs are labeled as blue lines on the DNA sequence. The resistance specific SNP that is located on the key WRKY binding site is labeled in red color.

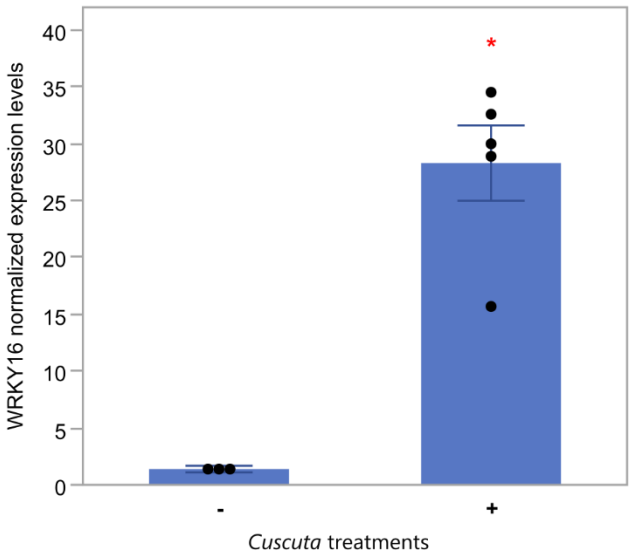

Supplemental Figure 10 | *SlWRKY16* expression level in different *Cuscuta* treatment condition. Normalized *SlWRKY16* expression level from qPCR data in M82 tomatoes with/without *Cuscuta* treatments. – and + indicates without or with *C. campestris* infection treatments respectively. Biologically independent replicates: M82-Cc, n = 3; M82+Cc, n = 5. Data presented are assessed using two-tailed t test. "*": p-values < 0.01. Value of the t-statistic: 8.10; degrees of freedom: 4.06.

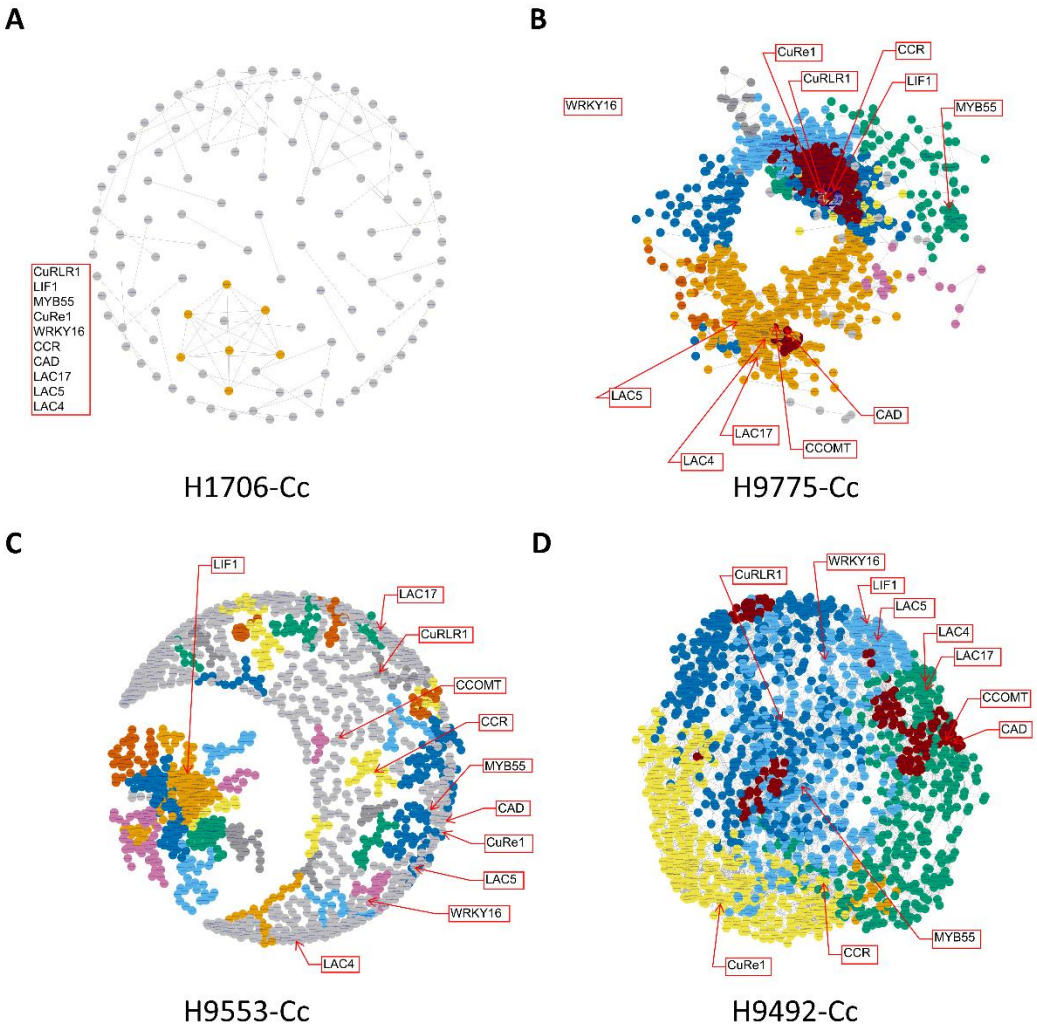

Supplemental Figure 11 | Gene co-expression network (GCN) analysis of identified key regulators. Gene co-expression networks (GCNs) of four different Heinz susceptible and resistant cultivars without *C. campestris* treatments. Based on BH-SNE analysis, 1676 genes in cluster 11, 17, 23, 39, 46 and CuRLR1 are selected for building GCNs. -Cc indicate without *C. campestris* infection treatments. The genes that are listed at the left of the GCN and not labeled in the network are the genes that have no coexpression connection with all the other genes in list.

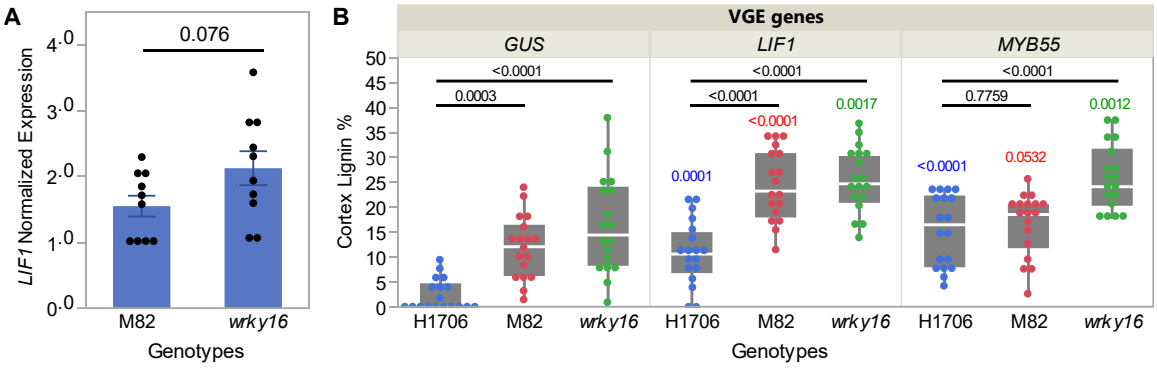

Supplemental Figure 12 | *LIF1* expression levels in *wrky16* and VGE overexpressing *SlMYB55* and *LIF1* in H1706, M82, and *wrky16*. (A) Normalized *LIF1* expression level from qPCR data in M82 and *wrky16* tomatoes. Data presented are assessed using Student's t test and p-value is labeled above the boxplot. Replicates: n = 10 for each plant genotype. (B) VGE overexpressing *SlMYB55* and *LIF1* in both susceptible H1706 and M82 tomatoes, and resistant *wrky16*. Data presented are assessed using Dunnett's test with H1706 as the control in each VGE overexpressing group and p-values are labeled above the boxplot in black. Data presented are also assessed using Dunnett's test with *GUS* as the negative control for each plant genotype. Each plant genotype group is labeled in specific color (H1706 in blue, M82 in red, *wrky16* in green) and p-values are labeled above the boxplot in the corresponding color. Replicates: n = 18 for each treatment.

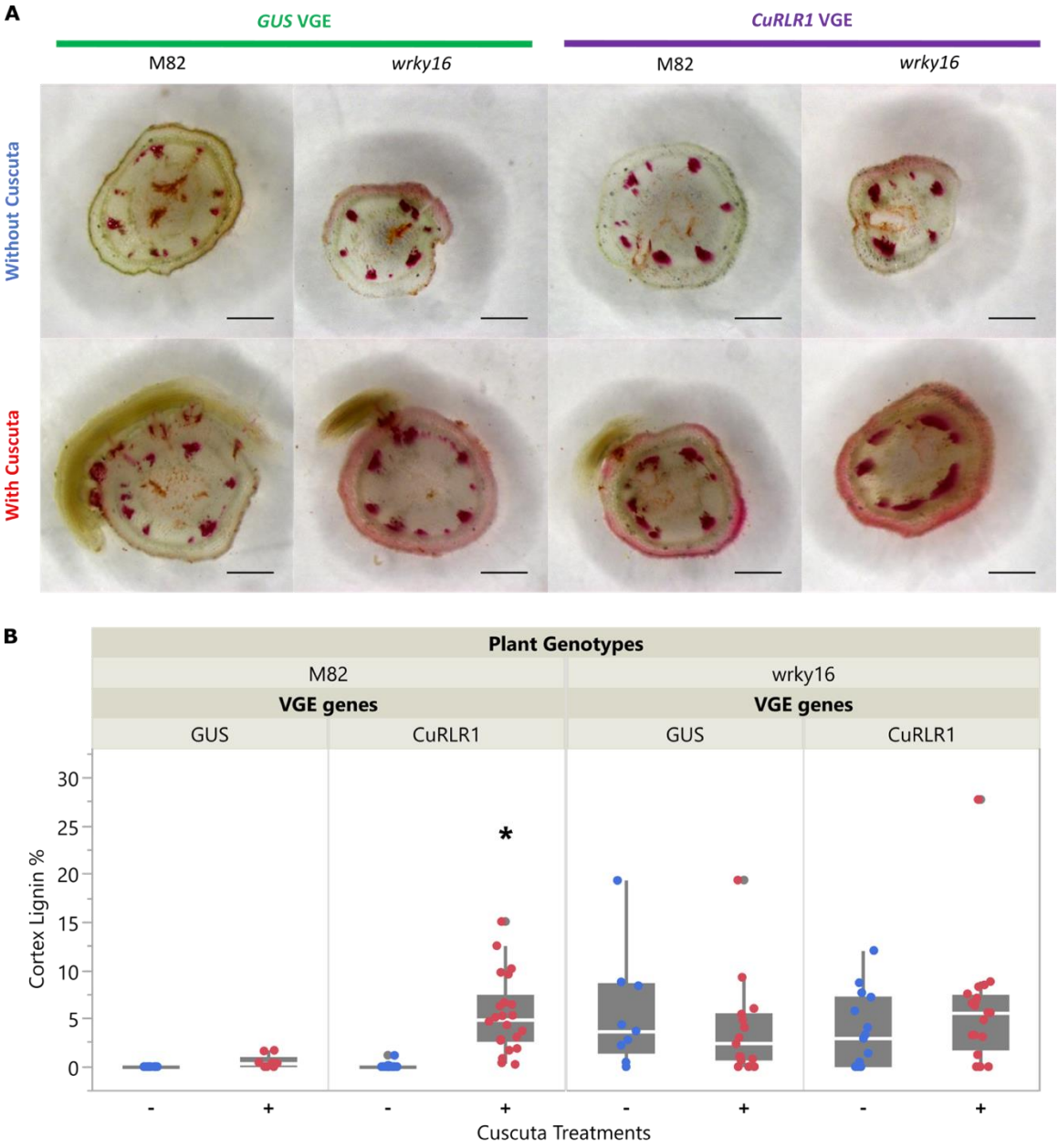

Supplemental Figure 13 | VGE overexpressing *CuRLR1* induced stem lignification in susceptible M82 tomatoes but not in *wrky16* tomatoes. (A) ~300 μm sections of the haustoria attachment sites stained with Phloroglucinol-HCl. Scale bar, 1 mm. (B) Cortex lignin area percentage in both susceptible M82 tomatoes and wrky16 tomatoes. – and + indicates without or with *C. campestris* infection treatments respectively. Data are assessed using Dunnett's test with *GUS*-Cc as the negative control for each genotype. "*": p-values < 0.01. Replicates: M82+*GUS*-

Cc, n = 10; M82+*GUS*+Cc, n = 9; M82+*CuRLR1*-Cc, n = 16; M82+*CuRLR1*+Cc, n = 22; *wrky16*+*GUS*-Cc, n = 9; *wrky16*+*GUS*+Cc, n = 15; *wrky16*+*CuRLR1*-Cc, n = 15; *wrky16*+*CuRLR1*+Cc, n = 20. Samples were collected at 10 DPI and 7 DPA.

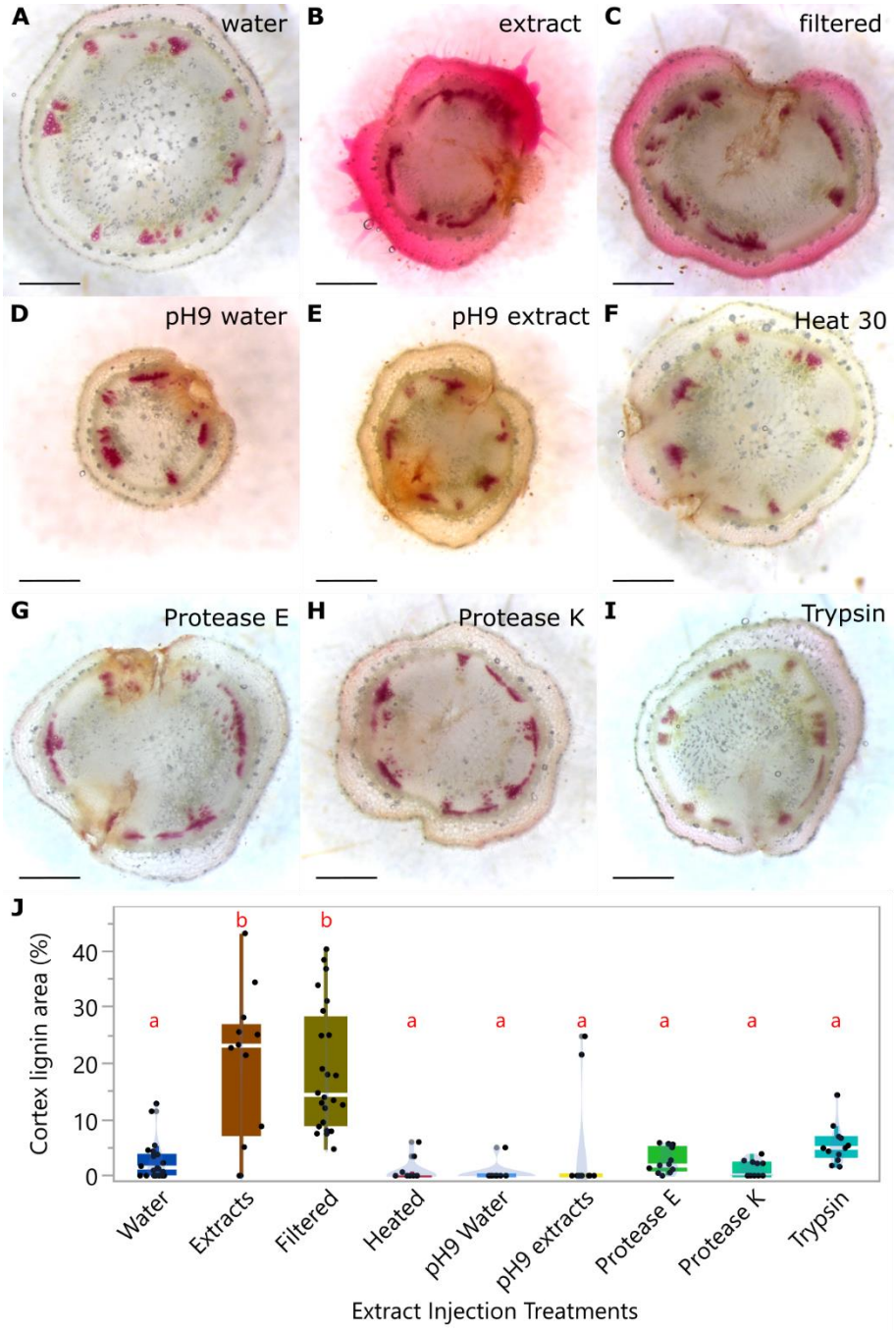

Supplemental Figure 14 | *C. campestris* extract injections to detect *Cuscuta* signals. (A-I) ~300 µm hand sections of resistant H9553 stems near injection sites stained with Phloroglucinol-HCl. Lignin is stained red. Data were collected at 7 days post injection (DPI). The H9553 plants are injected with (A) water, (B) untreated *C. campestris* extract, pH 5.8, (C) *C. campestris* extract

filtered with 0.2 μm filter, (D) pH 9 water, and (E) pH 9 *C. campestris* extract, (F) heat-treated *C. campestris* extract (95°C for 30 minutes), (G) Protease E-treated *C. campestris* extract, (H) Protease K-treated *C. campestris* extract, and (I) Trypsin-treated *C. campestris* extract. (J) Percentage of lignified cortex area in total stem area. The samples injected with water serve as negative controls. Different treated or untreated *C. campestris* extracts are compared to negative controls. Data presented are assessed using pair-wise comparisons with Tukey test. P-value of the contrasts between "a" and "b" are less than 0.01. Replicates: water, n = 22; untreated extract, n = 13; filtered extract, n = 24; heat-treated extract, n = 12; pH 9 water, n = 11; pH 9 extract, n = 12; Protease E-treated, n = 12; Protease K-treated, n = 12; Trypsin-treated, n = 12.

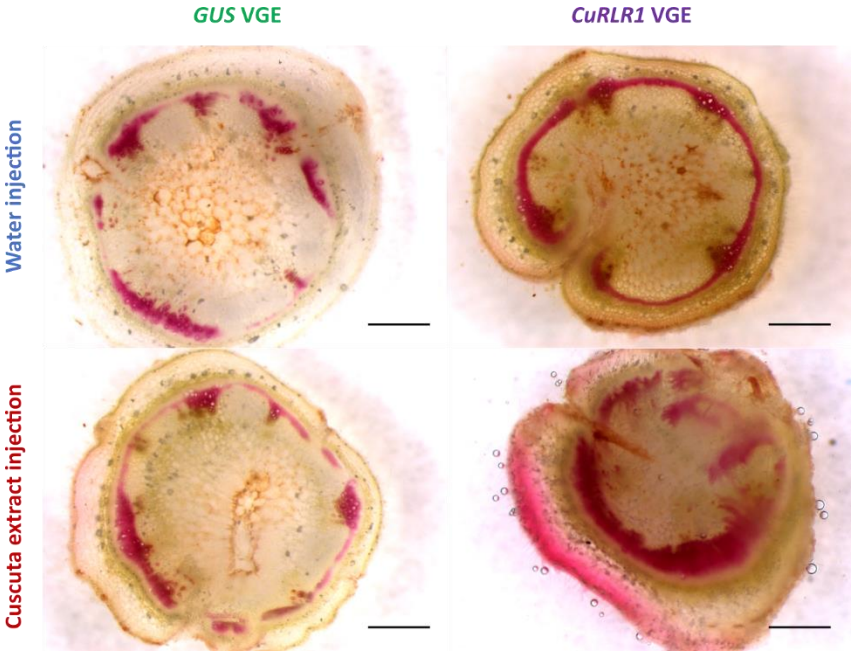

Supplemental Figure 15 | VGE overexpressing *CuRLR1* in H1706 with or without *Cuscuta* extract injections. These are ~300 μm sections of the haustoria attachment sites stained with Phloroglucinol-HCl. Scale bar, 1 mm. VGE overexpressing *GUS* served as a negative control for VGE. Water injection functions as a negative control for extract injections.

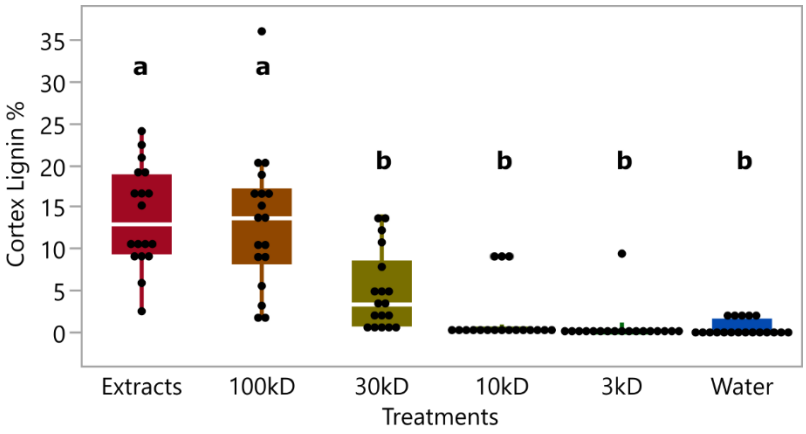

Supplemental Figure 16 | *Cuscuta* signal size analysis by using *Cuscuta* extract injections. Cortex lignin area percentage in H9553 cultivar with different size filtered Cuscuta extract injection. The *Cuscuta* extracts that flow through 3kD, 10kD, 30kD, and 100kD Amicon® Ultra Centrifugal Filter Devices are used to do injection on H9553 stems to test the size of *Cuscuta* signals. Data were assessed using pair-wise comparisons with Tukey test. P-values between "a" and "b" are < 0.05. Replicates: untreated extracts, n = 18; 100kD filtered extract, n = 18; 30kD filtered extract, n = 18; 10kD filtered extract, n = 18; 3kD filtered extract, n = 18; water, n = 19.

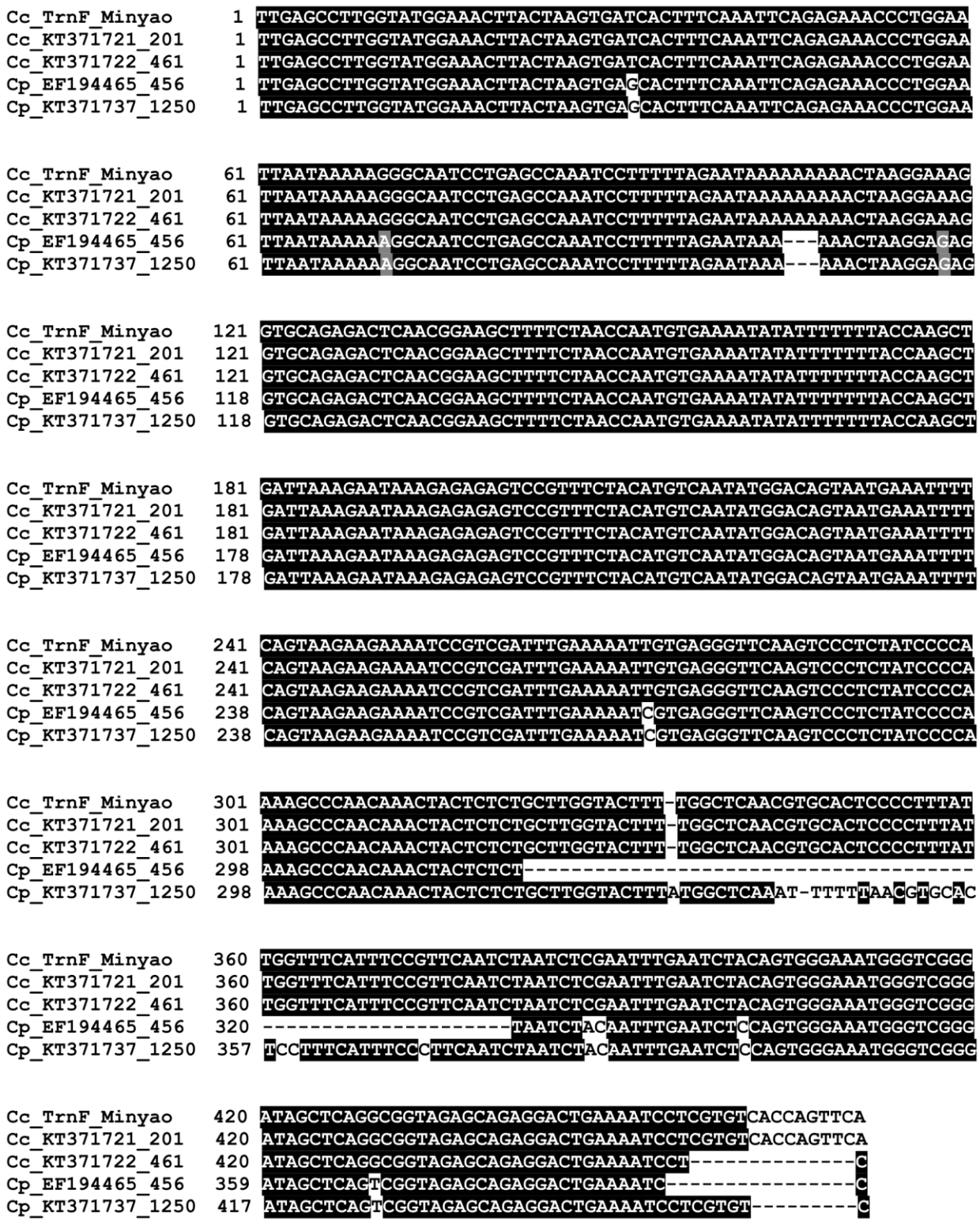

Supplemental Figure 17 | Sequence alignment of plastid *trnL-F* intron/spacer region sequences in our *Cuscuta campestris* isolate and published *Cuscuta campestris* and *Cuscuta*

***pentagona*.** The first sequence is from the *Cuscuta campestris* isolate we used in this research. The other sequences are from previously published *trnL-F* sequences of *Cuscuta campestris* (Cc) and *Cuscuta pentagona* (Cp) with GenBank accession numbers and following by DNA accession numbers.

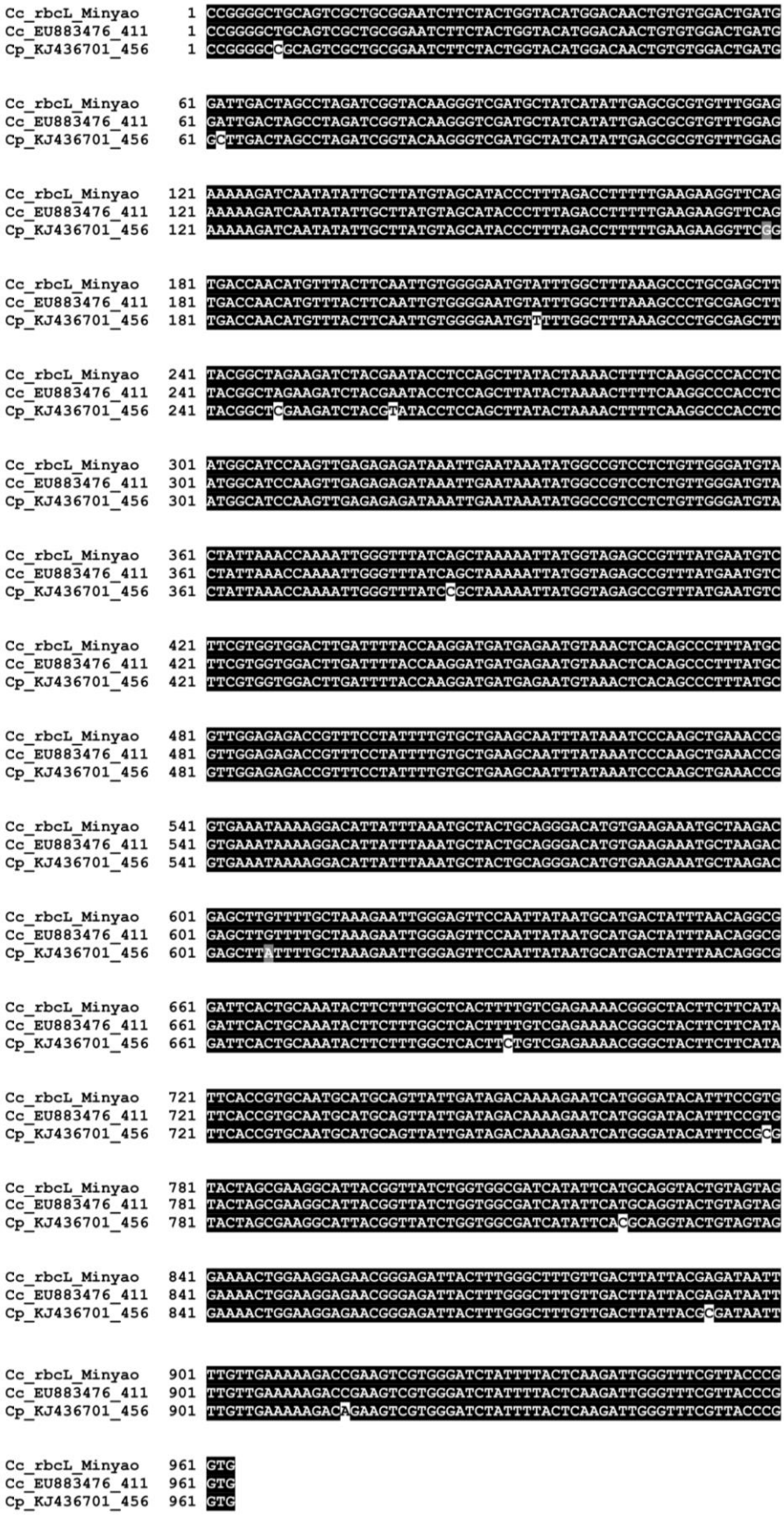
Cc_rbcL_Minyao 1 CCGGGGCTGCAGTCGCTGCGGAATCTTCTACTGGTACATGGACAACTGTGTGGACTGATG
Cc_EU883476_411 1 CCGGGGCTGCAGTCGCTGCGGAATCTTCTACTGGTACATGGACAACTGTGTGGACTGATG
Cp_KJ436701_456 1 CCGGGGCCGCAGTCGCTGCGGAATCTTCTACTGGTACATGGACAACTGTGTGGACTGATG
Cc_rbcL_Minyao 61 GATTGACTAGCCTAGATCGGTACAAGGGTCGATGCTATCATATTGAGCGCGTGTTTGGAG
Cc_EU883476_411 61 GATTGACTAGCCTAGATCGGTACAAGGGTCGATGCTATCATATTGAGCGCGTGTTTGGAG
Cp_KJ436701_456 61 GCTTGACTAGCCTAGATCGGTACAAGGGTCGATGCTATCATATTGAGCGCGTGTTTGGAG
Cc_rbcL_Minyao 121 AAAAAGATCAATATATTGCTTATGTAGCATACCCTTTAGACCTTTTTGAAGAAGGTTCAG
Cc_EU883476_411 121 AAAAAGATCAATATATTGCTTATGTAGCATACCCTTTAGACCTTTTTGAAGAAGGTTCAG
Cp_KJ436701_456 121 AAAAAGATCAATATATTGCTTATGTAGCATACCCTTTAGACCTTTTTGAAGAAGGTTCGG
Cc_rbcL_Minyao 181 TGACCAACATGTTTACTTCAATTGTGGGGAATGTATTTGGCTTTAAAGCCCTGCGAGCTT
Cc_EU883476_411 181 TGACCAACATGTTTACTTCAATTGTGGGGAATGTATTTGGCTTTAAAGCCCTGCGAGCTT
Cp_KJ436701_456 181 TGACCAACATGTTTACTTCAATTGTGGGGAATGTTTTTGGCTTTAAAGCCCTGCGAGCTT
Cc_rbcL_Minyao 241 TACGGCTAGAAGATCTACGAATACCTCCAGCTTATACTAAAACTTTTCAAGGCCCACCTC
Cc_EU883476_411 241 TACGGCTAGAAGATCTACGAATACCTCCAGCTTATACTAAAACTTTTCAAGGCCCACCTC
Cp_KJ436701_456 241 TACGGCTCGAAGATCTACGTATACCTCCAGCTTATACTAAAACTTTTCAAGGCCCACCTC
Cc_rbcL_Minyao 301 ATGGCATCCAAGTTGAGAGAGATAAATTGAATAAATATGGCCGTCCTCTGTTGGGATGTA
Cc_EU883476_411 301 ATGGCATCCAAGTTGAGAGAGATAAATTGAATAAATATGGCCGTCCTCTGTTGGGATGTA
Cp_KJ436701_456 301 ATGGCATCCAAGTTGAGAGAGATAAATTGAATAAATATGGCCGTCCTCTGTTGGGATGTA
Cc_rbcL_Minyao 361 CTATTAAACCAAAATTGGGTTTATCAGCTAAAAATTATGGTAGAGCCGTTTATGAATGTC
Cc_EU883476_411 361 CTATTAAACCAAAATTGGGTTTATCAGCTAAAAATTATGGTAGAGCCGTTTATGAATGTC
Cp_KJ436701_456 361 CTATTAAACCAAAATTGGGTTTATCCGCTAAAAATTATGGTAGAGCCGTTTATGAATGTC
Cc_rbcL_Minyao 421 TTCGTGGTGGACTTGATTTTACCAAGGATGATGAGAATGTAAACTCACAGCCCTTTATGC
Cc_EU883476_411 421 TTCGTGGTGGACTTGATTTTACCAAGGATGATGAGAATGTAAACTCACAGCCCTTTATGC
Cp_KJ436701_456 421 TTCGTGGTGGACTTGATTTTACCAAGGATGATGAGAATGTAAACTCACAGCCCTTTATGC
Cc_rbcL_Minyao 481 GTTGGAGAGACCGTTTCCTATTTTGTGCTGAAGCAATTTATAAATCCCAAGCTGAAACCG
Cc_EU883476_411 481 GTTGGAGAGACCGTTTCCTATTTTGTGCTGAAGCAATTTATAAATCCCAAGCTGAAACCG
Cp_KJ436701_456 481 GTTGGAGAGACCGTTTCCTATTTTGTGCTGAAGCAATTTATAAATCCCAAGCTGAAACCG
Cc_rbcL_Minyao 541 GTGAAATAAAAGGACATTATTTAAATGCTACTGCAGGGACATGTGAAGAAATGCTAAGAC
Cc_EU883476_411 541 GTGAAATAAAAGGACATTATTTAAATGCTACTGCAGGGACATGTGAAGAAATGCTAAGAC
Cp_KJ436701_456 541 GTGAAATAAAAGGACATTATTTAAATGCTACTGCAGGGACATGTGAAGAAATGCTAAGAC
Cc_rbcL_Minyao 601 GAGCTTGTTTTGCTAAAGAATTGGGAGTTCCAATTATAATGCATGACTATTTAACAGGCG
Cc_EU883476_411 601 GAGCTTGTTTTGCTAAAGAATTGGGAGTTCCAATTATAATGCATGACTATTTAACAGGCG
Cp_KJ436701_456 601 GAGCTTATTTTGCTAAAGAATTGGGAGTTCCAATTATAATGCATGACTATTTAACAGGCG
Cc_rbcL_Minyao 661 GATTCACTGCAAATACTTCTTTGGCTCACTTTTGTCGAGAAAACGGGCTACTTCTTCATA
Cc_EU883476_411 661 GATTCACTGCAAATACTTCTTTGGCTCACTTTTGTCGAGAAAACGGGCTACTTCTTCATA
Cp_KJ436701_456 661 GATTCACTGCAAATACTTCTTTGGCTCACTTCTGTCGAGAAAACGGGCTACTTCTTCATA
Cc_rbcL_Minyao 721 TTCACCGTGCAATGCATGCAGTTATTGATAGACAAAAGAATCATGGGATACATTTCCGTG
Cc_EU883476_411 721 TTCACCGTGCAATGCATGCAGTTATTGATAGACAAAAGAATCATGGGATACATTTCCGTG
Cp_KJ436701_456 721 TTCACCGTGCAATGCATGCAGTTATTGATAGACAAAAGAATCATGGGATACATTTCCGCG
Cc_rbcL_Minyao 781 TACTAGCGAAGGCATTACGGTTATCTGGTGGCGATCATATTCATGCAGGTACTGTAGTAG
Cc_EU883476_411 781 TACTAGCGAAGGCATTACGGTTATCTGGTGGCGATCATATTCATGCAGGTACTGTAGTAG
Cp_KJ436701_456 781 TACTAGCGAAGGCATTACGGTTATCTGGTGGCGATCATATTCACGCAGGTACTGTAGTAG
Cc_rbcL_Minyao 841 GAAAACTGGAAGGAGAACGGGAGATTACTTTGGGCTTTGTTGACTTATTACGAGATAATT
Cc_EU883476_411 841 GAAAACTGGAAGGAGAACGGGAGATTACTTTGGGCTTTGTTGACTTATTACGAGATAATT
Cp_KJ436701_456 841 GAAAACTGGAAGGAGAACGGGAGATTACTTTGGGCTTTGTTGACTTATTACGCGATAATT
Cc_rbcL_Minyao 901 TTGTTGAAAAAGACCGAAGTCGTGGGATCTATTTTACTCAAGATTGGGTTTCGTTACCCG
Cc_EU883476_411 901 TTGTTGAAAAAGACCGAAGTCGTGGGATCTATTTTACTCAAGATTGGGTTTCGTTACCCG
Cp_KJ436701_456 901 TTGTTGAAAAAGACAGAAGTCGTGGGATCTATTTTACTCAAGATTGGGTTTCGTTACCCG
Cc_rbcL_Minyao 961 GTG
Cc_EU883476_411 961 GTG
Cp_KJ436701_456 961 GTG

Supplemental Figure 18 | Sequence alignment of plastid ribulose-1,5-bisphosphate carboxylase/oxygenase large subunit (*rbcL*) sequences in our *Cuscuta campestris* isolate and published *Cuscuta campestris* and *Cuscuta pentagona*. The first sequence is from the *Cuscuta campestris* isolate we used in this research. The other sequences are from previously published rbcL sequences of *Cuscuta campestris* (Cc) and *Cuscuta pentagona* (Cp) with GenBank accession numbers and following by DNA accession numbers.

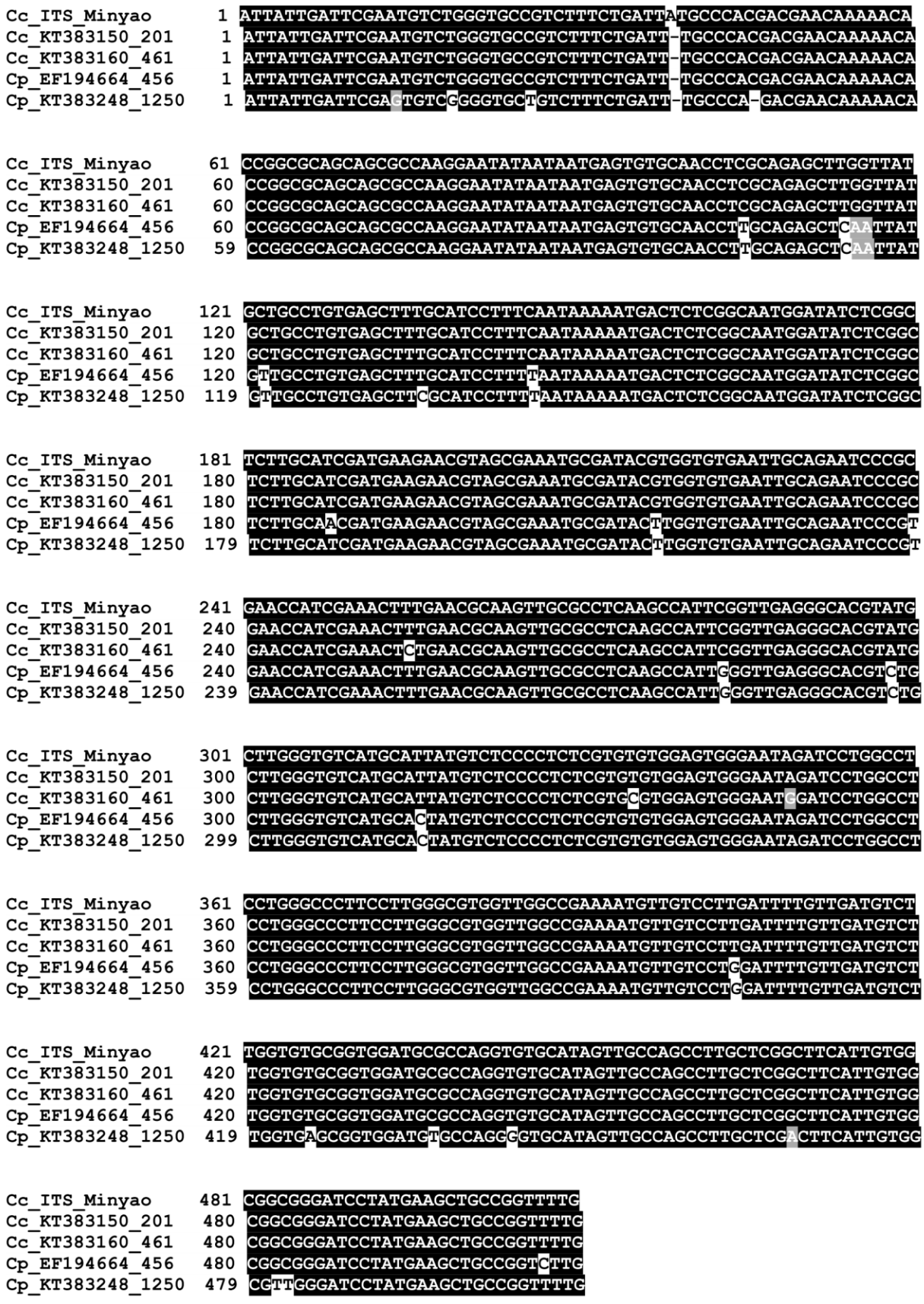
Cc_ITS_Minyao 1 ATTATTGATTCGAATGTCTGGGTGCCGTCTTTCTGATTATGCCCACGACGAACAAAAACA
Cc_KT383150_201 1 ATTATTGATTCGAATGTCTGGGTGCCGTCTTTCTGATT-TGCCCACGACGAACAAAAACA
Cc_KT383160_461 1 ATTATTGATTCGAATGTCTGGGTGCCGTCTTTCTGATT-TGCCCACGACGAACAAAAACA
Cp_EF194664_456 1 ATTATTGATTCGAATGTCTGGGTGCCGTCTTTCTGATT-TGCCCACGACGAACAAAAACA
Cp_KT383248_1250 1 ATTATTGATTCGAGTGTCGGGGTGCTGTCTTTCTGATT-TGCCCA-GACGAACAAAAACA
Cc_ITS_Minyao 61 CCGGCGCAGCAGCGCCAAGGAATATAATAATGAGTGTGCAACCTCGCAGAGCTTGGTTAT
Cc_KT383150_201 60 CCGGCGCAGCAGCGCCAAGGAATATAATAATGAGTGTGCAACCTCGCAGAGCTTGGTTAT
Cc_KT383160_461 60 CCGGCGCAGCAGCGCCAAGGAATATAATAATGAGTGTGCAACCTCGCAGAGCTTGGTTAT
Cp_EF194664_456 60 CCGGCGCAGCAGCGCCAAGGAATATAATAATGAGTGTGCAACCTTGCAGAGCTCAATTAT
Cp_KT383248_1250 59 CCGGCGCAGCAGCGCCAAGGAATATAATAATGAGTGTGCAACCTTGCAGAGCTCAATTAT
Cc_ITS_Minyao 121 GCTGCCTGTGAGCTTTGCATCCTTTCAATAAAAATGACTCTCGGCAATGGATATCTCGGC
Cc_KT383150_201 120 GCTGCCTGTGAGCTTTGCATCCTTTCAATAAAAATGACTCTCGGCAATGGATATCTCGGC
Cc_KT383160_461 120 GCTGCCTGTGAGCTTTGCATCCTTTCAATAAAAATGACTCTCGGCAATGGATATCTCGGC
Cp_EF194664_456 120 GTTGCCTGTGAGCTTTGCATCCTTTTAATAAAAATGACTCTCGGCAATGGATATCTCGGC
Cp_KT383248_1250 119 GTTGCCTGTGAGCTTCGCATCCTTTTAATAAAAATGACTCTCGGCAATGGATATCTCGGC
Cc_ITS_Minyao 181 TCTTGCATCGATGAAGAACGTAGCGAAATGCGATACGTGGTGTGAATTGCAGAATCCCGC
Cc_KT383150_201 180 TCTTGCATCGATGAAGAACGTAGCGAAATGCGATACGTGGTGTGAATTGCAGAATCCCGC
Cc_KT383160_461 180 TCTTGCATCGATGAAGAACGTAGCGAAATGCGATACGTGGTGTGAATTGCAGAATCCCGC
Cp_EF194664_456 180 TCTTGCAACGATGAAGAACGTAGCGAAATGCGATACTTGGTGTGAATTGCAGAATCCCGT
Cp_KT383248_1250 179 TCTTGCATCGATGAAGAACGTAGCGAAATGCGATACTTGGTGTGAATTGCAGAATCCCGT
Cc_ITS_Minyao 241 GAACCATCGAAACTTTGAACGCAAGTTGCGCCTCAAGCCATTCGGTTGAGGGCACGTATG
Cc_KT383150_201 240 GAACCATCGAAACTTTGAACGCAAGTTGCGCCTCAAGCCATTCGGTTGAGGGCACGTATG
Cc_KT383160_461 240 GAACCATCGAAACTCTGAACGCAAGTTGCGCCTCAAGCCATTCGGTTGAGGGCACGTATG
Cp_EF194664_456 240 GAACCATCGAAACTTTGAACGCAAGTTGCGCCTCAAGCCATTGGGTTGAGGGCACGTCTG
Cp_KT383248_1250 239 GAACCATCGAAACTTTGAACGCAAGTTGCGCCTCAAGCCATTGGGTTGAGGGCACGTCTG
Cc_ITS_Minyao 301 CTTGGGTGTCATGCATTATGTCTCCCCTCTCGTGTGTGGAGTGGGAATAGATCCTGGCCT
Cc_KT383150_201 300 CTTGGGTGTCATGCATTATGTCTCCCCTCTCGTGTGTGGAGTGGGAATAGATCCTGGCCT
Cc_KT383160_461 300 CTTGGGTGTCATGCATTATGTCTCCCCTCTCGTGCGTGGAGTGGGAATGGATCCTGGCCT
Cp_EF194664_456 300 CTTGGGTGTCATGCACTATGTCTCCCCTCTCGTGTGTGGAGTGGGAATAGATCCTGGCCT
Cp_KT383248_1250 299 CTTGGGTGTCATGCACTATGTCTCCCCTCTCGTGTGTGGAGTGGGAATAGATCCTGGCCT
Cc_ITS_Minyao 361 CCTGGGCCCTTCCTTGGGCGTGGTTGGCCGAAAATGTTGTCCTTGATTTTGTTGATGTCT
Cc_KT383150_201 360 CCTGGGCCCTTCCTTGGGCGTGGTTGGCCGAAAATGTTGTCCTTGATTTTGTTGATGTCT
Cc_KT383160_461 360 CCTGGGCCCTTCCTTGGGCGTGGTTGGCCGAAAATGTTGTCCTTGATTTTGTTGATGTCT
Cp_EF194664_456 360 CCTGGGCCCTTCCTTGGGCGTGGTTGGCCGAAAATGTTGTCCTGGATTTTGTTGATGTCT
Cp_KT383248_1250 359 CCTGGGCCCTTCCTTGGGCGTGGTTGGCCGAAAATGTTGTCCTGGATTTTGTTGATGTCT
Cc_ITS_Minyao 421 TGGTGTGCGGTGGATGCGCCAGGTGTGCATAGTTGCCAGCCTTGCTCGGCTTCATTGTGG
Cc_KT383150_201 420 TGGTGTGCGGTGGATGCGCCAGGTGTGCATAGTTGCCAGCCTTGCTCGGCTTCATTGTGG
Cc_KT383160_461 420 TGGTGTGCGGTGGATGCGCCAGGTGTGCATAGTTGCCAGCCTTGCTCGGCTTCATTGTGG
Cp_EF194664_456 420 TGGTGTGCGGTGGATGCGCCAGGTGTGCATAGTTGCCAGCCTTGCTCGGCTTCATTGTGG
Cp_KT383248_1250 419 TGGTGAGCGGTGGATGTGCCAGGGGTGCATAGTTGCCAGCCTTGCTCGACTTCATTGTGG
Cc_ITS_Minyao 481 CGGCGGGATCCTATGAAGCTGCCGGTTTTG
Cc_KT383150_201 480 CGGCGGGATCCTATGAAGCTGCCGGTTTTG
Cc_KT383160_461 480 CGGCGGGATCCTATGAAGCTGCCGGTTTTG
Cp_EF194664_456 480 CGGCGGGATCCTATGAAGCTGCCGGTCTTG
Cp_KT383248_1250 479 CGTTGGGATCCTATGAAGCTGCCGGTTTTG

Supplemental Figure 19 | Sequence alignment of nuclear internal transcribed spacer (*nrITS*) sequences in our *Cuscuta campestris* isolate and published *Cuscuta campestris* and *Cuscuta pentagona*. The first sequence is from the *Cuscuta campestris* isolate we used in this research. The other sequences are from previously published *nrITS* sequences of *Cuscuta campestris* (Cc) and *Cuscuta pentagona* (Cp) with GenBank accession numbers and following by DNA accession numbers.

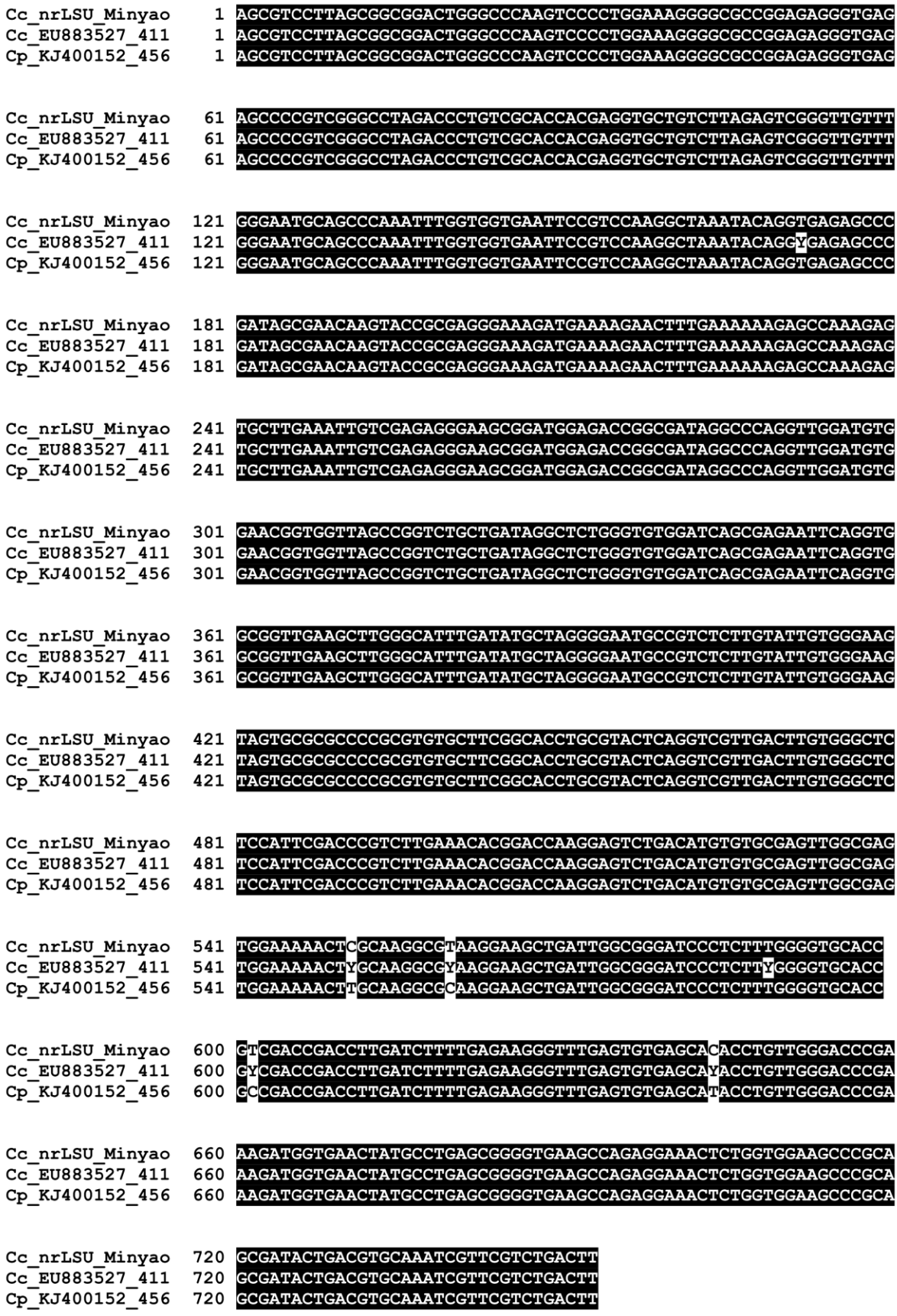
Cc_nrLSU_Minyao 1 AGCGTCCTTAGCGGCGGACTGGGCCCAAGTCCCCTGGAAAGGGGCGCCGGAGAGGGTGAG
Cc_EU883527_411 1 AGCGTCCTTAGCGGCGGACTGGGCCCAAGTCCCCTGGAAAGGGGCGCCGGAGAGGGTGAG
Cp_KJ400152_456 1 AGCGTCCTTAGCGGCGGACTGGGCCCAAGTCCCCTGGAAAGGGGCGCCGGAGAGGGTGAG
Cc_nrLSU_Minyao 61 AGCCCCGTCGGGCCTAGACCCTGTCGCACCACGAGGTGCTGTCTTAGAGTCGGGTTGTTT
Cc_EU883527_411 61 AGCCCCGTCGGGCCTAGACCCTGTCGCACCACGAGGTGCTGTCTTAGAGTCGGGTTGTTT
Cp_KJ400152_456 61 AGCCCCGTCGGGCCTAGACCCTGTCGCACCACGAGGTGCTGTCTTAGAGTCGGGTTGTTT
Cc_nrLSU_Minyao 121 GGGAATGCAGCCCAAATTTGGTGGTGAATTCCGTCCAAGGCTAAATACAGGTGAGAGCCC
Cc_EU883527_411 121 GGGAATGCAGCCCAAATTTGGTGGTGAATTCCGTCCAAGGCTAAATACAGGYGAGAGCCC
Cp_KJ400152_456 121 GGGAATGCAGCCCAAATTTGGTGGTGAATTCCGTCCAAGGCTAAATACAGGTGAGAGCCC
Cc_nrLSU_Minyao 181 GATAGCGAACAAGTACCGCGAGGGAAAGATGAAAAGAACTTTGAAAAAAGAGCCAAAGAG
Cc_EU883527_411 181 GATAGCGAACAAGTACCGCGAGGGAAAGATGAAAAGAACTTTGAAAAAAGAGCCAAAGAG
Cp_KJ400152_456 181 GATAGCGAACAAGTACCGCGAGGGAAAGATGAAAAGAACTTTGAAAAAAGAGCCAAAGAG
Cc_nrLSU_Minyao 241 TGCTTGAAATTGTCGAGAGGGAAGCGGATGGAGACCGGCGATAGGCCCAGGTTGGATGTG
Cc_EU883527_411 241 TGCTTGAAATTGTCGAGAGGGAAGCGGATGGAGACCGGCGATAGGCCCAGGTTGGATGTG
Cp_KJ400152_456 241 TGCTTGAAATTGTCGAGAGGGAAGCGGATGGAGACCGGCGATAGGCCCAGGTTGGATGTG
Cc_nrLSU_Minyao 301 GAACGGTGGTTAGCCGGTCTGCTGATAGGCTCTGGGTGTGGATCAGCGAGAATTCAGGTG
Cc_EU883527_411 301 GAACGGTGGTTAGCCGGTCTGCTGATAGGCTCTGGGTGTGGATCAGCGAGAATTCAGGTG
Cp_KJ400152_456 301 GAACGGTGGTTAGCCGGTCTGCTGATAGGCTCTGGGTGTGGATCAGCGAGAATTCAGGTG
Cc_nrLSU_Minyao 361 GCGGTTGAAGCTTGGGCATTTGATATGCTAGGGGAATGCCGTCTCTTGTATTGTGGGAAG
Cc_EU883527_411 361 GCGGTTGAAGCTTGGGCATTTGATATGCTAGGGGAATGCCGTCTCTTGTATTGTGGGAAG
Cp_KJ400152_456 361 GCGGTTGAAGCTTGGGCATTTGATATGCTAGGGGAATGCCGTCTCTTGTATTGTGGGAAG
Cc_nrLSU_Minyao 421 TAGTGCGCGCCCCGCGTGTGCTTCGGCACCTGCGTACTCAGGTCGTTGACTTGTGGGCTC
Cc_EU883527_411 421 TAGTGCGCGCCCCGCGTGTGCTTCGGCACCTGCGTACTCAGGTCGTTGACTTGTGGGCTC
Cp_KJ400152_456 421 TAGTGCGCGCCCCGCGTGTGCTTCGGCACCTGCGTACTCAGGTCGTTGACTTGTGGGCTC
Cc_nrLSU_Minyao 481 TCCATTCGACCCGTCTTGAAACACGGACCAAGGAGTCTGACATGTGTGCGAGTTGGCGAG
Cc_EU883527_411 481 TCCATTCGACCCGTCTTGAAACACGGACCAAGGAGTCTGACATGTGTGCGAGTTGGCGAG
Cp_KJ400152_456 481 TCCATTCGACCCGTCTTGAAACACGGACCAAGGAGTCTGACATGTGTGCGAGTTGGCGAG
Cc_nrLSU_Minyao 541 TGGAAAAACTCGCAAGGCGTAAGGAAGCTGATTGGCGGGATCCCTCTTTGGGGTGCACC
Cc_EU883527_411 541 TGGAAAAACTYGCAAGGCGYAAGGAAGCTGATTGGCGGGATCCCTCTTYGGGGTGCACC
Cp_KJ400152_456 541 TGGAAAAACTTGCAAGGCGCAAGGAAGCTGATTGGCGGGATCCCTCTTTGGGGTGCACC
Cc_nrLSU_Minyao 600 GTCGACCGACCTTGATCTTTTGAGAAGGGTTTGAGTGTGAGCACACCTGTTGGGACCCGA
Cc_EU883527_411 600 GYCGACCGACCTTGATCTTTTGAGAAGGGTTTGAGTGTGAGCAYACCTGTTGGGACCCGA
Cp_KJ400152_456 600 GCCGACCGACCTTGATCTTTTGAGAAGGGTTTGAGTGTGAGCATACCTGTTGGGACCCGA
Cc_nrLSU_Minyao 660 AAGATGGTGAACTATGCCTGAGCGGGGTGAAGCCAGAGGAAACTCTGGTGGAAGCCCGCA
Cc_EU883527_411 660 AAGATGGTGAACTATGCCTGAGCGGGGTGAAGCCAGAGGAAACTCTGGTGGAAGCCCGCA
Cp_KJ400152_456 660 AAGATGGTGAACTATGCCTGAGCGGGGTGAAGCCAGAGGAAACTCTGGTGGAAGCCCGCA
Cc_nrLSU_Minyao 720 GCGATACTGACGTGCAAATCGTTCGTCTGACTT
Cc_EU883527_411 720 GCGATACTGACGTGCAAATCGTTCGTCTGACTT
Cp_KJ400152_456 720 GCGATACTGACGTGCAAATCGTTCGTCTGACTT

Supplemental Figure 20 | Sequence alignment of nuclear large-subunit ribosomal DNA (*nrLSU*) sequences in our *Cuscuta campestris* isolate and published *Cuscuta campestris* and *Cuscuta pentagona*. The first sequence is from the *Cuscuta campestris* isolate we used in this research. The other sequences are from previously published *nrLSU* sequences of *Cuscuta campestris* (Cc) and *Cuscuta pentagona* (Cp) with GenBank accession numbers and following by DNA accession numbers.

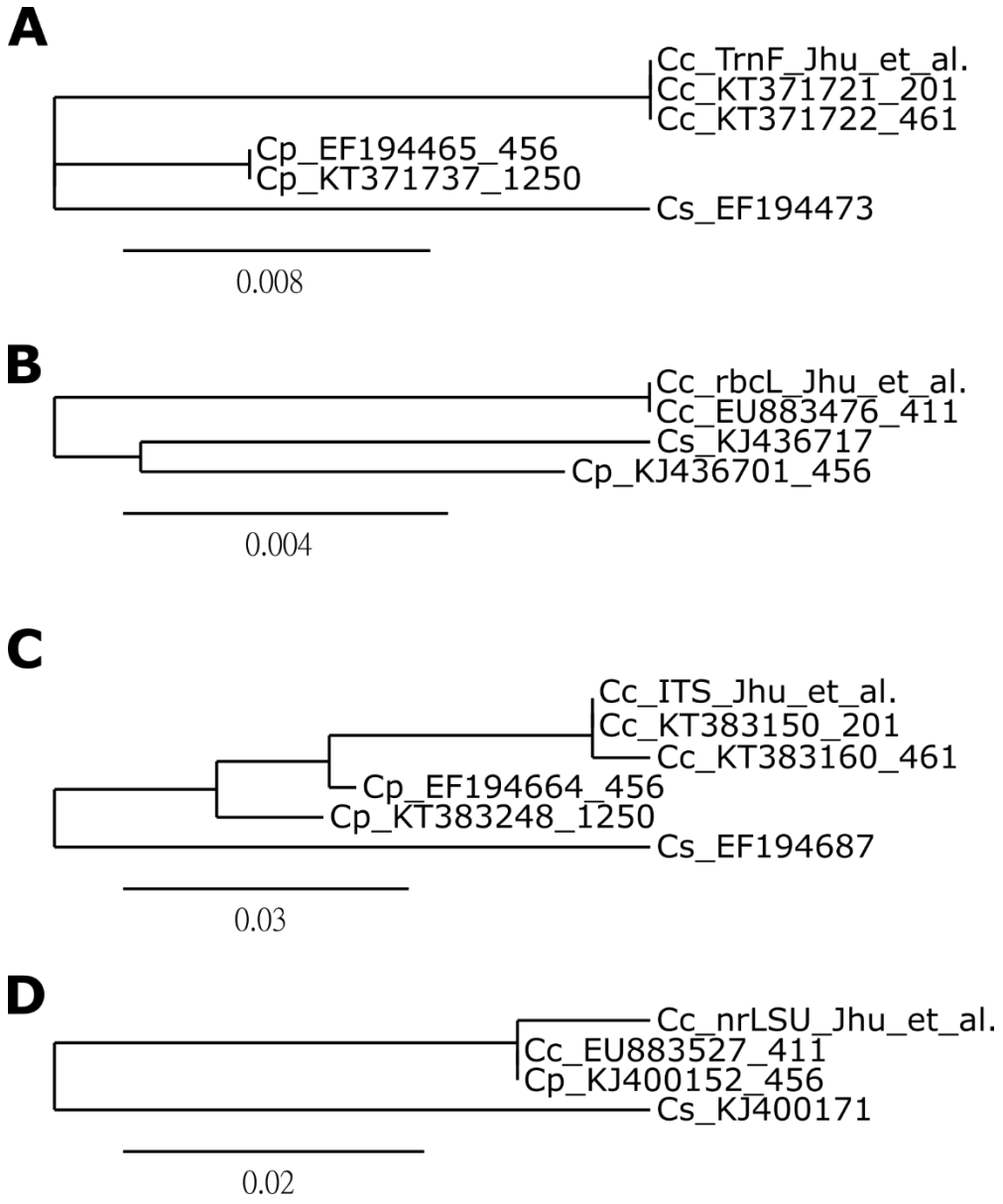

Supplemental Figure 21 | Phylogenetic relationships among our *Cuscuta campestris* isolate and published *Cuscuta campestris* and *Cuscuta pentagona* by Maximum-Likelihood Phylogenies. The first sequence of each tree is from the *Cuscuta campestris* isolate we used in this research. The other sequences are from previously published (A) *TrnL-F* (B) *rbcL* (C) *nrITS* (D) *nrLSU* sequences of *Cuscuta campestris* (Cc) and *Cuscuta pentagona* (Cp) with GenBank accession numbers and following by DNA accession numbers. These trees are rooted using *C.*

stenolepis (Cs) as functional outgroup. The number on the scale represents the percentage of genetic variation.

All Supplemental Tables are available on the bioRxiv Website. Please directly access them all at: https://www.biorxiv.org/content/10.1101/706861v3.supplementary-material**.**

Supplemental Data Set 1. DEG list of time-course RNA-Seq data.

Supplemental Data Set 2. DEG list of resistant and susceptible host response to C. campestris by using an interaction design model.

Supplemental Data Set 3. Vector pTAV (pMR315_pTAV-GW binary) sequence.

Supplemental Data Set 4. Haustorium infestation status quantification.

Supplemental Data Set 5. Resistant specific SNPs in all chromosome.

Supplemental Data Set 6. Resistant specific SNPs in *LIF1* promoter region.

Supplemental Data Set 7. Predicted transcription factor binding sites in *LIF1* promoter region.

Supplemental Data Set 8. DEG list of four different Heinz tomato cultivars response to *C. campestris* by ANOVA analysis.

Supplemental Data Set 9. Gene list in the Barnes-Hut t-distributed stochastic neighbor embedding (BH-SNE) generated clusters.

Chapter 4: Investigating host and parasitic plant interaction by tissue-specific gene analyses on tomato and dodder interface at three haustorial developmental stages

Abstract

Parasitic weeds cause billions of dollars in agricultural losses each year worldwide. *Cuscuta campestris* (*C. campestris*), one of the most widespread and destructive parasitic plants in the U.S., severely reduces yield in tomato plants. Reducing the spread of parasitic weeds requires understanding the interaction between parasites and hosts. Several studies have identified factors needed for parasitic plant germination and haustorium induction, and genes involved in host defense responses. However, knowledge of the mechanisms underlying the interactions between host and parasitic plants, specifically at the interface between the two organisms, is relatively limited. A detailed investigation of the crosstalk between the host and parasite at the tissue-specific level would enable development of effective parasite control strategies. To focus on the haustorial interface, we used laser-capture microdissection (LCM) with RNA-seq on early, intermediate and mature haustorial stages. In addition, the tomato host tissue that immediately surrounding haustoria was collected to obtain tissue- resolution RNA-Seq profiles for *C. campestris* and tomato at the parasitism interface. After conducting RNA-Seq analysis and constructing gene coexpression networks (GCNs), we identified *CcHB7*, *CcPMEI*, and *CcERF1* as putative key regulators involved in *C. campestris* haustorium organogenesis, and three potential regulators, *SlPR1*, *SlCuRe1-like*, and *SlNLR*, in tomatoes that are involved in perceiving signals from the parasite. We used host-induced gene silencing (HIGS) transgenic tomatoes to knock-down the candidate genes in *C. campestris* and produced CRISPR transgenic tomatoes to knock out candidate genes in tomatoes. The interactions of *C. campestris* with these

transgenic lines were tested and compared with that in wild-type tomatoes. The results of this study reveal the tissue-resolution gene regulatory mechanisms at the parasitic plant-host interface and provide the potential of developing a parasite-resistant system in tomatoes.

Introduction

Parasitic angiosperms are among the worst agricultural pests, reducing the yields of agricultural crops each year by billions of dollars worldwide (Agrios, 2005; Yoder and Scholes, 2010). Parasitic plants directly attach to host plants using specialized organs known as haustoria to extract nutrients and water from their hosts. Most standard herbicides and control techniques have not been effective or are too costly in managing parasitic plant infestations because of this tight physiological link between host plants and parasites. A better understanding of the mechanisms of parasitic signaling and haustorium development will allow us to develop more robust biocontrol approaches to eliminate the agricultural damage caused by parasitic plants.

Cuscuta species (dodders) lack functional roots and leaves and coil their stems counterclockwise as they grow on their host (Furuhashi et al., 2011; Alakonya et al., 2012). About 75% of *Cuscuta* species are found in the Americas (Furuhashi et al., 2011; García et al., 2014), including *Cuscuta campestris* (*C. campestris*). Many crop species are susceptible to *C. campestris* attack, including domesticated tomatoes (*Solanum lycopersicum*), leading to 50–72% yield reductions (Yaakov et al., 2001). In California, over 12,000 hectares of land are affected by *Cuscuta* (Lanini, 2005). Tomato is one of the most consumed fruit crops in the world, and the United States is one of the world's leading producers of tomatoes (Kimura and Sinha, 2008). In the United States, more than $2 billion in annual farm cash receipts are from fresh and processed tomatoes. Therefore, a detailed investigation of the haustorial development process in the

interactions between tomato and *Cuscuta* is essential to developing effective strategies to prevent agricultural losses that are caused by *Cuscuta* species.

However, the signals involved in haustorium development at specific developmental stages and the tissue-specific communication between host and parasite during the haustorium penetration process remain largely unknown. This is especially true for stem parasitic plant systems. Several studies have indicated that haustoria can transport not only water and nutrients, but also mRNA, miRNA, and small peptides. These bidirectional communications create a tight physiological connection between host and parasite. During the haustorium development process, parasitic plants change their host morphologically and physiologically by secreting hormones or effectors to help them establish haustorial connections. On the other hand, host plants deploy various defense strategies to counteract this infestation and prevent vascular connections. Understanding what parasitism-related genes have been explicitly activated at the interface between host and parasite could help develop a more efficient parasite-resistant system in crop plants.

Therefore, in this study, we used laser-capture microdissection (LCM) coupled with RNA-seq to zoom in on the interface between the host and parasite and to investigate the tissue-specific gene expression changes. We identified *CcHB7*, *CcPMEI*, and *CcERF1* as key regulators involved in haustorium organogenesis, and the functions of these candidate genes were validated by HIGS transgenic plants. We also identified three potential key regulators, *SlPR1*, *SlCuRe1-like*, and *SlNLR*, in tomatoes that may be involved in perceiving signals from the parasites, and two of them were further characterized with CRISPR knockout mutants.

Results

Transcriptomes at the host-parasite interface using laser-capture microdissection (LCM)

To investigate specific gene expression changes in penetrating haustoria, we used LCM with RNA-seq to analyze haustorial tissues from three different developmental stages. We defined three time points: early - the haustorium has just contacted the host, intermediate - the haustorium has developed searching hyphae, which are elongated tip-growing cells on haustoria, but has not formed vascular connections, and mature - a haustorium with continuous vascular tissue between host and parasite (Figure 1A-C).

We collected both parasite haustorial tissues and host tissues at the interface at these three-time points from *C. campestris* attached on *S. lycopersicum* cv. Heinz 1706 (H1706). To identify genes involved in *C. campestris* haustorial development during the penetration process, the protruding regions of haustoria were specifically collected from paraffin sections using LCM (Figure 1D-E). To capture the earliest host responses or defense mechanisms to combat *C. campestris* parasitism, we choose the same three developmental time points, early, intermediate, and mature stages of parasitism, to specifically collect the few layers of tomato cells that surround the penetrating *C. campestris* haustoria (Figure 1F). These host cells are most likely to exhibit the initial host defense response upon attacks by the parasite. These collected tomato and *C. campestris* tissues were processed for RNA extraction and library preparation for RNA-Seq and subsequent transcriptome analysis.

RNA-Seq analyses and gene coexpression networks (GCNs) across three developmental stages of *C. campestris* haustoria

We analyzed the transcriptome of LCM *C. campestris* haustorial tissues by mapping reads to the genome of *C. campestris* (Vogel et al., 2018). With multidimensional scaling analysis, the gene expression patterns among different samples showed that the early and intermediate stages are distinct from the mature stage (Supplemental Figure S1). We conducted a principal component analysis (PCA) analysis and coupled it with clustering analysis using self-organizing maps (SOM) to visualize the expression profile of each gene (Figure 2, Supplemental Table S1). To identify potential key regulators that are involved in *C. campestris* haustorium development at different stages, we conducted further gene coexpression analysis on specific SOM clusters.

First, we hypothesized that the genes highly up-regulated at the early stage of parasitism are most likely to be involved in the haustorium initiation and attachment process. Therefore, we focused on genes in SOM5, which is a cluster enriched with genes that are highly expressed in the early haustorial stage. Among these SOM5 genes, we constructed a gene coexpression network (GCN) to generate an overview of the potential molecular regulatory machinery and to identify central hub genes, which are genes with high degree of centrality in the coexpression network, that could be the regulators of the initiation and attachment mechanisms. Visualizing the network using Cytoscape (Cline et al., 2007), the SOM5 GCN is composed of four major modules (Fig. 3A-C, Supplemental Table S2) based on the fast greedy modularity optimization algorithm (Clauset et al., 2004). Using our previously published combined annotation profile, we conducted GO enrichment analysis using the matched TAIR ID for each *C. campestris* gene in the network to identify the major GO terms (FDR values < 0.05) for the target modules. We find the SOM5 module 1 enriched in biological process GO terms including “response to abiotic and biotic stimulus, response to stress, response to hormone, and response to far-red light” (Supplemental Table S5). This result indicates the genes contained in module 1 are likely involved in the

haustorium initiation process, which is responding to physical contact with the host and high far-red light environments, which are both important signals for haustorium induction in *Cuscuta* species.

To identify the key regulators in the haustorium initiation, we focused on genes in module 1 and calculated the degree centrality and betweenness centrality scores of each gene within this group because these gene are the potential master regulators. Many central hub genes in module 1 are protein kinases or enzymes involved in cell signaling. We focused on genes that are annotated as transcription factors to identify the potential master upstream key regulators of this developmental stage. Among these central hub transcription factors, a homeobox-leucine zipper protein (Cc014209) that is similar to transcription factor homeobox 7 (HB7) in *Arabidopsis* was identified (Figure 3B). Based on previous reports, *AtHB7* is a negative regulator of ABA response (Pehlivan, 2019) and modulates abscisic acid signaling by controlling the activity of protein phosphatases type 2C (PP2C) and ABA receptors (Valdés et al., 2012). Intriguingly, a recent study showed that ABA levels regulate haustoria formation in the root parasitic plant *Phtheirospermum japonicum* (Kokla et al., 2021). In *P. japonicum*, lowering ABA biosynthesis enabled haustoria to form in the presence of nitrates. Based on these pieces of evidence, we focus on *CcHB7* for further functional analysis.

Second, the genes highly up-regulated at the mature stage are most likely to be involved in establishment of vascular connection between host and parasite. Therefore, we also focused on genes in SOM3, which is a cluster enriched with genes that are highly expressed in the mature haustorial stage (Figure 3D). Using these SOM3 genes, we constructed a GCN to generate an overview of the potential molecular regulatory machinery. This SOM3 GCN is composed of five major modules based on the GCN community structure (Figure 3E, Supplemental Table S3). Using

GO enrichment analysis, we noticed that the SOM3 module 2 has enriched biological process GO terms including “root radial pattern formation” (Supplemental Table S5). This result matches our recent discovery that *C. campestris* also utilizes the root developmental program during haustorium organogenesis (Jhu et al., 2021). Therefore, we focused on SOM3 module 2 for further analysis. Based on the degree centrality and betweenness centrality scores, we noticed that many central hub genes in SOM3 module 2 are involved in cell wall modification, including expansins and several pectin methyl-esterase inhibitors (PMEIs) (Figure 3F). *CcPMEI* (Cc038093) is one of the central hub genes and has strong co-expression connection with other PMEIs. Thus, we focused on this *CcPMEI* for further functional analysis.

Last but not least, the previously identified key regulator in *C. campestris* haustorium development, transcription factor *LATERAL ORGAN BOUNDARIES DOMAIN 25* (*CcLBD25*) (Jhu et al., 2021) is classified in SOM6, which is enriched with genes that are highly expressed in the early and mature haustorial stage (Figure 3G). The SOM6 GCN is composed of four major modules based on the GCN community structure (Figure 3H, Supplemental Table S4). *CcLBD25* is located in module 2, which does not have any significantly enriched biological process GO terms (Supplemental Table S5). On the other hand, we noticed module 1 has enriched biological process GO term including “response to stimulus, response to hormone, response to organic substance.” Based on previous studies, auxin (Tomilov et al., 2005; Ishida et al., 2016) and ethylene (Cui et al., 2020) signaling play essential roles in parasitic plant haustorium development. Appropriate tactile stimuli, which come from the pressure coiling on the host, are also crucial for haustorium induction (Tada et al., 1996). Therefore, we zoomed in on SOM6 module 1 for further GCN analysis.

Many genes in SOM6 module 1 are enzymes that catalyze the degradation or modification of pectin, including pectin lyase (PL), pectin methyl esterase (PME), pectin methyltransferase (PMT), and pectin acetyl esterase (PAE) (Figure 3I). These findings coincide with several previous studies that cell wall modification, especially pectin structural dynamic and integrity, plays an important role in haustorium development (Vaughn, 2002; Johnsen et al., 2015; Hozumi et al., 2017). Besides cell wall remodeling, auxin and ethylene signaling also seem to play a role in the early and mature developmental stages. An auxin efflux carrier (Cc034373) and an auxin-responsive protein (Cc038909) were also located in SOM6 module 1 (Figure 3I). Furthermore, among the central hub genes in SOM6 module 1, the top central hub transcription factor is an ethylene responsive element binding factor 1 (*ERF1*, Cc002541), which is in the ERF/AP2 domain-containing transcription factor family. Intriguingly, a recent study showed that the root parasitic plant *Phtheirospermum japonicum* uses ethylene as a signal for host recognition and to tweak the haustorium development and penetration process (Cui et al., 2020). Our gene coexpression analysis suggests that this ethylene-mediated haustorial development regulatory pathway might be shared by both root and stem parasitic plants. Therefore, we focused on this *CcERF1* for further functional analysis.

Functional characterization of candidate *C. campestris* genes by host-induced gene silencing (HIGS)

Since an efficient transformation system for *C. campestris* is currently not available, to further validate the function of these candidate *C. campestris* genes, *CcHB7*, *CcPMEI*, and *CcERF1*, we used host-induced gene silencing (HIGS) to knock-down the candidate genes in *C. campestris*. Based on previous studies, cross-species transport of mRNAs, miRNAs and siRNAs between *C. campestris* and their hosts through haustoria vascular connections is common (Kim et

al., 2014; Johnson et al., 2019). These transported siRNAs can successfully down-regulate target gene transcription in *C. campestris*, via HIGS. Therefore, we generated transgenic tomatoes with hairpin RNAi constructs that target and down-regulate the candidate *C. campestris* genes, *CcHB7*, *CcPMEI*, and *CcERF1*, after the first successful attachment. If these genes are important in haustorium development, down-regulating these genes should influence haustorium penetration and parasitism.

To determine if these genes impact haustorium structure or the parasitism process, we grew *C. campestris* strands on the HIGS transgenic tomato. We collected tomato stem sections with *C. campestris* strands successfully attached on them and used vibratome sectioning to prepare 100 µm-thick fresh haustorium sections and subsequently stained them with Toluidine Blue O (O'Brien et al., 1964). We observed searching hyphae that entered the host cortex successfully and converted into xylic hyphae, which create the xylem bridge between host and parasite, or phloic hyphae, which mimic sieve elements and establish phloem-to-phloem connections, as they linked to the host xylem and phloem in sections of the haustoria growing on wild-type H1706 tomato plants (Figure 4A-C). However, we observed that many haustoria growing on *CcHB7* RNAi (Figure 4D-F), *CcPMEI* RNAi (Figure 4G-I), and *CcERF1* RNAi (Figure 4J-L) transgenic tomatoes seems to stop their penetration process at the cortex region. Furthermore, they also all shared a common phenotype that the host cortex cells that are surrounding the haustoria seem to enlarge and have a very loose cell wall structure, appearing degraded (Figure 4D-L). These *C. campestris* haustoria were not able to form vascular connections with their hosts and easily detached from their host stems.

This structural phenotype also corresponds well with our GCN results, especially the GCN for SOM3 and SOM6 (Figure 3). Several previous studies indicate that the interaction between

pectin methyl esterase (PME) and pectin methyl esterase inhibitor (PMEI) is a determinant factor in pectin degradation, cell wall loosening, strengthening, and organogenesis. Pectin acetyl esterases (PAEs) are involved in the enzymatic deacetylation of pectin and are used by plant pathogens to infect their hosts (Kong et al., 2019). However, the balance between different pectin enzyme functions might be precisely regulated by many key regulators. The down-regulation of these key regulators might disrupt the dynamic balance between enzymes and cause an out-of-control cell wall degradation, which lead to haustorium detachment from its host (Figure 4D-L).

Notably, since these plants are in a HIGS system, the first successful haustorial connection is necessary for the small interfering RNAs to transfer from the host to the parasite. Therefore, we often observed a successfully connected haustorium followed by several abnormal haustorium attachments, including the phenotype of overly degraded host cortex cell walls (Figure 4I). The overall plant phenotypes of *C. campestris* growing on the HIGS transgenic plants also showed very few haustorial connections and the inability to continue to form more attachments with the hosts compared to those growing on wild-type H1706 tomato plants (Supplemental Figure S2A-C). In addition, our preliminary biomass measurements also showed that the *C. campestris* plants growing on RNAi transgenic plants have reduced biomass compared with those growing on wild-type tomato plants (Supplemental Figure S2D). All of these results indicate that the down-regulation of these candidate gene expression levels by HIGS interfered with haustorium development and hampered *C. campestris* parasitism.

RNA-Seq analyses and gene coexpression networks (GCNs) across three developmental stages of host tissues surrounding *C. campestris* haustoria

On the other side of this host-parasite interface is the tomato host. We analyzed the LCM RNA-Seq data from the host tomato tissues surrounding *C. campestris* haustoria by mapping reads

to the tomato genome ITAG4.0 (Sato et al., 2012). Using multidimensional scaling analysis, the gene expression patterns in control host cell types (the regular tomato cortex cells that are not next to haustorium) are distinct from the cortex tissues surrounding *C. campestris* haustoria (Supplemental Figure S3). We also conducted a PCA coupled with SOM clustering analysis to visualize the expression profile of each gene (Figure 5, Supplemental Table S6). To identify potential key regulators of the interaction between host and parasite at different haustorium penetration stages, we conducted further gene coexpression analysis on specific SOM clusters.

First, the host genes that are highly up-regulated at the early stage are most likely to be involved in perceiving parasite signals, triggering pattern-triggered immunity (PTI) and effector-triggered immunity (ETI) to help the host repel *C. campestris* attacks. Based on previous reports, the changes in the levels of salicylic acid (SA) and jasmonic acid (JA) in hosts are most obvious in the early stage (4 days post attachment (DPA)) (Runyon et al., 2010). So, we hypothesized that the most pronounced gene expression changes of key regulators would be at the initial stage of infestation. Therefore, we focused on genes in SOM8, which is a cluster enriched with host genes that are highly expressed in the early haustorial stage (Figure 6A). Among the genes in SOM8, we noticed inclusion of *SlWRKY16* (Solyc07g056280), a negative regulator of the lignin-based resistance response (Jhu et al., 2020). The SOM8 GCN is composed of four major modules based on the GCN community structure (Figure 6B, Supplemental Table S7). *SlWRKY16* is located in module 2. Based on our GO enrichment analysis, there are some genes that matched the GO term "regulation of defense response, and defense response to fungus," but none of the GO terms were statistically significantly enriched in this module (Supplemental Table S9). However, one of the previously identified CuRe1 homologs (*CuRe1-like*, Solyc08g016210) (Fürst et al., 2016), which

is a leucine-rich repeat (LRR) receptor-like serine/threonine-protein kinase, is also located in module 2 (Figure 6B). Therefore, we zoomed in on the SOM8 module 2 for further GCN analysis.

Many other genes in SOM8 module 2 are involved in ethylene signaling (Figure 6C). Ethylene is known to play a vital role in activating plant defenses against various biotic stresses, including microbial pathogens and herbivores (Broekgaarden et al., 2015). Previous studies also used the emission of ethylene in *N. benthamiana* and *S. lycopersicum* as an indicator that the defense response was successfully triggered upon *Cuscuta reflexa* infestation (Hegenauer et al., 2016; Hegenauer et al., 2020). In addition to the CuRe1-like homolog, several LRR receptor-like protein kinases are also identified in SOM8 module 2 (Figure 6C). This result matches our hypothesis that the host genes that are highly up-regulated at the early stage are most likely to be involved in perceiving parasite signals. We suspect that *CuRe1-like* might play a role in sensing unknown *Cuscuta* signals, so we generated CRISPR-Cas9 edited *Cure1-like* mutant plants for further analysis.

Among the central hub genes in SOM8 module 2, *Pathogenesis-Related protein 1* (*PR1*, Solyc01g106600) was one of the top central hubs (*PR1* degree centrality = 64; median degree centrality in SOM8 = 13) (Figure 6C). PR1 proteins are known to be highly produced upon plant pathogen infection and have often been used as a marker for SA-mediated disease resistance (Breen et al., 2017). However, the role of PR1 in host plant responses upon parasitic plant attack is currently unknown. Therefore, we also focused on PR1 for further functional analysis using CRISPR-Cas9 gene editing.

Other than the host genes that are specifically only highly expressed at the early stage, another group of host genes are up-regulated at the early stage and gradually decrease their expression throughout parasitism. Genes with this expression pattern are found in SOM3 (Figure

6D). We suspected that these genes might also be involved in the parasite signal perceiving process. Hence, we focus on SOM3 for further GCN analysis. The SOM3 GCN is composed of four major modules based on the GCN community structure (Figure 6E, Supplemental Table S8). Based on our GO enrichment analysis, there are some genes in module 3 that matched the GO term "response to hormone," but none of the GO terms were statistically significantly enriched in this module (Supplemental Table S9). However, many genes in SOM3 module 3 are LRR receptor-like kinases or nucleotide-binding site–leucine-rich repeat (NBS-LRR, or NLR) proteins. Therefore, we focused on SOM3 module 3 for further analysis.

Among the genes in SOM3 module 3, four genes involved in ethylene signaling were identified, including an ethylene-responsive transcription factor, an ethylene-responsive proteinase inhibitor and an ethylene-inducing xylanase receptor. This result provides further support for the hypothesis that ethylene might also play an important role in plant resistance responses against parasitic plants. In addition to the ethylene signaling pathway, potential transcription factors or receptors are also enriched in SOM3 module 3. Three LRR proteins and two NLRs are identified in module 3. NLRs are common disease resistance genes (R genes) and are known to be involved in biotic stress detection, including various plant pathogens and herbivores (McHale et al., 2006; Van Ghelder et al., 2019). Therefore, we suspected that these NLRs are potentially involved in the process of detecting parasitic plants signals and choose the NLR with the highest degree centrality (Solyc07g056200 degree centrality = 7; median degree centrality of NLRs in SOM3 module 3 = 6.5) in SOM3 module 3 as our candidate genes for further functional analysis.

Functional characterization of tomato host genes by CRISPR-Cas9 gene editing

Since CRISPR knockout techniques (Pan et al., 2016) and tomato transformation systems are readily available, we designed and cloned synthetic guide RNAs (sgRNA) targeting our

candidate genes, *SlPR1*, *SlCuRe1-like*, *SlNLR*, and then produced transgenic tomato plants in the M82 background with CRISPR/Cas9 targeted candidate gene knockout mutations. We selected the T0 transgenic plants that had biallelic insertion or deletion or substitution mutations for further T1 plants analysis (Supplemental Figure S5). After obtaining these CRISPR transgenic tomato lines, we tested the interactions of *C. campestris* with these engineered tomato lines and compared their *C. campestris*-host interactions with those seen in wild-type M82 tomatoes by phenotyping the haustorium attachment sites.

Interestingly, the *SlCuRe1-like* CRISPR T0 transgenic tomato lines were very vulnerable to pathogens and insect herbivores, did not grow well in our greenhouse conditions and only produced very few seeds. This indicates that *SlCuRe1-like* might play a role in the plant defense responses to other pathogens and herbivores in addition to any possible role in plant parasitism. As a result, due to low seed set we were unable to phenotype these CRISPR tomato lines, so *SlCuRe1-like* phenotyping is excluded from our current analysis.

When compared with wild-type M82 tomato plants (Figure 7A-B), *SlPR1* CRISPR T1 tomato plants (Figure 7E-F) and *SlNLR* CRISPR T1 tomato plants (Figure 7I-J) did not have an obvious difference in their overall plant or tissue phenotypes without *C. campestris* infestation, based on the fresh vibratome sections. However, the differences were apparent when these CRISPR tomato plants were infested by *C. campestris*. On wild-type M82 tomato plants, we observed that searching hyphae entered the host cortex and linked to the host xylem and phloem, but *C. campestris* did not change the overall host stem structure much, other than penetrating and forming vascular connections (Figure 7C-D).

In contrast, *SlPR1* CRISPR tomato plants seem to be more susceptible to *C. campestris* attack and have hypertrophy symptoms, which is abnormal plant outgrowth caused by

cell enlargement, at the haustorium attachment sites (Figure 7G-H). The vascular connections between host and parasite, especially the xylem bridges, were enlarged. Based on previous reports, hypertrophy improves the efficiency of root parasitic plant *Phtheirospermum japonicum* parasitism (Spallek et al., 2017). This parasite-derived modification can change host tissue morphology and help with parasite fitness. Similarly, *C. campestris* haustoria not only penetrated and formed vascular connections with *SlNLR* CRISPR tomato vascular tissue, but also changed the overall host stem vascular tissue arrangement, causing a reduction in the secondary xylem in the region of haustorium penetration (Figure 7K-L). This phenotype also indicates that *SlNLR* CRISPR tomato plants are more vulnerable to *C. campestris*.

The overall plant phenotypes of wild-type M82 tomatoes and CRISPR transgenic plants with *C. campestris* infestation also showed that the *SlPR1* and *SlNLR* CRISPR transgenic plants have stunted growth after being parasitized by *C. campestris* (Supplemental Figure S4). The CRISPR transgenic plants with *C. campestris* infestation are much shorter than wild-type M82 with *C. campestris* infestation. Notably, the *SlPR1* and *SlNLR* CRISPR transgenic plants without *C. campestris* infestation have no significant height difference comparing to wild-type M82 (Supplemental Figure S4C). This result indicates that the CRISPR-mediated mutations do not lead to the stunted growth phenotype directly; however, the *SlPR1* and *SlNLR* knockout mutations cause a growth penalty in the presence of *C. campestris*. These results also suggest that the knockout of candidate genes might interfere with the host defense response and make these CRISPR plants more susceptible to *C. campestris* parasitism.

Discussion

In this study, we use LCM captured *C. campestris* haustorial tissues and tomato host tissues surrounding haustoria, coupled with RNA-seq analysis to reveal the potential tissue-resolution

molecular regulatory machinery and the complexity of gene coexpression networks involved in haustorium organogenesis and host defense responses. We identified three potential key regulators in *C. campestris* that are involved in the early or/and mature stage of haustorium development, and all three of them were validated by using HIGS transgenic plants. We also identified three potential key regulators in tomato plants that are involved in perceiving signals from the parasite, and two of them were further verified with CRISPR knockout mutants.

Pectin dynamic regulation in *Cuscuta* parasitism and haustorium development

The chemical structure and mechanical properties of plant cell walls play an important role in organogenesis (Chebli and Geitmann, 2017). Several reports indicate that the physical interactions between pectins and other cell wall components regulate many vital aspects of plant development (Saffer, 2018). Pectin composition and mechanical characteristics have also been found to control the parasitism process and the development of haustorium in *Cuscuta* species. For example, a previous study discovered that *Cuscuta pentagona* secretes de-esterified pectins at the host and parasite interface (Vaughn, 2002). These low-esterified pectins function as a cement to help adhesion to their hosts during the early stage of the *Cuscuta* parasitism process. Similar de-esterified pectin accumulation phenomena have also been reported in *Cuscuta reflexa*, *Cuscuta campestris*, and *Cuscuta japonica* to facilitate the formation of strong adhesion (Johnsen et al., 2015; Hozumi et al., 2017). De-esterified pectin is a good substrate for pectate lyases, which are also found to be highly expressed at haustoria in *C. reflexa* (Johnsen et al., 2015). High levels of pectate lyases suggest that *Cuscuta* utilizes these enzymes to remodel their host cell walls to achieve successful penetration. The SOM5 and SOM6 GCNs of *C. campestris* genes also identified several highly expressed pectate lyases and pectin methyl-esterases at early and/or mature stages (Figure 3A-C and 3G-I). Our GCN analysis is not only consistent with previous findings but also

provides a more comprehensive potential gene regulatory machinery at specific haustorial developmental stages.

The interplay between PME and PMEI is also known to regulate the chemical and physical characteristics of the cell wall, including cell wall porosity and elasticity (Wormit and Usadel, 2018). Although cell wall loosening is a necessary step for haustorium penetration, an out-of-control cell wall degradation could lead to haustorium detachment from its host (Figure 4). The balance between different pectin enzyme functions might be precisely regulated by many key regulators. The down-regulation of these key regulators might disrupt the dynamic balance between enzymes and lead to abnormal cell wall degradation. Therefore, regulation of the enzymes that likely help with the haustorium penetration process may be disrupted, leading to over-degradation of the host cell wall, resulting in haustorium detachment (Figure 4D-L). Therefore, loosening the host plant cell wall should be precisely regulated during the parasitism process. Several highly expressed PMEIs are found in the SOM3 GCN at the mature stage, verifying this hypothesis (Figure 3D-F). Furthermore, in SOM6 module 1 (Figure 3G-I), tight connections between several enzymes that catalyze the modification of pectin, including PLs, PME, PMT, and PAE, reveal the complexity of dynamic pectin regulation in the haustorium penetration process and the importance of balancing various aspects of cell wall modification.

Auxin and ethylene in haustorium development

Regulating auxin transport and distribution is a pivotal factor in plant organogenesis (Benková et al., 2003). Regional auxin accumulation is commonly seen in root development, lateral root initiation, and root hair formation. Previous studies also indicate that spatial and temporal auxin accumulation play an important role in the early stage of haustorium organogenesis in root parasitic plants, like *Phtheirospermum japonicum* and *Triphysaria versicolor* (Tomilov et

al., 2005; Ishida et al., 2016), which adopted the root morphogenesis program into haustorium development (Yoshida et al., 2016). Our SOM5 and SOM6 GCNs also included several genes that are auxin transporters or auxin-responsive proteins at the early stage of haustorium development (Figure 3). This suggests that auxin-mediated regulation of haustorium initiation might be shared by both root and stem parasitic plants, and also further validates our hypothesis that stem parasitic also co-opted the root parasite program into haustorium development.

Other than auxin regulation, ethylene accumulation has also been observed in the early stage of haustorium development in *T. versicolor* (Tomilov et al., 2005). A recent study further discovered that ethylene signaling plays an important role in regulating cell proliferation and differentiation in the haustorial development process of *P. japonicum* (Cui et al., 2020). This root parasitic plant utilizes host-produced ethylene as a signal for host recognition to help with the haustorium penetration process (Cui et al., 2020). However, whether ethylene is also involved in haustorium development in stem parasitic plant remains an open question. The identification of ethylene signaling-related genes in SOM5 GCN (Figure 3C) and *ERF1* as one of the central hub genes in our SOM6 GCN (Figure 3I) provides some clues that ethylene signaling might also play a vital role in regulating haustorium initiation at the early haustorium initiation stage, and later cell differentiation at the mature haustorium stage in *C. campestris*.

Ethylene and abscisic acid (ABA) in host responses upon *C. campestris* infestation

Besides regulating cell wall modification and organogenesis, ethylene is also known as a key hormone involved in plant defense response against various biotic stresses, including pathogens and herbivores (Adie et al., 2007; Liu et al., 2013; Tintor et al., 2013; Böhm et al., 2014). The production of ethylene has often been observed in host plants upon parasitic plant infestation. For example, an ethylene biosynthesis gene (Dos Santos et al., 2003) and an ethylene-responsive

element-binding factor (Vieira Dos Santos et al., 2003) were activated in *A. thaliana* upon *O. ramosa* infestation. Similarly, ethylene emission was induced in *N. benthamiana* and *S. lycopersicum* upon *Cuscuta reflex* infestation (Hegenauer et al., 2016; Hegenauer et al., 2020). The identification of many ethylene-responsive transcription factors in our tomato SOM8 and SOM3 GCNs and their tight connections with many LRR and NLR genes (Figure 6) suggesting that ethylene may also play a key role in host defense against *C. campestris* by triggering and regulating local and systemic immune responses.

Many previous studies also indicate that ethylene has complex crosstalk with other hormone pathways, including ABA, which is another major phytohormone regulating stress responses (Veselov et al., 2003; Ku et al., 2018; Berens et al., 2019). Although ABA is often known to be involved in responses to abiotic stress (Ku et al., 2018; Berens et al., 2019), induction of ABA biosynthesis and signaling were also observed in the interaction between host and parasitic plants. For example, ABA levels increased in both leaves and roots of tomatoes upon the infestation of root parasitic plant *Phelipanche ramose* (Cheng et al., 2017). ABA concentrations also increased in maize leaves upon *Striga hermonthica* infestation (Taylor et al., 1996). The induction of ABA was also observed in tomatoes at 36 hours after *C. pentagona* infestation and continued to accumulate through 120 hours (Runyon et al., 2010). Furthermore, in the early stage of *P. ramosa* infestation, elevated gene expression levels of ABA-responsive and biosynthesis genes were also reported. An ABA signaling-related gene has also been included in SOM8 module 2 (Figure 6C) suggests that ABA might play a role in host defense response at the early stage of perceiving *C. campestris* attack.

Parasitic plant-induced hypertrophy

Hypertrophy, abnormal plant outgrowth caused by cell enlargement, is also a common plant symptom that can be induced by various pathogens, herbivores, or parasites (Bowman, 2019). Hyperplasia is abnormal plant outgrowth caused by excessive cell division, leading to increased cell numbers, resulting in the formation of plant galls that can be induced by viruses, pathogens, parasites, or insects (Bowman, 2019). Parasitic plant-induced hypertrophy and hyperplasia have also been reported in several different systems (Heide-Jørgensen, 2008). For example, hypertrophy has also been observed on crabapple trees, *Malus toringoides*, induced by the stem parasitic plant European mistletoe, *Viscum album* (Spallek et al., 2017). Similarly, the root parasitic plant *Phtheirospermum japonicum* induced hypertrophy at the haustorial attachment site in both *A. thaliana* and tomato roots (Spallek et al., 2017). This hypertrophy phenotype enlarged the width of xylem tissues in the host root right above haustoria attachment sites, which could help the parasites uptake more water and nutrients from the host. The induction of cytokinin and ethylene might be one reason for the hypertrophy phenotype (Spallek et al., 2017; Mignolli et al., 2020). However, the detailed mechanism underlying parasitic plant-induced hypertrophy remains unknown.

In this study, our fresh sections showed that *C. campestris* induced xylem bridge cell enlargement in *PR1*-CRISPR transgenic tomato plants (Figure 7). This might allow *C. campestris* to obtain water and nutrients more efficiently from host plants and help with the fitness of the parasite. At the same time, this result also suggests that wild-type tomatoes might originally have a PR1-mediated defense mechanism to prevent hypertrophy upon parasitism. The removal of PR1 makes these transgenic plants more vulnerable to *C. campestris* and these plants have obviously stunted growth upon *C. campestris* infestation (Figure 7, Supplemental Figure S4). Investigating the connection between PR1 and hypertrophy would be of interest for future research

because this could help us to not only understand a potential new defense mechanism against parasitic plants but also know how parasites and host plants influence each other physiologically and morphologically.

Potential receptors and factors involved in detecting *C. campestris* signals

Detecting pathogens or herbivores is the essential first step in triggering plant innate immunity and the following defense responses. Many plant immune receptors have the leucine-rich repeat (LRR) domain (Padmanabhan et al., 2009). More recent studies have indicated that host plants can identify stem and root parasitic plants by utilizing the mechanisms that are similar to the systems for recognizing bacterial and fungal pathogens. For example, the previously identified *CUSCUTA RECEPTOR 1* (*CuRe1*) encodes a leucine-rich repeat receptor-like protein (LRR-RLP) in tomatoes (Hegenauer et al., 2016). This cell surface receptor-like protein bind with a Cuscuta factor, glycine-rich protein (GRP), or its minimal peptide epitope Crip21 to trigger resistance responses, including hypersensitive responses (HRs) and induced ethylene synthesis (Hegenauer et al., 2016; Hegenauer et al., 2020).

However, the host plants that lack CuRe1 are still fully resistant to *C. reflexa*, indicating that CuRe1 is not the only receptor involved in defense responses against parasitic plants (Hegenauer et al., 2016). Recent studies indicate that multilayered resistance mechanisms are deployed by plants to ensure efficient defense against pathogens and parasites (Jhu et al., 2020). Therefore, investigating other potential receptors is important for identifying other potential layers of defense mechanisms and could help with developing parasitic plant resistant systems in crops. In our LCM RNA-Seq analysis results, many LRR genes, including a CuRe1-like gene, are highly expressed in tomato hosts at the early stage of haustorium penetration and are included in SOM8 module 2 and SOM3 module 3 GCNs (Figure 6). These discoveries not only provide some

evidence for the multilayered resistance hypothesis but also identify potential receptors that might be able to perceive different unknown *Cuscuta* signals.

In addition to LRRs, many NLRs encoded by R genes also have been identified to detect parasitic plants. For example, the *RSG3-301* gene encodes a coiled-coil nucleotide-binding site leucine-rich repeat protein (CC-NBS-LRR) protein in the resistant cowpea, which can trigger the hypersensitive response upon *S. gesnerioides* attack (Li and Timko, 2009). Similarly, *Cuscuta R-gene for Lignin-based Resistance 1* (*CuRLR1*) encodes an N-terminal CC-NBS-LRR, which can induce lignin-based resistance responses in the stem cortex of specific resistant Heinz tomato upon *C. campestris* infestation (Jhu et al., 2020). The two NLRs (Solyc07g056200, Solyc12g006040) that are identified in SOM3 module 3 suggest that other NLRs might also be involved in the defense response again *C. campestris*. The tight gene co-expression connection between NLRs and LRRs indicates either that there is potential crosstalk among different layers of resistance mechanisms, or that these receptors might be regulated by common master regulators.

The results of this study reveal the detailed tissue-resolution gene regulatory mechanisms at the parasitic plant and host interface and identifies key regulators of parasitism in both the parasitic plant *C. campestris* and its tomato host. These findings will not only shed light on the field of plant parasitism and haustorium development but also help to develop a parasite-resistant system in tomatoes to reduce economic losses in agriculture. Parasitic weeds-resistant crops will be effective approaches for regulating parasitic plant infestations, reduce the usage of herbicides, and help with developing sustainable agriculture.

Materials and Methods

Cuscuta campestris materials

The dodder materials used in this study were generous gifts from W. Thomas Lanini, who collected dodder seeds from tomato fields in California. By using molecular phylogenetics of plastid DNA, and nuclear large-subunit ribosomal DNA (*nrLSU*) sequences (Stefanović et al., 2007; García et al., 2014; Costea et al., 2015), we have verified that this dodder isolate is the same as *Cuscuta campestris* 201, Rose 46281 (WTU) from USA, CA (Jhu et al., 2020) by comparing with published sequences (Costea et al., 2015).

Haustorium section preparation

To capture specific tissues at the host and parasitic plant interface, we prepared haustorium paraffin sections for further analysis. About four-leaf-stage Heinz 1706 tomato (*Solanum lycopersicum*) plants were infested with 10-15 cm long *C. campestris* strands. First, sections of tomato stem with haustoria, about 0.75 cm long, were collected for histology. Second, these stem sections were fixed in formaldehyde – acetic acid – alcohol (FAA). Third, these samples were dehydrated by the ethanol series for one hour at each step (75%, 85%, 95%, 100%, 100%, 100% ethanol) and proceeded through xylene in ethanol series for two hours each (25%, 50%, 75%, 100%, 100% xylene). Fourth, these stem sections were then incubated at 42°C in paraffin and xylene solution series and kept in 100% paraffin and changed twice daily for three days at 55°C. Finally, these stem sections were embedded in paraffin (Paraplast X-TRA, Thermo Fisher Scientific). 10 μm thick paraffin sections were prepared using a Leica RM2125RT rotary microtome. These paraffin section strips were placed on polyethylene naphthalate (PEN)-coated membrane slides (Leica), dried at room temperature, and deparaffinized with 100% xylene.

Laser-capture microdissection (LCM) sample collection

Comparing with our previous transcriptome that used the whole tomato stem tissues near the haustorial attachments (Jhu et al., 2020) or the whole *Cuscuta* strands with haustoria (Ranjan et al., 2014) for RNA library construction, to zoom in on the interface between the host and parasite, laser-capture microdissection (LCM) was used for tissue sample collection in this project. With this method, the tissue of *C. campestris* haustorium protruding region and the tomato host tissue that were surrounding the haustoria from paraffin sections were specifically captured for RNA library construction. Targeted haustorial and host tissues were dissected on a Leica LMD6000 Laser Microdissection System (Figure 1). Based on the haustorial structures, we classified haustoria into three different developmental stages. "Early" indicates that the haustorium has just penetrated the tomato stem cortex region. "Intermediate" indicates that the haustorium has penetrated the tomato stem cortex and formed searching hyphae, but has not formed vascular connections with the host vascular system. "Mature" indicates that the haustorium has formed continuous vasculatures with the host (Figure 1). Both haustorial tissues and tomato host tissues were microdissected from each of the three developmental stages. These tissues were collected in lysis buffer from RNAqueous®-Micro Total RNA Isolation Kit (Ambion) and stored at -80°C. Collected tissues were processed within one month of fixation to ensure RNA quality. Approximately 30 regions of 10 um thickness each were cut from each slide, and three to four slides were used per library preparation.

LCM RNA-seq library preparation and sequencing

RNAs of these collected tissues were extracted using RNAqueous-Micro Total RNA Isolation Kit (Ambion) and amplified using WT-Ovation Pico RNA Amplification System (ver. 1.0, NuGEN Technologies Inc.) following manufacturer instructions. RNA-seq libraries for

Illumina sequencing were constructed following a previously published method (Kumar et al., 2012) with slight modifications. Libraries were quantified, pooled to equal amounts, and their quality was checked on a Bioanalyzer 2100 (Agilent). Libraries were sequenced on a HiSeq2000 Illumina Sequencer at the Vincent J Coates Genomics Sequencing Laboratory at UC Berkeley.

RNA-Seq data mapping and processing

After receiving raw reads data for these LCM libraries, we separated them into two groups based on tissue origin, *C. campestris* (dodder) and *S. lycopersicum* (tomato). For the LCM RNA-Seq data from *C. campestris*, these raw reads were mapped to the published genome of *C. campestris* (Vogel et al., 2018) with Bowtie 2 (Langmead and Salzberg, 2012). For the LCM RNA-Seq data from tomato, these raw reads were mapped to the published current tomato genome version ITAG4.0 (Sato et al., 2012) with Bowtie 2 (Langmead and Salzberg, 2012). Both data were then analyzed by using EdgeR (Robinson et al., 2009) to get normalized trimmed means of M values (TMM) for further analysis.

MDS and PCA with SOM clustering

After the normalization steps, to visualize the overall expression profiles of each library, the function "cmdscale" in the R stats package was used to create multidimensional scaling (MDS) data matrix and then generate MDS plots. For both *C. campestris* and tomato LCM RNA-Seq data, genes in the upper 50% quartile of coefficient of variation were selected for further analysis. For principal component analysis (PCA), principal component (PC) values were calculated using the "prcomp" function in the R stats package. The expression profiles of selected genes were visualized in a two-dimensional (2D) plot for PC1 and PC2.

These selected genes were then clustered for multilevel three-by-two hexagonal SOM using the som function in the "kohonen" package (Wehrens and Buydens, 2007). The SOM clustering results were then visualized in PCA plots. The complete gene lists for all SOM units in *C. campestris* and tomato LCM RNA-Seq data with SOM distances and PCA principal component values are included in Supplemental Table S1 and S2, respectively. For both *C. campestris* and tomato LCM RNA-Seq data, we specifically focused on the SOM groups with genes that are highly expressed in the early developmental stage (4 DPA). From *C. campestris* libraries, these genes are likely involved in the mechanisms of haustorium early development and penetration process. From tomato libraries, these genes are likely regulating the early host responses or defense mechanism upon parasitic plant attacks.

Construction of gene co-expression networks (GCNs)

To identify potential key regulators, we use the genes that are classified in selected SOM groups to build GCNs. The R script is modified from our previously published method (Ichihashi et al., 2014), and the updated script is uploaded to GitHub and included in code availability. For the GCN of *C. campestris* LCM data, we used the selected SOM gene list and constructed the GCN of these genes based on the expression profiles in *C. campestris* LCM data with the following normal quantile cutoff. The SOM5 GCN cutoff = 0.97. The SOM3 GCN cutoff = 0.98. The SOM6 GCN cutoff = 0.95. For the GCN of tomato LCM data, we used the selected SOM gene list and constructed the GCN of these genes based on the expression profiles in tomato LCM data with the following normal quantile cutoff. The SOM3 GCN cutoff = 0.80. The SOM8 GCN cutoff = 0.90. These networks were then visualized using Cytoscape version 3.8.0. Based on the number of connections, we identified the central hub genes with the highest connections as our candidate genes (Supplemental Table S2, 3, 4, 7, 8).

Functional annotation and GO enrichment analysis of RNA-Seq data

For tomato genes, the current published tomato genome ITAG4.0 is well-annotated, so the gene name and functional annotation that is currently available on the Sol Genomics Network website (https://solgenomics.net/) were used in this study. For *C. campestris* genes, since many genes are not functionally annotated in the current published *C. campestris* genome (Vogel et al., 2018), we used our previously published master list for annotated *C. campestris* transcriptome (Ranjan et al., 2014) combined with *C. campestris* genome gene IDs to create a more complete functional annotation (Jhu et al., 2021). TAIR ID hits were used for GO Enrichment Analysis on http://geneontology.org/ for gene clusters and modules. After obtaining these functional annotations, we specifically focused on our candidate genes that are annotated as transcription factors (TFs) or receptors for further analysis.

HIGS RNAi and CRISPR transgenic plants

For HIGS RNAi constructs for *C. campestris* candidate genes, we used the previously published destination vector pTKO2 vector (Snowden et al., 2005; Brendolise et al., 2017). This pTKOS2 vector contains two GATEWAY cassettes positioned at opposite directions that are separated by an Arabidopsis ACT2 intron, and the whole construct is under the control of the constitutive 35S promoter. To avoid off-target effects on influencing potential homologs in tomatoes, we used BLAST to identify a sequence fragment that is specific to each *C. campestris* candidate gene. The sequences that are used in HIGS RNAi constructs are listed in Supplemental Table S10. This RNAi fragment was amplified from *C. campestris* genomic DNA and cloned into pCR8/GW-TOPO (Life Technologies), and then *in vitro* recombined with the destination vector pTKO2 to generate a final expression clone. The final plasmids were verified by Sanger sequencing and introduced into *A. tumefaciens* EHA105.

For CRISPR constructs of candidate genes, we identified guide RNA (gRNA) sequences that were specific to the target genes using CCTop - CRISPR/Cas9 target predictor (Stemmer et al., 2015; Labuhn et al., 2017). Among CCTop provided candidates, we identified two sequences that are 50~150 bp apart at the 5' of the coding sequence and that are scored highly by the CRISPRscan software (Moreno-Mateos et al., 2015). The gRNA sequences that were used in CRISPR constructs are listed in Supplemental Table S11. One of these two gRNAs was cloned into pDONR_L1R5_U6gRNA and another was cloned into pDONR_L5L2_AtU6-26gRNA. Both plasmids were digested with BbsI, which places gRNAs under a U6 promoter. Using the *in vitro* CRISPR assay, we verified that the selected gRNAs are functional by expressing gRNAs from a T7 promoter (NEB HiScribe T7 High Yield RNA Synthesis Kit E2040S), generating targets by PCR with gene specific primers, and then mixing them with commercial Cas9 protein (NEB *Streptococcus pyogenes* Cas9, M0641S). Next, both gRNA expression cassettes were recombined by multi-site GATEWAY LR cloning into binary plant transformation vector pMR290, in which an Arabidopsis codon-optimized *Streptococcus pyogenes Cas9* is placed under the control of 2x35S constitutive promoter. The final plasmids were verified by Sanger sequencing and transformed into *A. tumefaciens* EHA105.

All of these HIGS RNAi and CRISPR constructs were sent to the Ralph M. Parsons Plant Transformation Facility at the University of California Davis to generate transgenic tomato plants. HIGS RNAi transgenic tomato plants are in Heinz 1706 background. To verify that these transgenic plants contained HIGS RNAi constructs, all T0 transgenic plants were selected for kanamycin resistance, and their genomic DNAs were extracted and tested by PCR. CRISPR transgenic tomato plants are in the M82 background. To verify that transgenic plants contained CRISPR mutations in the target gene, a region spanning and extending the regions

between the two gRNAs targets were amplified by PCR and sequenced. The sequence results and the mutations generated by CRISPR are shown in Supplemental Figure S5 for each candidate gene.

Figures

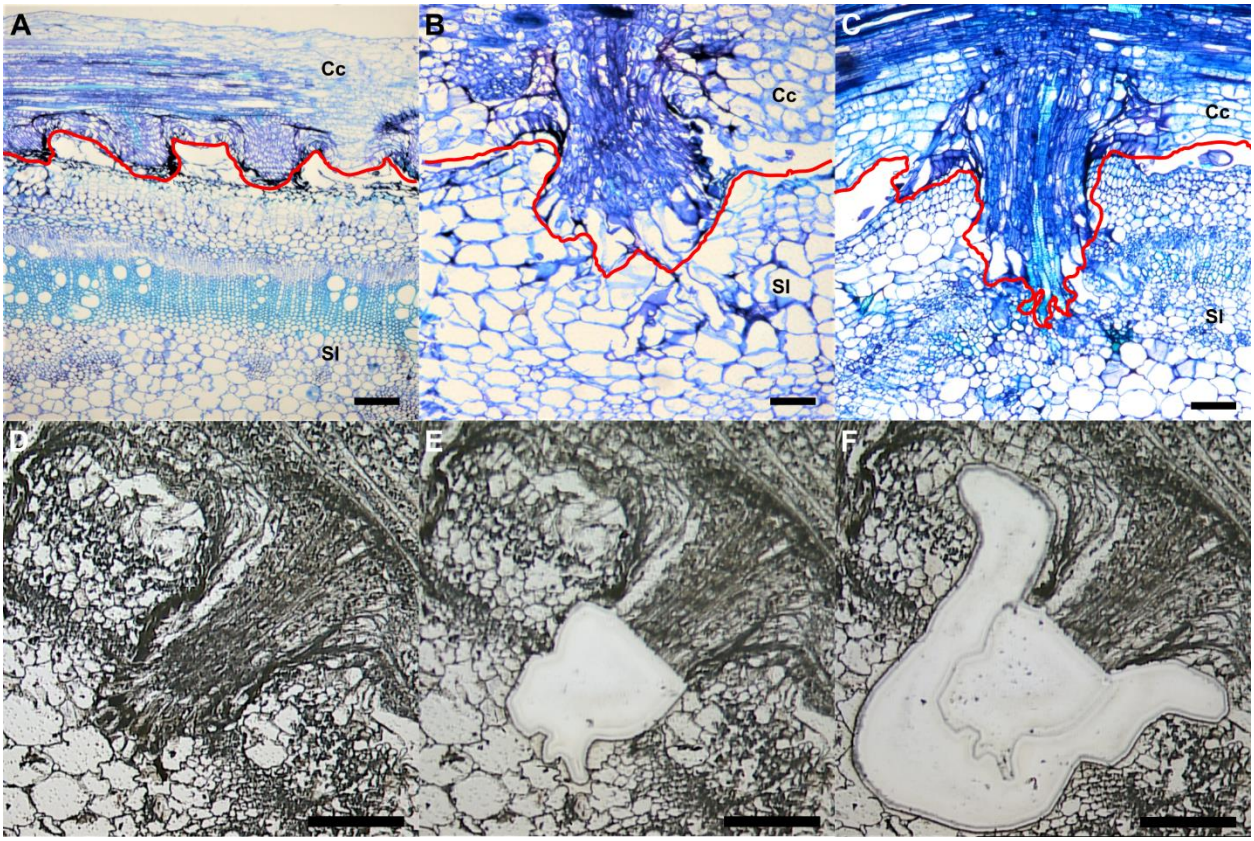

Figure 1. Laser-capture microdissection (LCM) of *C. campestris* haustoria penetrating tomato stems at three developmental stages. (A-C) Toluidine blue O stained paraffin sections of tomato stem with *C. campestris* early (A), intermediate (B), and mature stage (C) haustoria. Red line indicates the interface between *C. campestris* and host tomato. Cc indicates *C. campestris*; Sl indicates *S. lycopersicum*. (D-F) *C. campestris* haustorial tissues and host tissues were collected using LCM. A paraffin section of an intermediate stage haustorium before collection (D), after haustorial tissue collection (E), and after host tissue collection (F). (A) and (C), scale bars = 250 μm. (B), (D), (E), and (F), scale bars = 100 μm.

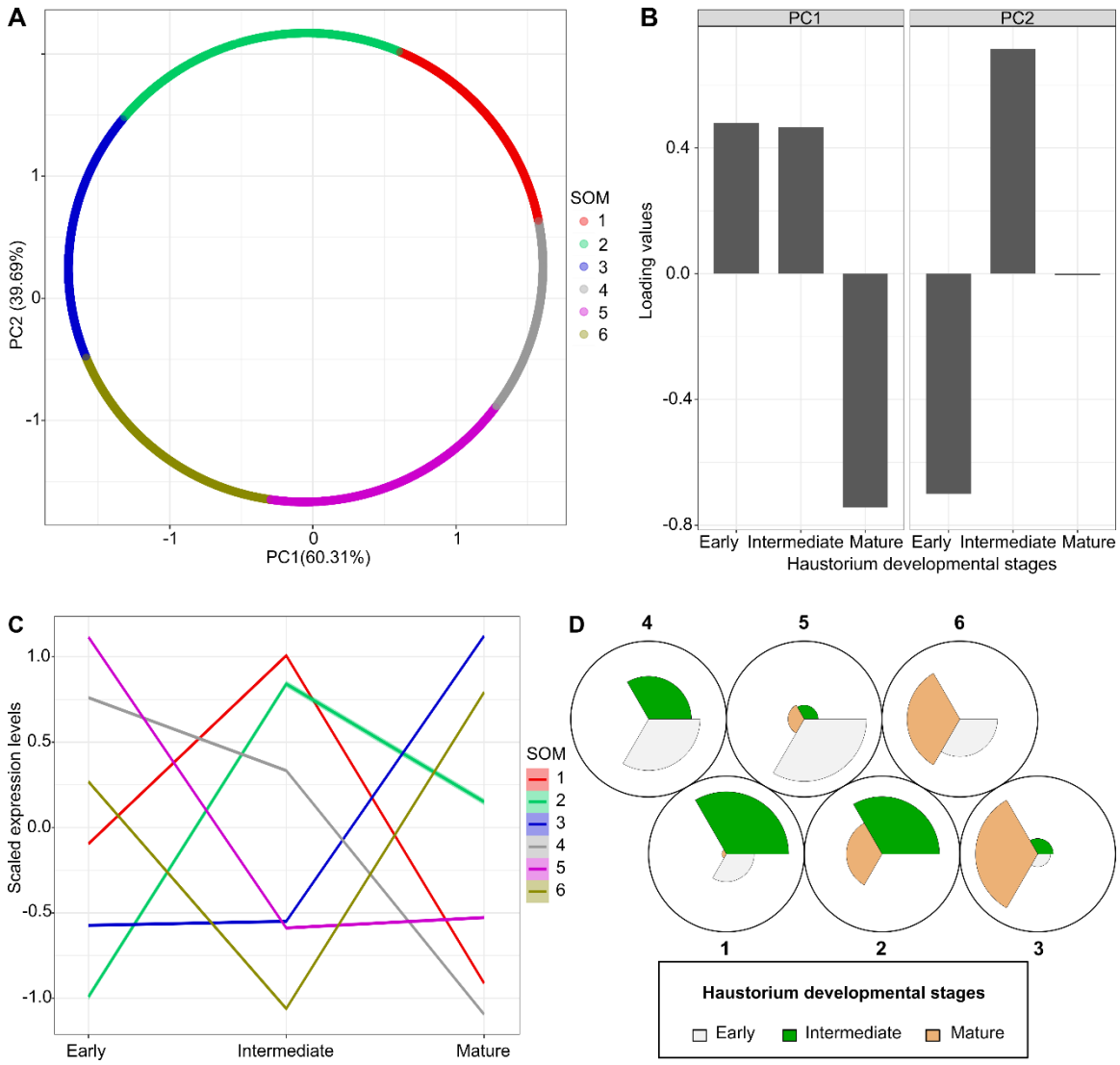

Figure 2. Principal component analysis (PCA) analysis results coupled with self-organizing maps (SOM) clustering in *C. campestris* haustoria across three developmental stages from LCM RNA-Seq data. (A) PCA plot of the first and second principal components (PC1 and PC2) and colored indicate their corresponding SOM groups. Each dot represents a gene. (B) Loading values of PC1 and PC2. PC1 separates the mature stage-specific genes from the early and intermediate stages-specific genes. PC2 separates the genes specifically expressed in the early stage from those specifically expressed in the intermediate stage. (C) A plot of each SOM group's scaled expression levels at three *C. campestris* haustorial developmental stages. The color of each

line represents the SOM group it belongs to. The 95 percent confidence interval is indicated by the shaded area around the lines. (D) A code plot of SOM clustering showing which developmental phases are dominant in each SOM group based on sector size. Each sector represents a developmental stage and is colored according to the stage it represents.

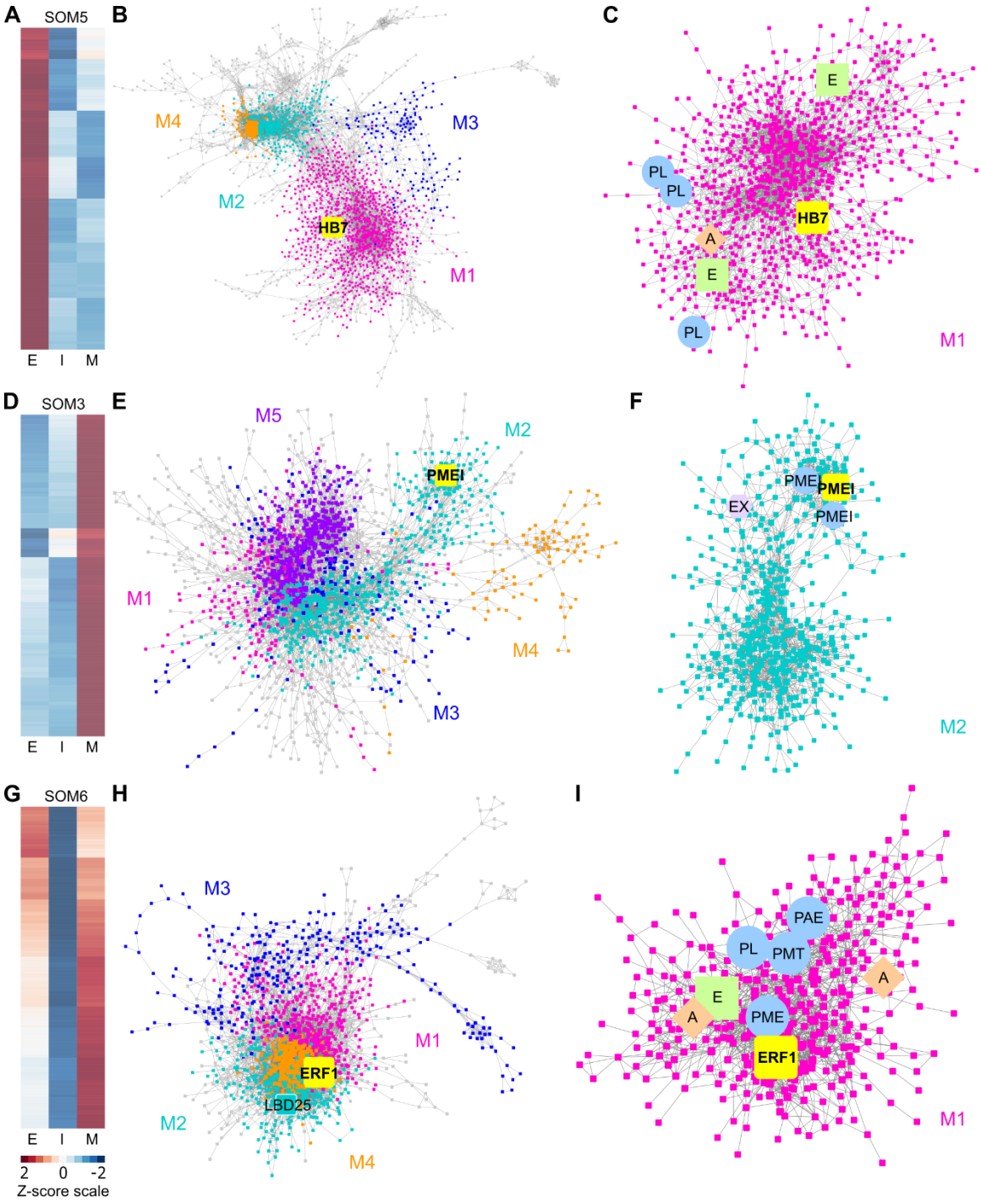

Figure 3. Heatmaps and gene-coexpression networks (GCNs) of *C. campestris* haustorial tissues across three developmental stages. (A) A heatmap of gene expression profiles in z-scores for SOM5, which includes genes that are highly expressed in the early stage. (B) A GCN of genes in SOM5. This SOM5 GCN is composed of four major modules. Magenta indicates genes in

Module 1, which has enriched biological process GO term including “response to abiotic and biotic stimulus, stress, hormone, far-red light.” The transcription factor HB7 is enlarged and labeled in yellow. (C) GCN of genes that are classified in SOM5 Module 1. PL, pectin lyase-like superfamily protein. A, auxin response factor 1. E, ethylene signaling-related genes. (D) A heatmap of gene expression profiles in z-scores for SOM3, which includes genes that are highly expressed in the mature stage. (E) A GCN of genes that are in SOM3. The SOM3 GCN is composed of five major modules. Cyan indicates genes in Module 2, which has enriched biological process GO term including “root radial pattern formation.” Selected pectin methyl-esterase inhibitor (PMEI) is enlarged and labeled in yellow. (F) GCN of genes that are classified in SOM3 Module 2. PMEI, pectin methyl-esterase inhibitor. EX, expansin. (G) A heatmap of gene expression profiles in z-scores for SOM6, which includes genes that are relatively highly expressed in the early and mature stage. (H) A GCN of genes in SOM6. This SOM6 GCN is composed of four major modules. Magenta indicates genes in Module 1, which has enriched biological process GO term including “response to stimulus, hormone, organic substance.” Ethylene responsive element binding factor 1 (ERF1) is enlarged and labeled in yellow. The transcription factor LBD25 is enlarged and labeled in cyan as other genes in Module 2. (I) GCN of genes that are classified in SOM6 Module 1. PL, pectin lyase-like superfamily protein. A, auxin transporter or auxin-responsive protein. E, ethylene signaling-related genes. PL, pectin lyase-like superfamily protein. PME, pectin methylesterase. PMT, pectin methyltransferase-like. PAE, pectin acetylesterase family protein. The complete gene lists for all SOM units with SOM distances and PCA principal component values are included in Supplemental Table SX.

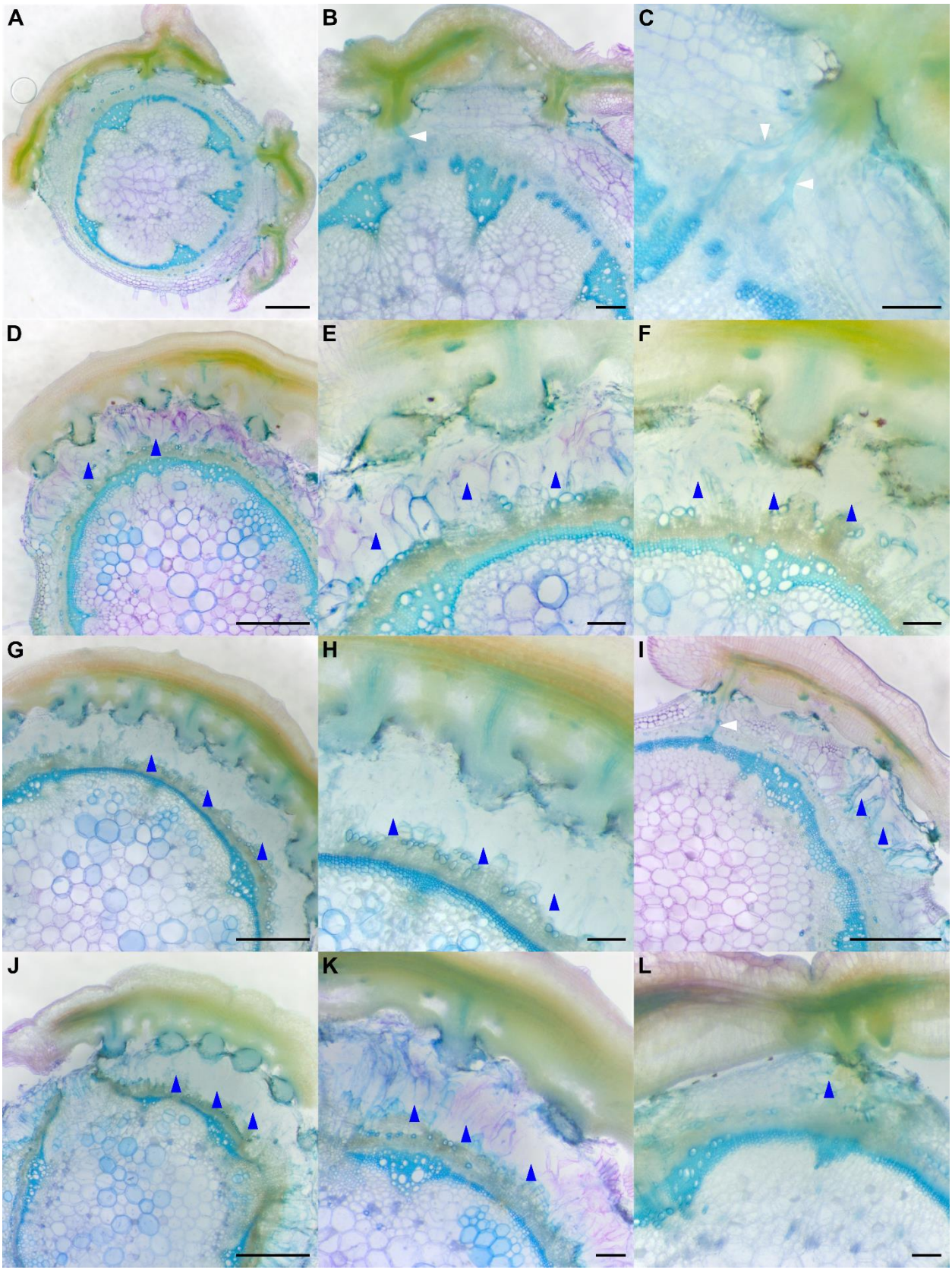
A
B
C
D
E
F
G
H
I
J
K
L

Figure 4. Haustorium phenotypes of *C. campestris* growing on Heinz tomato wild-types and HIGS RNAi transgenic plants. *C. campestris* haustoria that were growing on wild-type H1706 tomato hosts (A-C), on HB7 RNAi transgenic tomato plants (D-F), on PMEI RNAi transgenic tomato plants (G-I), on ERF1 RNAi transgenic tomato plants (J-L). (A, D, G, I, J) Scale bars = 1 mm. (B, C, E, F, H, K, L) Scale bars = 200 µm. (A-L) 100 µm thick vibratome sections of fresh haustorium stained with Toluidine Blue O. White arrowhead indicates normal haustorial vascular connections. Blue arrowhead indicates the phenotype of overly degraded host cortex cell walls.

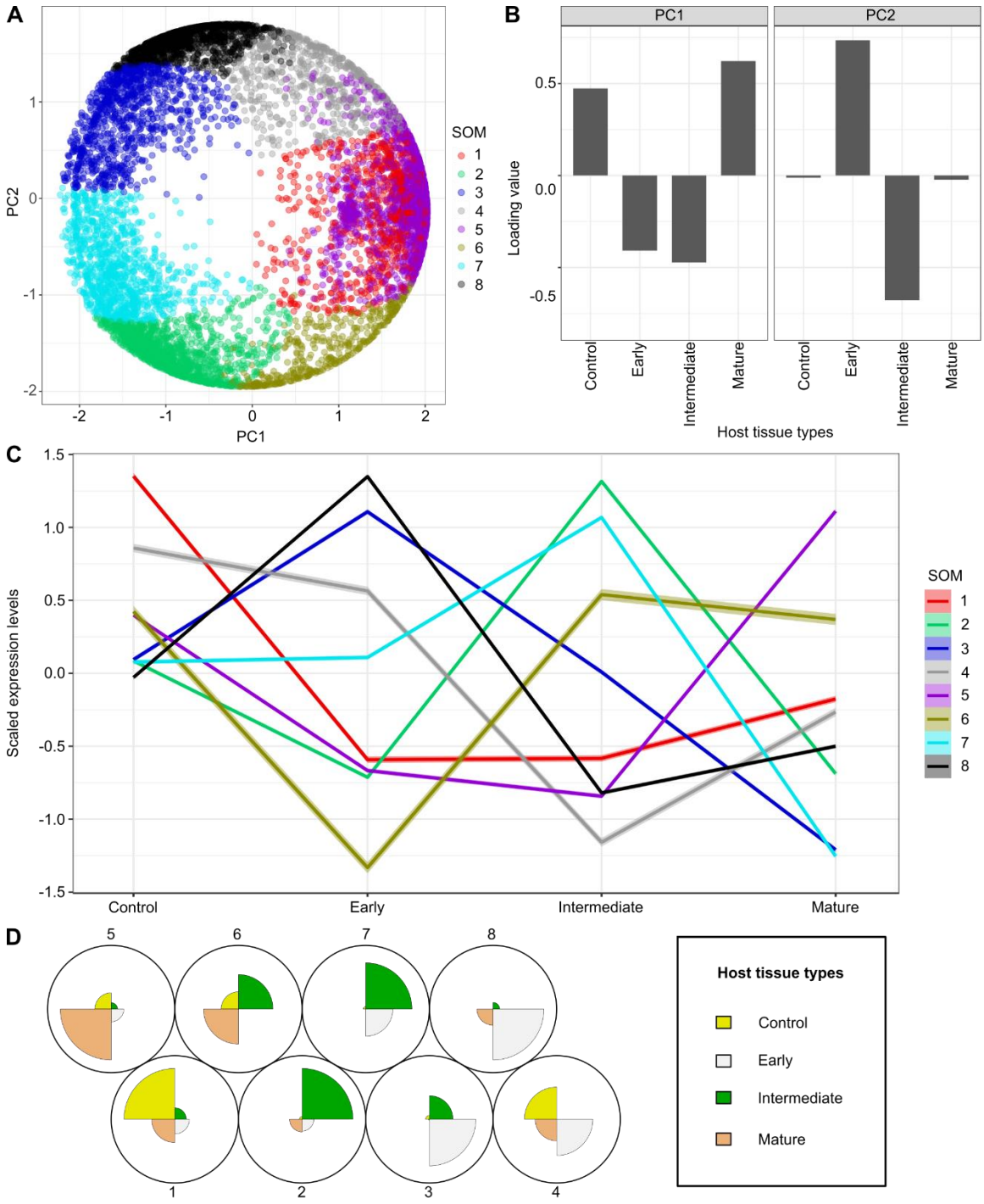

Figure 5. Principal component analysis (PCA) and self-organizing maps (SOM) clustering of LCM RNA-Seq data from the host tomato tissues surrounding *C. campestris* haustoria. (A) PCA plot of the first and second principal components (PC1 and PC2) and colored indicate their corresponding SOM groups. Each dot represents a gene. (B) Loading values of PC1 and PC2.

"Control" means the tomato stem cortex tissue samples that are not next to *C. campestris* haustoria, which serve as negative controls in this experiment. PC1 separates the genes specifically expressed in host tissues sounding the early and intermediate-stage haustoria from those specifically expressed in other stages. PC2 separates the genes specifically expressed in host tissues surrounding the intermediate-stage haustoria from those expressed explicitly at the mature stage. (C) A plot of each SOM group's scaled expression levels at four types of host tomato tissue surrounding *C. campestris* haustoria at different developmental stages. The color of each line represents the SOM group it belongs to. The shaded area around the lines indicates the 95 percent confidence interval. (D) A code plot of SOM clustering showing which group of genes are dominant in each SOM group based on sector size. Each sector represents the host tissues surrounding *C. campestris* haustoria at a developmental stage and is colored according to the types it represents.

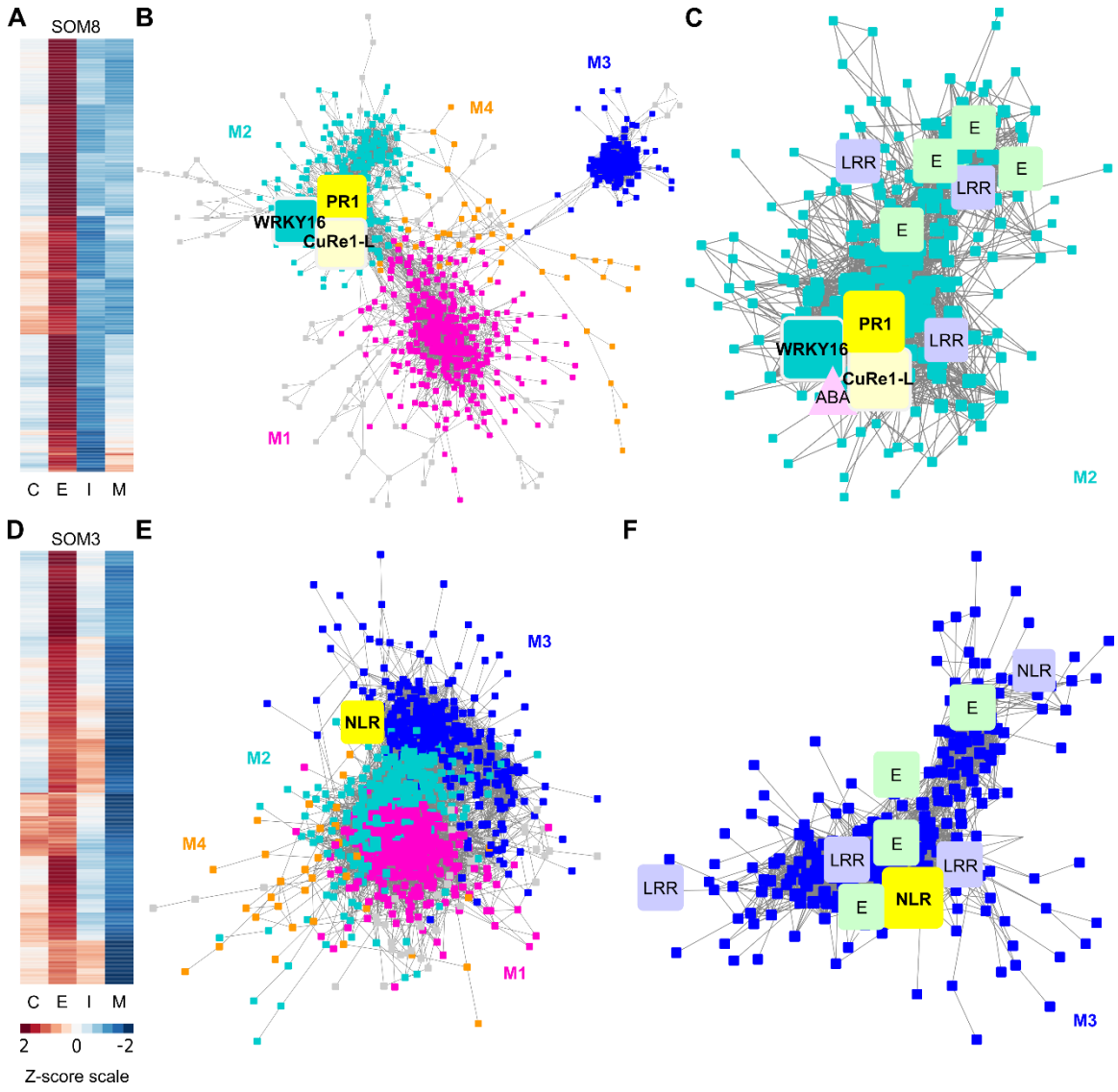

Figure 6. Heatmaps and gene-coexpression networks (GCNs) of LCM RNA-Seq data from the host tomato tissues surrounding *C. campestris* haustoria. (A) A heatmap of gene expression profiles in z-scores for SOM8, which includes genes specifically highly expressed in the early stage. (B) A GCN of genes in SOM8. This SOM8 GCN is composed of four major modules. Cyan indicates genes in Module 2. The transcription factor WRKY16 is enlarged and labeled in cyan as other genes in Module 2. PR1 is enlarged and labeled in yellow. CuRe1-like receptor (CuRe1-L) is enlarged and labeled in light yellow. (C) GCN of genes that are classified in SOM8 Module 2. CuRe1-L, CuRe1-like receptor. LRR, Leucine-rich repeat receptor-like protein kinase. ABA,

Abscisic acid stress ripening 5. E, ethylene-responsive transcription factor. (D) A heatmap of gene expression profiles in z-scores for SOM3, including genes that have high expression levels in the early stage and moderate expression levels in the intermediate stage. (E) A GCN of genes in SOM3. This SOM3 GCN is composed of four major modules. Blue indicates genes in Module 3. NBS is enlarged and labeled in yellow. (F) GCN of genes that are classified in SOM3 Module 3. LRR, Leucine-rich repeat receptor-like protein kinase. E, ethylene-responsive transcription factor. NLR, NBS-LRR protein. The complete gene lists for all SOM units with SOM distances and PCA principal component values are included in Supplemental Table SX.

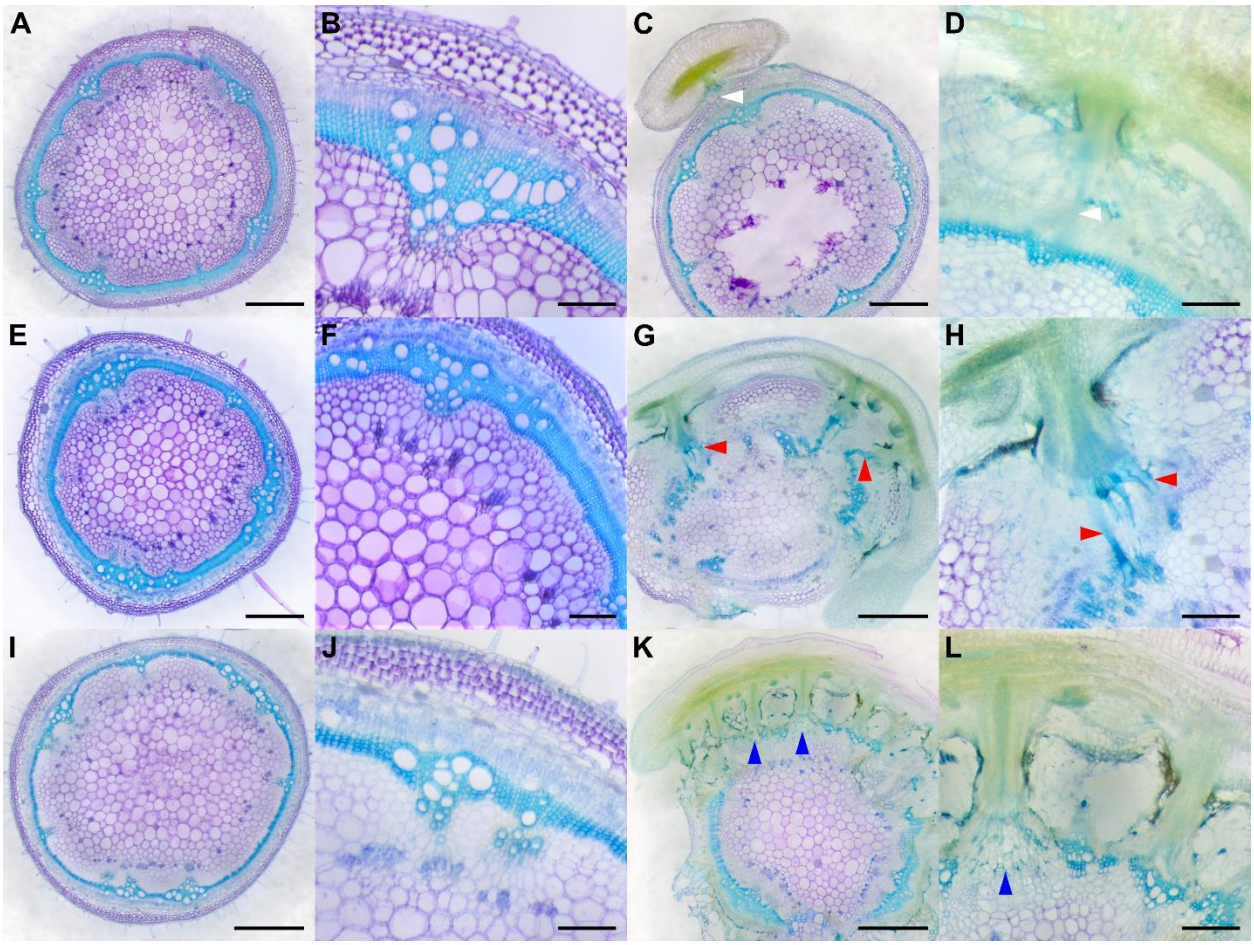

Figure 7. Haustorium phenotypes of *C. campestris* growing on M82 tomato wild-types and candidate genes-CRISPR transgenic plants. *C. campestris* haustoria that were growing on wild-type M82 tomato hosts (A-D), on PR1-CRISPR T1 transgenic tomato plants (E-H), on NBS-LRR-CRISPR T1 transgenic tomato plants (I-L). (A, C, E, G, I, K) Scale bars = 1 mm. (B, D, F, H, J, L) Scale bars = 200 µm. (A-L) 100 µm thick vibratome sections of fresh haustorium stained with Toluidine Blue O. White arrowhead indicates normal haustorial vascular connections. Red arrowhead indicates the hypertrophy symptom with enlarged xylem bridges. Blue arrowhead indicates the phenotype of disrupted host stem vascular tissue arrangement.

References

Adie, B., Chico, J.M., Rubio-Somoza, I., and Solano, R. (2007). Modulation of Plant Defenses by Ethylene. *Journal of Plant Growth Regulation* 26**,** 160-177.

Agrios, G.N. (2005). "chapter thirteen - PLANT DISEASES CAUSED BY PARASITIC HIGHER PLANTS, INVASIVE CLIMBING PLANTS, AND PARASITIC GREEN ALGAE," in *Plant Pathology (Fifth Edition)*. (San Diego: Academic Press), 705-722.

Alakonya, A., Kumar, R., Koenig, D., Kimura, S., Townsley, B., Runo, S., Garces, H.M., Kang, J., Yanez, A., David-Schwartz, R., Machuka, J., and Sinha, N. (2012). Interspecific RNA Interference of *SHOOT MERISTEMLESS-Like* Disrupts *Cuscuta pentagona* Plant Parasitism. *The Plant Cell* 24**,** 3153-3166.

Böhm, H., Albert, I., Fan, L., Reinhard, A., and Nürnberger, T. (2014). Immune receptor complexes at the plant cell surface. *Current Opinion in Plant Biology* 20**,** 47-54.

Benková, E., Michniewicz, M., Sauer, M., Teichmann, T., Seifertová, D., Jürgens, G., and Friml, J. (2003). Local, efflux-dependent auxin gradients as a common module for plant organ formation. *Cell* 115**,** 591-602.

Berens, M.L., Wolinska, K.W., Spaepen, S., Ziegler, J., Nobori, T., Nair, A., Krüler, V., Winkelmüller, T.M., Wang, Y., Mine, A., Becker, D., Garrido-Oter, R., Schulze-Lefert, P., and Tsuda, K. (2019). Balancing trade-offs between biotic and abiotic stress responses through leaf age-dependent variation in stress hormone cross-talk. *Proceedings of the National Academy of Sciences* 116**,** 2364-2373.

Bowman, C. (2019). *Plant Virology*. EDTECH.

Breen, S., Williams, S.J., Outram, M., Kobe, B., and Solomon, P.S. (2017). Emerging Insights into the Functions of Pathogenesis-Related Protein 1. *Trends Plant Sci* 22**,** 871-879.

Broekgaarden, C., Caarls, L., Vos, I.A., Pieterse, C.M.J., and Van Wees, S.C.M. (2015). Ethylene: Traffic Controller on Hormonal Crossroads to Defense. *Plant physiology* 169**,** 2371-2379.

Chebli, Y., and Geitmann, A. (2017). Cellular growth in plants requires regulation of cell wall biochemistry. *Curr Opin Cell Biol* 44**,** 28-35.

Cheng, X., Floková, K., Bouwmeester, H., and Ruyter-Spira, C. (2017). The Role of Endogenous Strigolactones and Their Interaction with ABA during the Infection Process of the Parasitic Weed Phelipanche ramosa in Tomato Plants. *Frontiers in Plant Science* 8.

Clauset, A., Newman, M.E.J., and Moore, C. (2004). Finding community structure in very large networks. *Physical Review E* 70**,** 066111.

Cline, M.S., Smoot, M., Cerami, E., Kuchinsky, A., Landys, N., Workman, C., Christmas, R., Avila-Campilo, I., Creech, M., Gross, B., Hanspers, K., Isserlin, R., Kelley, R., Killcoyne, S., Lotia, S., Maere, S., Morris, J., Ono, K., Pavlovic, V., Pico, A.R., Vailaya, A., Wang, P.-L., Adler, A., Conklin, B.R., Hood, L., Kuiper, M., Sander, C., Schmulevich, I., Schwikowski, B., Warner, G.J., Ideker, T., and Bader, G.D. (2007). Integration of biological networks and gene expression data using Cytoscape. *Nat. Protocols* 2**,** 2366-2382.

Costea, M., García, M.A., Baute, K., and Stefanović, S. (2015). Entangled evolutionary history of Cuscuta pentagona clade: A story involving hybridization and Darwin in the Galapagos. *TAXON* 64**,** 1225-1242.

Cui, S., Kubota, T., Nishiyama, T., Ishida, J.K., Shigenobu, S., Shibata, T.F., Toyoda, A., Hasebe, M., Shirasu, K., and Yoshida, S. (2020). Ethylene signaling mediates host invasion by parasitic plants. *Science Advances* 6**,** eabc2385.

Dos Santos, C.V., Letousey, P., Delavault, P., and Thalouarn, P. (2003). Defense Gene Expression Analysis of Arabidopsis thaliana Parasitized by Orobanche ramosa. *Phytopathology*® 93**,** 451-457.

Fürst, U., Hegenauer, V., Kaiser, B., Körner, M., Welz, M., and Albert, M. (2016). Parasitic Cuscuta factor(s) and the detection by tomato initiates plant defense. *Communicative & Integrative Biology* 9**,** e1244590.

Furuhashi, T., Furuhashi, K., and Weckwerth, W. (2011). The parasitic mechanism of the holostemparasitic plant Cuscuta. *Journal of Plant Interactions* 6**,** 207-219.

García, M.A., Costea, M., Kuzmina, M., and Stefanović, S. (2014). Phylogeny, character evolution, and biogeography of Cuscuta (dodders; Convolvulaceae) inferred from coding plastid and nuclear sequences. *American Journal of Botany* 101**,** 670-690.

Hegenauer, V., Fürst, U., Kaiser, B., Smoker, M., Zipfel, C., Felix, G., Stahl, M., and Albert, M. (2016). Detection of the plant parasite *Cuscuta reflexa* by a tomato cell surface receptor. *Science* 353**,** 478-481.

Hegenauer, V., Slaby, P., Körner, M., Bruckmüller, J.-A., Burggraf, R., Albert, I., Kaiser, B., Löffelhardt, B., Droste-Borel, I., Sklenar, J., Menke, F.L.H., Maček, B., Ranjan, A., Sinha, N., Nürnberger, T., Felix, G., Krause, K., Stahl, M., and Albert, M. (2020). The tomato receptor CuRe1 senses a cell wall protein to identify Cuscuta as a pathogen. *Nature Communications* 11**,** 5299.

Heide-Jørgensen, H. (2008). *Parasitic flowering plants.* Brill.

Hozumi, A., Bera, S., Fujiwara, D., Obayashi, T., Yokoyama, R., Nishitani, K., and Aoki, K. (2017). Arabinogalactan Proteins Accumulate in the Cell Walls of Searching Hyphae of

the Stem Parasitic Plants, Cuscuta campestris and Cuscuta japonica. *Plant and Cell Physiology* 58**,** 1868-1877.

Ichihashi, Y., Aguilar-Martínez, J.A., Farhi, M., Chitwood, D.H., Kumar, R., Millon, L.V., Peng, J., Maloof, J.N., and Sinha, N.R. (2014). Evolutionary developmental transcriptomics reveals a gene network module regulating interspecific diversity in plant leaf shape. *Proceedings of the National Academy of Sciences* 111**,** E2616-E2621.

Ishida, J.K., Wakatake, T., Yoshida, S., Takebayashi, Y., Kasahara, H., Wafula, E., Depamphilis, C.W., Namba, S., and Shirasu, K. (2016). Local Auxin Biosynthesis Mediated by a YUCCA Flavin Monooxygenase Regulates Haustorium Development in the Parasitic Plant Phtheirospermum japonicum. *Plant Cell* 28**,** 1795-1814.

Jhu, M.-Y., Farhi, M., Wang, L., Philbrook, R.N., Belcher, M.S., Nakayama, H., Zumstein, K.S., Rowland, S.D., Ron, M., Shih, P.M., and Sinha, N.R. (2020). Lignin-based resistance to *Cuscuta campestris* parasitism in Heinz resistant tomato cultivars. *bioRxiv***,** 706861.

Jhu, M.-Y., Ichihashi, Y., Farhi, M., Wong, C., and Sinha, N.R. (2021). LATERAL ORGAN BOUNDARIES DOMAIN 25 functions as a key regulator of haustorium development in dodders. *Plant Physiology*.

Johnsen, H.R., Striberny, B., Olsen, S., Vidal-Melgosa, S., Fangel, J.U., Willats, W.G.T., Rose, J.K.C., and Krause, K. (2015). Cell wall composition profiling of parasitic giant dodder (Cuscuta reflexa) and its hosts: a priori differences and induced changes. *New Phytologist* 207**,** 805-816.

Johnson, N.R., Depamphilis, C.W., and Axtell, M.J. (2019). Compensatory sequence variation between trans-species small RNAs and their target sites. *eLife* 8**,** e49750.

Kim, G., Leblanc, M.L., Wafula, E.K., Depamphilis, C.W., and Westwood, J.H. (2014). Genomic-scale exchange of mRNA between a parasitic plant and its hosts. *Science* 345**,** 808-811.

Kimura, S., and Sinha, N. (2008). Tomato (Solanum lycopersicum): A Model Fruit-Bearing Crop. *Cold Spring Harbor Protocols* 2008**,** pdb.emo105.

Kokla, A., Leso, M., Zhang, X., Simura, J., Cui, S., Ljung, K., Yoshida, S., and Melnyk, C.W. (2021). Nitrates increase abscisic acid levels to regulate haustoria formation in the parasitic plant Phtheirospermum japonicum. *bioRxiv***,** 2021.2006.2015.448499.

Kong, G., Wan, L., Deng, Y.Z., Yang, W., Li, W., Jiang, L., Situ, J., Xi, P., Li, M., and Jiang, Z. (2019). Pectin acetylesterase PAE5 is associated with the virulence of plant pathogenic oomycete Peronophythora litchii. *Physiological and Molecular Plant Pathology* 106**,** 16-22.

Ku, Y.-S., Sintaha, M., Cheung, M.-Y., and Lam, H.-M. (2018). Plant Hormone Signaling Crosstalks between Biotic and Abiotic Stress Responses. *International journal of molecular sciences* 19**,** 3206.

Kumar, R., Ichihashi, Y., Kimura, S., Chitwood, D., Headland, L., Peng, J., Maloof, J., and Sinha, N. (2012). A High-Throughput Method for Illumina RNA-Seq Library Preparation. *Frontiers in Plant Science* 3.

Labuhn, M., Adams, F.F., Ng, M., Knoess, S., Schambach, A., Charpentier, E.M., Schwarzer, A., Mateo, J.L., Klusmann, J.-H., and Heckl, D. (2017). Refined sgRNA efficacy prediction improves large- and small-scale CRISPR–Cas9 applications. *Nucleic Acids Research* 46**,** 1375-1385.

Langmead, B., and Salzberg, S.L. (2012). Fast gapped-read alignment with Bowtie 2. *Nature Methods* 9**,** 357-359.

Lanini, W., And Kogan, M. (2005). Biology and Management of *Cuscuta* in Crops. *CIENCIA E INVESTIGACION AGRARIA* 32**,** 127-141.

Li, J., and Timko, M.P. (2009). Gene-for-Gene Resistance in *Striga*-Cowpea Associations. *Science* 325**,** 1094-1094.

Liu, Z., Wu, Y., Yang, F., Zhang, Y., Chen, S., Xie, Q., Tian, X., and Zhou, J.-M. (2013). BIK1 interacts with PEPRs to mediate ethylene-induced immunity. *Proceedings of the National Academy of Sciences* 110**,** 6205-6210.

Mchale, L., Tan, X., Koehl, P., and Michelmore, R.W. (2006). Plant NBS-LRR proteins: adaptable guards. *Genome Biology* 7**,** 212.

Mignolli, F., Todaro, J.S., and Vidoz, M.L. (2020). Internal aeration and respiration of submerged tomato hypocotyls are enhanced by ethylene-mediated aerenchyma formation and hypertrophy. *Physiologia Plantarum* 169**,** 49-63.

Moreno-Mateos, M.A., Vejnar, C.E., Beaudoin, J.-D., Fernandez, J.P., Mis, E.K., Khokha, M.K., and Giraldez, A.J. (2015). CRISPRscan: designing highly efficient sgRNAs for CRISPR-Cas9 targeting in vivo. *Nature Methods* 12**,** 982-988.

O'brien, T.P., Feder, N., and Mccully, M.E. (1964). Polychromatic staining of plant cell walls by toluidine blue O. *Protoplasma* 59**,** 368-373.

Padmanabhan, M., Cournoyer, P., and Dinesh-Kumar, S.P. (2009). The leucine-rich repeat domain in plant innate immunity: a wealth of possibilities. *Cellular microbiology* 11**,** 191-198.

Pan, C., Ye, L., Qin, L., Liu, X., He, Y., Wang, J., Chen, L., and Lu, G. (2016). CRISPR/Cas9-mediated efficient and heritable targeted mutagenesis in tomato plants in the first and later generations. 6**,** 24765.

Pehlivan, N. (2019). Stochasticity in transcriptional expression of a negative regulator of Arabidopsis ABA network. *3 Biotech* 9**,** 15.

Ranjan, A., Ichihashi, Y., Farhi, M., Zumstein, K., Townsley, B., David-Schwartz, R., and Sinha, N.R. (2014). De Novo Assembly and Characterization of the Transcriptome of the Parasitic Weed Dodder Identifies Genes Associated with Plant Parasitism. *PLANT PHYSIOLOGY* 166**,** 1186-1199.

Robinson, M.D., Mccarthy, D.J., and Smyth, G.K. (2009). edgeR: a Bioconductor package for differential expression analysis of digital gene expression data. *Bioinformatics* 26**,** 139-140.

Runyon, J.B., Mescher, M.C., Felton, G.W., and De Moraes, C.M. (2010). Parasitism by Cuscuta pentagona sequentially induces JA and SA defence pathways in tomato. *Plant, Cell & Environment* 33**,** 290-303.

Saffer, A.M. (2018). Expanding roles for pectins in plant development. *J Integr Plant Biol* 60**,** 910-923.

Sato, S., Tabata, S., Hirakawa, H., Asamizu, E., Shirasawa, K., Isobe, S., Kaneko, T., Nakamura, Y., Shibata, D., Aoki, K., Egholm, M., Knight, J., Bogden, R., Li, C., Shuang, Y., Xu, X., Pan, S., Cheng, S., Liu, X., Ren, Y., Wang, J., Albiero, A., Dal Pero, F., Todesco, S., Van Eck, J., Buels, R.M., Bombarely, A., Gosselin, J.R., Huang, M., Leto, J.A., Menda, N., Strickler, S., Mao, L., Gao, S., Tecle, I.Y., York, T., Zheng, Y., Vrebalov, J.T., Lee, J., Zhong, S., Mueller, L.A., Stiekema, W.J., Ribeca, P., Alioto, T., Yang, W., Huang, S., Du, Y., Zhang, Z., Gao, J., Guo, Y., Wang, X., Li, Y., He, J., Li, C., Cheng, Z., Zuo, J., Ren, J., Zhao, J., Yan, L., Jiang, H., Wang, B., Li, H., Li, Z., Fu, F., Chen, B., Han, B., Feng, Q., Fan, D., Wang, Y., Ling, H., Xue, Y., Ware, D., Richard Mccombie, W., Lippman, Z.B., Chia, J.-M., Jiang, K., Pasternak, S., Gelley, L., Kramer, M., Anderson, L.K., Chang, S.-

B., Royer, S.M., Shearer, L.A., Stack, S.M., Rose, J.K.C., Xu, Y., Eannetta, N., Matas, A.J., Mcquinn, R., Tanksley, S.D., Camara, F., Guigó, R., Rombauts, S., Fawcett, J., Van De Peer, Y., Zamir, D., Liang, C., Spannagl, M., Gundlach, H., Bruggmann, R., et al. (2012). The tomato genome sequence provides insights into fleshy fruit evolution. *Nature* 485**,** 635-641.

Spallek, T., Melnyk, C.W., Wakatake, T., Zhang, J., Sakamoto, Y., Kiba, T., Yoshida, S., Matsunaga, S., Sakakibara, H., and Shirasu, K. (2017). Interspecies hormonal control of host root morphology by parasitic plants. *Proceedings of the National Academy of Sciences* 114**,** 5283-5288.

Stefanović, S., Kuzmina, M., and Costea, M. (2007). Delimitation of major lineages within Cuscuta subgenus Grammica (Convolvulaceae) using plastid and nuclear DNA sequences. *American Journal of Botany* 94**,** 568-589.

Stemmer, M., Thumberger, T., Del Sol Keyer, M., Wittbrodt, J., and Mateo, J.L. (2015). CCTop: An Intuitive, Flexible and Reliable CRISPR/Cas9 Target Prediction Tool. *PLOS ONE* 10**,** e0124633.

Tada, Y., Sugai, M., and Furuhashi, K. (1996). Haustoria of Cuscuta japonica, a Holoparasitic Flowering Plant, Are Induced by the Cooperative Effects of Far-Red Light and Tactile Stimuli. *Plant and Cell Physiology* 37**,** 1049-1053.

Taylor, A., Martin, J., and Seel, W.E. (1996). Physiology of the parasitic association between maize and witchweed (Striga hermonthica): is ABA involved? *Journal of Experimental Botany* 47**,** 1057-1065.

Tintor, N., Ross, A., Kanehara, K., Yamada, K., Fan, L., Kemmerling, B., Nürnberger, T., Tsuda, K., and Saijo, Y. (2013). Layered pattern receptor signaling via ethylene and endogenous

elicitor peptides during *Arabidopsis* immunity to bacterial infection. *Proceedings of the National Academy of Sciences* 110**,** 6211-6216.

Tomilov, A.A., Tomilova, N.B., Abdallah, I., and Yoder, J.I. (2005). Localized hormone fluxes and early haustorium development in the hemiparasitic plant Triphysaria versicolor. *Plant physiology* 138**,** 1469-1480.

Valdés, A.E., övernäs, E., Johansson, H., Rada-Iglesias, A., and Engström, P. (2012). The homeodomain-leucine zipper (HD-Zip) class I transcription factors ATHB7 and ATHB12 modulate abscisic acid signalling by regulating protein phosphatase 2C and abscisic acid receptor gene activities. *Plant Molecular Biology* 80**,** 405-418.

Van Ghelder, C., Parent, G.J., Rigault, P., Prunier, J., Giguère, I., Caron, S., Stival Sena, J., Deslauriers, A., Bousquet, J., Esmenjaud, D., and Mackay, J. (2019). The large repertoire of conifer NLR resistance genes includes drought responsive and highly diversified RNLs. *Scientific Reports* 9**,** 11614.

Vaughn, K.C. (2002). Attachment of the parasitic weed dodder to the host. *Protoplasma* 219**,** 227-237.

Veselov, D., Langhans, M., Hartung, W., Aloni, R., Feussner, I., Götz, C., Veselova, S., Schlomski, S., Dickler, C., Bächmann, K., and Ullrich, C.I. (2003). Development of Agrobacterium tumefaciens C58-induced plant tumors and impact on host shoots are controlled by a cascade of jasmonic acid, auxin, cytokinin, ethylene and abscisic acid. *Planta* 216**,** 512-522.

Vieira Dos Santos, C., Delavault, P., Letousey, P., and Thalouarn, P. (2003). Identification by suppression subtractive hybridization and expression analysis of Arabidopsis thaliana

putative defence genes during Orobanche ramosa infection. *Physiological and Molecular Plant Pathology* 62**,** 297-303.

Vogel, A., Schwacke, R., Denton, A.K., Usadel, B., Hollmann, J., Fischer, K., Bolger, A., Schmidt, M.H.W., Bolger, M.E., Gundlach, H., Mayer, K.F.X., Weiss-Schneeweiss, H., Temsch, E.M., and Krause, K. (2018). Footprints of parasitism in the genome of the parasitic flowering plant Cuscuta campestris. *Nature Communications* 9**,** 2515.

Wehrens, R., and Buydens, L. (2007). Self- and Super-organizing Maps in R: The kohonen Package. *Journal of Statistical Software* 21**,** 1-19.

Wormit, A., and Usadel, B. (2018). The Multifaceted Role of Pectin Methylesterase Inhibitors (PMEIs). *International Journal of Molecular Sciences* 19**,** 2878.

Yaakov, G., Lanini, W.T., and Wrobel, R.L. (2001). Tolerance of Tomato Varieties to Lespedeza Dodder. *Weed Science* 49**,** 520-523.

Yoder, J.I., and Scholes, J.D. (2010). Host plant resistance to parasitic weeds; recent progress and bottlenecks. *Current Opinion in Plant Biology* 13**,** 478-484.

Yoshida, S., Cui, S., Ichihashi, Y., and Shirasu, K. (2016). The Haustorium, a Specialized Invasive Organ in Parasitic Plants. *Annual Review of Plant Biology* 67**,** 643-667.

Supplemental Data

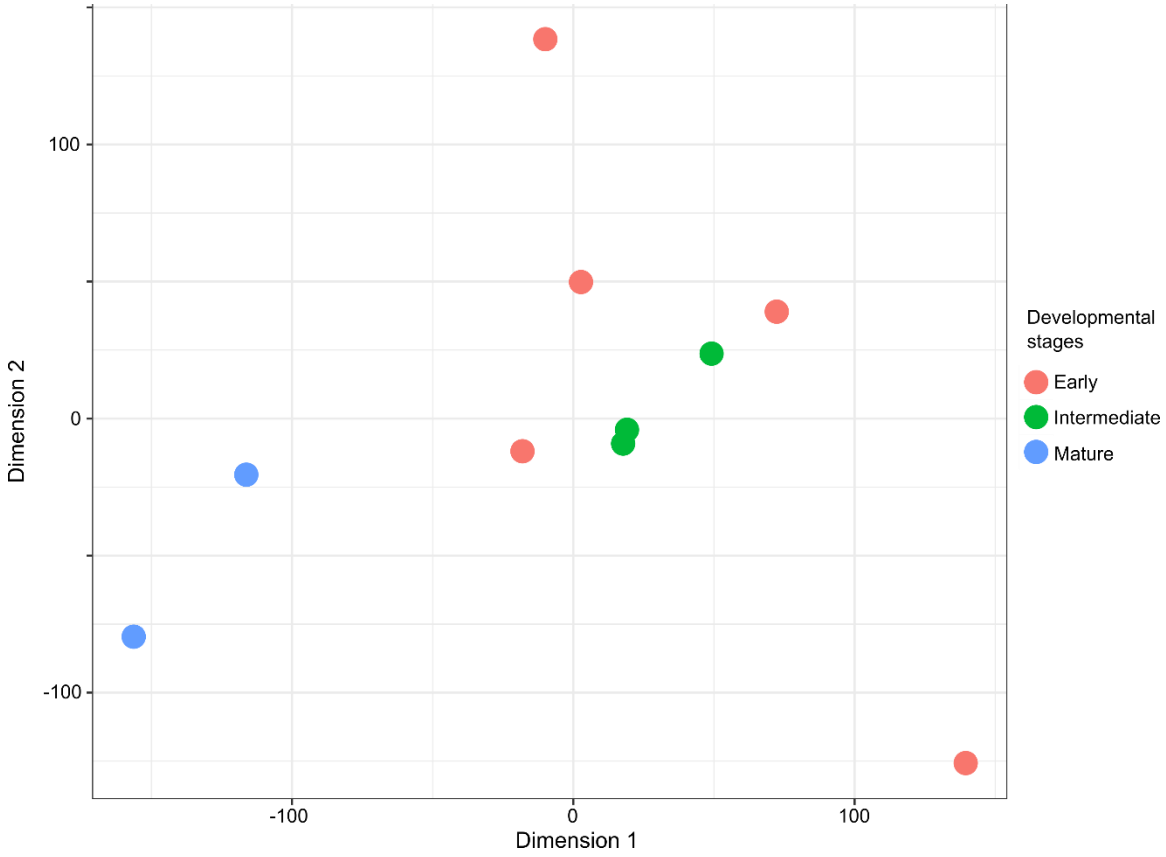

Supplemental Figure S1. Multidimensional scaling (MDS) plot of RNA expression profile in all libraries from LCM of three different *C. campestris* developmental stages mapped to *C. campestris* genome. The early stage has five libraries. The intermediate stage has three libraries. The mature stage has two libraries.

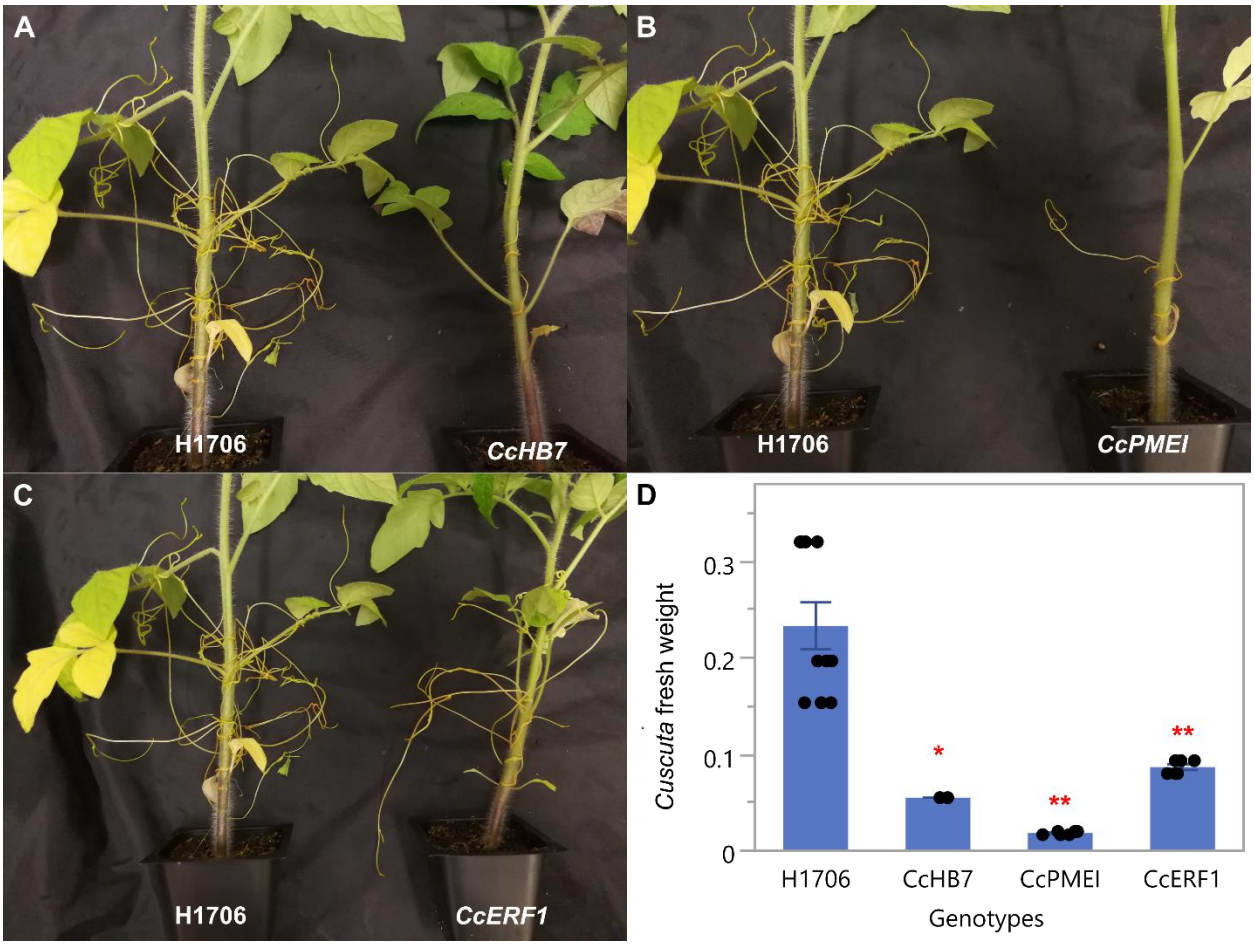

Supplemental Figure S2. Phenotypes of *C. campestris* growing on Host-Induced Gene Silencing (HIGS) RNAi transgenic plants. (A) *C. campestris* growing on wild-type H1706 tomatoes and T1 *CcHB7* RNAi transgenic plants. (B) *C. campestris* growing on wild-type H1706 tomatoes and T1 *CcPMEI* RNAi transgenic plants. (C) *C. campestris* growing on wild-type H1706 tomatoes and T1 *CcERF1* RNAi transgenic plants. (D) Biomass of *C. campestris* growing on wild-type H1706 tomatoes and T1 *CcHB7*, *CcPMEI*, and *CcERF1*RNAi transgenic plants. Fresh net weights of *C. campestris* were measured in grams (g). Data presented are assessed using Dunnett's test with wild-type H1706 as control. "*" p-value < 0.0005. "**" p-value < 0.0001.

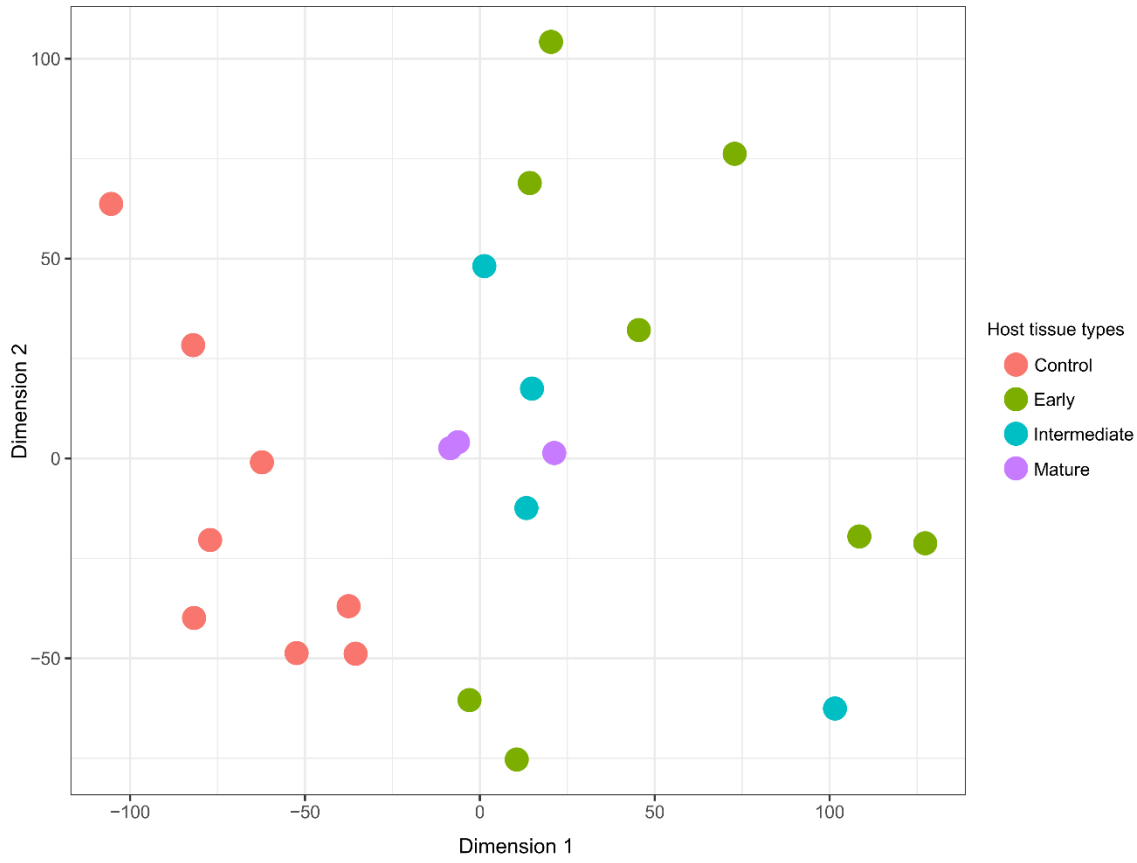

Supplemental Figure S3. Multidimensional scaling (MDS) plot of LCM RNA-Seq data from the host tomato tissues surrounding *C. campestris* haustoria. "Control" means the tomato stem cortex tissue samples that are not next to *C. campestris* haustoria, which serve as negative controls in this experiment. The control has eight libraries. The early stage has eight libraries. The intermediate stage has four libraries. The mature stage has three libraries.

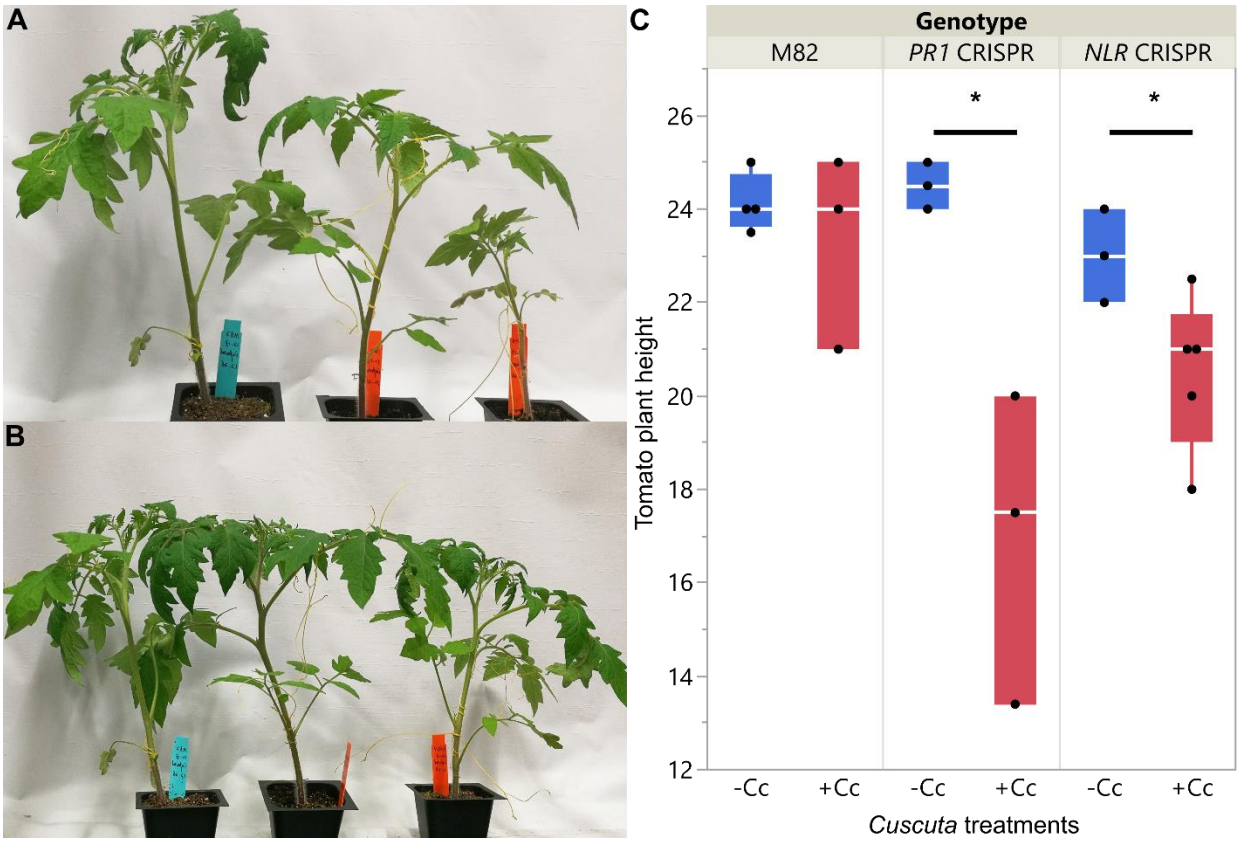

Supplemental Figure S4. Phenotypes of wild-types and CRISPR transgenic plants with *C. campestris* infestation. (A) Wild-type M82 tomatoes and T1 *SlPR1* CRISPR transgenic plants with *C. campestris* infestation. (B) Wild-type M82 tomatoes and T1 *SlNLR* CRISPR transgenic plants with *C. campestris* infestation. (C) Plant height of wild-type H1706 tomatoes and CRISPR transgenic plants with *C. campestris* infestation. The plant height of host tomato plants was measured in centimeters (cm). Data presented are assessed using one-tailed t-test with wild-type M82 as control. "*****" p-value < 0.05.

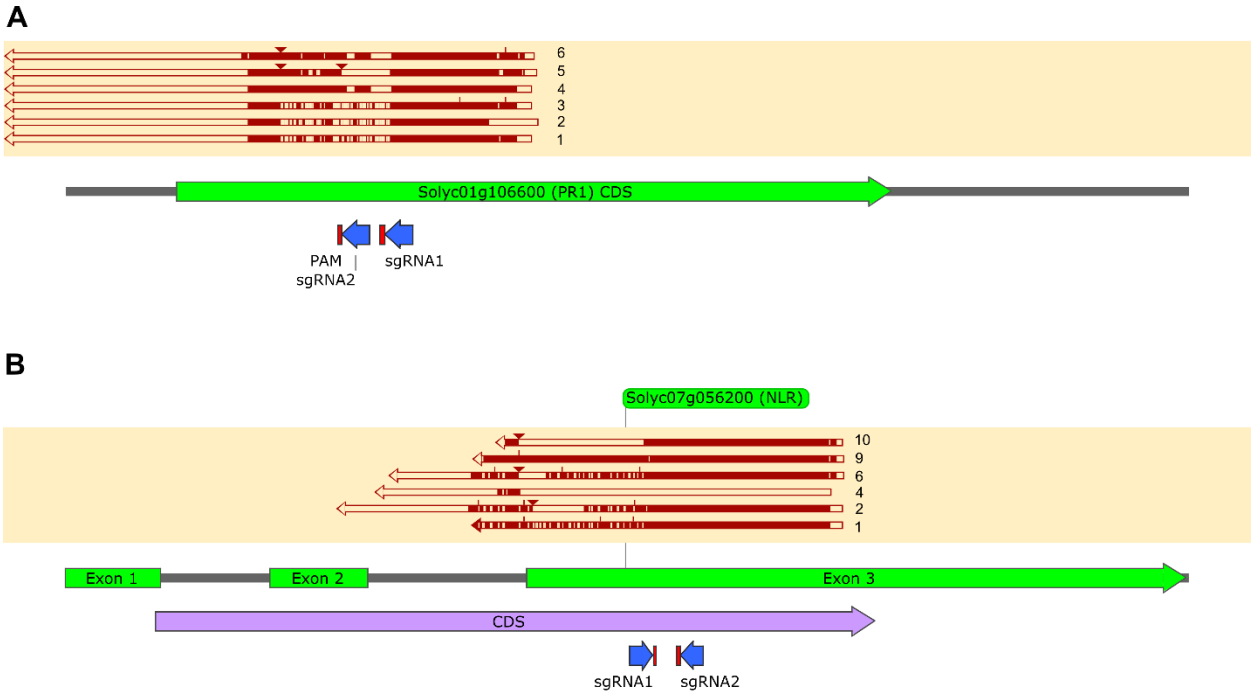

Supplemental Figure S5. Genotyping results of the T1 CRISPR transgenic plants that are used in this study. (A) Genomic DNA PCR product sequencing result of PR1 T1 CRISPR plants. T1 plant #1-3 have similar mixed peaks were present next to the sgRNA1, indicating a biallelic mutation. T1 plant #4 and #6 both have a 14 base pair (bp) deletion and a 6 bp deletion next to the two gRNAs. T1 plant #6 also has a 20 bp insertion. T1 plant #5 has a 33 bp deletion, a 14 bp insertion and a 20 bp insertion. (B) Genomic DNA PCR product sequencing result of NLR T1 CRISPR plants. T1 plant #1, 2, 6 have similar mixed peaks were present next to the sgRNA1, indicating a biallelic mutation. T1 plant #2 also has a 44 bp deletion and a 42 bp insertion. T1 plant #6 also has a 23 bp deletion and a 26 bp insertion. T1 plant #4 has a large section of deletion (>150 bp) next to the two gRNAs. T1 plant #9 has 1 bp deletion next to the sgRNA1. T1 plant #10 has a 107 bp deletion and a 292 bp insertion. (A-B) The dark red line indicates the sequencing result. The section filled with dark red color indicates regions of perfect sequence match; the empty boxes indicate regions of sequence mismatch. The gRNAs are labeled as blue arrows. The gRNA

sequences that were used in these CRISPR constructs are listed in Supplemental Table S11. The protospacer adjacent motif (PAM) sites are labeled as small red boxes that are right next to gRNAs.

All Supplemental Tables are available in the Supplemental Data Excel files.

Supplemental Table S1. The SOM clustering gene list in *C. campestris* haustorial tissue LCM RNA-Seq data and results of PCA analysis and multilevel SOM clustering using selected genes in the upper 50% quartile of coefficient of variation.

Supplemental Table S2. The gene list of SOM5 GCN modules from *C. campestris* haustorial tissue LCM RNA-Seq data.

Supplemental Table S3. The gene list of SOM3 GCN modules from *C. campestris* haustorial tissue LCM RNA-Seq data.

Supplemental Table S4. The gene list of SOM6 GCN modules from *C. campestris* haustorial tissue LCM RNA-Seq data.

Supplemental Table S5. The GO enrichment results and statistics of SOM3, 5, 6 GCN target modules from *C. campestris* haustorial tissue LCM RNA-Seq data.

Supplemental Table S6. The SOM clustering gene list in tomato host tissue LCM RNA-Seq data and results of PCA analysis and multilevel SOM clustering using selected genes in the upper 60% quartile of coefficient of variation.

Supplemental Table S7. The gene list of SOM8 GCN modules from tomato host tissue LCM RNA-Seq data.

Supplemental Table S8. The gene list of SOM3 GCN modules from tomato host tissue LCM RNA-Seq data.

Supplemental Table S9. The GO enrichment results and statistics of SOM3, 8 GCN target modules from tomato host tissue LCM RNA-Seq data.

Supplemental Table S10. The sequences that are used in HIGS RNAi constructs for *C. campestris* candidate genes.

Supplemental Table S11. The gRNA sequences that are used in CRISPR constructs for tomato candidate genes.

Chapter 5: Conclusions

Parasitic plants have a unique heterotrophic lifestyle, which makes them a perfect system to study plant-plant interactions. However, the tight physiological connections between hosts and parasitic plants also makes them difficult to eradicate using traditional herbicides and control methods, including management of soil fertility, hand weeding, and sanitation, leading to serious agricultural issues. Developing potential biocontrol approaches to contain the damage that parasitic plants cause will be much more efficient and environmental-friendly. Understanding the mechanisms involved in haustorium development and host-parasitic plant interaction is necessary for deployment of these control strategies.

The first chapter of this dissertation looked at the current knowledge of how host plants detect stem and root parasitic plants, followed by how diverse host pre-attachment and post-attachment resistance responses defend against these parasites. This chapter also summarized existing knowledge and examples of cross-organ parasitism reported but not well-reviewed. Most current research overlooks the importance of organ specialization in resistance responses. Understanding if host plants use similar defense mechanisms to resist both major organ parasitism and cross-organ parasitism might reveal new information about host-parasite relationships.

The second chapter of this dissertation investigated the mechanism of haustorium organogenesis in the stem parasitic plant *C. campestris*. With the transcriptome of six *C. campestris* tissues and detailed transcriptome analyses, *LATERAL ORGAN BOUNDARIES DOMAIN 25* (*CcLBD25*) was identified as a critical regulator of haustorium development. The discovery of this research supports the hypothesis that stem parasitic plants, like root parasitic plants, also adapted the lateral root formation program into haustorium development. This finding

also opens a new potential path for generating parasitic weed-resistant crops that can prevent both stem and root parasitic plant attacks.

The third chapter of this dissertation investigated mechanisms underlying the resistance of hybrid Heinz tomato cultivars to *C. campestris* attacks. These cultivars trigger post-attachment lignification in the stem cortex upon *C. campestris* infection. The genes that encode key regulators involved in the lignin-based defense response were found using comprehensive RNA-Seq and DNA-Seq analyses. Two transcription factors, *SlMYB55* and *LIF1* (*Lignin induction Factor 1*, an *AP2*-like protein), were identified as crucial factors conferring host resistance by regulating lignin biosynthesis positively. One transcription factor, *SlWRKY16* is upregulated upon *C. campestris* infestation and acts as a negative regulator of *LIF1* function. *CuRLR1* (*Cuscuta R-gene for Lignin-based Resistance 1*, a *CC-NBS-LRR*) may play a role in signaling or function as a receptor for receiving *Cuscuta* signals or effectors. The identification of these four regulators in the lignin-based resistance response lays the groundwork for further research on multilayer resistance against *Cuscuta* species.

The fourth chapter of this dissertation focused on the haustorial interface between tomato hosts and *C. campestris*. *C. campestris* haustorial tissue and their surrounding tomato host tissue were collected by laser-capture microdissection (LCM) for tissue-resolution RNA-Seq analyses. Based on RNA-Seq analysis and gene co-expression networks (GCNs) module membership, network properties and associated predicted function, *CcHB7* (homeobox 7 transcription factor), *CcPMEI* (pectin methyl esterase inhibitor), and *CcERF1* (ethylene-responsive element binding factor 1) were identified as likely important regulators engaged in *C. campestris* haustorium organogenesis. Gene function was validated by host-induced gene silencing (HIGS). *SlPR1* (Pathogenesis-related protein 1), *SlCuRe1-like* (a CuRe1 homolog),

and *SlNLR* (nucleotide-binding domain leucine-rich repeat, NBS-LRR) are three possible regulators in tomatoes that are involved in receiving parasite signals, and *SlPR1* and *SlNLR* were further characterized with CRISPR knockout mutants. These findings demonstrate a complex tissue-resolution gene regulation system at the parasitic plant-host interface and uncover critical parasitism regulators in *C. campestris* and important resistance regulators in tomato hosts.

In conclusion, to stop parasitic plants from hampering crop growth and causing food shortages in many regions around the world, an understanding of the mechanisms involved in parasitic plant haustoria development and host plant defense responses is essential and critical. These are also the top priorities in setting future parasitic plant research directions. I hope the knowledge presented in this dissertation provides a foundation for developing parasitic plant-resistant systems in crops to eliminate agricultural losses and solve food security issues.